



Heterogeneous photo-fenton process for removal of micropollutants at very low concentration from Meurthe river

Hawraa Ayoub

► To cite this version:

Hawraa Ayoub. Heterogeneous photo-fenton process for removal of micropollutants at very low concentration from Meurthe river. Chemical and Process Engineering. Université de Lorraine; Université libanaise, 2018. English. NNT : 2018LORR0025 . tel-01920215

HAL Id: tel-01920215

<https://hal.univ-lorraine.fr/tel-01920215>

Submitted on 15 Apr 2019

HAL is a multi-disciplinary open access archive for the deposit and dissemination of scientific research documents, whether they are published or not. The documents may come from teaching and research institutions in France or abroad, or from public or private research centers.

L'archive ouverte pluridisciplinaire **HAL**, est destinée au dépôt et à la diffusion de documents scientifiques de niveau recherche, publiés ou non, émanant des établissements d'enseignement et de recherche français ou étrangers, des laboratoires publics ou privés.



AVERTISSEMENT

Ce document est le fruit d'un long travail approuvé par le jury de soutenance et mis à disposition de l'ensemble de la communauté universitaire élargie.

Il est soumis à la propriété intellectuelle de l'auteur. Ceci implique une obligation de citation et de référencement lors de l'utilisation de ce document.

D'autre part, toute contrefaçon, plagiat, reproduction illicite encourt une poursuite pénale.

Contact : ddoc-theses-contact@univ-lorraine.fr

LIENS

Code de la Propriété Intellectuelle. articles L 122. 4

Code de la Propriété Intellectuelle. articles L 335.2- L 335.10

http://www.cfcopies.com/V2/leg/leg_droi.php

<http://www.culture.gouv.fr/culture/infos-pratiques/droits/protection.htm>

Thèse En Cotutelle

Une thèse soumise pour l'obtention du titre de Docteur
Spécialité : Génie des Procédés et des Produits

l'Université de Lorraine

Ecole Doctoral RP2E

Science et Ingénierie, Ressources, Procédés, Produits et Environnement

ET

l'Université Libanaise

Ecole Doctorale des Sciences et Technologies (EDST)

Présentée et soutenue publiquement le 27 March 2018 by :

Hawraa AYOUB

Procédé photo-Fenton hétérogène pour l'élimination des micropolluants à très faible concentration de la rivière Meurthe

Membre du jury :

Joachim HANSEN	<i>Pr-CNRS, Université of Luxembourg</i>	Rapporteur
Stéphanie OGNIER	<i>MC-CNRS, Université of Pierre et Marie Curie</i>	Rapporteur
Souad AMMAR	<i>Pr-CNRS, Université Paris Diderot</i>	Examineur
Thibault ROQUES-CARMES	<i>MC-CNRS, Université de Lorraine</i>	Directeur (France)
Bachar KOUBAISSY	<i>Pr-CNRS, Lebanese University</i>	Directeur (Lebanon)
Olivier POTIER	<i>MC-CNRS- University of Lorraine</i>	Co-Directeur (France)
Joumana TOUFAILY	<i>Pr-CNRS, Université Libanaise</i>	Co-Directeur (Lebanon)
Cédric GUIGNARD	<i>SS-CNRS, Luxembourg institute of science and technology</i>	Invité
Tayssir HAMIEH	<i>Pr-CNRS, Université Libanaise</i>	Invité

Cotutelle Thesis

A thesis submitted for the title of Doctor
Specialty: Process and Product Engineering

University of Lorraine

Doctoral School RP2E
Science and Engineering, Resources, Processes, Products and Environment

And

Lebanese University

Doctoral School of Science and Technology (EDST)

Presented and defended on March 27, 2018 by:

Hawraa AYOUB

**Heterogeneous photo-fenton process for removal of micropollutants at very low
concentration from Meurthe river**

Members of the jury:

Joachim HANSEN	<i>Pr-CNRS, Université de Luxembourg</i>	Reviewer
Stéphanie OGNIER	<i>MC-CNRS, Université de Pierre et Marie Curie</i>	Reviewer
Souad AMMAR	<i>Pr-CNRS, Université Paris Diderot</i>	Examinor
Thibault ROQUES-CARMES	<i>MC-CNRS, Université de Lorraine</i>	Director (France)
Bachar KOUBAISSY	<i>Pr-CNRS, Lebanese University</i>	Director (Lebanon)
Olivier POTIER	<i>MC-CNRS- University of Lorraine</i>	Co-Director (France)
Joumana TOUFAILY	<i>Pr-CNRS, Université Libanaise</i>	Co-Director (Lebanon)
Cédric GUIGNARD	<i>SS-CNRS, Luxembourg institute of science and technology</i>	Invited
Tayssir HAMIEH	<i>Pr-CNRS, Université Libanaise</i>	Invited

Acknowledgement

First and above all, I praise God, the almighty for granting me the capability to proceed successfully through the three years. What I have achieved till now and whatever I will do for then it will be the result of his presence beside me.

I would like to express my thanks to Mr. Joachim Hansen and Mrs. Stéphanie Ognier for giving me the honor to be the reviewers of this thesis. I also would like to thank the members of the jury, Mrs. Souad Ammar, Mr. Cédric Guignard and Mr. Tayssir Hamieh for their remarks and notes. My great gratitude to Mr. Cedric guignard and Mrs. Audrey Lenouvel for welcoming me in their laboratory LIST in Luxembourg, increasing my knowledge in the analytical part by your beneficial remarks and suggestions and helping me to apply the analysis.

I would like to express my big thanks to my supervisor, Mr. Thibault Roques-Carmes for the help, encouragement and trust you gave me through our work together. Thanks to Mr. Olivier Potier, my co-supervisor, for the support and effective discussions you provided. Thank you both for the care you were always showing for me.

A special thanks to my Lebanese supervisor Mr. Bachar Koubaissy for giving always the necessary advice and guidance and being available for any help. Thanks to my co-supervisor Mrs. Joumana Toufaily for providing me this chance for pursuing our high research study and having a trust in my abilities to achieve our goal successfully.

Special appreciation to Mr. Steve Pontvianne for the help you provided me to carry on different experiments and analysis, and the exchange of the English-French languages we tried to do. Thanks also to Mrs. Helene Poirot for your help in analysis and sampling even in rainy weather conditions. I would like to express my gratitude to Mr. Emmanuel Mousset for the beneficial and effective knowledge you shared with me, and for your availability to provide me with any help.

A great thanks to the 'Association of Specialization and Scientific Orientation' in Lebanon for funding this thesis, allowing me to persue my study.

Beside the scientific experience in Nancy, I want to express my gratitude to the friends whom I shared with them this path. First, Zahraa, Batoul, Zeinab (In chronological order :p), every one of you represents a separate special graded experience for me. Enaamo, we strated the research together in M2 and we shared it together here. Rana, you came after a time as an office neighbor, we shared different moments and the precious neighbor, mine, Hassan. Even not mentioning the names, I can't forget all the other people I have met through the years of my stay here and my LRGP lab mates.

My biggest support, my family, my mother Hoda, my father Ayoub, my 3 sisters, Zahraa, Batoul and Nour, my friend sister Bayan, my cousin hamodi who was the indirect reason for my presence here, my all cousins, Tita and aunts. You are the strongest support everyone pray to have, without your presence all it will not be beautiful like this.

Table of Content

Acknowledgement.....	1
Table of Content.....	2
Abbreviations	4
Abstract.....	6
Résumé	7
Main Introduction.....	8
References.....	12
Résumé Du Rapport en Français	14
Chapter I.....	42
Bibliograpghy.....	42
1 Water pollution.....	43
2 Occurrence of emerging micropollutants in water and their regulations	44
3 Types and groups of micropollutants	48
3.1 Pharmaceuticals.....	48
3.2 Endocrine disruptor chemicals.....	49
3.3 Perfluorinated compounds	50
3.4 Personal care products (PCPs)	53
4 Source and fate of micropollutants	53
5 Consequences and impacts	57
6 Treatment of wastewater in wastewater treatment plants (WWTP).....	60
7 Treatment of micropollutants in WWTP: Fate and removal	62
7.1 Removal of micropollutants by conventional processes	64
7.2 Removal of micropollutants by non-conventional processes in tertiary treatment.....	66
7.2.1 Phase changing technology:.....	66
7.2.2 Biological treatment	67
7.2.3 Advanced oxidation processes	68
8 Heterogeneous photocatalysis	69
9 Photo-Fenton processes.....	71
9.1 Zeolites catalyst for heterogeneous photo-Fenton process.....	81

10	Analytical methodology for analysis, detection and quantification of micropollutants in water	84
10.1	Solid phase extraction (SPE)	84
10.2	Liquid chromatography coupled to double mass spectrometry (LC-MS/MS)	86
11	Selected compounds studied.....	89
11.1	Diclofenac	89
11.2	Phenol.....	90
	References.....	93
	Chapter II.....	108
	Detection and Quantification of Micropollutants at Very Low Concentrations from River Water	108
	Abstract.....	109
1	Introduction.....	110
2	Materials and Methods	111
2.1	River system and Sampling	111
2.2	Compounds selection	113
2.3	Preparation and analytical processes.....	116
2.4	Flux and mass balance calculations.....	117
2.5	Characterizations of macropollutants	118
3	Results and Discussion	118
3.1	Macropollutants analysis.....	118
3.1.1	Total Organic Carbon (TOC)	118
➤	Non-Purgeable Organic Carbon (NPOC)	121
➤	Inorganic Carbon (IC).....	121
➤	Total Nitrogen (TN).....	121
➤	Flux and Mass Balance.....	122
3.1.2	UV-Visible Spectroscopic analysis.....	123
3.1.3	Synchronous fluorescence spectroscopy	126
3.2	Quantification of micropollutants in river water	130
3.2.1	Site position effect	134
3.2.2	Variation with the time	139
3.3	Release of micropollutants by the wastewater treatment plant.....	143
3.4	Mass balance study	146
3.5	Detection of micropollutants in drinking water.....	147
4	Conclusion	149
	References.....	151

Chapter III	154
Iron impregnated zeolite catalyst for efficient removal of micropollutants at very low concentration from Meurthe river: Comparison with heterogeneous TiO₂ photocatalysis	154
Abstract.....	155
1 Introduction.....	156
2 Materials and methods	159
2.1 Chemicals.....	159
2.2 Catalyst preparation.....	159
2.3 Catalyst characterizations.....	160
2.4 Photo-Fenton reactions with model pollutant	160
2.5 Catalyst reusability	163
2.6 Photo-Fenton tests with real water	163
3 Results and discussion.....	165
3.1 Characterization of the Fe impregnated Faujasite.....	165
3.2 Photo-Fenton degradation of phenol pollutant.....	171
3.3 Study of the catalyst reusability.....	179
3.4 Photo-Fenton removal of diclofenac.....	181
4 Photo-Fenton degradation of micropollutants from real water	184
5 Heterogeneous photocatalysis of pollutants using TiO ₂	196
5.1 Photocatalytic degradation of model macropollutants	196
5.2 Photocatalytic degradation of micropollutants	197
6 Comparison between titania photocatalytic and iron impregnated Faujasite photo-Fenton degradation of micropollutants	210
7 Conclusion	217
Supporting Information	222
Conclusion and Perspectives.....	229

Abbreviations

AOPs	Advanced oxidation processes
ARB	Antimicrobial resistance bacteria
BET	Brunauer–Emmett–Teller
BOD	Biological oxygen demand
DWTP	Drinking water treatment plant
E1	Estrone
E2	17-beta-estradiol
EDCs	Endocrine disruptor compounds
ED	endocrine disruptors
EE2	17-alpha-ethinyl estradiol
EMs	Emerging micropollutants
EPA	Environmental protection agency
ESI	Electro-spray ionization
EU	European Union
GW	ground water
IC	Inorganic carbon
IPCS	International program of chemical safety
IT	Ion trap
LITs	Linear ion trap
LLE	Liquid-liquid extraction
LOD	Limit of detection
LOQ	Limit of quantification
MF	Membrane filtration
MP	Micropollutants
NPOC	Non-purgeable organic carbon
NSAIDs	Non-steroidal anti-inflammatory drugs
OECD	Organization of economic and cooperative development
PCPs	personal care products
PFCA	Perfluorocarboxylic acids
PFCs	Perfluorinated compounds
PFOA	Perfluorooctanoic acid
PFOS	Perfluorooctane sulfonic acid
PPCPs	Pharmaceutical and personal care products
QqLIT	Quadrupolelinear ion trap
QqQ	Triplequadropole
QqTOF	Quadrupoletime of flight
SEM	Scanning electron microscope
SPE	Solid phase extraction
SW	Surface water
TN	Total nitrogen
TOC	Total organic carbon
UF	Ultrafiltration
UHPLC	Ultra-high pressure liquid chromatography
WHO	World health organization
WWTPs	Wastewater treatment plant
XRD	X-ray diffraction

Abstract

Twenty one 21 micropollutants including pharmaceuticals, personal cares product, endocrine disruptors and perfluorinated compounds presenting at ng/L in the real water of Meurthe river, were successfully quantified and removed using heterogeneous photo-Fenton process. To achieve this goal, an analytical-catalytic methodology was developed and the work steps were performed linked together in a cycle-like manner. The use of the sensitive and efficient multi-residual SPE-LC-MS/MS analytical method allowed us to analyze and quantify the mixture of micropollutants present in a complex matrix during 3 periods of the year with different weather conditions, from 5 sampling sites. Results showed that the highest concentrations of most of the present micropollutants are observed in October at ng/L, Moulin Noir sampling site found to contain the largest number and type of these pollutants, the WWTP was not efficient in the removal of the micropollutants present in water and the drinking water used from tab was totally safe from micropollutants. The calculation of the fluxes and estimation of the mass balance at the rivers confluence confirmed the good precision and reliability of our measurement methodology, and specify the most suitable site for water to be taken from to be used in the removal tests which was Moulin Noir. Having the appropriate water sample, an efficient iron impregnated Faujasite catalyst was developed and used in a photo-Fenton process for the micropollutant removal tests. After characterization and optimization of the different experimental factors using the 2 model macropollutants, phenol and diclofenac, the real tests were performed on real water samples from Moulin Noir. The results demonstrated the good efficiency of the photo-Fenton process with the cocktail of 21 micropollutants. Except for sulfamethoxazole and PFOA, the concentrations of all the other micro-contaminants became lower than the limit of quantification of the LC-MS/MS after 30 minutes or 6 hours of photo-Fenton treatment depending on their initial concentrations under the effect of both adsorption and Fenton mechanisms. Comparing the photo-Fenton process to heterogeneous photocatalytic degradation over TiO_2 , Faster micropollutants removal occurred with the zeolite.

Résumé

Ce travail de thèse concerne le développement de catalyseurs Fe/faujasite afin de dégrader un cocktail de micropolluants provenant d'une eau réelle de rivière dans la Meurthe (France) avec le procédé photo-Fenton hétérogène. Les micropolluants étudiés appartiennent à 4 grandes familles : des principes actifs pharmaceutiques, des produits de soins cosmétiques, des perturbateurs endocriniens, et des composés perfluorés. Pour la première fois, dans cette thèse, la dégradation d'un mélange de 21 micropolluants à l'état de traces (2 – 88 ng/L) provenant d'une réelle eau de rivière non-dopée a été effectuée. Cependant, le fait de travailler avec des concentrations très faibles en polluants reste un challenge notamment en ce qui concerne les aspects de chimie analytiques. Ce travail de thèse est donc divisé en deux grandes parties. Dans un premier temps, il a été nécessaire de trouver la meilleure eau réelle contenant un nombre élevé de micropolluants de différentes natures à des concentrations de l'ordre de quelques ng/L mais inférieures à 100 ng/L. Pour cela différentes campagnes de prélèvement ont été effectuées dans les deux principales rivières de la région Lorraine, la Meurthe et la Moselle, en différents lieux et différentes périodes de l'année. L'eau provenant du site de Moulin Noir a été choisie. Dans une deuxième partie, nous avons développé des catalyseurs fer/faujasite pour pouvoir tester leur efficacité pour la dégradation des micropolluants provenant du site de Moulin Noir par le procédé photo-Fenton hétérogène. Dans une étape intermédiaire, l'optimisation des paramètres opératoires du procédé photo-Fenton avec nos catalyseurs a été effectuée en utilisant deux macropolluants modèles, phénol et diclofenac.

Main Introduction

Introduction

Currently, the pollution of the global water cycle with persistent organic contaminants remains one of the major challenges of the 21st century, and its minimization is one of today's main areas of scientific research (Aleksić et al. 2010). Since the end of the last century, large amounts of new contaminants such as medicines, pesticides, dyes, personal care products, disinfectants, food additives and laundry detergents have been detected in rivers, lakes and ground water in low concentrations (Grassi et al. 2012). These chemicals were named contaminants of emerging concerns or simply emerging contaminants ECs because they proved to have adverse negative effects on living organisms and environment even at low doses (Trapido et al. 2014; Bramard 2016) but the risk they pose is not yet fully understood (Water Quality Association). Being not monitored in the environment and unregulated, new concerns have been released regarding their occurrence, fate and adverse effects on living things (Thomaidis et al. 2012). Significant efforts have been made over the last few years to improve our understanding of the presence of emerging contaminants, their level in the environment and their effects in order to drive the necessary protection and treatment actions (Bramard 2016). This results in better monitoring of such emerging compounds. The exploratory monitoring campaigns in 2011 and 2012 on rivers, lakes, littoral waters and groundwater throughout mainland France and its overseas territories showed that substances such as pharmaceuticals, personal care products and endocrine disrupting compounds are the mostly detected emerging substances under the name micropollutants (Bramard 2016). In Germany, up to 16000 tons of pharmaceuticals were disposed each year from human medical care through flushing down the toilets or disposed of with household waste. In United Kingdom, 74.7 % of the unfinished bought pharmaceuticals are discarded in household waste or into sink. In United States, several kinds of drugs have been present at detectable levels in many surface waters (Kolpin et al. 2002). Furthermore, several micropollutants can be introduced into groundwater through surface water leakage and groundwater recharge (Zhang et al. 2008). The detection of micropollutants in ground water across Europe raised important questions related to the quality of the drinking water consumed from the tap, and how much it is clean and pure (Tousova et al. 2017). Being present in wastewater from different sources, the treatment of this water in the wastewater treatment plants (WWTP) before its discharge to the rivers does not solve the problem. On the contrary, WWTP act as the main gateway for micropollutants into water bodies due to the fact that conventional treatment methods used in WWTP don't provide an effective barrier against ECs (Hamid and Eskicioglu 2012; Stackelberg et al. 2004). For example, 80 % of 32 selected drugs were detectable in at least one sewage treatment plant effluent, and 20 different drugs and four corresponding metabolites were

detected in rivers and streams (Ternes 1998). Therefore, the development of efficient treatment technologies that achieve effective and complete removal and even mineralization of micropollutants from water need to be recognized and is of important consideration in the WWTP responsible for the release of wastewater into the environment and in the production of safe drinking water (Rossner et al. 2009).

Several treatment methods are considered for the removal of emerging contaminants from wastewater and drinking water as well. These include adsorption, membrane technology and biological treatments. However, these methods have several drawbacks including high cost, generation of secondary pollution, and complex treatment procedure (Aleksić et al. 2010). Advanced oxidation processes (AOPs) are considered to be the most effective treatment methods for the removal of micropollutants from water based on the generation of the highly active oxidizing hydroxyl radicals' species. AOPs include several oxidation methods such as Fenton processes, photocatalytic treatments (homogeneous or heterogeneous), ozonation, and much more. Fenton processes using iron salts are the most cost effective source of hydroxyl radicals with easy operation procedure. It is widely proved that among the different Fenton processes, UV assisted heterogeneous photo-Fenton process overcome the disadvantages of all the other Fenton processes including mainly less iron leaching and the ability to operate at milder pH conditions. Different types of catalyst supports can be used in such processes such as synthetic and natural zeolites, pillared clay and bentonites. Among them, synthetic zeolites are the most efficient catalyst mainly due to its unique properties and ability to adsorb smaller organic compounds (Aleksić et al. 2010; Blanco et al. 2014).

In order to study the efficiency of the selected treatment in the removal of micropollutants from water, there is a need for an efficient analytical methodology for detection and quantification of these compounds at such low concentration. Recently, new approaches combining the sensitivity of the used tools with sophisticated chemical analysis have been developed to cover a wide range of emerging contaminants in complex water matrix (Tousova et al. 2017). Due to the low and fluctuating concentrations of such compounds (ng/L), pre-concentration techniques have been developed. The main and mostly used pre-concentration technique is the solid phase extraction that pre-concentrates, cleans and allows direct quantification of the identified compounds in the analyzed sample (Dimpe and Nomngongo 2016). The quantification of micropollutants have been carried out by ultra-high performance liquid chromatography (UHPLC) or by gas chromatography (GC) both coupled to tandem mass spectrometry (MS/MS) for their sensitivity and good resolution (Tousova et al. 2017; Sordet et al. 2016). LC-MS/MS have shown high performance in multi-residual analysis of organic micropollutants in water and their quantification down to sub-ng/L (Leendert et al. 2015).

Large improvements have been made due to the combination of SPE-LC-MS/MS based on atmospheric pressure ionization (ESI) which have shown high recoveries and quantification values (Zwiener and Frimmel 2004). Despite of the high performance of such multi-residual methodology, the analysis of micropollutants at very low concentration level is an analytical challenge for several studies. Since the availability of laboratories with the special needed equipment's is limited and the need for complex multi-steps analysis make researchers prefer to perform their analysis on samples with relatively high pollutants' concentration instead of working with such very low concentrations.

Being able to work and quantify the micropollutants presenting at very low concentration, allows us to implement the treatment method on real river water samples that contain a real mixture of different micropollutants, in a complex water matrix containing a variety of organic and inorganic pollutants. Taking water samples from a river is affected by different factors related to the river itself, the environmental conditions and the city surrounding it. Nancy city is crossed by the Moselle river of 545 km length flowing through France, Luxembourg and Germany, in addition to a small part that drains Belgium. The Moselle has a catchment area of 28,286 Km² where the French part covers 15360 Km² (about 54 % of the total catchment). Many cities in France are located along it such as Nancy, Epinal, Toul and Metz. Meurthe is one of the 10 largest tributaries of Moselle of 161 Km length flowing in north-eastern France through Nancy city in Lorraine. Meurthe river flows into the Moselle at Pompey on the northern edge of Nancy. Water samples from the Meurthe river and Moselle river are considered as an important field for the study of the removal efficiency of the heterogeneous photo-Fenton treatment method.

The analysis of 21 micropollutants of different groups in a real river water samples from the Meurthe river and Moselle river in the Nancy city using multi-residual SPE-LC-MS/MS analytical method is studied in chapter II. The effect of different factors such as flow rate, weather conditions, surrounding area, and site sampling position on the quantification of low concentration contaminants in real water is evaluated. The analysis in real water allows finding the best real water conditions and position for good, precise and reliable measurements. The Fe-Faujasite catalyst is synthesized and characterized by several techniques. In chapter III, the catalyst efficiency is tested first on synthetic solutions using phenol and diclofenac as the model pollutants to optimize the different experimental parameters before applying the removal treatment on real water samples. The efficiency of degradation of the Fe/Faujasite photo-Fenton system towards the removal of 21 micropollutants is compared with that of TiO₂ photocatalysis.

References

- Aleksi M, Kušić H, Koprivanac N, Leszczynska D, Lončarić Božić A (2010) Heterogeneous Fenton Type Processes for the Degradation of Organic Dye Pollutant in Water-The Application of Zeolite Assisted AOPs. *Desalination* 257 (1–3): 22–29.
- Blanc M, Martinez A, Marcaide A, Aranzabe E, Aranzabe A (2014) Heterogeneous Fenton Catalyst for the Efficient Removal of Azo Dyes in Water. *Am. J. Analyt. Chem.* 05 (08): 490–99.
- Bramard M (2016) Monitoring Micropollutants in French Aquatic Environments: Recent Advances. http://www.eaufrance.fr/IMG/pdf/campex_201603_EN.pdf.
- Dimpe K.M, Nomngongo P.N (2016) Current Sample Preparation Methodologies for Analysis of Emerging Pollutants in Different Environmental Matrices. *TRAC-Trend. Anal. Chem.* 82 (September): 199–207.
- Grass M, Kaykioglu G, Belgiorno V, Lofrano G (2012) Removal of Emerging Contaminants from Water and Wastewater by Adsorption Process. In: Lofrano G. (eds) *Emerging Compounds Removal from Wastewater*: 15–37.
- Hamid H, Eskicioglu C (2012) Fate of Estrogenic Hormones in Wastewater and Sludge Treatment: A Review of Properties and Analytical Detection Techniques in Sludge Matrix. *Water Res.* 46 (18): 5813–33.
- Kolpin D.W, Furlong E.T, Meyer M.T, Michael Thurman E, Zaugg S.T, Barber L.B, Buxton H.T (2002) Pharmaceuticals, Hormones, and Other Organic Wastewater Contaminants in U.S. Streams, 1999–2000: A National Reconnaissance. *Envi. Sci. Tech.* 36 (6): 1202–11.
- Leendert V, Langenhove H.V, Demeestere K (2015) Trends in Liquid Chromatography Coupled to High-Resolution Mass Spectrometry for Multi-Residue Analysis of Organic Micropollutants in Aquatic Environments. *TRAC-Trend. Anal. Chem.* 67 (April):192–208.
- Rossner A, Snyder S.A, Knappe D.R.U (2009) Removal of Emerging Contaminants of Concern by Alternative Adsorbents.” *Water Res.* 43 (15):3787–96.
- Sordet M, Berlioz-Barbier A, Buleté A, Garric J, Vulliet E (2016) Quantification of Emerging Micropollutants in an Amphipod Crustacean by Nanoliquid Chromatography Coupled to Mass Spectrometry Using Multiple Reaction Monitoring Cubed Mode.” *J. Chromatogr. A.* 1456 (July): 217–25.
- Stackelberg P.E, Furlong E.T, Meyer M.T, Zaugg S.D, Henderson A.K, Reissman D.B (2004) Persistence of Pharmaceutical Compounds and Other Organic Wastewater Contaminants in a Conventional Drinking-Water-Treatment Plant. *Sci. Total Environ.* 329 (1–3): 99–113.

- Ternes T.A (1998) Occurrence of Drugs in German Sewage Treatment Plants and rivers. *Water Res.* 32 (11): 3245–60.
- Thomaidis N.S, Asimakopoulos A.G, Bletsou A.A (2012) Emerging Contaminants: A Tutorial Mini-Review. *Global NEST J.* 14, 2012, no. 1 edition.
- Tousova Z, Oswald P, Slobodnik J, Blaha L, Muz M, Hu M, Brack W, et al (2017) European Demonstration Program on the Effect-Based and Chemical Identification and Monitoring of Organic Pollutants in European Surface Waters.” *Sci. Total Environ.* 601–602 (December): 1849–68.
- Trapido M, Epold I, Bolobajev J, Dulova N (2014) Emerging Micropollutants in Water/Wastewater: Growing Demand on Removal Technologies. *Environ. Sci. Pollut. R.* 21 (21): 12217–22.
- Water quality association. Contaminants of Emerging Concern. <https://www.wqa.org/whats-in-your-water/emerging-contaminants>.
- Zhang Y, Geißen S.U, Gal C (2008) Carbamazepine and Diclofenac: Removal in Wastewater Treatment Plants and Occurrence in Water Bodies. *Chemosphere* 73 (8): 1151–61.
- Zwiener C, Frimmel F.H (2004) LC-MS Analysis in the Aquatic Environment and in Water Treatment Technology? A Critical Review. *Anal. Bioanal. Chem.* 378 (4): 862–74.

Résumé Du Rapport en Français

Résumé

La protection de l'environnement, et particulièrement de l'eau, demeure un enjeu fondamental, en raison de sa détérioration à cause des activités industrielles et anthropiques. A l'heure actuelle la contamination se répercute également sur l'eau douce et notamment les eaux de surface, qui se trouve détériorée par divers polluants provenant de diverses sources. Celles-ci peuvent être industrielles, provenir de l'agriculture intensive, du transport, des déchets domestiques, des produits de santé, des déchets urbains, de la pollution aérienne soluble dans l'eau, etc. Des recherches récentes reportent la présence d'un large groupe de polluants organiques présents dans les effluents provenant de diverses sources à des gammes de concentrations de l'ordre du ng/L et µg/L. Cette nouvelle classe de polluants est appelée micropolluants. Ces substances incluent notamment les principes actifs pharmaceutiques, les produits de soins cosmétiques, les perturbateurs endocriniens, et les composés perfluorés. La grande majorité de ces composés est considérée comme dangereuses mêmes lorsque ces composés sont présents à l'état de traces : cancérogènes, perturbateur endocriniens, etc. Les procédés de traitement dans les stations d'épuration ne permettent pas d'éliminer toute la pollution présente dans les effluents et de nombreux micropolluants demeurent présents dans les eaux en sortie des stations. En outre, le rejet de ces polluants pose également des problèmes pour le fonctionnement de l'écosystème.

Il devient donc nécessaire de développer des technologies innovantes et de nouveaux procédés de façon à éliminer, à un coût acceptable, les traces de mélanges micropolluants les plus indésirables tout en préservant l'écosystème. Les procédés d'oxydation avancée (AOPs) apparaissent comme une bonne alternative en pleine expansion pour la décontamination de l'eau. Ils présentent une complémentarité intéressante aux techniques habituelles de floculations, précipitations, adsorption sur charbon actif ou osmose inverse en tant que traitements tertiaires de finition. Le principe des AOPs repose sur la production d'agent oxydant très puissant tel que les radicaux hydroxyles ($\cdot\text{OH}$) qui possèdent un potentiel d'oxydation très élevé ($E^\circ = 2.80 \text{ V vs SHE}$). Parmi ces techniques d'oxydation avancée, le procédé photo-Fenton présente l'avantage d'oxyder de très nombreux contaminants de l'eau tels que les engrais, les pesticides, les colorants, les molécules pharmaceutiques jusqu'à leur destruction complète (minéralisation) grâce à la production de radicaux $\cdot\text{OH}$ au travers de réactions de type Fenton et Fenton-like en présence de peroxyde d'hydrogène (H_2O_2) avec les ions ferreux (Fe^{2+}) et ferrique (Fe^{3+}) :

Fenton:



Fenton-like :



Deux sources additionnelles d' $\cdot\text{OH}$ peuvent être obtenues par photolyse en présence de lumière :

Photo-Fenton :



Cependant, le procédé photo-Fenton homogène présente de nombreux désavantages. Il entraîne la formation de boues contenant des ions fers qui doivent être retirés à la sortie des stations d'épurations. De plus, la régulation en continu du pH à des pH acides autour de pH 3 fait que le procédé homogène n'est pas adapté pour être utilisé dans des stations d'épurations. De fait, le développement du procédé hétérogène, i.e. photo-Fenton hétérogène, apparaît comme une solution pour résoudre ces problèmes. De nombreux supports ont d'ores et déjà été développés : nafion, zeolite, silice, argile, et charbon actif. L'utilisation de support de type zéolite apparaît très prometteuse en raison de leurs propriétés spécifiques qui augmentent l'efficacité et, surtout, réduisent la formation de sous-produits de dégradation comparés aux autres procédés d'oxydation avancée (AOPs). Récemment, des zéolites contenant des métaux (composites formés de nanoparticules métalliques déposées sur zéolites) apparaissent comme des catalyseurs efficaces et prometteurs pour l'oxydation par photo-Fenton de différents groupes de polluants organiques en présence de peroxyde d'hydrogène. Plus particulièrement, des catalyseurs à base de fer immobilisés sur des zéolites permettent d'atteindre de grande efficacité de dégradation. Les Faujasites sont un type particulier d'aluminosilicate zéolites qui combinent un réseau en trois dimensions de pores accessibles (0.74 nm) et proviennent d'une synthèse en l'absence de produits organiques. C'est ce type de zéolite qui a été choisie dans cette thèse comme support du catalyseur à base de fer.

La dégradation de micropolluants par des AOPs (photo-Fenton, photocatalyse, etc.) a déjà été étudiée auparavant. Cependant, la très grande majorité des travaux ont été conduits avec des eaux reconditionnées, c'est-à-dire des eaux synthétiques « synthetic waters » ou de l'eau réelle (provenant des sorties de station d'épuration ou de l'eau naturelle) mais « dopée » (spiked) avec des solutions de micropolluants. Dans le même temps, dans ces études la concentration en micropolluant est généralement élevée i.e. entre le $\mu\text{g L}^{-1}$ et le mg L^{-1} . Seulement quelques études travaillent avec des micropolluants provenant d'eaux réelles. Par exemple, Miralles-Cuevas et al. (2014) ont reportées la dégradation de micropolluants provenant d'eaux municipales par le procédé photo-Fenton. Ils se sont intéressés à 9 micropolluants pharmaceutiques de la même famille mais à des concentrations relativement grandes comprises entre 200 $\mu\text{g/L}$ et 0.86 $\mu\text{g/L}$. Il est également intéressant de mentionner que la dégradation, notamment par le procédé photo-Fenton, de certains micropolluants, tels que les composés perfluorés, PFCs, a été rarement évaluée en raison de la liaison carbone-fluore.

Il apparaît donc très intéressant de conduire une étude avec de l'eau réelle contenant différentes familles de produits chimiques. Ce travail de thèse concerne le développement de catalyseurs Fe/Faujasite afin de dégrader un cocktail de micropolluants provenant d'une eau réelle de rivière dans la Meurthe (France) avec le procédé photo-Fenton hétérogène. Les micropolluants étudiés appartiennent à 4 grandes familles : des principes actifs pharmaceutiques, des produits de soins cosmétiques, des perturbateurs endocriniens, et des composés perfluorés. Pour la première fois, dans cette thèse, la dégradation d'un mélange de 21 micropolluants à l'état de traces (0.8 – 88 ng/L) provenant d'une réelle eau de rivière non-dopée a été effectuée. Il est important de mentionner le fait que la dégradation de micropolluants à ces très faibles niveaux de concentration est représentative des niveaux de concentrations en micropolluant émergents (ng.L^{-1}) rencontrés à la sortie des stations d'épurations (STEP). Par conséquent, les résultats de nos travaux seront directement applicables dans les STEPs. Cependant, le fait de travailler avec des concentrations très faibles en polluants reste un challenge notamment en ce qui concerne les aspects de chimie analytiques. En effet, la majorité des études de ce type dans la littérature évitent ces concentrations trop faibles en raison de la complexité de l'analyse par LC-MS/MS, du grand nombre d'étapes pour effectuer une mesure, et également du prix très élevé de ce type d'appareillage, ce qui fait que seulement un nombre limité de laboratoire en possèdent. Dans le cadre de cette thèse, nous ne disposons pas de ce type d'appareillage dans nos laboratoires ni à Nancy, ni au Liban. Les mesures n'ont pu être effectuées que grâce à une collaboration avec le Luxembourg Institute of Science and Technology (LIST) et plus particulièrement via une collaboration avec madame Audrey Lenouvel et monsieur Cédric Guignard.

Ce travail de thèse est donc divisé en deux grandes parties (Fig. 1):

1) Dans un premier temps, il a été nécessaire de trouver la meilleure eau réelle contenant un nombre élevé de micropolluants de différentes natures à des concentrations de l'ordre de quelques ng/L mais inférieures à 100 ng/L. Pour cela différentes campagnes de prélèvement ont été effectuées dans les deux principales rivières de la région Lorraine, la Meurthe et la Moselle, en différents lieux et différentes périodes de l'année. Nous verrons que l'eau provenant du site de Moulin Noir a été choisie.

2) Dans une deuxième partie, nous avons développé des catalyseurs fer/Faujasite pour pouvoir tester leur efficacité pour la dégradation des micropolluants provenant du site de Moulin Noir par le procédé photo-Fenton hétérogène. Dans une étape intermédiaire, l'optimisation des paramètres opératoires du procédé photo-Fenton avec nos catalyseurs a été effectuée en utilisant deux macropolluants modèles, phénol et diclofenac.

Ce travail se situe donc à la rencontre de la chimie analytique, la catalyse, les matériaux, le traitement de l'eau, ceci dans le cadre d'une collaboration internationale entre la France, le Liban et le Luxembourg. Ceci constitue une des originalités de ce travail de thèse.

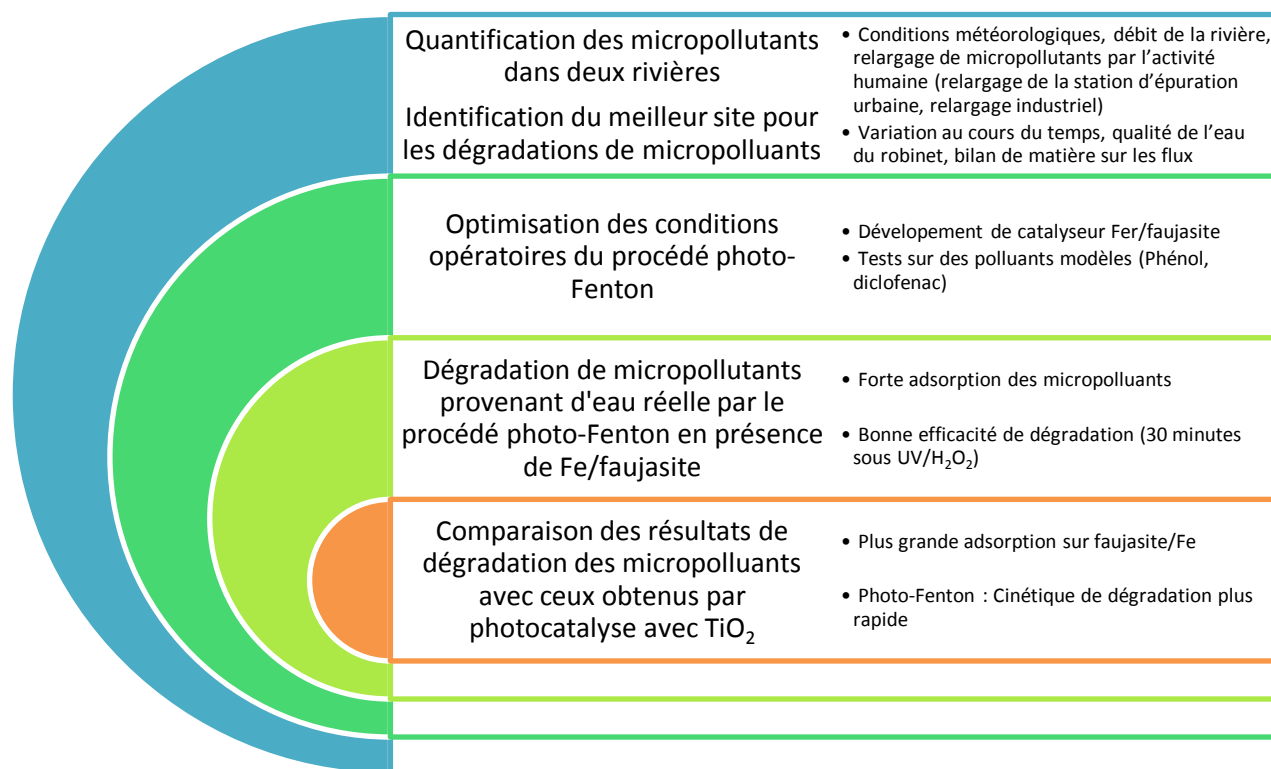


Fig. 1. Résumé des étapes de la thèse.

La première partie de ce travail a pour objectif de caractériser et de quantifier les divers micropolluants présents dans les deux rivières afin de trouver le point de prélèvement le plus favorable pour les expériences de dégradation au laboratoire, c'est-à-dire le lieu présentant le plus grand nombre de micropolluants différents à tout moment. La quantification des différents groupes de micropolluants (principes actifs pharmaceutiques, produits de soins cosmétiques, perturbateurs endocriniens, et composés perfluorés) présents dans les rivières de Meurthe et de Moselle a été effectuée par analyse LC-MS/MS. Il est important de noter qu'une étape de pré-concentration s'avère nécessaire avant l'analyse. Durant une période de 1 an, l'eau des rivières a été prélevée et analysée 3 fois, à savoir en septembre 2015, janvier 2016 et octobre 2016. Les prélèvements ont été effectués dans 5 différents endroits de la Meurthe et de la Moselle. Ceci nous permet d'étudier différents facteurs telles que les conditions météorologiques, le débit de la rivière, le relargage de micropolluants par l'activité humaine, et notamment de la station d'épuration, et la qualité de l'eau que nous buvons au robinet. La Fig. 2 précise les positions de chacun des sites de prélèvements.

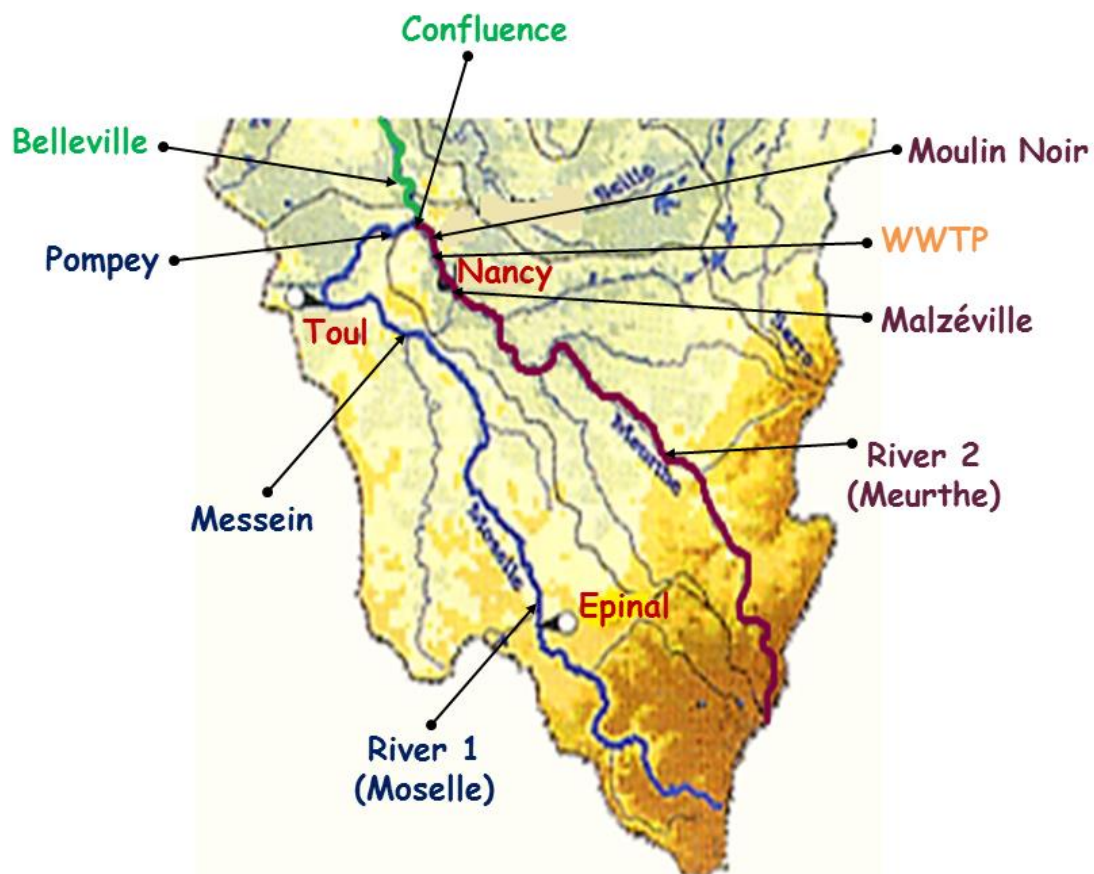


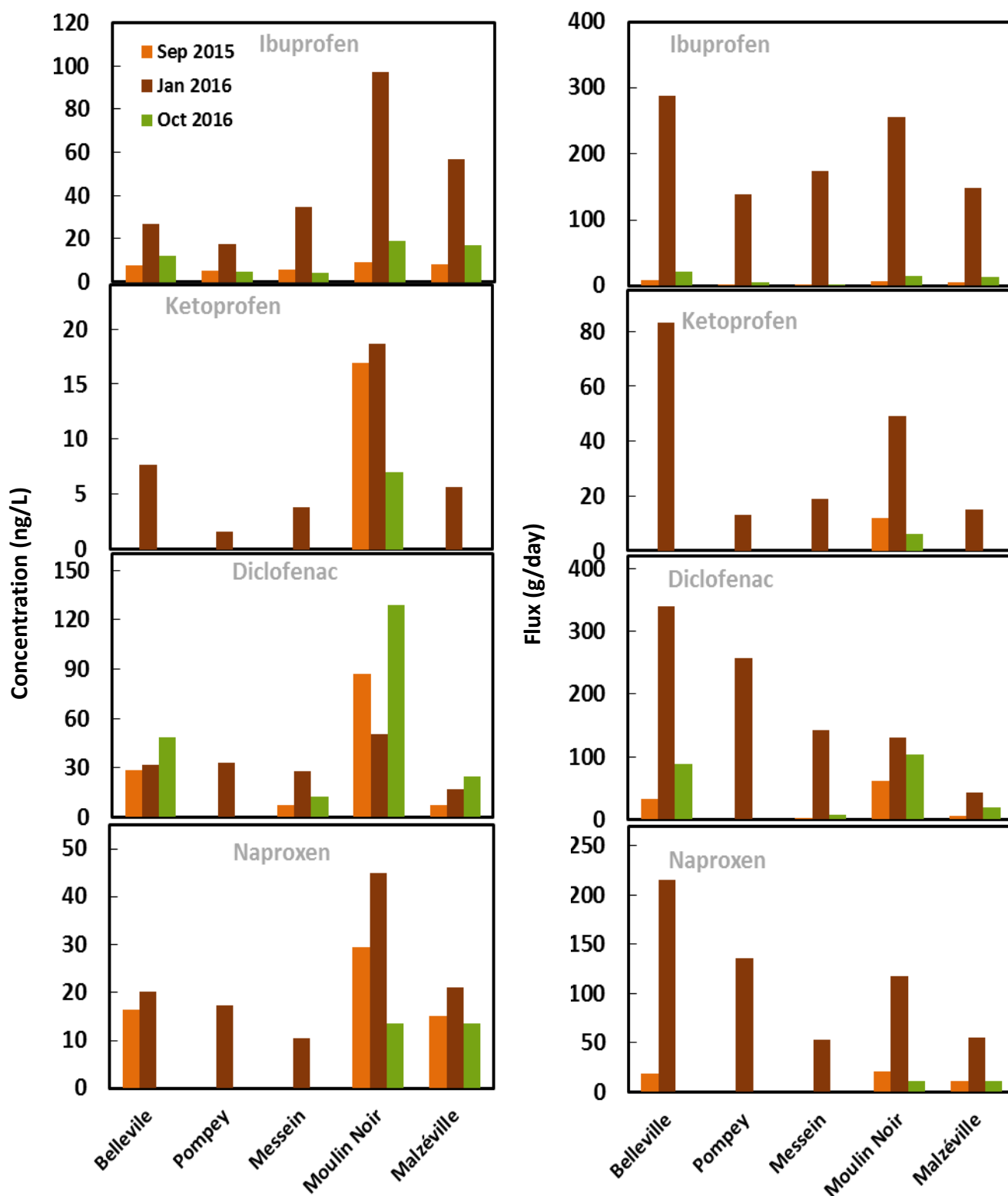
Fig. 2. Positions de chacun de sites de prélèvements sur la Meurthe et la Moselle.

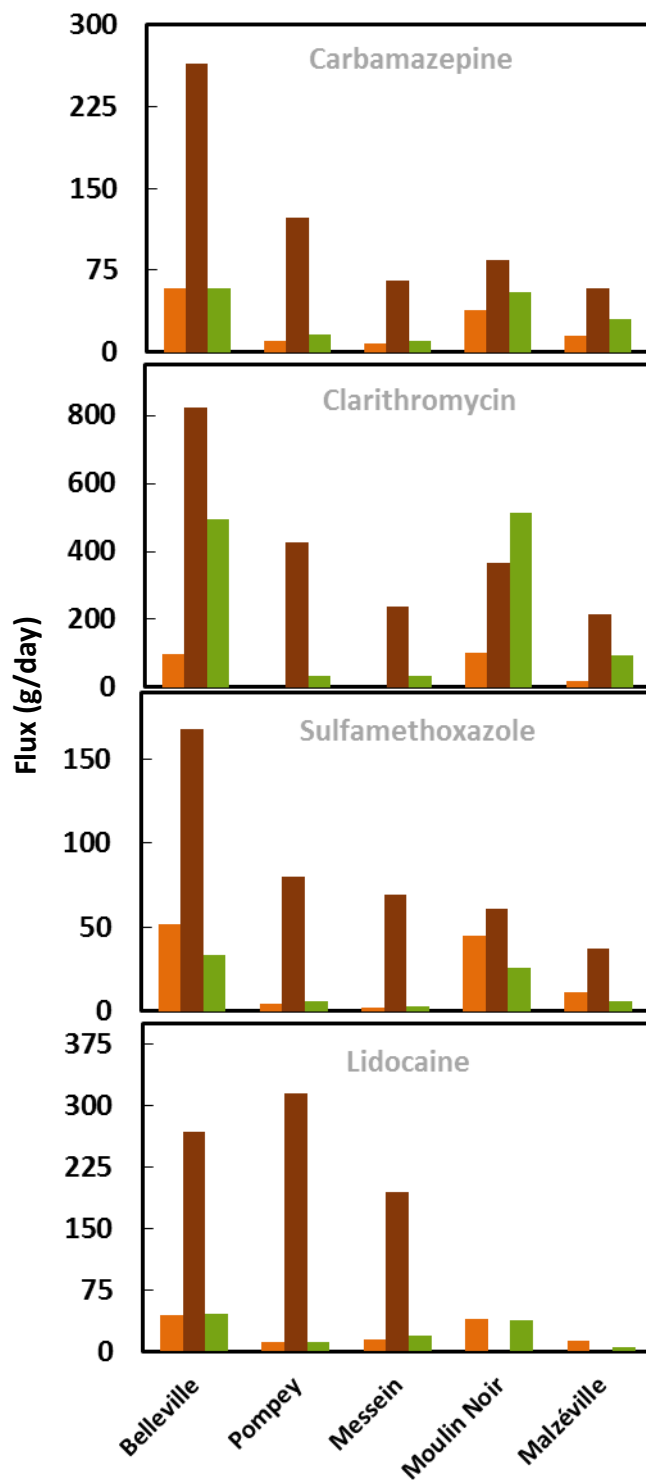
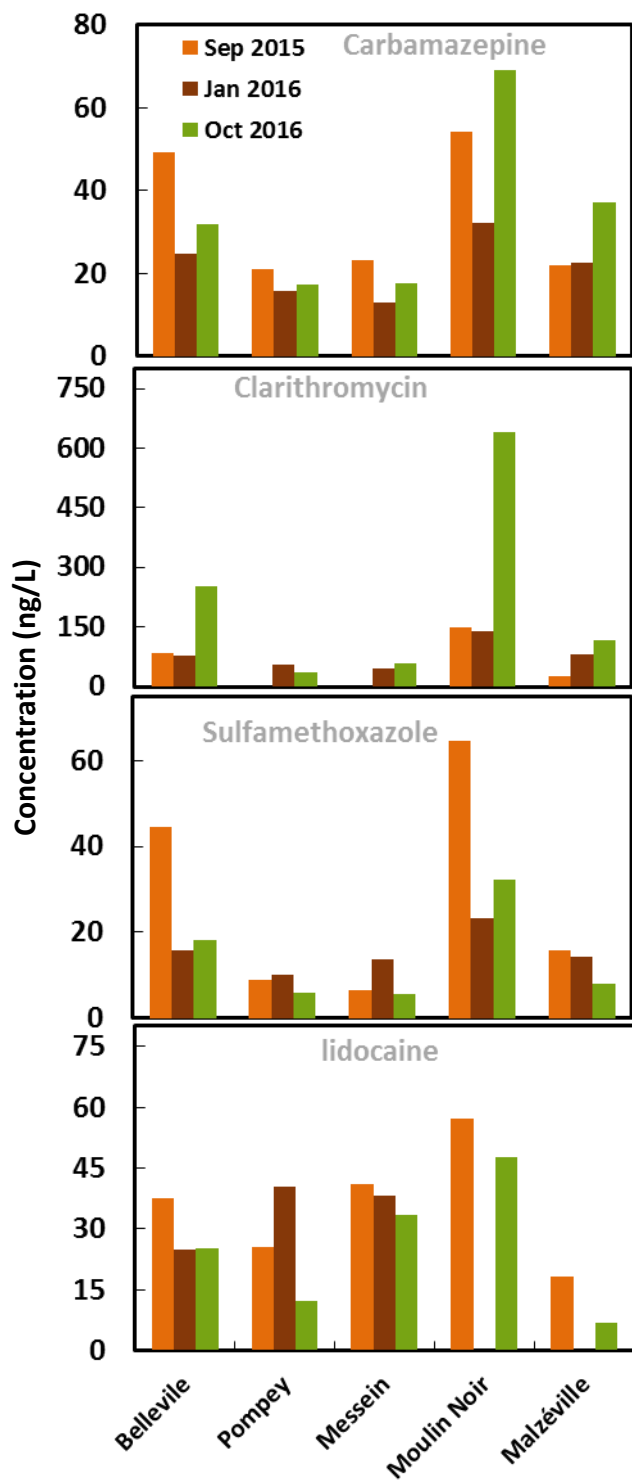
Les résultats majeurs de cette étude sont les suivants (Fig. 3):

- 1) Nous avons réussi à quantifier 21 micropolluants à de très faibles concentrations de l'ordre de quelques ng/L. Pour chaque polluant, la concentration dépend du site de prélèvement et également des conditions météorologiques. Par exemple, les concentrations inhabituelles de triclosan mesurées dans la Meurthe, ainsi que celles de PFOA dans la Moselle peuvent être attribuées à la présence d'usine.
- 2) Calcul des flux et analyse des changements sur les 5 différents sites en tenant compte du débit de la rivière à différents moments durant une année. Nous avons montré que les concentrations de polluant sont affectées par le débit de la rivière. Le flux de micropolluant dépend également des rejets effectués autour des différents sites. Ceux-ci varient selon la saison pour certains polluants. A titre d'exemple, le flux de carbamazépine ne dépend pas de la période de l'année ni des conditions météorologiques, du fait qu'elle est un antiépileptique utilisé tous les jours en traitement de fond. De la même façon, le bisphénol A est utilisé en continu tout au long de l'année, ainsi son flux reste similaire durant l'année. En revanche, pour le diclofenac, le flux change durant l'année car son utilisation est fortement impactée par la période de l'année.
- 3) Des bilans matières ont été effectués avant et après la confluence de la Meurthe et de la Moselle. En tenant compte des incertitudes lors de la mesure de ces faibles concentrations en micropolluant, les résultats des bilans sont très satisfaisants. L'erreur est de l'ordre de 6,5 % à 23,3 % pour neuf des douze micropolluants présents au niveau de la confluence, ce qui renseigne sur la précision et la fiabilité de nos mesures de concentration.
- 4) Le relargage de la station d'épuration pour la dégradation des micropolluants a été évaluée. Pour ce faire, nous avons estimé la concentration des différents groupes de micropolluants avant et après la STEP. Le flux de micropolluant augmente en sortie de la STEP, ce qui met en évidence la relative inefficacité de la STEP pour détruire les micropolluants. C'est pour cette raison que la concentration en micropolluant sur le site de Moulin Noir est la plus élevée car les micropolluants proviennent à la fois de la STEP et de la rivière.
- 5) En ce qui concerne la qualité de l'eau que nous buvons, nous avons analysé l'eau du robinet du laboratoire en la comparant à l'eau de la rivière Moselle à Messein au niveau de captage (pour la production d'eau potable de la Métropole de Nancy). Toutes les concentrations des 21 micropolluants analysés sont en-dessous de la limite de quantification du LC/MS-MS avec préconcentration. La comparaison de ces valeurs avec celles obtenues sur le site de Messein, met clairement en évidence que la station de potabilisation (drinking water

treatment plant, DWTP) est très efficace. Elle permet de détruire les micropollutants présents dans l'eau.

- 6) Le lieu le plus intéressant pour le prélèvement d'eau pour les expériences de biodégradation est le site de Moulin Noir. C'est le site d'analyse qui présente une eau contenant le plus grand nombre de micropolluants différents, et ceci pour les trois périodes différentes de prélèvement.





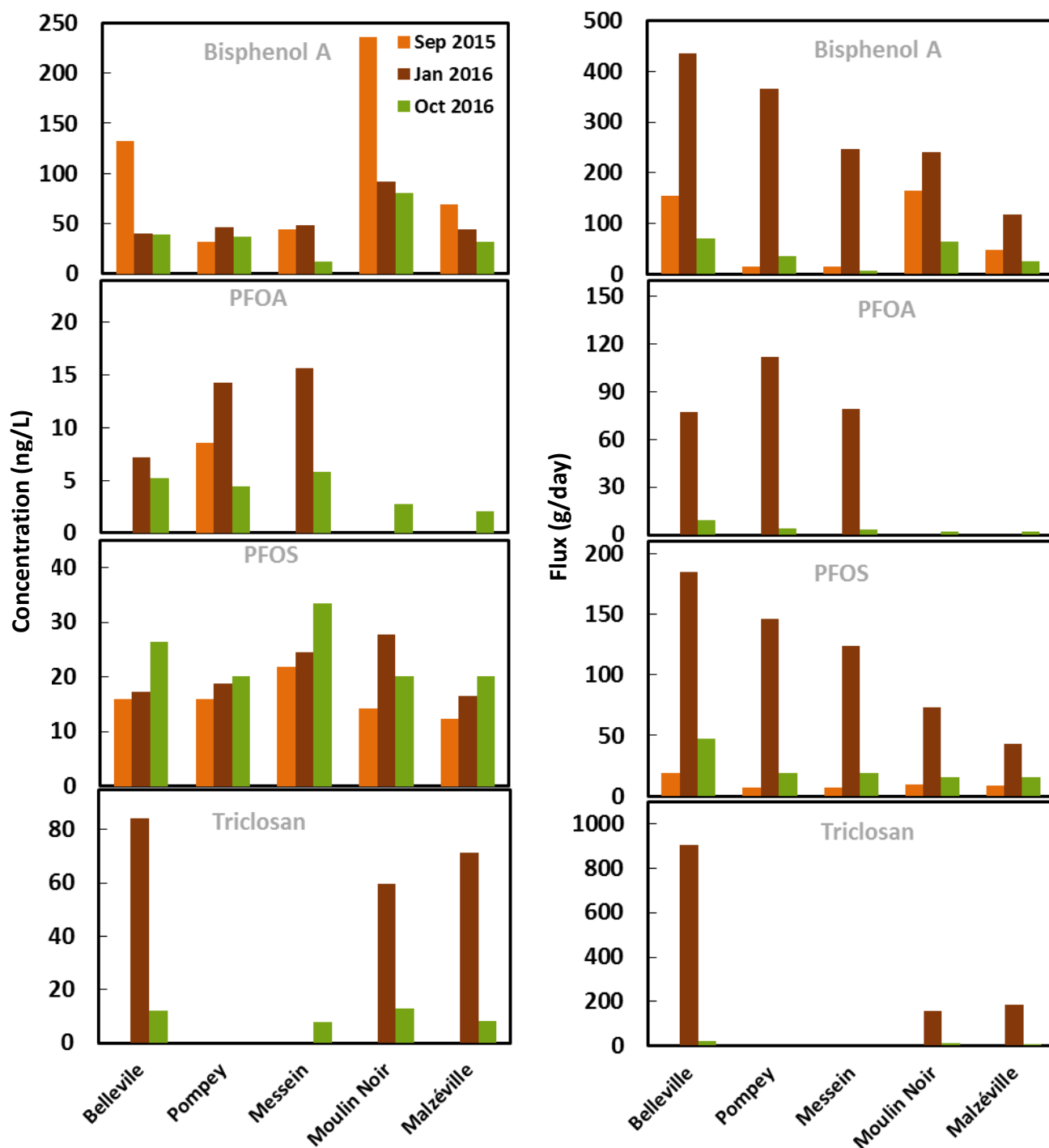


Fig. 3. Concentration et flux de chacun des micropolluants sur les différents sites pour 3 différentes périodes.

La deuxième partie de ce travail de thèse a pour objectif de (a) développer des catalyseurs fer/Faujasite, (b) optimiser les performances du procédé photo-Fenton avec ces catalyseurs en utilisant principalement un polluant modèle (phénol), et surtout (c) de tester l'efficacité de ce système pour traiter l'eau réelle contenant un cocktail de micropolluants provenant du site de Moulin noir. L'efficacité sera ensuite comparée avec celle du dioxyde de titane et du procédé de photocatalyse pour la dégradation de ces micropolluants (d).

Le catalyseur est préparé par la méthode d'imprégnation par voie humide en utilisant du nitrate de fer (III) comme précurseur de fer. Les méthodes de caractérisations, MEB couplé à de la spectroscopie à rayons X à dispersion d'énergie (EDS), diffraction de rayons X, spectrophotométrie UV-visible, et mesures de potentiel zeta ont permis de confirmer la présence de fer, principalement sous la forme de particules de Fe_2O_3 déposées sur la surface de la Faujasite.

L'optimisation des performances du procédé photo-Fenton avec ces catalyseurs a été évaluée en étudiant la dégradation du phénol utilisé comme macropolluant modèle. Nous avons plus particulièrement envisagé l'influence de quatre paramètres fondamentaux, à savoir la concentration en peroxyde d'hydrogène, la nature (UV et visible) et l'intensité de la lumière, la quantité de fer déposée sur la zéolite, et l'influence du pH de la solution. La dégradation complète de 10 mg/L de phénol a été obtenue en présence de Faujasite contenant 20% en masse de fer, sous irradiation UV, en présence de 0,007 mol/L de H_2O_2 à pH 5,5 (Fig. 4).

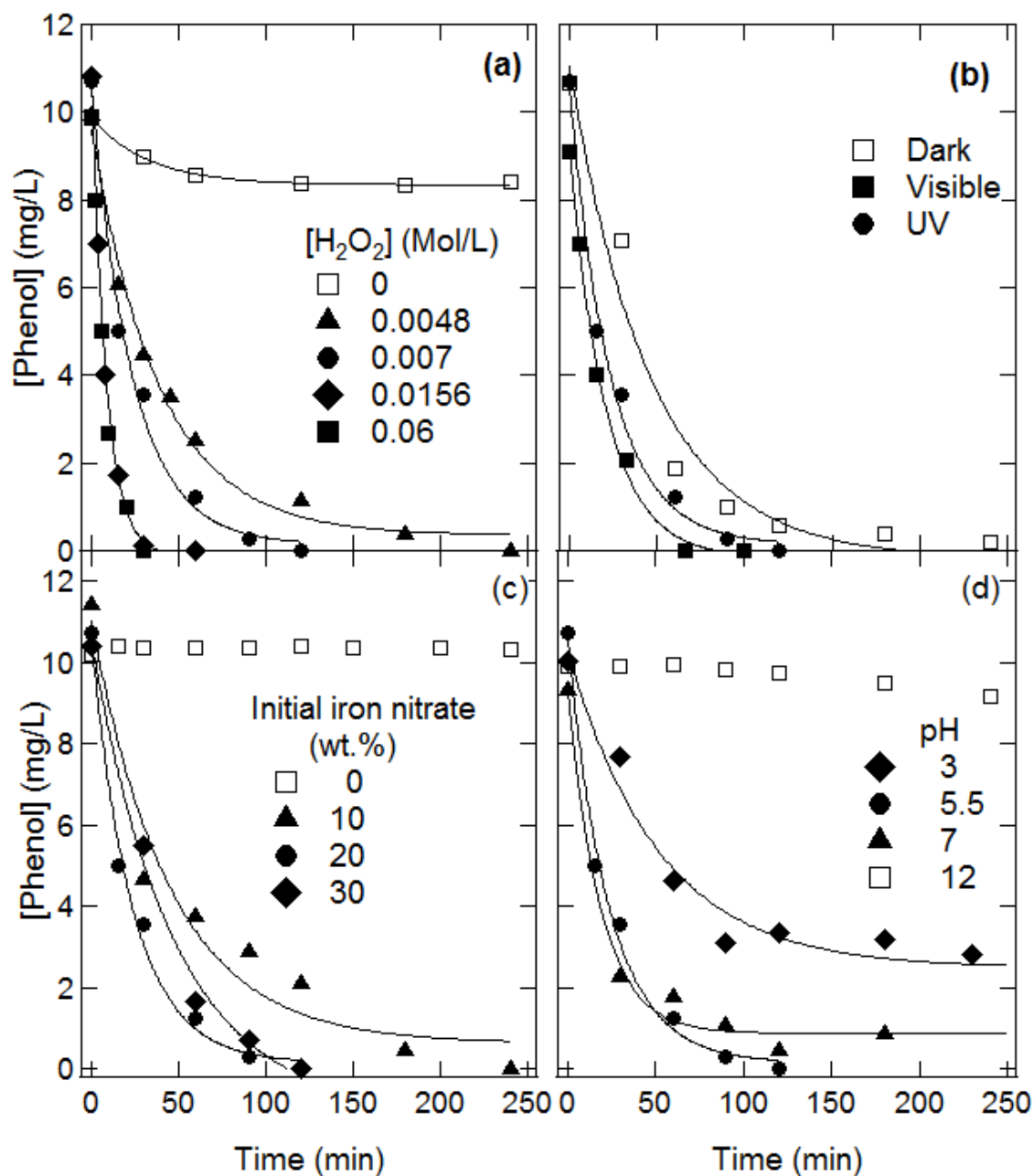


Fig. 4. Optimisation des paramètres expérimentaux durant la dégradation par le procédé photo-Fenton du phénol en présence de Fe/Faujasite. (a) Effet de la concentration en H_2O_2 . Conditions expérimentales: catalyseur = 1 g/L, irradiation UV, et pH 5,5. (b) Influence de la nature de la lumière. Conditions expérimentales: catalyseur = 1 g/L, 0,007 M H_2O_2 , et pH 5,5. (c) Effet de la masse initiale en du nitrate de fer (III) utilisée pour préparer le catalyseur. Conditions expérimentales: catalyseur = 1 g/L, 0,007 M H_2O_2 , irradiation UV, et pH 5,5. (d) Influence du pH. Conditions expérimentales: catalyseur = 1 g/L, 0,007 M H_2O_2 , et irradiation UV. Les lignes correspondent au fit des données expérimentales par une fonction du type $A \exp(-k t)$ représentative d'une cinétique du premier ordre

Par la suite, nous avons testé l'efficacité de ce système pour traiter l'eau réelle contenant un cocktail de micropolluants provenant du site de Moulin noir. La capacité d'adsorption du catalyseur a été évaluée. La majorité des micropolluants ont une forte affinité pour la surface de la Faujasite imprégnée de fer. Cela indique que la grande majorité des micropolluants peuvent être retirée de l'eau par adsorption sur la Faujasite modifiée. En effet, après 2 heures d'adsorption la concentration résiduelle devient inférieure à la limite de quantification du LC/MS-MS (Fig. 5).

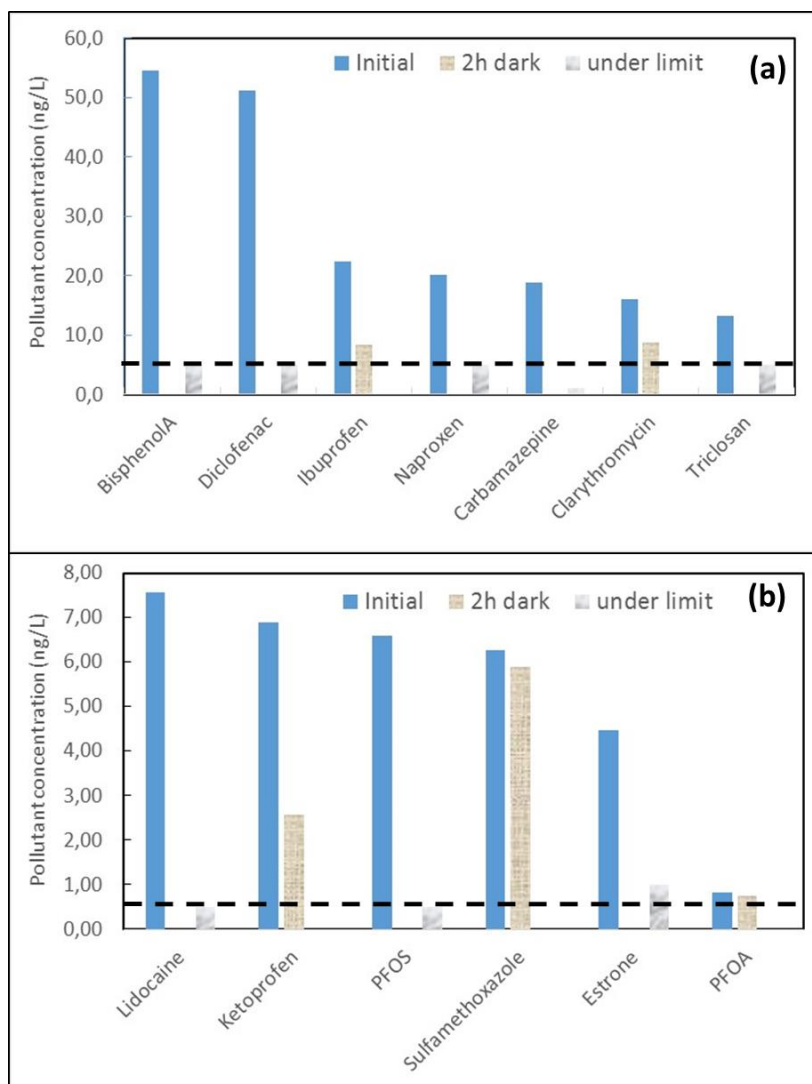


Fig. 5. Adsorption des micropolluants sur la Faujasite imprégnée de fer. La notation "Initial" indique la concentration initiale en micropolluants avant l'adsorption, tandis que "2h dark" correspond à la concentration en micropolluant restante en solution à la fin des deux heures de contact entre l'eau et le catalyseur dans le noir et en absence de H_2O_2 . La légende spécifique "under limit" indique que la concentration devient plus faible que la limite de quantification du LC-MS/MS. Les lignes pointillées donnent également la limite de quantification du LC-MS/MS. Conditions expérimentales: catalyseur = 1 g/L, et pH 5,5.

Le résultat majeur de cette étude est la très bonne efficacité de dégradation photo-Fenton des micropolluants avec nos Faujasite modifiées. Pour la grande majorité des micropolluants (à l'exception du sulfamethoxazole et du PFOA), la concentration de tous les autres micropolluants (bisphenol A, carbamazépine, carbamazépine-10,11-époxyde, clarithromycine, diclofenac, estrone, ibuprofène, kétoprofène, lidocaïne, naproxène, PFOS, triclosan) devient plus faible que la limite de quantification de notre appareil analytique (LC-MS/MS) après 30 minutes ou 6 heures de traitement (Fig. 6 et 7). Cependant, la dégradation du PFOA demeure négligeable. Un autre résultat intéressant est que la dégradation du sulfaméthoxazole suit une cinétique de dégradation du premier ordre en présence du cocktail de micropolluants (Fig. 8b).

Nous avons également pu montrer l'absence de dégradation en absence de catalyseur mais en présence de lumière UV et de peroxyde d'hydrogène pour la grande majorité des polluants. Cependant, la dégradation par photolyse de la kétoprofène a été observée. La comparaison de la dégradation des micropolluants en présence et en absence de lumière, i.e. photo-Fenton vs. Fenton conduit à des efficacités de dégradation assez proche même si le rendement reste supérieur en présence de lumière UV (Fig. 8a).

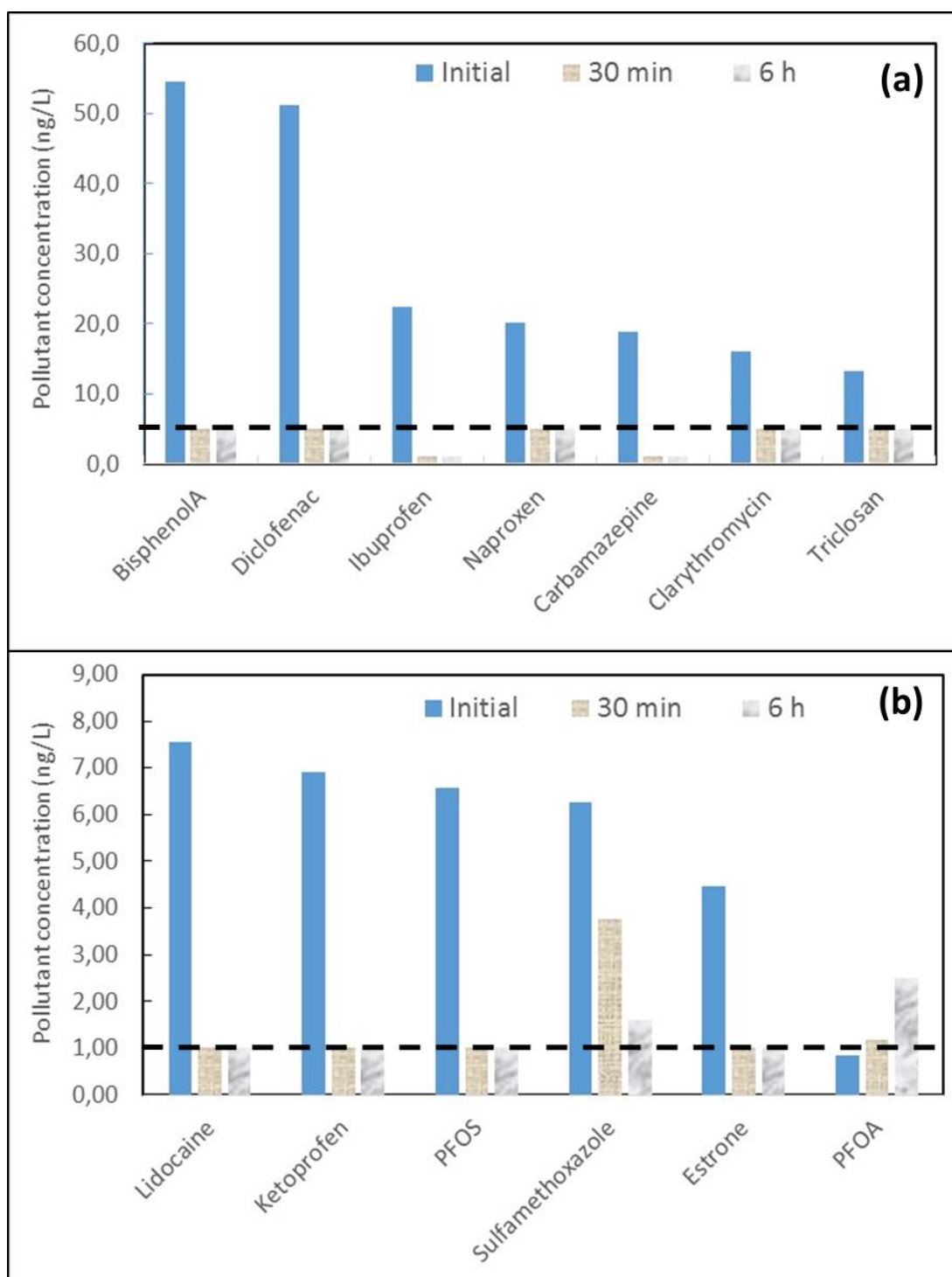


Fig. 6. Photo-Fenton traitement de l'eau en présence de Fe/Faujasite. L'eau a été prélevée en mars 2017. La notation "Initial" indique la concentration initiale en micropolluants avant l'adsorption, tandis que les notations "30 min" et "6 h" correspondent aux concentrations en micropolluant restantes dans l'eau après 30 min et 6 heures de procédé photo-Fenton. Les lignes pointillées donnent la limite de quantification du LC-MS/MS. Conditions expérimentales: catalyseur = 1 g/L, 0,007 M H_2O_2 , irradiation UV, et pH 5,5.

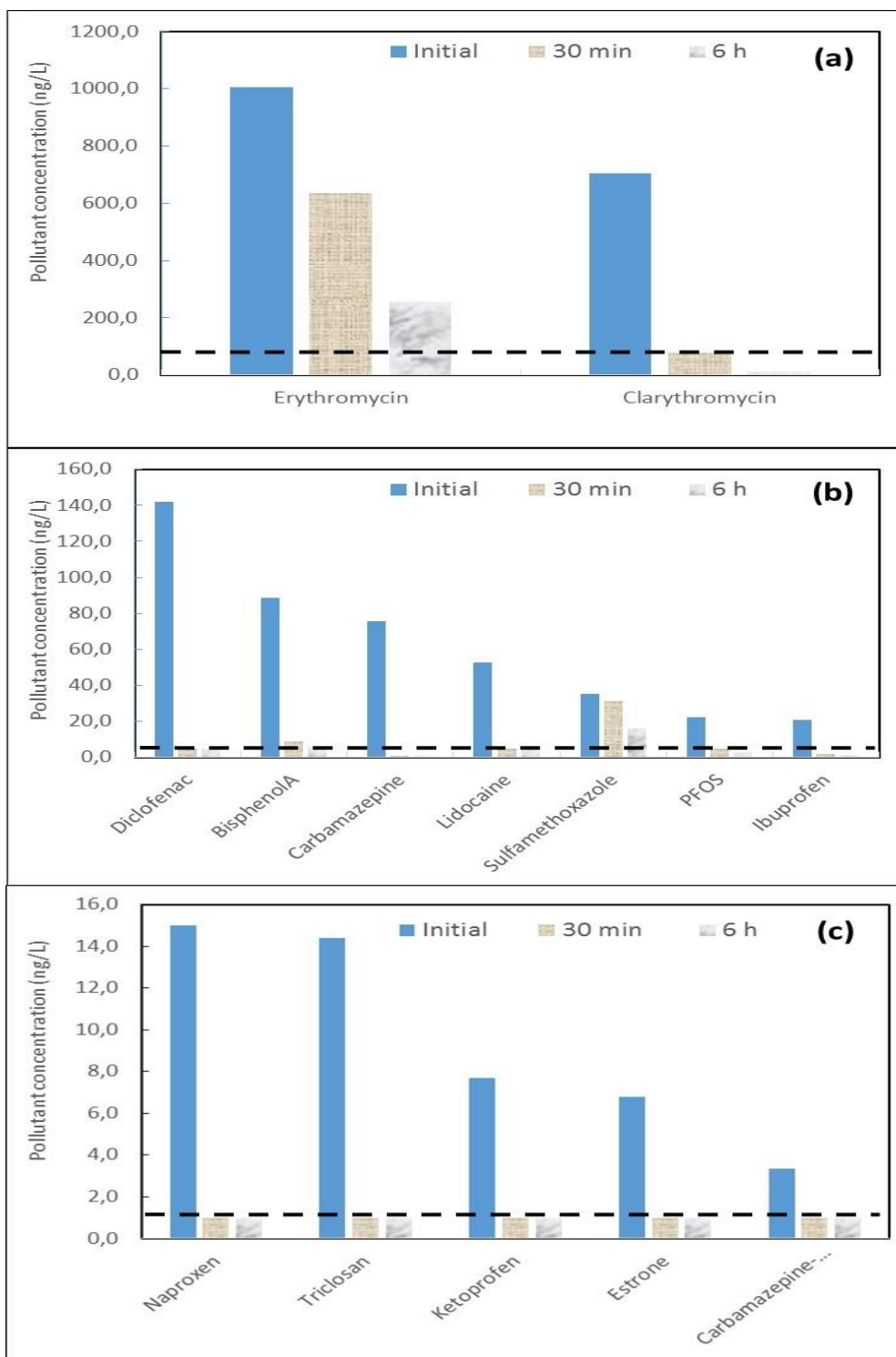


Fig. 7. Photo-Fenton traitement de l'eau en présence de Fe/Faujasite. L'eau a été prélevée en Octobre 2016. La notation "Initial" indique la concentration initiale en micropolluants avant l'adsorption, tandis que les notations "30 min" et "6 h" correspondent aux concentrations en micropolluant restantes dans l'eau après 30 min et 6 heures de procédé photo-Fenton. Les lignes pointillées donnent la limite de quantification du LC-MS/MS. Conditions expérimentales: catalyseur = 1 g/L, 0,007 M H_2O_2 , irradiation UV, et pH 5,5.

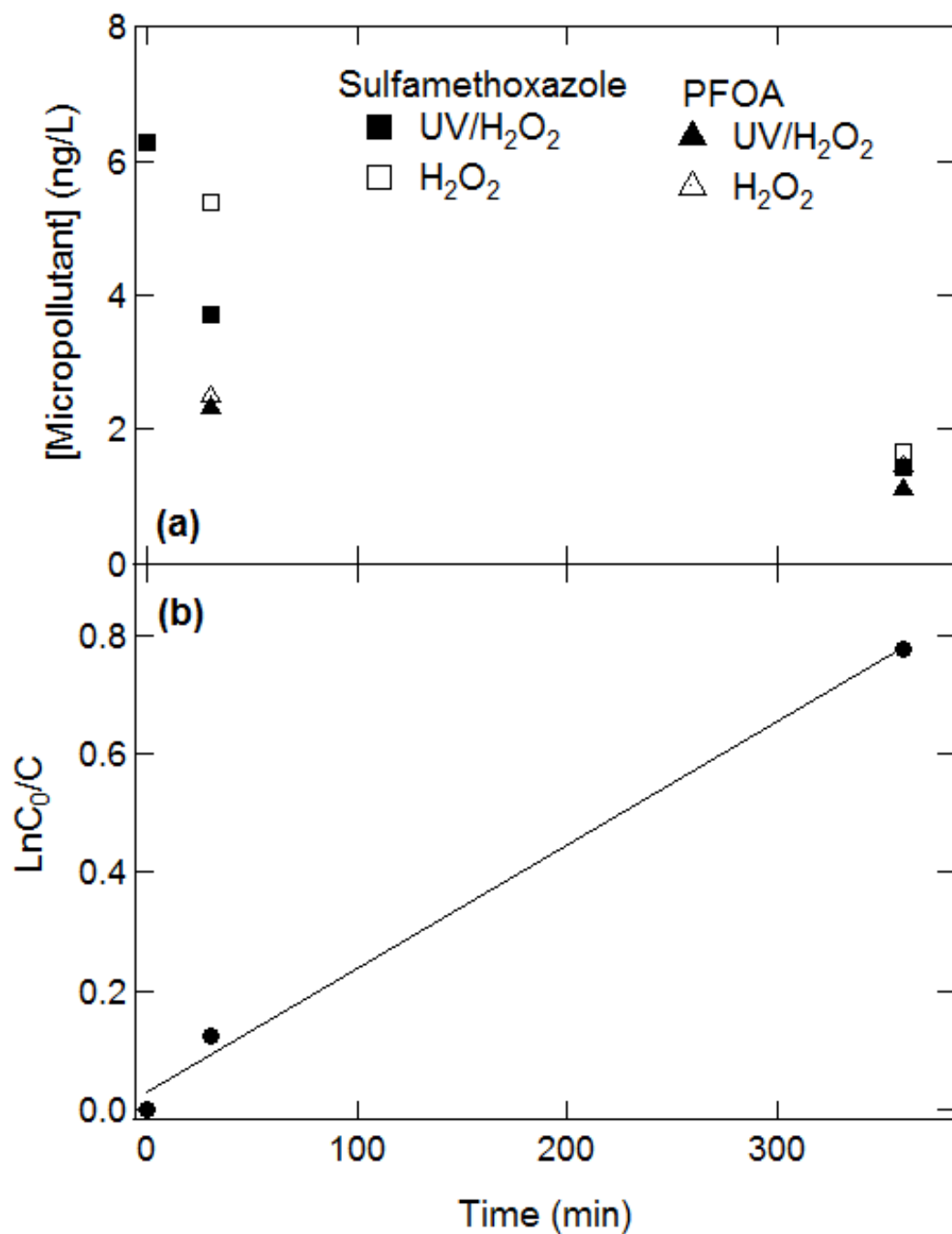


Fig. 8. (a) Effet de l'illumination sur les performances du procédé. Le procédé photo-Fenton ("UV/H₂O₂") est comparé au procédé Fenton en absence de lumière ("H₂O₂") pour deux micropolluants sulfamethoxazole et PFOA. (b) Cinétique de dégradation photo-Fenton du sulfamethoxazole. La ligne représente la linéarisation donnée par $\ln(C_0/C) = 0.0021 \text{ Time} + 0.029$ ($R^2 = 0.9947$). Conditions expérimentales: catalyseur = 1 g/L, 0,007 M H₂O₂, et pH 5,5.

Il nous a paru fondamental de comparer les propriétés de dégradation de ces micropolluants par nos catalyseurs via le procédé photo-Fenton à d'autres procédés d'oxydation avancés et catalyseurs. Nous avons donc comparé nos résultats à ceux obtenus par le procédé de photocatalyse hétérogène. Le procédé de photocatalyse repose sur l'action simultanée de photons et d'une couche de catalyseur (Fig. 9). Le catalyseur le plus utilisé est le dioxyde de titane (TiO_2) pour des raisons d'efficacité, stabilité et de faible coût de production. L'activité photocatalytique de TiO_2 est basée sur la génération de paires électron-trou à la surface du matériau sous rayonnement ultraviolet. La forme anatase présentant une bande interdite (gap) de 3,23 eV (384 nm) qui correspond au domaine ultraviolet est photoactive. Un photon d'énergie supérieure ou égale au gap pourra être absorbé par celui-ci. Les électrons de la bande de valence sont alors excités et promus dans la bande de conduction. Il en résulte la création de porteurs de charges sous forme de photoélectrons e^- et de trous électroniques h^+ . Ces paires électron-trou peuvent alors migrer vers la surface du matériau pour former des sites oxydants et réducteurs. Des réactions d'oxydoréduction peuvent avoir lieu avec des groupements accepteurs ou donneurs adsorbés en surface. Le fort pouvoir oxydant des trous h^+ peut entraîner la formation de radicaux hydroxyles $\cdot\text{OH}$ ou $\text{R}\cdot$ très réactifs, via l'oxydation de l'eau, des groupements OH superficiels ou encore de produits organiques R adsorbés à la surface. Ces radicaux sont des oxydants très puissants qui peuvent à leur tour réagir avec les polluants adsorbés à la surface du matériau.

Nous avons donc effectué les mêmes mesures de dégradation par le procédé de photocatalyse hétérogène en utilisant un photocatalyseur à base de TiO_2 de type P25.

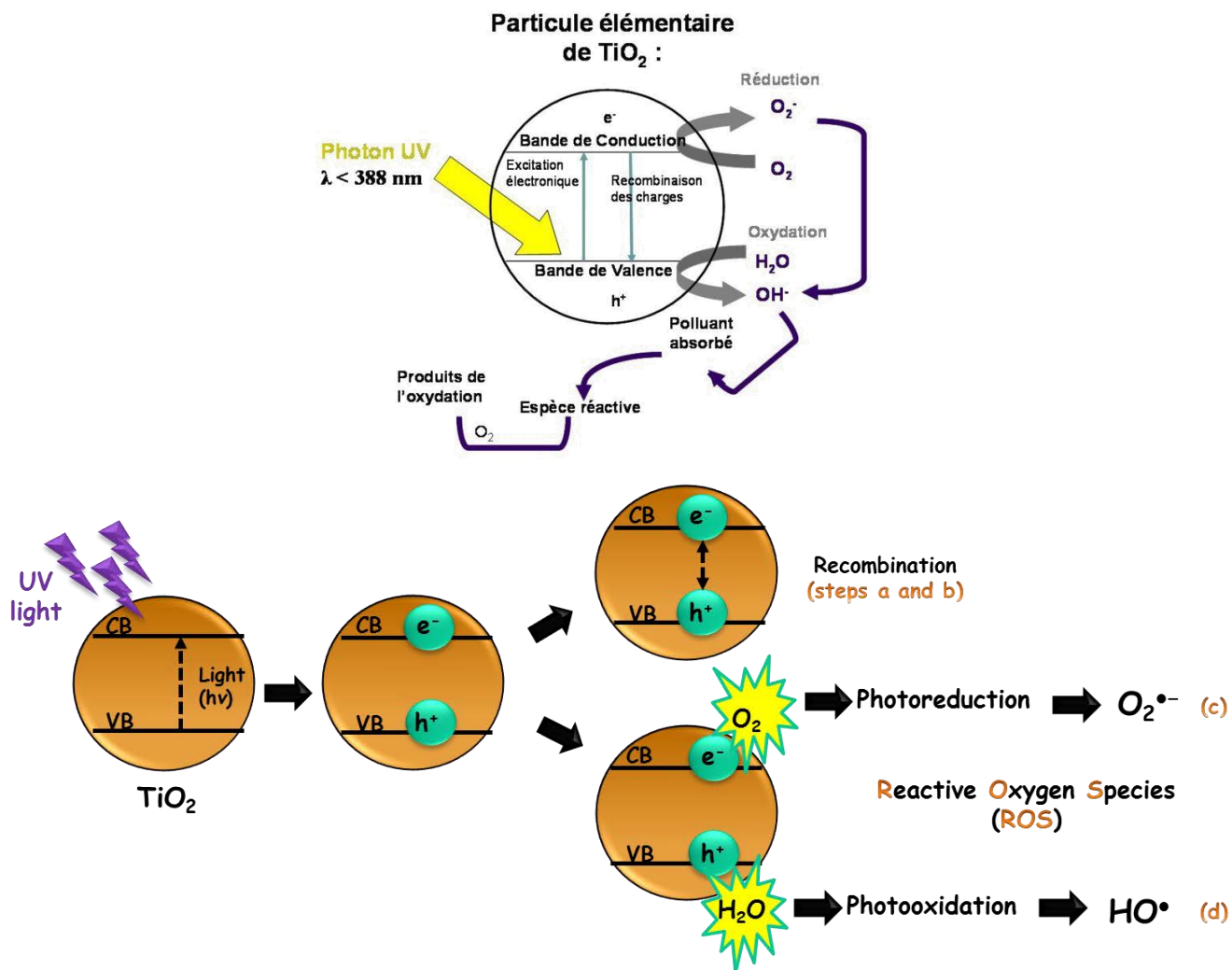


Fig. 9. Schéma général de la photocatalyse avec TiO₂.

L'adsorption des micropolluants sur le TiO₂ a été étudiée. La capacité d'adsorption des micropolluants sur le TiO₂ reste assez faible. En effet, parmi les 21 polluants testés, seuls la carbamazepine-10,11-époxyde et le naproxène présentent une concentration résiduelle inférieure à la limite de quantification du LC/MS-MS après 2 heures d'adsorption. Afin d'évaluer plus en détail l'impact de la nature et de la concentration initiale en micropolluant sur l'adsorption, nous avons

reporté la quantité de micropolluants adsorbés sur le TiO₂ ($\Gamma = \frac{(C_0 - C(2\text{heures})) \times V}{m_{\text{TiO}_2}}$) en fonction

de la concentration initiale en micropolluant sur la Fig. 10. Pour tous les micropolluants, la quantité adsorbée augmente avec la concentration en contaminant. On peut noter le faible impact de la nature du micropolluant sur la quantité adsorbée.

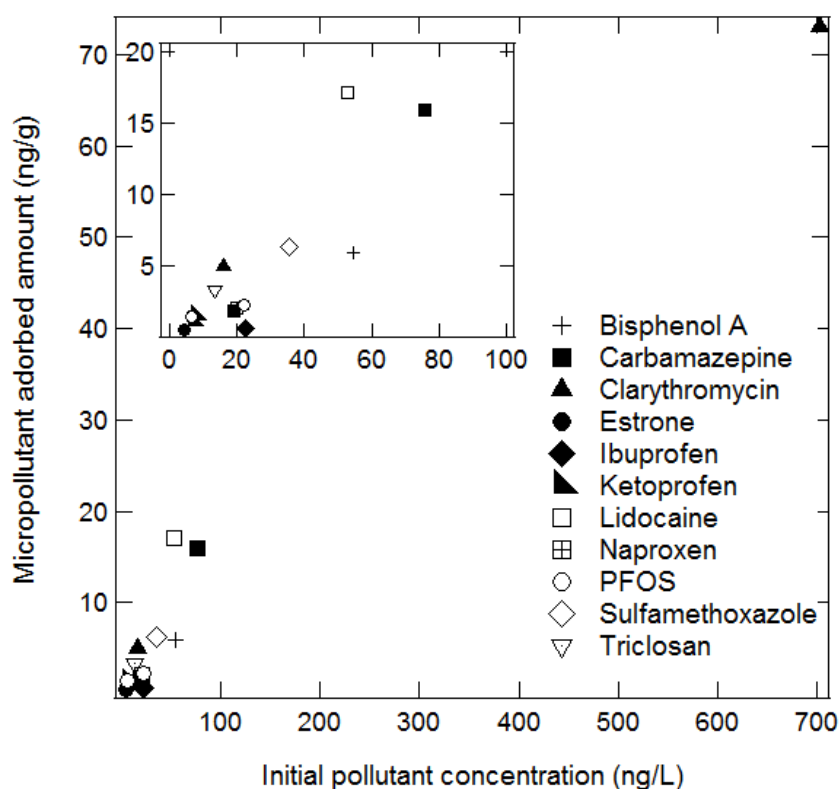


Fig. 10. Adsorption des micropollutant sur le dioxyde de titane en fonction de la concentration initiale en micropollutant.

L'activité photocatalytique a également été évaluée en étudiant la dégradation des 21 micropolluants. Les expériences ont été conduites sous illumination UV (Figures 11 et 12). Pour tous les micropolluants, la concentration de chacun des micropolluants diminue avec la durée d'irradiation ce qui confirme l'activité photocatalytique de dégradation du cocktail des 21 micropolluants. Après 6 heures d'irradiation, la concentration de la grande majorité des micropolluants devient plus faible que la limite de détection du LC/MS-MS (diclofenac, carbamazepine, lidocaine, sulfamethoxazole, estrone, ketoprofen, naproxen, clarithromycin, and triclosan). Cependant, pour les deux prélèvements, l'ibuprofen, le PFOA et le PFOS restent présents dans l'eau à la fin du procédé tandis que la présence d'erythromycin et de bisphenol A n'a été détectée que dans l'eau prélevée en octobre 2017. Cependant, les taux de dégradation X (

$$X = \left(\frac{C_0 - C(6\text{hours})}{C_0} \right) \times 100$$

sont de l'ordre de 95 % pour l'ibuprofen, 65% pour le bisphenol A, 56% pour le PFOS, et 18% pour erythromycin.

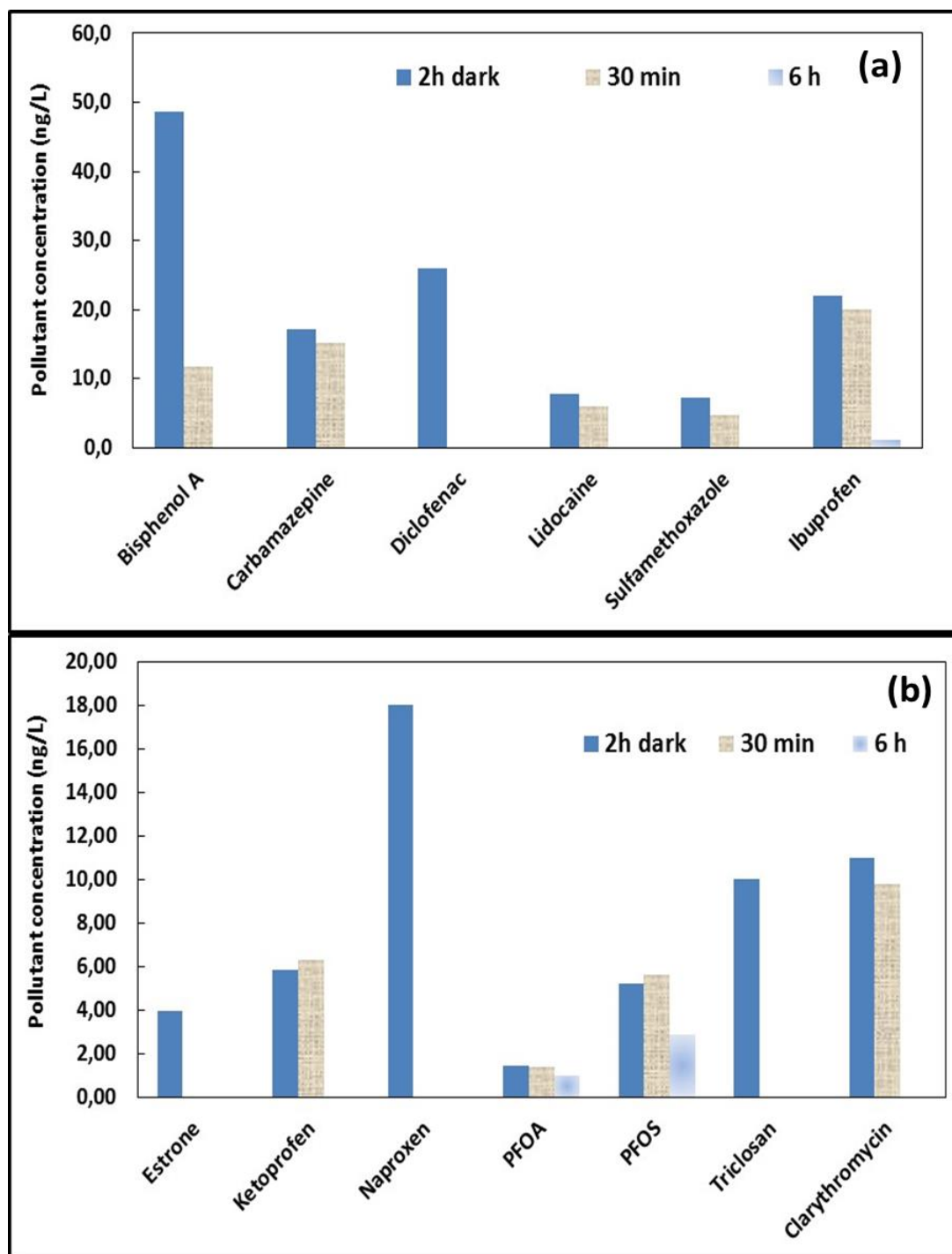


Fig. 11. Photocatalytique traitement de l'eau en présence de TiO_2 . L'eau a été prélevée en mars 2017. La notation "2h dark" correspond à la concentration en micropolluant restante en solution à la fin des deux heures de contact entre l'eau et le TiO_2 dans le noir, tandis que les notations "30 min" et "6 h" correspondent aux concentrations en micropolluant restantes dans l'eau après 30 min et 6 heures de procédé de photocatalyse. Conditions expérimentales: catalyseur = 1 g/L, et irradiation UV.

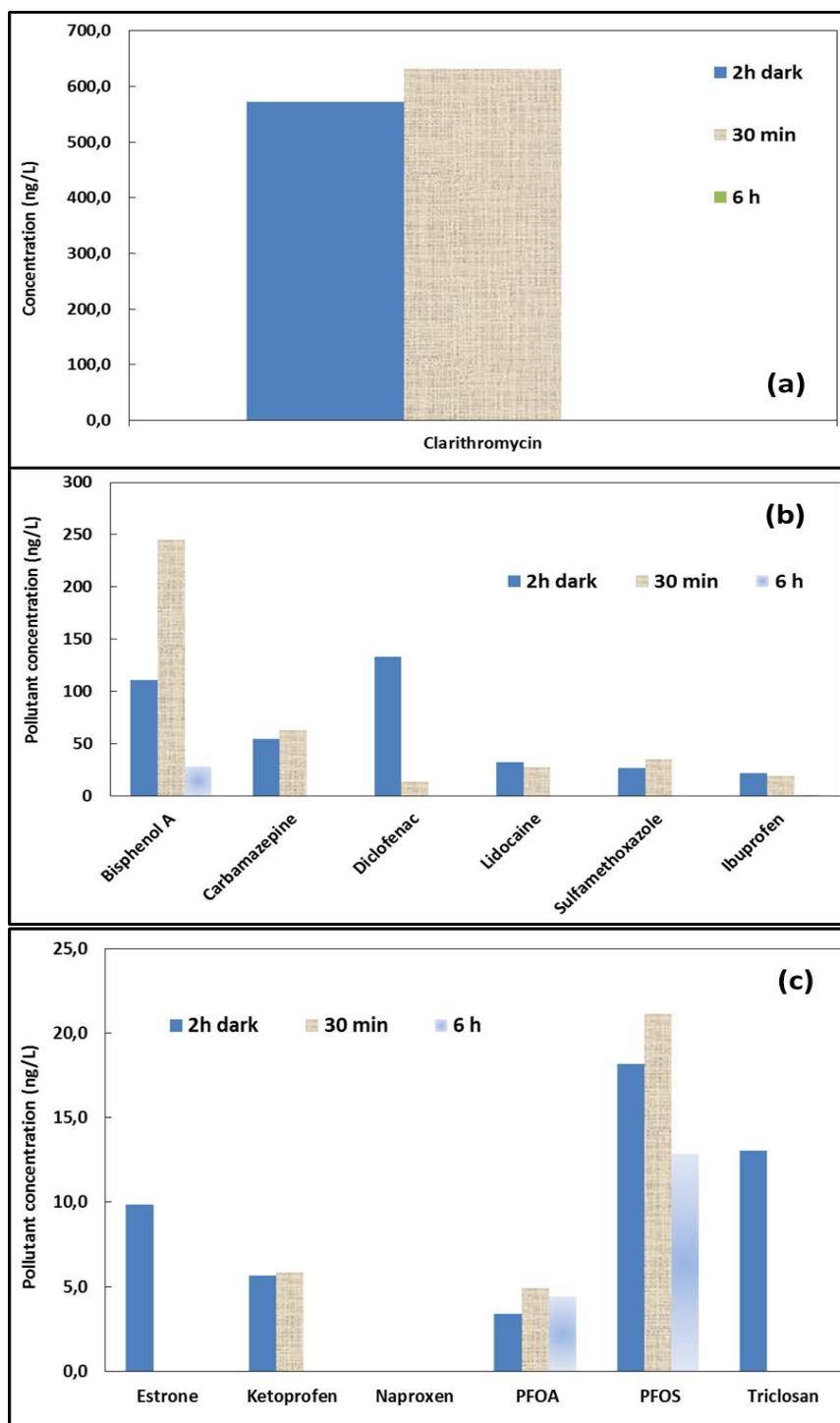


Fig. 12. Photocatalytique traitement de l'eau en présence de TiO_2 . L'eau a été prélevée en octobre 2016. La notation "2h dark" correspond à la concentration en micropolluant restante en solution à la fin des deux heures de contact entre l'eau et le TiO_2 dans le noir, tandis que les notations "30 min" et "6 h" correspondent aux concentrations en micropolluant restantes dans l'eau après 30 min et 6 heures de procédé de photocatalyse. Conditions expérimentales: catalyseur = 1 g/L, et irradiation UV.

Nous avons pu étudier la cinétique de dégradation photocatalytique. Cependant, il apparaît que la cinétique de dégradation est affectée par la nature des micropolluants. Il nous a semblé intéressant de discuter la relation entre la vitesse de dégradation après 30 minutes de procédé photocatalytique avec la concentration initiale en micropolluant en tenant compte de la nature du micropolluant (Fig. 13). La vitesse de dégradation photocatalytique est donnée par

$$r = \frac{C_0 - C(30\text{minutes})}{t_i} \quad (10)$$

avec t_i fixé à 30 minutes, C_0 et $C(30\text{minutes})$ sont les concentrations en micropolluants initiales et après 30 minutes de traitement sous UV en présence de TiO_2 .

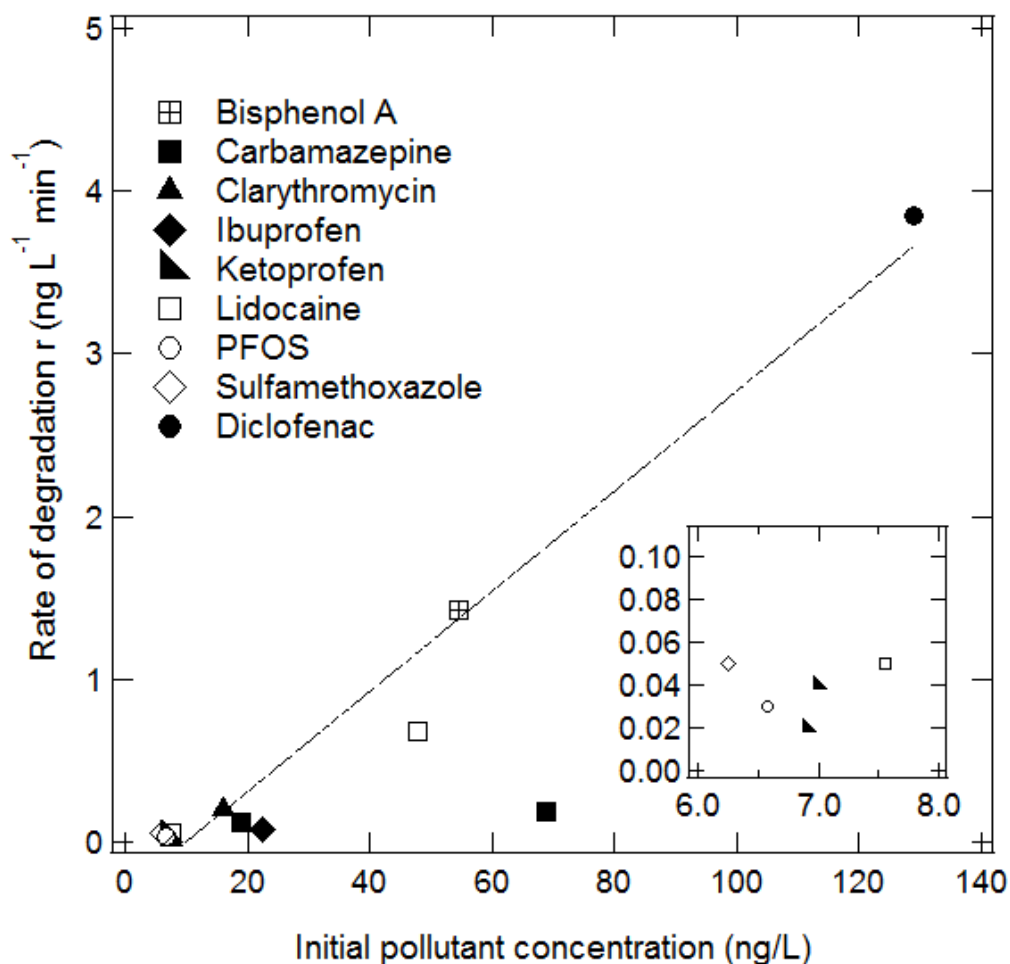


Fig. 13. Effet de la concentration initiale en micropolluant ($[\text{Micropollutant}]$) sur la vitesse de dégradation r . La ligne représente la régression linéaire donnée par $r = 0.0307 [\text{Micropollutant}] - 0.3045$ ($R^2 = 0.9645$).

La vitesse de dégradation dépend fortement de la concentration initiale en micropolluant. En utilisant l'ensemble des données, il apparaît qu'une relation linéaire peut-être extraite malgré une dispersion certaine des valeurs expérimentales autour de la droite. Un autre résultat intéressant est que la dégradation de l'ibuprofène suit une cinétique de dégradation du premier ordre en présence du cocktail de micropolluants.

Dans une dernière partie, il nous a paru fondamental de comparer les propriétés de dégradation de ces micropolluants par nos catalyseurs via le procédé photo-Fenton à ceux obtenus par le procédé de photocatalyse hétérogène en utilisant le photocatalyseur à base de TiO_2 de type P25. La comparaison des quantités de micropolluants adsorbés sur la faujasite modifiée (Fe/Faujasite) et les particules de TiO_2 sont reportées sur les Figures 14 et 15 pour les eaux prélevées en mars 2017 et octobre 2016, respectivement. L'adsorption de tous les micropolluants est plus élevée sur la zéolite que sur le dioxyde de titane. Ce résultat peut être expliqué à partir de la surface spécifique des deux solides. La surface spécifique de la Faujasite modifiée est beaucoup plus élevée ($640 \text{ m}^2 \text{ g}^{-1}$) que celle des particules de TiO_2 ($59 \text{ m}^2 \text{ g}^{-1}$). Nous avons également mis en évidence que la surface de Fe/Faujasite est plus polaire que celle du TiO_2 .

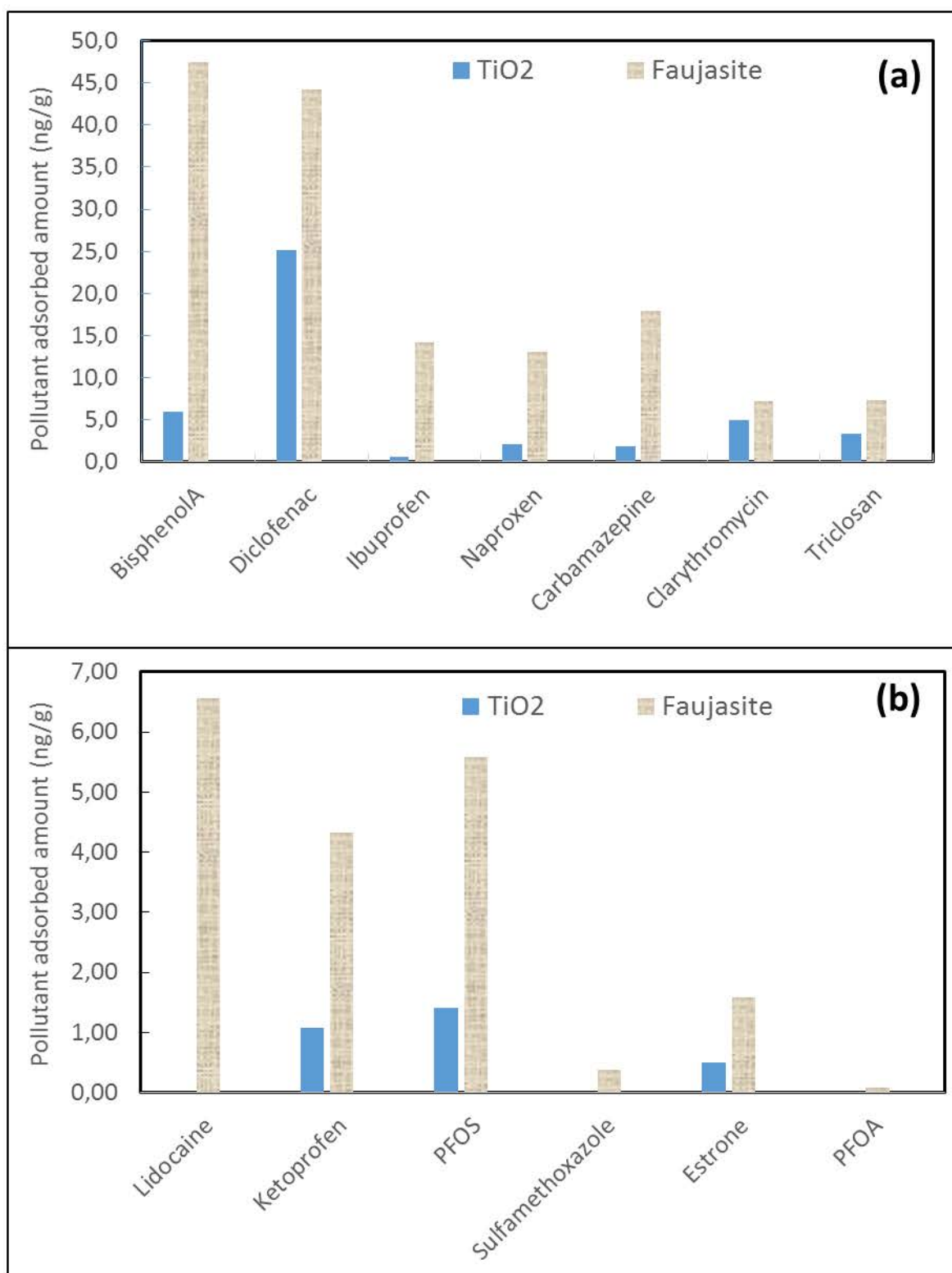


Fig. 14. Comparaison des quantités de micropollutants adsorbées sur le TiO₂ et la Faujasite modifiée.

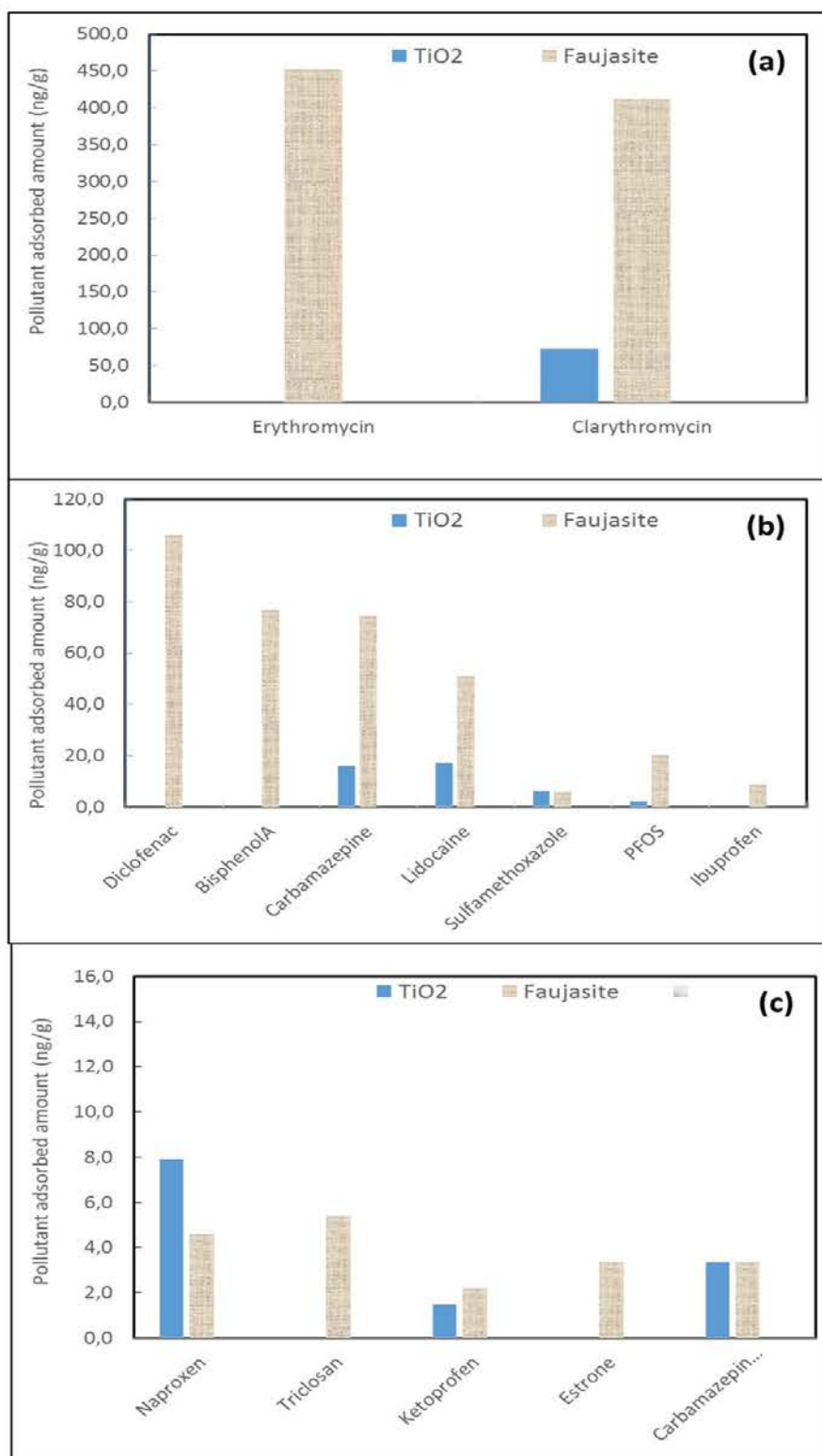


Fig. 15. Comparaison des quantités de micropollutants adsorbées sur le TiO₂ et la Faujasite modifiée.

Les deux catalyseurs, et surtout les deux procédés (photocatalyse et photo-Fenton), conduisent à des performances similaires. Après 6 heures de traitement par les 2 procédés, la majorité des micropolluants sont détruits. Pour être plus précis, les concentrations restantes en micropolluant sont plus faibles que la limite de détection du LC/MS-MS. De fait, on peut considérer que la carbamazépine, la carbamazépine-10,11-époxyde, la clarithromycine, le diclofénac, l'estrone, la kétoprofène, la lidocaïne, le naproxène, et le triclosan sont totalement éliminés par les deux procédés. A la fin du procédé, seul le PFOA, PFOS, l'ibuprofène, le bisphénol A, et l'érythromycine sont encore présents en solution. La concentration restante est plus élevée après le procédé de photocatalyse qu'après le traitement photo-Fenton. Afin d'être plus quantitatif, il apparaît pertinent de discuter les résultats en terme de taux de dégradation X après 6h de procédé. La Fig. 16 compare les taux de dégradations obtenus avec le TiO_2 et la Fe/Faujasite. Les nanoparticules de Faujasite modifiées (photo-Fenton) possèdent une activité de dégradation des micropolluants supérieure à celle du TiO_2 sous lumières UV.

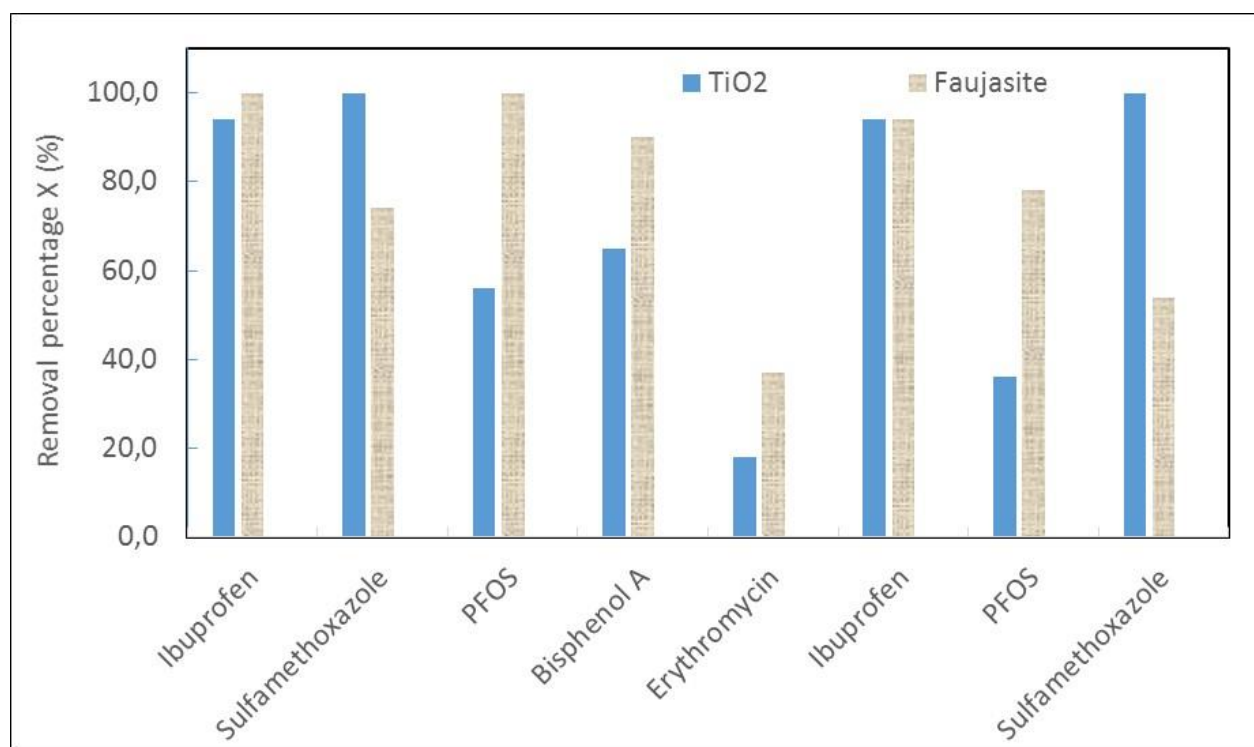


Fig. 16. Comparaison du taux de dégradation X (après 6 h de procédé) par photocatalyse (TiO_2) et par photo-Fenton (Fe/faujasite).

Afin d'analyser les cinétiques de dégradation, il semble intéressant de discuter le temps nécessaire pour totalement dégrader chacun des micropolluants par les deux procédés. Le Tableau 1 donne les temps caractéristiques de dégradation obtenus par photocatalyse et photo-Fenton hétérogène. Pour la majorité des micropolluants, les micropolluants sont totalement dégradés après 30 minutes de procédés photo-Fenton tandis qu'il faut 6 heures par le procédé de photocatalyse hétérogène.

La plus rapide dégradation en présence de Fe/faujasite provient de deux causes : (i) la plus grande quantité de micropolluants adsorbées sur la faujasite, et (ii) la plus grande quantité de radicaux produits par le procédé photo-Fenton. Le procédé photo-Fenton permet de produire une plus forte quantité de radicaux hydroxyles (OH°) que par photocatalyse. La formation supplémentaire de radicaux OH° à travers la réaction Fenton provient de la présence de peroxyde d'hydrogène (Equations (1)-(6)).

Tableau 1. Comparaison du temps nécessaire pour totalement dégrader chacun des micropolluants par photocatalyse (TiO_2) et par photo-Fenton (Fe/faujasite).

Temps	Mars 2017 TiO_2	Mars 2017 Faujasite	Octobre 2016 TiO_2	Octobre 2016 Faujasite
Bisphenol A	6 h	30 min	-	-
Carbamazepine	6 h	30 min	6 h	30 min
Carbamazepine-10,11-epoxide	-	-	30 min	30 min
Clarithromycin	6 h	30 min	6 h	6 h
Diclofenac	30 min	30 min	6 h	30 min
Estrone	30 min	30 min	30 min	30 min
Ibuprofen	-	30 min	-	-
Ketoprofen	6 h	30 min	6 h	30 min
Lidocaine	6 h	30 min	6 h	30 min
Naproxen	30 min	30 min	30 min	6 h
PFOS	-	30 min	-	-
Sulfamethoxazole	6 h	-	6 h	-
Triclosan	30 min	30 min	30 min	30 min

Chapter I

Bibliograpghy

In this chapter, we will present the previous work performed on the emerging contaminants and their removal. We will discuss more particularly four types of micropollutants (pharmaceuticals, personal care products, endocrine disruptors, perfluorinated compounds) and two advanced oxidation processes (Fenton processes and photocatalysis). The aim of this chapter is to give the basis of the AOP processes and the analytical methodology which will be used in the following chapters.

1 Water pollution

The rapid increase in human population, rapid development of technological advancement, poor agricultural practices, inadequate wastewater treatment facilities and drought caused by global climate change increased the water pollution to a level that have not been seen before (Tijani et al. 2013). It is considered as one of the global environmental challenges of the 21st century as a result of release of a wide variety of toxic substances. About 100,000 of synthetic organic chemicals over the past 30 years have been commercially used in the United States and European Union (EU) (Muir et al. 2006, Thomas A. Ternes 2010). These chemicals find their way into different water systems and natural water through different sources such as wastewater streams, agriculture, chemical pills and other sources (Schwarzenbach et al. 2006). This made water unsafe for both human consumption and aquatic animals (Liu et al. 2009, Tijani et al. 2013). Also the use of renewable fresh water and ground water is accompanied by contamination with different organic and inorganic chemical compounds that are used in different applications in industry, health, agriculture and household purposes (Field et al. 2006). In addition to that, the viability of water reuse of treated municipal or industrial water effluents is being affected by contamination with different organic substances such as substituted phenols, pesticides and non-biodegradable chlorinated solvents that are difficult to be removed from water (Esplugas et al. 2007). All this had increased the demand for clean water resources and good quality potable water since water is crucial to all living organisms, used for multiple human activities and it is so difficult and even impossible to live without the availability of safe drinking water (Cortes Munoz et al. 2013, Barbosa et al. 2016a).

Beside the deep scientific investigations of various water contaminants such as microbial pollutants, heavy metals, nutrients and other pollutants, recent researchers reported the presence of a wide group of organic contaminants originating from diverse sources presenting in water in concentrations ranging from ng/L to pg/L (Rodriguez-Narvaez et al. 2017a) named as emerging micropollutants. They are termed emerging since they are only recently recognized as water pollutants with significant effect on water quality, living organisms and ecosystems. The emerging contaminants include pharmaceuticals and personal care products (PPCPs), persistent organic pollutants, pesticides and herbicides, disinfection by-products, endocrine-disrupting chemicals (EDCs), perflorinated compounds (PFCs), and other micro constituents. The number of these emerging micropollutants in different water systems and treated wastewater is expected to increase. In addition, real effects of such contaminants have been observed on humans and aquatic organisms such as endocrine disturbances in aquatic organisms, brain damage, carcinogenic diseases,

cardiovascular disease, liver damage, and lung defects beside disturbances in gene expression resulting in feminization of aquatic organisms (Diamanti-Kandarakis et al. 2009). However, these studies are still very limited with few of them discussing the identification of efficient and appropriate treatment, making the reuse of water contaminated with emerging micropollutants an ongoing challenge (Rodriguez-Narvaez et al. 2017a).

2 Occurrence of emerging micropollutants in water and their regulations

Micropollutants are non-regulated organic pollutants presenting at trace concentrations of ng/L to few µg/L, just recently introduced or newly detected due to advanced analytical technologies (Luo et al. 2014). They are still considered as emerging compounds since their regulations and limits have not yet been specifically made (Kosma et al. 2010, Tran et al. 2017a) or in process of regularization (Esplugas et al. 2007). Over the last few decades, the occurrence of micropollutants in the aquatic environment has become a worldwide issue of increasing environmental concern (Luo et al. 2014). They took a great attention over drinking water safety (Yang et al. 2017) due to their ability to induce undesirable effect on human health and ecosystem (Jelic et al. 2011).

Emerging micropollutants include a wide variety of natural occurring substances and anthropogenic compounds (Luo et al. 2014) coming from different anthropogenic activities such as industrial discharges, discharges of treated effluents from wastewater treatment plants (WWTPs) (Al Aukidy et al. 2012), sewer leaking (Wolf et al. 2012), sewer overflow and surface runoff (Pedersen et al. 2005). Emerging contaminants include pharmaceuticals and personal care products, endocrine disrupting chemicals (EDCs), steroid hormones, pesticides, industrial chemicals, perfluorinated compounds and many other emerging substances (Luo et al. 2014, Tran et al. 2017a). Both their low concentration and variety create a need for not only develop the detection and quantification techniques but also find the efficient water and wastewater treatment processes (Luo et al. 2014). The occurrence of emerging micropollutants in the aquatic environment has taken an increasing concern reflected in being studied in thousands of publications during the last decades and discussed by many authors (Barbosa et al. 2016a). Until 2011 (Bell et al. 2011), several review papers were published annually since 2007 focusing on the occurrence, fate, transport and treatment of micropollutants. Since 2012 (da Silva et al. 2013), the treatment of micropollutants was discussed separately from the other topics due to the big challenges given for the removal of micropollutants in water and wastewater effluents (Luo et al. 2014, Barbosa et al. 2016a). This is due to the fact that the current conventional wastewater treatment plants (WWTPs) are not efficiently and specifically

designed to eliminate micropollutants. In addition, monitoring rules and precautions for micropollutants have not been well specified in most WWTPs (Luo et al. 2014). Therefore, these compounds persist in the treatment effluents and find their way into different water bodies such as surface water, river water (Luo et al. 2014), ground water (Lapworth et al. 2012), wastewater (Deblonde et al. 2011). Consequently, their occurrence in the aquatic environment causes real threats to wildlife (Luo et al. 2014) reflected in a number of negative effects such as effects on the hormonal control of development in aquatic organisms (Esplugas et al. 2007), short-term and long-term toxicity, disruption of endocrine systems (Esplugas et al. 2007) and antibiotic resistance of microorganisms (Pruden et al. 2006). Moreover, the detection of micropollutants in finished drinking water induces a real trouble for drinking water industry and is considered as another public health concern (Rivera-Utrilla et al. 2013a, Luo et al. 2014). This is due to the fact that little information is known about the effect of long term ingestion of drinking water containing a mixture of the micropollutants (Rivera-Utrilla et al. 2013a). Until now, there are no standards and legal discharge guidelines limits are not yet being done for most micropollutants (Luo et al. 2014). However, regulations have been published for a small group of micropollutants in some countries (Barbosa et al. 2016a). The Directive 2000/60/EC was the first mark in the European water policy, that put a strategy to specify the high risk substances to be prioritized (Directive 2000). In the Directive 2008/105/EC, 33 priority substances/groups of substances (PSs) and the respective environmental quality standards (EQS) were stipulated (Directive 2008) such as that of nonylphenol, diuron, bisphenol A, and DEHP (Luo et al. 2014). At the same time, nonylphenol have also been classified as toxic compound by the Canadian government (Canadian Environmental Protection Act 1999). In 2013, the monetarization and treatment processes for a group of 45 pharmaceuticals were studied in the European Union Directive 2013/39/EU (Directive, 2013) (Barbosa et al. 2016a) for the protection of human health and aquatic environment. In 2015, a first watch list of 10 substances/group of substances for European Union-wide monitoring was created in the Decision 2015/495/EU of 20 March 2015. This watch list included the 2 pharmaceuticals: non-steroid anti-inflammatory diclofenac and the synthetic hormone 17-alpha-ethinylestradiol-EE2, a natural hormone 17-beta-estradiol-E2 and Estrone-E1, three macrolide antibiotics: azithromycin, clarithromycin and erythromycin, pesticides, a UV filter and an antioxidant commonly used as food additive, listed in Table 1 (Barbosa et al. 2016a).

Due to the frequent occurrence of different groups of micropollutants in the aquatic environment and the inefficiency of the conventional WWTPs to remove these pollutants, regulatory agencies as European Commission and scientific community is working on covering a larger groups

of toxic micropollutants, not only to set their regulatory limits and study the impact on individual, but also their additive, antagonistic effects and new treatment processes (Luo et al. 2014, Barbosa et al. 2016a).

Table 1. The first watch list of the 10 compound created in the Decision 2015/495/EU.

Name of substance/group of substances	Substance	Concentration (ng/L)/ Matrix/ Location
17-Alphaethinylestradiol (EE2)	17-Alphaethinylestradiol (EE2)	<1-8/ WW/ Korea (n = 120), Germany (n.a.), South Africa (n = 12) 0.2-1.9/ SW/ China (n = 3), Korea (n = 120), Germany (n.a.), France (n = 73) 0.5-230/ GW/ France (n = 73), USA (n.a.)
Natural hormones	17-Beta-estradiol (E2)	<1-88/ WW/ China (n = 3), Korea (n = 120), Sweden (n = 3), UK (n.a.), Germany (n.a.) 0.2-10.1/ SW/ China (n = 3), Korea (n = 120), Germany (n.a.), Japan (n = 517), France (n = 71) 0.3-147/ GW/ France (n = 73), USA (n.a.)
	Estrone (E1)	WW/ China (n = 3), Korea (n = 120), Sweden (n = 3), UK (n.a.), Germany (n.a.) 0.5-69.1/ SW/ China (n = 3), Korea (n = 120), Germany (n.a.), France (n = 71) 0.7-79/ GW/ France (n = 73), USA (n.a.)
Diclofenac	Diclofenac	14.9-4425/ WW/ Spain (n.a.), Italy (n = 3), USA (n.a.), Portugal (n = 4) 0.8-1043/ SW/ Spain (n.a.), Vietnam (n.a.), Costa Rica (n = 86), Greece (n = 30) 1.17-380/ GW/ Spain (n = 30), France (n = 70)
2,6-di-tert-butyl-4-methylphenol	2,6-di-tert-butyl-4-Methylphenol	49-620/ SW/ USA (n = 19), Sweden (n.a.)
2-ethylhexyl-4-methoxycinnamate	2-ethylhexyl-4-methoxycinnamate	4.7-505/ WW/ China (n = 17), Norway (n = 5) 12-1040/ SW/ Japan (n = 23) 770/ GW/ Spain (n = 7)

Macrolide antibiotics	Azithromycin	0.4-1220/ WW/ Italy (n = 3), Slovakia (n = 3), USA (n.a.), Portugal (n = 4) 0.6-90.8/ SW/ Vietnam (n = 2), China (n = 24) 0.6-1620/ GW/ Spain (n.a), China (n = 69)
	Clarithromycin	54-1890/ WW/ Spain (n.a.), Italy (n = 3), Slovakia (n = 3), USA(n.a) 0.01-778/ SW/ Vietnam (n = 2), Spain (n = 18), China (n = 24) 0.2-20.5/ GW/ Spain (n.a.), China (n = 15)
	Erythromycin	16-147.9/ WW/ Spain (n.a.), Slovakia (n = 3), USA (n.a.), China(n = 3) 0.28-2246/ SW/ Vietnam (n = 2), Spain (n = 18) 4.8-154.3/ GW/ Spain (n = 121), China (n = 54)
Methiocarb		4.73-14.92/ WW/ Spain (n = 55)
Neonicotinoids	Imidacloprid	2-34.44/ WW/ Spain (n = 55) 1.1-105/ SW/ Spain (n = 24), USA (n = 35), Greece (n = 89), Portugal (n.a.), Australia (n = 13)
	Thiacloprid	20-400/ SW/ Australia (n = 13)
	Thiamethoxam	0-1580/ SW/ Brasil (n.a.), Vietnam (n = 11), Australia (n = 13)
	Clothianidin	20-420/ SW/ Australia (n = 13)
	Acetamiprid	20-380/ SW/ Australia (n = 13)
Oxadiazon		4-1440/ SW/ Canada (n = 8)
Triallate		n.a.

n.a. not available

WW: wastewater, SW: surface water, GW: ground water

3 Types and groups of micropollutants

Emerging micropollutants constitute a large number of chemical groups and grows continuously as new compounds are being classified as a part of ECs (Rodriguez-Narvaez et al. 2017a). Micropollutants include pharmaceuticals, personal care products, endocrine disrupting compounds (EDCs) including hormones having adverse effects on wildlife and human endocrine systems (Rodriguez-Narvaez et al. 2017a), perfluorinated compounds (Rodriguez-Narvaez et al. 2017a), pesticides and biocides, industrial compounds (Ribeiro et al. 2015a), surfactants (Luo et al. 2014), persistent organic pollutants as household chemicals, heavy metals and polycyclic aromatic hydrocarbons (Margot 2015). Richardson and Ternes (Rodriguez-Narvaez et al. 2017a) mentioned in their biannual review of ECS in water different compounds to the EC group such as sunscreens and UV filters, sucralose and other artificial sweeteners, flame retardants, nanomaterials, drinking water and swimming pool disinfection by-products, naphthenic acids, siloxanes and algal toxins. Recently, scientists are showing high importance to monitor ECs especially with the increase in the release of variety of other compounds classified as ECs having harmful effect on humans and wildlife even little agreement exists on the list of substances that should be monitored (Rodriguez-Narvaez et al. 2017a). Pharmaceuticals, endocrine disrupting chemicals and perfluorinated compounds, 3 main groups of emerging contaminants, are studied in our work and described below.

3.1 Pharmaceuticals

Pharmaceuticals are considered as a large and important group of emerging micropollutants (Rodriguez-Narvaez et al. 2017a) because they are still unregulated or in the process of regulation (Rivera-Utrilla et al. 2013a). They include synthetic chemicals and drugs that are largely used by humans and animals (Maletz et al. 2013) and continuously introduced into the environment (Esplugas et al. 2007). Even though they have been present in water for decades, they have been recently quantified and studied as harmful to wildlife (Rivera-Utrilla et al. 2013a). They have received increasing attention among scientists and researchers in different developed countries such as European Union, USA and China since the early 1990s (Tijani et al. 2013a). Actually their presence in water systems as ground water, surface water and wastewater generated several harmful effects on humans, aquatic life (Rodriguez-Narvaez et al. 2017a) and water quality reflected its impact directly on drinking water (Esplugas et al. 2007, Rivera-Utrilla et al. 2013a). This group of ECs includes about 3000 different compounds such as anti-inflammatory drugs, antibiotics, antidiabetics, painkillers, beta blockers, antiseptics, contraceptives, antidepressants, lipid regulators,

anti-epileptic, antimicrobials and impotence drugs (Rodriguez-Narvaez et al. 2017a) (Tijani et al. 2013a). Table 2 shows some of the pharmaceutical compounds of our study and their origin and usage (Potter et al. 1998, Esplugas et al. 2007, Grassi et al. 2013b, Tijani et al. 2013). Pharmaceuticals are largely consumed which increase their detection in different water bodies (Rodriguez-Narvaez et al. 2017a). For example, in Western Europe, more than 300 mg of active ingredients are daily consumed per inhabitant (Margot 2015).

Table 2. List of the studied pharmaceuticals and their origin and usage.

Pharmaceutical group	Compounds	Origin/Use
Non-steroidal anti-inflammatories (NSAIDs)	Diclofenac, ibuprofen, ketoprofen, naproxen, phenazone, indomethacine	NSAIDs are the most used and abused drugs in the world today. All NSAIDs have analgesic, antipyretic and anti-inflammatory effect
Antibiotics/antimicrobials	Sulfonamides, sulfadimethoxine, erythromycin, sulfamethoxazole, sulfathiazole, clarithromycin	Antibiotics/antimicrobials are vital medicines for the treatment of bacterial infections in both humans and animals
Antiepileptic	Carbamazepine, carbamazepine-10,11-epoxide	Antiepileptics are commonly used in medicine to stop, prevent, or control seizures (convulsions, partial seizures, etc.)
Anesthetic	Lidocaine	This medication is used on the skin to stop itching and pain from certain skin conditions.

3.2 Endocrine disruptor chemicals

Endocrine disrupting chemicals were defined by the Organization of Economic and Cooperative Development (OECD) as exogenous substances that are able to modify the functions of the endocrine system causing several health problems in organisms (Esplugas et al. 2007). Endocrine system is responsible for controlling some of the body physiological activities such as embryonic development, metabolic development and sex differentiation (Tijani et al. 2013). EDCs affect these

activities, block the hormonal growth in the endocrine system (Schug et al. 2011), alter the metabolism of natural hormones and the hormones receptors in a cell (Olujimi et al. 2010). EDCs include more than 38,000 toxic compounds that were proven to have endocrine disrupting function (Esplugas et al. 2007, Tijani et al. 2013). Some are natural while others are synthetic (Tijani et al. 2013). Steroid hormones constitute a large group of the EDCs due to their main hormonal activity as mentioned before (Tijani et al. 2013a). They include estrogens that are the mostly abundant type in water systems (Barbosa et al. 2016a, 495). They can be natural as estrone (E1) and 17-estradiol (E2) or synthetic as ethinylestradiol (EE2). EDCs also include pesticides as vinclozolin and atrazine, alkyl-phenols as nonylphenol and octylphenol, organohalogens as dioxins, plasticizers and heavy metals as lead and mercury (Esplugas et al. 2007). Table 3 shows the groups, compounds, origin and usage of EDCs which are studied in our work (Esplugas et al. 2007, Barbosa et al. 2016a).

Table 3. List of endocrine disruptor compounds studied and their origin and usage.

EDCs group	Compound	Origin/Usage
Bisphenols	Bisphenol A	Bisphenol A is used in the manufacture of rubber chemicals, flame retardants and polymers as epoxy resins.
Natural hormones	Estrone, 17-estradiol	Estrogens naturally and daily excreted in the human urine and animals.
Synthetic steroids	17-ethinylestradiol	Used for therapy during menopause, causes injurious effects to living organisms.

3.3 Perfluorinated compounds

Perfluorinated compounds (PFCs) are synthetic anthropogenic chemicals produced in large quantities since 1950s (Adeleye 2016). They are considered as one of the most detected emerging contaminants around the world at concentration of ng/L to mg/L in different water systems (Lai et al. 2016). They are characterized by a carbon chain in which the hydrogen atoms are substituted by fluorine atoms (Du et al. 2014). They have special amphiphilic properties gained from their unique structure that is made up of hydrophobic perfluorinated tail responsible for its hydrophobic property that is proportional to their carbon chain length and hydrophilic functional group head (Du et al. 2014) that could be neutral (e.g. perfluoroalkyl sulfonamides ($-\text{SO}_3\text{NH}_2$)), positively (quaternary

ammonium group) or negatively charged (e.g. sulfonates (-SO₃⁻) and carboxylates (-COO⁻)) (Adeleye 2016) as shown in Fig. 1.

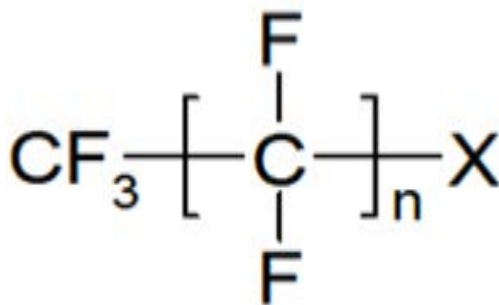


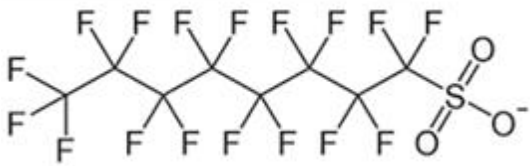

Fig. 1. General formula of perfluorinated compounds.

This unique amphiphilic structure makes them usable in a wide range of applications such as industrial surfactants, paper and fabric protection, household products for creating water or stain resistant surfaces, coatings and firefighting foams, photolithography (Du et al. 2014), some cosmetics, window cleaners and many other applications (Margot J. 2015). On the other hand, their hydrophilic functional groups which make them highly soluble in water (Adeleye 2016) and the high energy of the covalent bond between fluorine and carbon atoms (about 110 kcal/mol) (Du et al. 2014) make PFCs very persistent, highly chemically stable and non-degradable in the aquatic environment (Du et al. 2014, Margot 2015). They are also resistant to acids, UV light or photolysis, oxidation and reduction (even at high temperatures). It was confirmed in the recent studies the hazardous and harmful effect of PFCs to both animals and humans (Du et al. 2014).

PFCs include more than hundred organic compounds. They can be classified into 3 families: perfluoroalkyl sulphonates C_nF_{2n+1}SO₃H (PFASs), where one sulphonate group is attached to the perfluorinated carbon chain, perfluorocarboxylic acids C_nF_{2n}COOH (PFCA) having carboxylic acid chains in the perfluorinated compound, and fluorotelomers that are not fully fluorinated, having one remaining hydrocarbon group comprising of double carbon atoms (-CH₂CH₂-) (Margot 2015). Two of the PFCs which are mostly used, highly detected in the aquatic systems and greatly toxic are Perfluorooctanesulfonic acid (PFOS) belonging to PFAS family and perfluorooctanoic acid (PFOA) belonging to PFCA (Adeleye A.P. 2016). PFOS and PFOA are the mostly detected PFCs in raw municipal wastewaters, with average concentrations of about 5-50 ng/L in comparison to the total concentrations of the most common PFCs which is stated in the range of 30-150 ng/L (Margot 2015). Both compounds were added to the list of the Stockholm convention on persistent organic pollutants (POPs) and the relevant regulations in America, Canada and Germany (Du et al. 2014). PFOSs have a sulfonic acid functional group and a straight perfluoroalkyl 8-carbon chain (Adeleye 2016). It was

classified as primary hazardous substance in the EU because of its bioaccumulation ability and very high persistence in the environment. PFOA is being more studied due to its toxic properties and high persistence (Post et al. 2012). Although some developing countries have restricted the use of PFCs, they are still used in some fields as manufacturing, electroplating and electronic industries (Du et al. 2014). Table 4 reports some of the structural, physical and chemical properties of the 2 studied PFCs, namely PFOS and PFOA.

Table 4. Some of the physical and chemical properties of the studied PFCs (Adeleye A.P. 2016)

	PFOS	PFOA
Structure/Formula	 $\text{CF}_3(\text{CF}_2)_7\text{SO}_3^-$	 $\text{CF}_3(\text{CF}_2)_6\text{COOH}$
Molecular weight (g/mol)	538	414
Origin/Use	It is a degradation end product of many POSF, used in many commercial and industrial products	It is used mainly as a reactive intermediate, wetting agents, produce non-stick coating on cookware, employed in electronic manufacture
Solubility in pure water (g/L)	0.57	3.4
Melting point (M.p)/boiling point (B.p) in °C	M.p ≥ 400 B.p = 133	M.p = 45-50 B.p = 189
Vapour pressure	3.31×10^{-4} Pa at 200 °C	10 mm Hg
Log K_{ow}	4.30	3.60
pKa	-3.27	2.8

n.a. = not available

3.4 Personal care products (PCPs)

Personal care products (PCPs) include chemicals found in sunscreens, skin care products, cosmetics, perfumes, hair styling products, etc. The most studied PCPs are antiseptics/disinfectants, fragrances (polycyclic and nitro musks), UV filters, antimicrobial and preservatives (Margot 2015) (Rodriguez-Narvaez et al. 2017a). They are widely consumed and designed for external usage. For this reason, no metabolic changes occur in their chemical structure and they enter easily into the aquatic environment including ground water, municipal wastewater through wash-off during showering and urban runoff (Rodriguez-Narvaez et al. 2017a).

Triclosan is a synthetic antiseptic agent widely used to slow or stop the growth of microorganisms on the external surfaces of the body and help to prevent infections. It should be distinguished from disinfectants that destroy microorganisms on non-living objects, and antibiotics that destroy microorganisms inside the body (Esplugas et al. 2007). Triclosan is widely used in the United States since 1960s. It has been classified as one of the personal care products as antimicrobial agent and preservative. Streams, wastewater, seawater, sediments, fish are being contaminated with triclosan caused by the release of different triclosan-containing products. Scientific concerns regarding the widespread contamination of triclosan in the aquatic environment have emerged. These includes development of cross-resistance to antibiotics, production of more toxic chemicals, toxic effects on ecological health (Roh et al. 2009).

4 Source and fate of micropollutants

Micropollutants including PPCPs, EDCs and PFCs have been detected in different water bodies and wastewater effluents at low concentration levels, ranging from nanograms per liter to micrograms per liter (Esplugas et al. 2007, Grassi et al. 2013a). The diverse sources of micropollutants in the aquatic environment are listed in Table 5 (Luo et al. 2014).

Table 5. Sources of the studied groups of micropollutants.

Group	Subgroup	Major sources	
		Distinct	Common
Pharmaceuticals	NSAIDs, anticonvulsants, antibiotics, lipid regulator	Domestic wastewater from excretion Hospital effluents Run-off from agriculture and CAFOs	Industrial wastewater from product manufacturing discharges Landfill leachate from improper disposal of used, improper or expired items.
Personal care products	Fragrances, insect repellents, disinfectants	Domestic wastewater from bathing, shaving, spraying, etc.	
Steroid hormones	Estrogens	Domestic wastewater from excretion Run-off from agriculture and CAFOs ^a	
Industrial chemicals	Plasticizers	Domestic wastewater by leaching out from the materials	

^aCAFOs : concentrated animal feeding operations

Originating from different sources, micropollutants find their way into surface water, ground water (Yu et al. 2007) and some of them are even detected in drinking water (Heberer 2002) as shown in Fig. 2

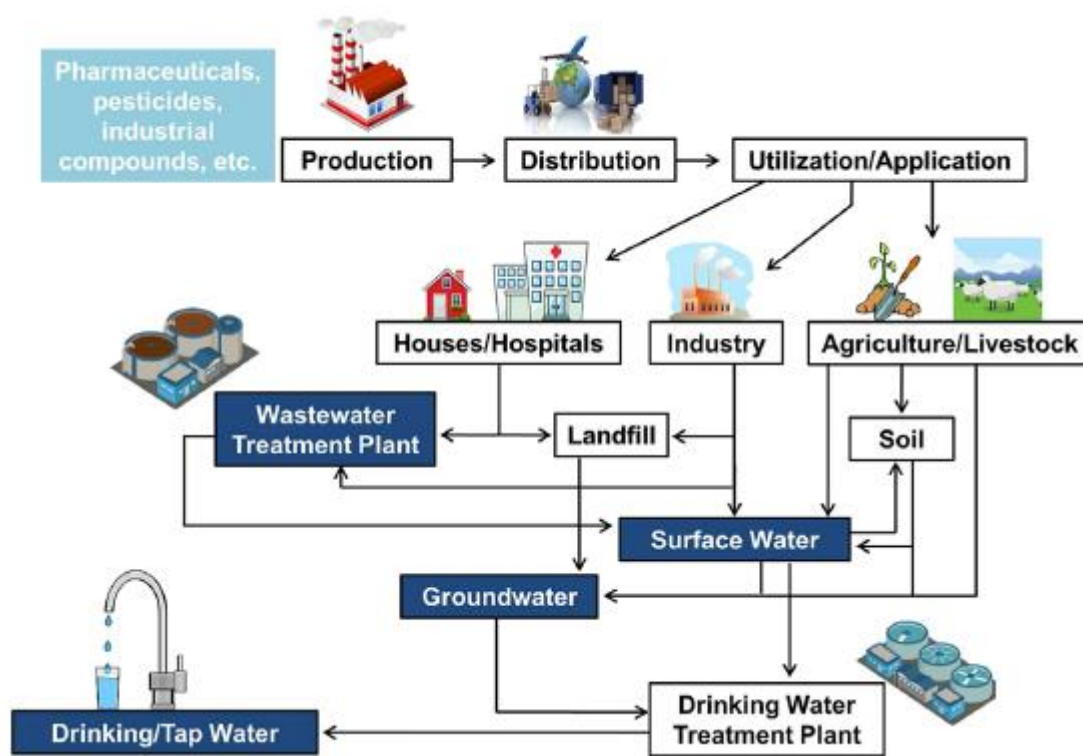


Fig. 2. Representative diagram for the different sources and fate of micropollutants in the aquatic environment (Barbosa et al. 2016a).

Starting from sewage sludge and soil, micropollutants including nonbiodegradable pharmaceuticals (Grassi et al. 2013a), fertilizers and pesticides (used for better productivity), steroid hormones and antibiotics (used for livestock) (Iglesias et al. 2014), run off from agriculture and livestock areas into surface water (Barbosa et al. 2016a). Such micropollutants can also pass by direct leaching into ground water which may contaminate the drinking water as well (Feng et al. 2013). Also the leakage of different micropollutants from landfills, industrial waste systems, septic and manure storage tanks find their way into surface water and ground water as well (Matthiessen et al. 2006). Moreover, the irrigation of the agricultural lands with treated wastewater leads to contamination of these fields by the receiving water that contains many emerging contaminants and their intermediates as well (Pedersen et al. 2003, Esplugas et al. 2007, Grassi et al. 2013a). Beside these sources, the main source for the presence of micropollutants including PPCPs, endocrine disruptors and PFCs into the aquatic systems is the wastewater treatment plants effluent disposal

(Tijani et al. 2013a, Adeleye 2016, Lai et al. 2016). The wastewater treated in such plants comes from different sources including domestic activities, industrial activities and hospitals disposal as shown in Fig. 3. The domestic activities are primarily related to the use of pharmaceuticals and personal care products by people (Grassi et al. 2013a). Literature data shows that more than 300 mg of pharmaceutical active ingredients are daily consumed per inhabitant in Western Europe (Ortiz de García et al. 2013), with the availability of about 3000 pharmaceutical compounds in Europe. These pharmaceuticals enter the sewage by showering, bathing, and washing (Margot 2015). The total average amount of pharmaceuticals entering the sewers is estimated to be around 70 mg/d.capita corresponding to 200-250 $\mu\text{g/L}$ (Ortiz de García et al. 2013). Depending on the consumption and excretion rate of pharmaceuticals, concentrations of individual pharmaceuticals in raw wastewater ranges from less than 1 ng/L to over 100 $\mu\text{g/L}$ including mainly ibuprofen, naproxen, diclofenac, sulfamethoxazole, carbamazepine and many other compounds (Margot 2015). Beside the domestic activities, industrial activities that discharge different kinds of PFCs, PCPs and other micropollutant compounds in addition to the hospital wastewater disposal that contain large amounts of pharmaceuticals and PFCs, are other sources of wastewater treated in the WWTP (Barbosa et al. 2016a, Lai et al. 2016). Reaching the WWTP, the removal of micropollutants is not complete, thus they persist in the effluents and released into receiving water systems (Esplugas et al. 2007).

Released from different sources into different water bodies, the presence of the different groups of micropollutants in water even at low concentration proved to have series negative impacts on aquatic life.

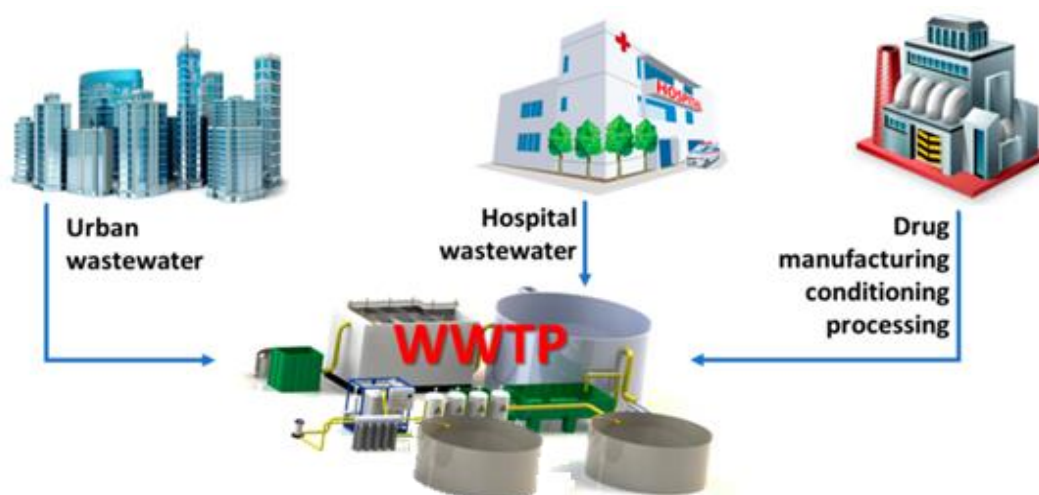


Fig. 3. Different sources of wastewater directed to the WWTPs for treatment.

5 Consequences and impacts

In the last few years, a great concern about the effects of the occurrence of micropollutants in different environmental compartments such as surface water, ground water, soil and drinking water on aquatic organisms and human's health has been highlighted (Daughton 2010). The inadvertent exposure of non-target organisms to these compounds can arise serious potential impacts (Santos et al. 2010). Due to the very low individual concentrations of micropollutants, it is difficult to predict their direct negative effects (Quinn et al. 2009). However, it was proven that their effect does not depend only on their concentrations in the environment. It depends also on many other factors such as exposition time, persistence, bioaccumulation and the mechanisms of eliminations and biotransformation (Esplugas et al. 2007). Thus, the potential effects of micropollutants require much more investigations and studies. For this reason, nowadays, many organizations, governmental and non-governmental, such as the World Health Organization (WHO), the European Union (EU), the International Program of Chemical Safety (IPCS), and the North American Environmental Protection Agency (EPA) are working on this problem by making directives and frameworks to have a clear idea about the effect of such micropollutants on aquatic organisms and humans. Table 6 lists some information concluded by these organizations, showing that these emerging micropollutants have a great potential to cause serious chronic effects (Esplugas et al. 2007). This was confirmed by several studies (Kidd et al. 2007) which reported that the simultaneous presence of micropollutants recalcitrant compounds as complex mixtures and their long term exposition (Barbosa et al. 2016a), lead to constant but imperceptible effects that can accumulate gradually resulting in irreversible effects on wildlife and human being as well (Jjemba 2006, Barbosa et al. 2016a).

Table 6. Information related to different policies about micropollutants.

Year	Organization	Title of project/document
1995	US EPA	Research needs for the risk assessment of health and environmental effects of endocrine disruptors: a report of the U.S.
1996	US EPA	Development of a research strategy for assessing the ecological risk of endocrine disruptors.
1997	US EPA	Special report on environmental endocrine disruption: an effects assessment and analysis.
1998	OECD	The second meeting of the OECD validation management group (VMG) for the screening and testing of endocrine disruptors.
1999	CSTEE	CSTEE opinion on human and wildlife health effects of endocrine disrupting chemicals, with emphasis on wildlife and ecotoxicology test method.
2001	EU	On the implementation of the community strategy for endocrine disruptors, a range of substances suspected of interfering with the hormone systems of human and wildlife.
2002	EU	Study on the scientific evaluation of 12 substances in the context of endocrine disrupter priority list of actions.
2002	OECD	Appraisal of test methods for sex hormone disrupting chemicals.
2002	WHO	Global assessment of the state of the science of endocrine disruptors.
2003	IEH	Information exchange and international co-ordination on endocrine disruptors.
2003	EU	ERAVMIS: environmental risk assessment of veterinary medicines in slurry.
2004	EU	POSEIDON: assessment of technologies for the removal of pharmaceuticals and personal care products in sewage and drinking water facilities to improve the indirect potable water reuse.
2004	EU	Commission staff working document: on implementation of the community strategy for endocrine disruptors-a range of substances suspected of interfering with the hormone system of humans and wildlife COM (1999).

Regarding pharmaceuticals and personal care products, toxicological studies have shown that they might have direct toxicity towards certain aquatic organisms (Crane et al. 2006), with chronic effect at small concentrations (from ng/L to µg/L) (Schwaiger et al. 2004) and acute effect at higher concentrations (typically milligrams per liter) (Rizzo et al. 2009a, Rizzo et al. 2009b). For example, the large use of antibiotics and antimicrobial agents can result in the development of antimicrobial resistance bacteria (ARB) (Esplugas et al. 2007, Santos et al. 2010, Rizzo et al. 2013) and antimicrobial resistance genes (ARG), which reduces the therapeutic potential against animal bacteria pathogens and humans (Tran et al. 2017a). PPCPs can also cause harmful effects to the

endocrine system. Moreover, several studies have showed that pharmaceuticals present in the treated wastewater, used for irrigation, reach the soil and may be taken by plants causing their direct damage. This is due to pharmaceuticals' uptake or antimicrobial action on soil microorganisms (Grassi et al. 2013a). As a proof for this effect, a lab scale experiment tests was done using fluoroquinolone enrofloxacin, which is a spectrum of synthetic antibiotic used in medicine for human and veterinary, to study its toxic effects and uptake in plants (Migliore et al. 2003, Grassi et al. 2013a). After 30 days of plant exposure to concentrations between 50 and 5000 µg/L, toxic effect and hormesis were induced in the plants by modifying the length of primary root, hypocotyl, cotyledons, and the number/length of leaves. The authors attributed this effect to the efficient plant drug uptake (Grassi et al. 2013a).

Concerning EDCs, their effect on human health and wildlife biology were first reported in the 1930s, and the real research progressed in the late 1970s and early 1980s (Möder et al. 2007). After this, several studies documented the impacts of exposure of aquatic organisms to low concentration (ng/L) of EDCs (Shin et al. 2007, Hecker et al. 2008). Literature data reported several abnormalities and health problems of EDCs on environment and human beings which are presented in Fig. 4. (Tijani et al. 2013a).

Concerning human beings, their exposure to EDCs could be through dermal absorption or contaminated media such as water, food, air, and soil (Tijani, Fatoba, et Petrik 2013a). The major concern is related to fetuses and newborn babies due to their higher sensitivity (Barbosa et al. 2016a). Recently, a study by Kabir et al. (2015) has reviewed the mechanism of action and harmful effects of EDCs on human health (Kabir et al. 2015). Another study highlighted the EDCs risk assessment, particularly issues related to long-term and combined exposure, transgenerational and mixture effects (Futran Fuhrman et al. 2015).

Moreover, some studies reported an effect of EDCs toward animals. Several fish species has been feminized due to presence of estrogenic substances, such as natural estrogens (e.g. estrone [E1] or 17 β-estradiol [E2]) and synthetic estrogen (e.g. 17α- ethinylestradiol [EE2]) even at ng/L concentration levels (Tran et al. 2017a). Kidd et al. (2007) conducted a 7-years experiment, that showed that the exposure of the fish population *Pimephales promelas* to EE2 at concentration of 5-6 ng/L during the 7 years, lead to a significant collapse of the fish population as a result of feminization of the male fish and altered oogenesis in females (Kidd et al. 2007, Barbosa et al. 2016a, Tran et al. 2017a).

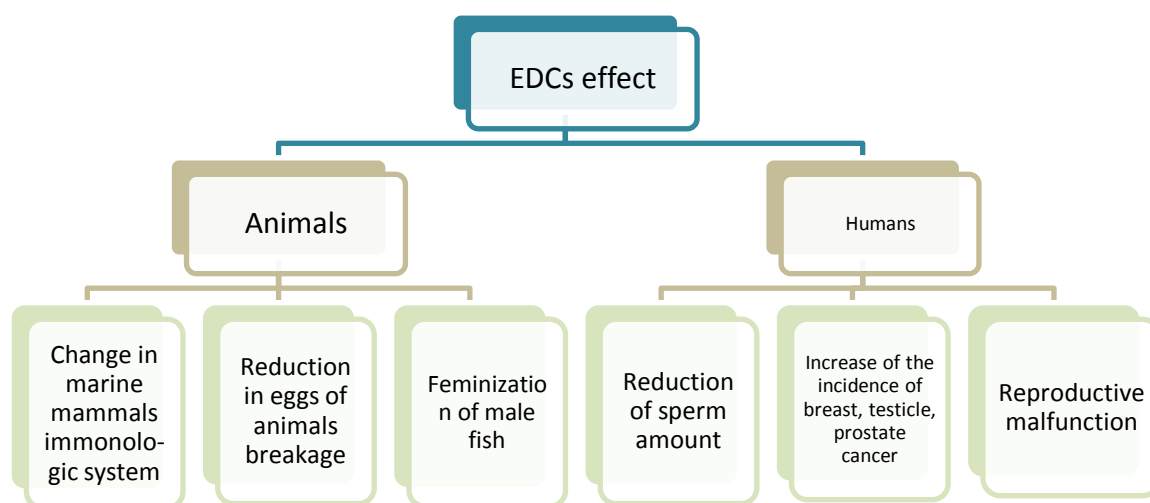


Fig. 4. Main negative effects of EDCs on environment and human health (Barbosa et al. 2016a, Tijani et al. 2013).

The wide distribution of PFCs, including PFOS and PFOA, increases their bioaccumulation and bio-concentrations. As a result of their persistence and long-term accumulation, fish, piscivorous birds and other biota are exposed to PFOS and PFOA. PFOS is founded to accumulate to important levels in fish tissue. The estimated bio-concentration factor in fish ranges from 1,000 to 4,000. As of 2013, PFCs have been reported in the 5-year reviews of the 14 hazardous waste on the EPA National Priorities List by the Superfund Information Systems Database (Environmental Protection Agency EPA 2014).

Therefore, it is necessary to treat the effluents containing PPCPs, EDCs and PFCs adequately before discharging them into different water bodies due to their significant adverse negative effects on wildlife and aquatic living things.

6 Treatment of wastewater in wastewater treatment plants (WWTP)

Wastewater from hospitals, urban industries, drug manufacturing industries, agriculture and human activities enter into WWTPs for treatment and removal of organic and inorganic pollutants including micropollutants presenting at low concentrations. The treatment comprises a pre-treatment followed by primary, secondary and tertiary systems as shown in Fig. 5. The pre-treatment step remove coarse wastes (bar screen), sand (decantation channel) and grease tank where skimmers

collect the floating fat (Margot 2015). Primary treatment is based on physicochemical process (Rivera-Utrilla et al. 2013a) where coagulants such as alum, ferric chloride, and polymers are used to remove colloidal and suspended solids through primary clarifier. In the process, organics attached with dissolved humic substances and particles can also be removed (Das et al. 2017a). Secondary system consists of biological reactor formed by activated sludge (Rivera-Utrilla et al. 2013a) where easily biodegradable dissolved organics or residual solid are removed by biodegradation (Margot 2015). The thickened sludge from both primary and secondary clarifiers is digested anaerobically (biosolids) prior to disposal (Das et al. 2017a).

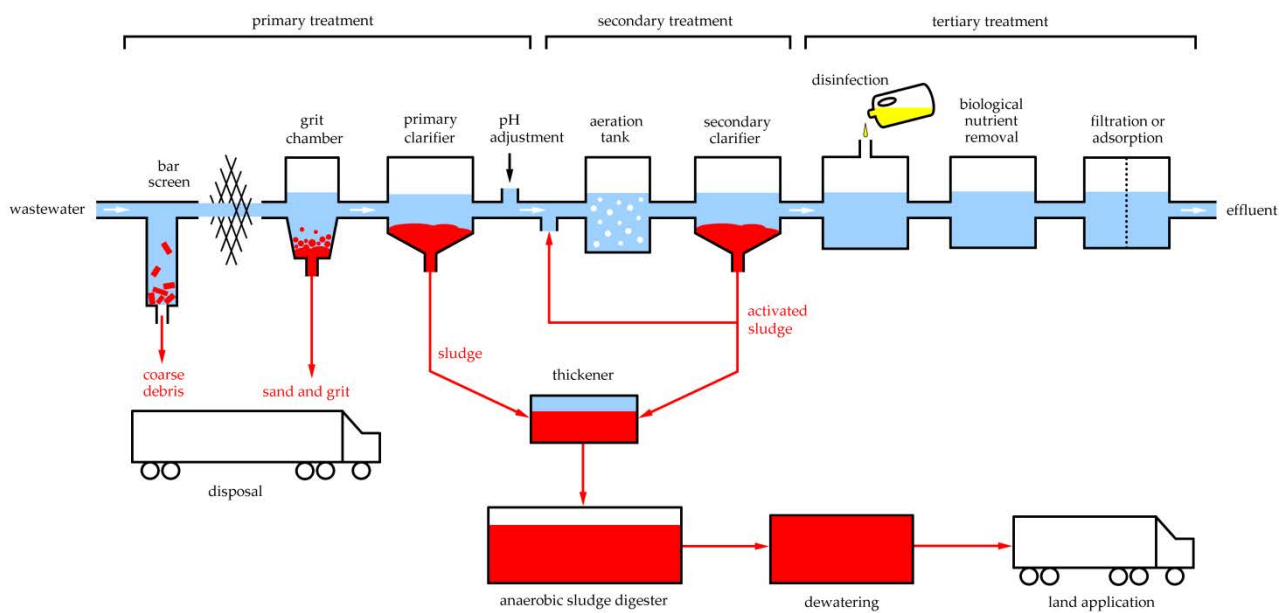


Fig. 5. Normal treatment steps followed in conventional WWTP (Margot 2015).

In general, through these systems, WWTPs are able to remove solid wastes, suspended solids, biodegradable dissolved organics and nutrients (Das et al. 2017a). But, in fact, it is proven that most of the conventional WWTP do not completely eliminate micropollutants at low concentrations (Daughton et Ternes 1999, Tijani et al. 2013) since they cannot be metabolized by microorganisms as source of carbon and they can even inhibit the activity of microorganisms (Rivera-Utrilla et al. 2013a). Thus, these compounds persists in the WWTP effluents and are then detected in the surface water as presented in Fig. 6.

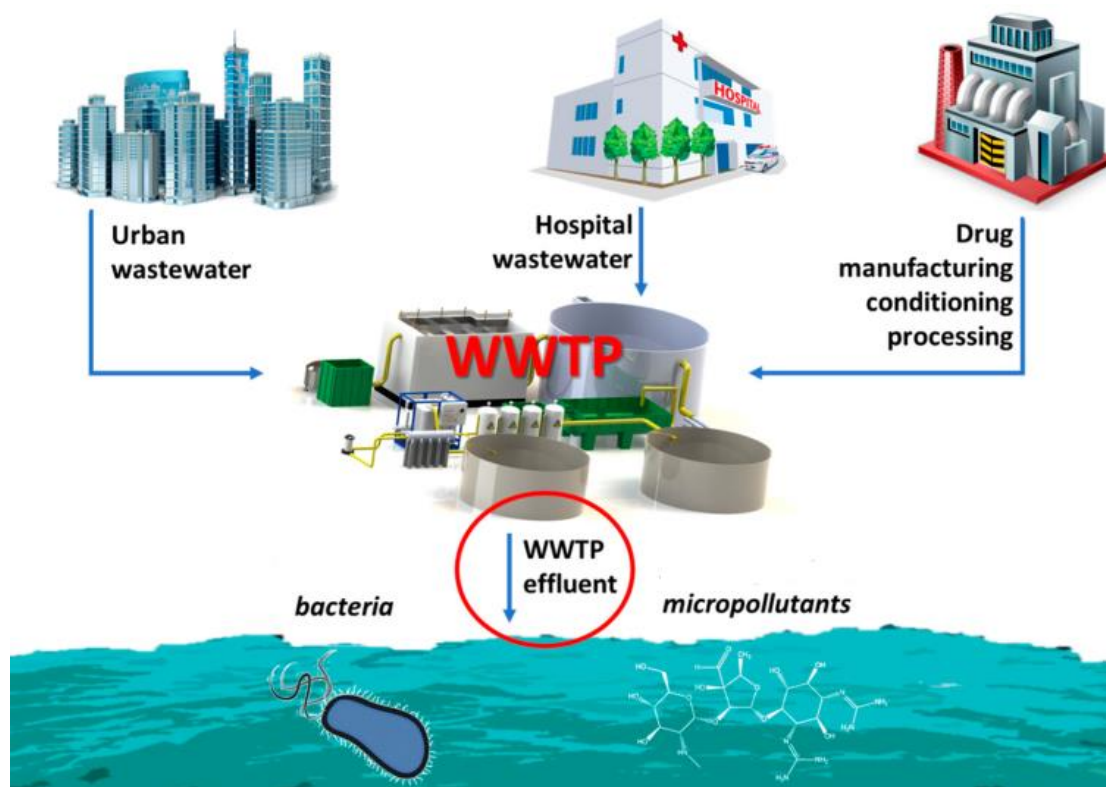


Fig. 6. Discharge of micropollutants in WWTP effluents into natural water.

Therefore, the upgrade of the WWTPs with advanced treatment technologies to improve the removal efficiency of micropollutants before their discharge into receiving water becomes necessary (Klamerth et al. 2010, De Luca et al. 2013, Sudhakaran et al. 2013a). For this aim, tertiary treatment methods based on non-conventional treatment technologies include biological systems, adsorption on activated carbon, membrane filtration and AOPs are adapted for final treatment of effluents to remove micropollutants at low concentrations before their discharge (Rivera-Utrilla et al. 2013a).

7 Treatment of micropollutants in WWTP: Fate and removal

The removal of micropollutants in WWTP depends on their physical-chemical properties such as solubility, octanol-water partition coefficient K_{ow} , and Henry's constant, beside the treatment process employed (Grassi et al. 2013, Barbosa et al. 2016, Das et al. 2017). Table 7 lists some of the micropollutants and their concentrations in wastewater effluent and surface water, and their physical properties.

Table 7. Concentration of some micropollutants in WWTP effluent and in surface water in addition to some of their physical-chemical properties (Das et al. 2017).

Micropollutants	Average		Solubility (mg/L)	Log K _{ow}	pK _a	Henry's constant (atm·m ³ /mol) [*]
	concentration (ng/L)					
	WWTP effluent	Surface water				
Bisphenol A	331	840	0.12	3.32	9.6	1 × 10 ⁻¹¹
Estradiol	3	2	0.0213	4.01	10.33	3.64 × 10 ⁻¹¹
Estrone	15	2	0.00394	3.13	10.33	3.8 × 10 ⁻¹⁰
Ethinylestradiol	2	5	0.00677	3.63	10.33	7.94 × 10 ⁻¹²
Carbamazepine	832.3	-	0.152	2.45	15.96	1.08 × 10 ⁻¹⁰
Clarithromycin	276	30	0.00033	3.16	8.9	1.73 × 10 ⁻²⁹
Diclofenac	647	65	0.00447	4.98	4	4.73 × 10 ⁻¹²
Erythromycin	42	25	0.459	2.37	12.44	1.46 × 10 ⁻²⁹
Ibuprofen	394	35	0.0684	3.5	4.85	1.50 × 10 ⁻⁰⁷
Ketoprofen	86.0	-	0.0213	3.12	4.45	2.12 × 10 ⁻¹¹
Naproxen	462	37	0.0511	3.29	4.19	3.39 × 10 ⁻¹⁰
Sulfadiazine	3.5	-	0.601	-0.09	6.36	1.58 × 10 ⁻¹⁰
Sulfamethoxazole	238	26	0.459	0.79	6.16	6.42 × 10 ⁻¹³
Triclosan	74.8	-	0.00605	5.53	7.9	4.99 × 10 ⁻⁰⁹
PFOS	-	-	3.1	6.28	0.14	-

The fate and removal processes for MPs in a WWTP start in primary and secondary systems based on conventional processes that include mainly: adsorption on suspended particulates, dissolved humic substances, primary and secondary sludge, coagulation and sedimentation, biodegradation, biological and/or chemical transformation. Then, they continue in the tertiary system using non-conventional treatment technologies including adsorption on activated carbon, advanced oxidation, and membrane filtration as shown in Fig. 7. Volatilization of the MPs during any of the treatment steps is negligible due to their very low Henry's constant ($< 10^{-5}$ atm-m³/mol) (Table 7) (Barbosa et al. 2016b, Das et al. 2017b).

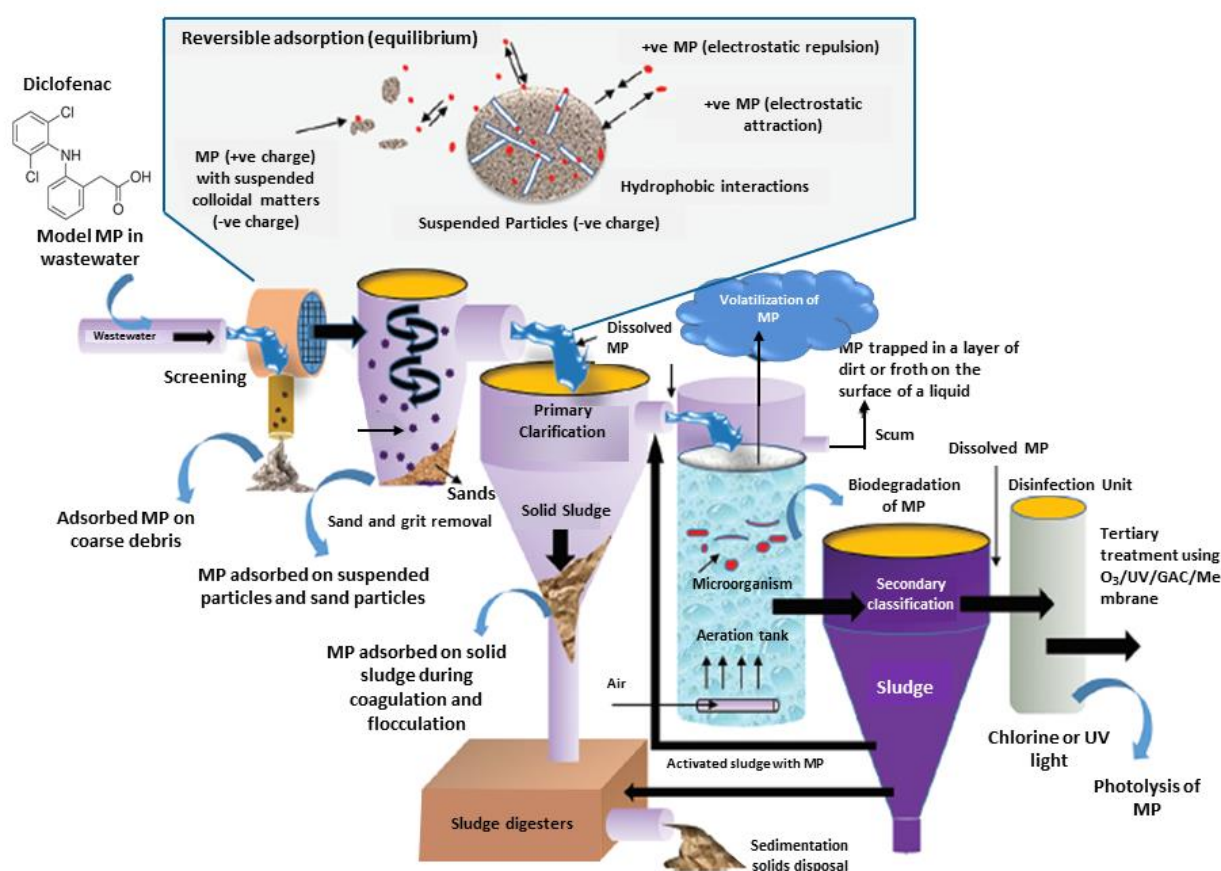


Fig. 7. Conventional model of the fate and removal processes of a micropollutant in a typical WWTP (Das et al. 2017b).

7.1 Removal of micropollutants by conventional processes

Before the removal process, micropollutants in wastewater can be adsorbed on suspended solids in both primary and secondary treatment. Adsorption may occur due to the hydrophobic

interactions between the aliphatic and aromatic groups of the compounds with the fat and lipid fractions in primary sludge, and the lipophilic cell membrane of the microorganisms in secondary sludge, respectively. Also micropollutants can be adsorbed by electrostatic interactions that occur between the positively charged groups in the MPs and the negatively charged microorganisms in secondary sludge. Many micropollutants especially acidic pharmaceuticals are negatively charged at neutral pH, and their sorption on sludge is negligible. The removal of MPs by coagulation-flocculation and sedimentation processes is not very effective for most of the micropollutants (Das et al. 2017b).

In the secondary treatment, the most common employed processes are conventional activated sludge (CAS) and membrane biological reactors (MBR). The physical-chemical properties of the compounds, the nature of the microbial community and the operational factors (such as temperature, hydraulic retention time (HRT) and the sludge retention time (SRT)) control the efficiency of a CAS in the removal of MPs in wastewater (Petrovic et al. 2009, Oulton et al. 2010). MBRs emerged as an alternative technique to CAS since it combines both biological treatment (aerobic biodegradation) and membrane separation (micro and ultrafiltration) (Oulton et al. 2010, Das et al. 2017). In addition, MBRs is characterized by its higher SRT compared to CAS (Petrovic et al. 2009), which increases the biodiversity of the microorganisms making the opportunity for adaptation of specific microorganisms to the persistent compounds greater (Das et al. 2017b). Previous studies reported that 90 % of MPs are not removed or bio-transformed using these biological treatments (Das et al. 2017b). For example, Nakada et al. (2006) investigated that pharmaceuticals, such as ketoprofen, naproxen, carbamazepine, and crotamiton exhibited poor removal in five WWTPs in Tokyo using a combination of primary and secondary treatment (Tran et al. 2017). In another study, Radjenovic et al. (2009) investigated the fate of pharmaceuticals in biological wastewater treatment by conventional activated sludge (CAS) and membrane bioreactor (MBR) systems, and they concluded that some pharmaceuticals have poor removal efficiencies in either CAS or MBR system (Tran et al. 2017b). Another point is that the efficiency of the conventional methods in the removal of micropollutants do not distinguish between adsorption and biotransformation, and most of the data gives the overall removal based on the influent and effluent concentrations with no information about the intermediate steps (Das et al. 2017). Moreover, other challenges in such treatments at this point are the absence of information regarding the fate of metabolites, transformation products of micropollutants and their complex chemistry (Das et al. 2017b). For this reason, the implementation of advanced treatment technologies (non-conventional treatment processes during the tertiary treatment) that allow the transformation of micropollutants into less harmful substances (or even

mineralize them), is one of the promising strategies research studies are working to achieve Hybridization of natural systems with advanced treatment processes for organic micropollutant removals: New concepts in multi-barrier treatment (Sudhakaran et al. 2013, Barbosa et al. 2016a).

7.2 Removal of micropollutants by non-conventional processes in tertiary treatment

The advanced treatment methods for removal of emerging contaminants in WWTPs during the tertiary system are mostly categorized into three approaches (Liu et al. 2009, Rivera-Utrilla et al. 2013, Rodriguez-Narvaez et al. 2017). These are the physical methods (phase changing methods), the biological treatment, and the advanced oxidation processes.

7.2.1 Phase changing technology:

Phase changing technologies are based on the movement of the contaminants from one phase (such as water) into another (such as solid). They have been widely reported for the removal of emerging contaminants. They include 2 main processes: adsorption and membrane filtration (Rodriguez-Narvaez et al. 2017b).

➤ Adsorption

Adsorption processes have been extensively studied for the removal of several different pollutants (Homem et al. 2011, Rodriguez-Narvaez et al. 2017a). Several types of adsorbents are stated in the literature for removal of ECs in water. Activated carbon adsorbent is the mostly used material due to its high porosity and specific surface area properties (Sotelo et al. 2012, Rivera-Utrilla et al. 2013c) that make it highly adsorptive and effective in the removing of emerging contaminants (Rodriguez-Narvaez et al. 2017a). Other types of adsorbents include biochar, carbon nanotubes and clay (Rodriguez-Narvaez et al. 2017b). The type of the adsorbent material is one of the most important factors that should be taken into consideration, since it determines other important features that affect the adsorption efficiency such as pore size, metallic or nonmetallic nature and the ability to couple with a second treatment method. From this point, adsorption process is sometimes coupled with other treatment processes especially oxidation processes where adsorbents such as zeolite, miso- and micro- porous materials, and metal oxides enhance the total removal efficiency (Hou et al. 2010a, Ahmed et al. 2015).

➤ Membrane technology

Membrane filtration technology is mostly used for the removal of dyes, micro-organisms and salts from wastewater. The most common membrane technologies can be divided into 2 groups: i) the low pressure systems, such as microfiltration (MF) and ultra-filtration (UF) at 5 and 10 bar respectively and ii) the high pressure systems, including nanofiltration (NF) up to 50 bar and reverse osmosis (RO) up to 70 bar. Recent studies are focusing on the application of this technology in the removal of emerging contaminants (Barbosa et al. 2016a). It has been shown that high pressure systems have the ability to remove micropollutants more efficiently than the lower pressure systems (Esplugas et al. 2007).

Being quite effective; phase changing processes do not perfectly remove micropollutants including EDCs and PPCPs in water (Nowotny et al. 2007). Also they are not highly effective in the case of low concentrations of micropollutants in water (Rodriguez-Narvaez et al. 2017a). Moreover, the retention capacity of both methods can be reduced through blockage by natural organic matter in water (Rivera-Utrilla et al. 2013c). Moreover, their high operation costs limit their use also (Grassi et al. 2013c).

Concerning adsorption process separately, its main drawback is the regeneration cost especially if thermal process is integrated (Grassi et al. 2013c). As for membrane technology, one of its major disadvantages is the production of concentrate containing all the retained compounds (15-25 % of the flow with high micropollutants concentrations) (Barbosa et al. 2016a) that are commonly discharged into the different water bodies (Justo et al. 2015). Thus, the need to treat such a concentrate wastewater separately before their discharge into the aquatic system still limits its use at full-scale (Tambosi et al. 2010, Margot 2015, Barbosa et al. 2016a). As a conclusion, such processes can be used, but mostly as a concentrate pretreatment coupled with other removal treatments mainly AOPs that are able to degrade ECs in water (Justo et al. 2013, Ana Justo et al. 2014).

7.2.2 Biological treatment

Biological system includes several different processes mainly activated sludge under aerobic and anaerobic conditions, and soil and biological filtration (Rodriguez-Narvaez et al. 2017a). The choice of the type of biological process depends on the type of the contaminant, and it is usually coupled with other tertiary treatment processes (Martín et al. 2015). These processes proved to have some good removal efficiencies in the removal of emerging contaminants in water. Some research studies investigate that only easily biodegradable ECs such as caffeine, diclofenac, trimethoprim

can be eliminated by biological systems, whereas compounds with low biodegradability such as sulpiride, metoprolol, bezafibrate may not be eliminated at all. The main disadvantage of such method is the absence of accurate analytical methodologies that is able to identify and quantify micropollutants in such complex matrix. Moreover, the microorganisms used for ECs degradation are not identified, it is only reported that activated sludge is the removal key. In addition, studies on biological processes do not include experimental development or detailed characterization of many of the used processes resulting in several unanswered questions about the fundamental process mechanism. Therefore, it is necessary to find efficient advanced treatment technologies for the complete removal of micropollutants in WWTP before they pass into the aquatic environment (Rodriguez-Narvaez et al. 2017a).

7.2.3 Advanced oxidation processes

Although phase changing technology and biological processes can effectively remove micropollutants in wastewater, they are not able to degrade them completely to low concentration levels essential for the use of the effluent (Rivera-Utrilla et al. 2013c). From this point, AOPs proved to overcome the other advanced technologies by their ability to completely mineralize the micropollutants (Tijani et al. 2013b).

AOPs are chemical oxidation techniques characterized by the generation of hydroxyl radical (oxidation potential, 2.8 V) (Rodriguez-Narvaez et al. 2017a) the strongest known oxidant beside fluorine. It is capable of oxidizing and mineralizing, unselectively, the organic pollutants into carbon dioxide and water (Esplugas et al. 2007, Tijani et al. 2013b, Barbosa et al. 2016a) with high reaction rate constants ranging from 10^6 to 10^9 /M.s (Esplugas et al. 2007). These radicals can generate several AOP systems making them highly versatile (Rivera-Utrilla et al. 2013c). Although the main characteristic of AOPs is the production of hydroxyl radicals, the type of the production reaction and the experimental conditions are highly important (Rodriguez-Narvaez et al. 2017a). Different types of AOPs are employed for the treatment of micropollutants in water and real matrices, and are implemented in WWTP for wastewater treatment. They can be used as pre-treatment or post treatment of a biological process. As pre-treatment, single or a sequence of complementary AOPs is implemented to improve the biodegradability of the effluent by transforming the initially recalcitrant micropollutants into more biodegradable intermediates. After that the resulting effluent is transferred to a conventional biological treatment system. When used as post-treatment, AOPs degrade the micropollutants and their by-products into CO_2 , H_2O and inorganic ions, yielding a clean effluent that can be discharged directly into the natural water compartments (Barbosa et al. 2016a, Mirzaei et

al. 2017). During the last years, the performance of AOPs in the degradation of ECs is similarly and relatively high for all the studies, the main difference being the nature of the process and its experimental conditions provided for the removal (Tijani et al. 2013b, Rodriguez-Narvaez et al. 2017a). The main AOP techniques are characterized by the presence of oxidants such as hydrogen peroxide and ozone, and the use of UV light radiation. They include ozonation (O_3 /with and without UV), heterogeneous photocatalysis (mainly UV/ TiO_2), Fenton and photo-Fenton processes (homogeneous and heterogeneous) and more other techniques (Ribeiro et al. 2015b). The major debate concerning the use of these processes is the formation of oxidation by-products (or transformation products) from micropollutants. But research data indicated that these byproducts have in significant estrogenic and antimicrobial activity compared to the parent compounds beside their low concentration levels (Luo et al. 2014). In the following, we will discuss briefly the heterogeneous photocatalysis and with more details the Fenton processes because they will be used in our study later.

8 Heterogeneous photocatalysis

Heterogeneous photocatalysis is one of the AOP processes that have been widely investigated for mineralization of organic compounds in wastewater (Tijani et al. 2013a). The process is based on the use of semiconductors with wide band-gap that generate electrons and holes when irradiated with photons of energy higher than the semi-conductor band-gap (i.e. $h\nu \geq E_G$) (Barbosa et al. 2016a). The valence band holes (h_{vb}^+) can initiate oxidative pathways by reacting with adsorbed H_2O to produce $\cdot OH$, while conduction band electrons (e_{cb}^-) react with adsorbed O_2 electron accepting species, including some contaminants. Fig. 8 represents the photocatalytic mechanism through hydroxyl radical (Carbonaro et al. 2013).

9 Photo-Fenton processes

Among AOPs, Fenton-type processes have been identified as the effective methods for the removal of micropollutants in water based on the production of hydroxyl radicals by the reaction between iron salts and hydrogen peroxide (Fenton 1894, Barbosa et al. 2016a, Mirzaei et al. 2017). Fenton processes can be performed with or without light source (Fenton or photo-Fenton) and with or without a support material (homogeneous or heterogeneous). Thus several Fenton type processes exist. This includes homogeneous Fenton/photo-Fenton processes and heterogeneous Fenton/photo fenton processes according to the equations below. The difference in their experimental factors has a great effect on their efficiency in the removal of micropollutants in water. Homogeneous Fenton process or Fenton-like process requires the presence of Fe^{2+} or Fe^{3+} iron species respectively that react with hydrogen peroxide to produce the oxidizing hydroxyl radical species according to Eq. 1 and Eq. 2 (Sreeja et al. 2016, Mirzaei et al. 2017).



Even though Fenton process is an important oxidation treatment, only few papers targeting the removal of EDCs and PPCPs are found in the literature (Esplugas et al. 2007, Mirzaei et al. 2017). The main advantages of this process are its high efficiency, cheap reagents, the consequent easy implementation and operation (Barbosa et al. 2016a), and the smooth transition from laboratory scale to large scale due to its ability to operate at room temperature and normal pressure without complicate apparatus (Tran et al. 2017a). Fenton processes have been successfully used to remove herbicides and antibiotics in wastewater. As an example, Mackulak et al. (2006) successfully removed 13 drugs to concentrations below the detection limit from a wastewater treatment plant by Fenton and Fenton-like processes (Mirzaei et al. 2017). Moreover, it is reported that when treating micropollutants in real wastewater, the presence of dissolved organic matter seems to enhance the micropollutants removal during all Fenton processes which is an important advantage of the Fenton process over other AOPs namely TiO_2 photocatalysis (Luo et al. 2014). Comparing different AOPs processes that have been scaled to a treatment plant, it can be observed that Fenton processes surpass the other processes (Rodriguez-Narvaez et al. 2017a). Prieto-Rodriguez et al. (2013) compared the removal efficiencies of solar photo-Fenton, ozonation and solar TiO_2 photocatalytic treatment in the removal of a combination of 66 ECs including 16 PhACs. The results showed highest removal

efficiency for solar photo-Fenton system with 98 % ECs removal achieved in only few minutes of reaction. Another study done by Radjenovic et al. (2009) who reported higher removal efficiency for photo-Fenton degradation of AAP and ATL compared to the degradation by photocatalytic treatment with TiO₂. Furthermore, the removal Ofloxacin in WWTP effluent was studied by Michael et al. (2010) who demonstrated that the photo-Fenton process was more efficient than TiO₂ not only for the ofloxacin degradation but also for the DOC removal (Table 8).

Table 8. A summary of some removal processes for the treatment of emerging contaminants.

Emerging contaminant	Process implied	Experimental conditions	Results	Ref.
B-Lactams Amoxicillin 5.0 ×10 ⁻⁴ M	Ozonation	Deionized water 1.6 ×10 ⁻⁴ M O ₃ pH = 2.5-7.2	90 % removal after 4 min and 18 % mineralization after 20 min. Low degree of mineralization, even for long treatment times.	(Andreozzi et al. 2005)
Penicillin COD = 1555 mg/L	Ozonation Direct and indirect photolysis photo-Fenton process	Formulation effluent ozonation: 2760 mg/(L h) O ₃ , pH = 3-11.5 Photolysis: LP UV at 254 nm, pH = 7 0-40 mM H ₂ O ₂ Photo-Fenton: LP UV at 254 nm, pH = 3 20 mM H ₂ O ₂ , 1 mM Fe ³⁺	Ozonation was pH-dependent and the highest COD and TOC removals occurred in alkaline conditions (after 60 min of treatment, the maximum COD removal was 49 %). Photolysis proved to be a less effective method. Fenton-like processes: COD with Fe ³⁺ /H ₂ O ₂ (61 % COD removal). Poor improvement of biodegradability	(Alaton et al. 2004)
[Paracetamol] ₀ = 50 mg/L	Homogeneous photo-Fenton vs Photolysis	FeSO ₄ ·7H ₂ O Distilled water pH 2.5-2.8 Temperature = 25 °C [H ₂ O ₂] = 120 mg/L [Catalyst] = 0.05 mM Reaction time = 300 min Solar radiation simulator (1100 W xenon arc lamp).	No photolysis of PCT was observed at natural pH (4.2) after 300 min irradiation. 100 % PCT removal was achieved after 120 min by FeSO ₄ and 180 min by FeOx. 79 % TOC removal was reported by FeSO ₄ and 58% by FeOx after 300 min.	(Trovó et al. 2012)

[Ibuprofen] ₀ = 0.87 mM	Homogeneous Fenton vs UV/H ₂ O ₂	FeSO ₄ ·7H ₂ O Distilled water pH 3 Temperature = 30 °C [H ₂ O ₂] = 0.32 mM [Catalyst] = 1.2 mM Reaction time = 120 min Xe lamp 1 kW 6.9 mE/s (290-400 nm)	UV/H ₂ O ₂ process led to the 30 % IBP removal after 2 h, however, TOC did not decrease. Maximum 60 % and 10 % IBP and TOC removal were achieved by Fenton process. About 100 % IBP (after 60 min) and 40 % TOC removal were reported by the photo-Fenton reaction. Biodegradability was improved at the end of the process (BOD ₅ was reached to less than 1 mg/L from 25 mg/L).	(Méndez-Arriaga et al. 2010)
[AAP] ₀ = 10 mg/L [ATL] ₀ = 10 mg/L	Photo-Fenton treatment vs photocatalytic treatment with TiO ₂	Distilled water & S.E. [Fe ²⁺] = 5 mg/L [H ₂ O ₂] = 10-20 mg/L Light source: Sunlight Illuminated volume: 36 L Total volume: 150 L pH 2.6-2.8	Primary experiments confirmed that no hydrolysis and photolysis of PhACs occurred without the catalyst. Total degradation of AAP and ATL were reported after 12 and 3.8 min of illumination by solar photo-Fenton in DW, respectively. Total degradation of AAP and ATL were reported after 21.8 and 30 min of illumination by solar photo-Fenton in S.E., respectively. The photo-Fenton treatment was more efficient for the degradation of ATL and ACTP than the photocatalytic treatment with TiO ₂ .	(Radjenović et al. 2009)
Combination of 66 ECs include 16 PhACs [DOC] ₀ = 13-23 mg/L [COD] ₀ = 32-63 mg/L	Comparison: Solar photo-Fenton, ozonation, solar/TiO ₂	MWTP [Fe ²⁺] = 5 mg/L [H ₂ O ₂] = 60 mg/L Light source: Sunlight Illuminated volume: 44.6 L Total volume: 75 L Temperature = 35 °C pH 2.8	The removal efficiency of solar photo-Fenton, ozonation and solar/TiO ₂ used as the posttreatment after the secondary biological treatment process showed the following trend: Solar photo-Fenton > ozonation > solar/TiO ₂ . Over 98 % ECs removal was achieved in only a few minutes of reaction by the photo-Fenton process that	(Prieto-Rodríguez et al. 2013)

			<p>produced an effluent with extremely low (nontoxic) inhibition.</p> <p>Solar photo-Fenton is a potential advanced treatment in MWTPs with treatment costs of $<0.4 \text{ V/m}^3$.</p>	
<p>[Ofloxacin]₀ = 10 mg/L</p>	<p>Photo-Fenton treatment vs photocatalytic treatment with TiO₂</p>	<p>FeSO₄·7H₂O (Riedel-de Haen)</p> <p>WWTP effluent (secondary treated)</p> <p>pH 3</p> <p>Temperature = 25 °C</p> <p>[H₂O₂] = 2.714 mM</p> <p>[Catalyst] = 5 mg/L</p> <p>Reaction time = 120 min</p> <p>Solar radiation simulator (1 kW Xenon lamp)</p>	<p>Less than 6 % OFX removal was observed after 120 min by photolysis.</p> <p>Total removal of OFX was achieved after 90 min by Fenton reaction while by photo-Fenton reaction 30 min was required.</p> <p>Photo-Fenton was more efficient than TiO₂ not only for the OFX degradation but also for the DOC removal.</p> <p>At optimum conditions, 50 % and 10 % DOC removal were achieved by photo-Fenton and TiO₂, respectively.</p> <p>First order rate constant of OFX degradation by the photo-Fenton process was 0.1128/min, and t_{1/2} was 6.14 min.</p>	<p>(Michael et al. 2010)</p>
<p>Amoxicillin 104 mg/L</p> <p>Ampicillin 105 mg/L</p> <p>Cloxacillin 103 mg/L</p>	<p>Fenton</p>	<p>Distilled water</p> <p>pH = 2-4</p> <p>H₂O₂/COD molar ratio = 1.0-3.5</p> <p>H₂O₂/Fe²⁺ molar ratio = 2-150</p>	<p>Under the optimal conditions (H₂O₂/Fe²⁺ molar ratio = 10, pH = 3) it was achieved the complete degradation of the antibiotics in 2 min.</p> <p>The biodegradability was improved from 0 to 0.37 in 10 min and COD and DOC degradation were 81.4 % and 54.3 %, respectively in 60 min.</p> <p>Fenton process was effective in the treatment of solutions containing these antibiotics.</p>	<p>(Elmolla et Chaudhuri 2009)</p>
<p>Amoxicillin 104 mg/L</p> <p>Ampicillin 105 mg/L</p>	<p>Photo-Fenton</p>	<p>Distilled water</p> <p>pH= 2-4</p> <p>H₂O₂/COD molar ratio = 1.5, H₂O₂/Fe²⁺ molar ratio = 20, pH = 3)</p>	<p>Under the optimal conditions (H₂O₂/COD = 1.5, H₂O₂/Fe²⁺ molar ratio = 20, pH = 3) it was achieved that</p>	<p>(Elmolla et Chaudhuri 2009)</p>

mg/L		ratio = 1.0-2.5	the complete degradation of the	
Cloxacillin 103		H ₂ O ₂ /Fe ²⁺ molar	antibiotics in 2 min.	
mg/L		Ratio = 10-150	The biodegradability was improved	
		UV light (6 W) at 365 nm	from 0 to 0.4 and COD and DOC	
			degradation were 80.8 % and 58.4 %,	
			respectively in 50 min.	
			Mineralization of organic carbon	
			occurred.	
Amoxicillin 104	Semiconductor	Distilled water	No significant degradation	(Elmolla et
mg/L	photocatalysis	UV light (6 W) at 365 nm	occurred by 300 min of UV	Chaudhuri
Ampicillin 105		0.5-2.0 g/L TiO ₂	irradiation.	2010)
mg/L		50-300 mg/L H ₂ O ₂	At pH = 5 and 1.0 g/L TiO ₂ , 50 %	
Cloxacillin 103		pH = 3-11	degradation was achieved for all	
mg/L			compounds (81 % DOC removal).	
Ref 3			Addition of 100 mg/L H ₂ O ₂ at pH = 5	
			and 1.0 g/L TiO ₂ resulted in complete	
			degradation after 30 min and 40 %	
			mineralization after 24 h.	

The photo-Fenton process can be more efficient than Fenton alone. In the presence of light, hydroxyl radicals are produced according to Eq. 3, 4 and 5. The higher performance of the photo-Fenton processes is mainly due to the faster regeneration of Fe²⁺ that result from the reaction of the formed complex Fe(OH)²⁺ with light Eq. 5 and Eq.6 (Barbosa et al. 2016a).



The importance of light integration is also reflected by the low TOC removal observed in most of the AOPs dark treatments and not only Fenton treatment (Esplugas et al. 2007). Table 9 shows the efficiency of different Fenton processes with various experimental conditions in the removal of micropollutants.

Table 9. The efficiency of several types of Fenton processes in the removal of micropollutants with different experimental conditions.

Emerging contaminant	Process	Experimental conditions	Results	Ref
[Sulfathiazole] ₀ = 47 µmol/L	Homogeneous	FeSO ₄ ·7H ₂ O	84 % PhAC removal was observed after 8 min reaction.	(Velasquez et al. 2014)
	Fenton	pH 3	30 % TOC removal was achieved after 60 min reaction.	
		[Fe ²⁺] = 192 µmol/L [H ₂ O ₂] = 1856 µmol/L Reaction time = 60 min	40 % COD removal was reported after 15 min reaction. Oxamic acid as a byproduct remained stable after long periods of reaction.	
[Sulfathiazole] ₀ = 47 µmol/L	Homogeneous	FeSO ₄ ·7H ₂ O	95 % removal was achieved after 60 min reaction.	(Velasquez et al. 2014)
	photo-Fenton	pH 3	75 % TOC removal was reported after 60 min reaction.	
		[Fe ²⁺] = 157 µmol/L [H ₂ O ₂] = 1219 µmol/L Reaction time = 60 min 6 × 20 W solarium lamps (365 nm), 3.5 mW/cm	90 % COD removal was achieved after 15 min reaction. Photo-Fenton reaction was twice faster than Fenton reaction.	
[Sulfathiazole] ₀ = 195 µmol/L	Heterogeneous	Synthesized nano	Process could be conducted in a wide range of pH value	(Niu et al. 2011)
	Fenton	Fe ₃ O ₄ /HA	in Fe ₃ O ₄ /HA- H ₂ O ₂ system.	
		Deionized water, pH 3.5 Temperature = 40 °C [Catalyst] = 3 g/L [H ₂ O ₂] = 0.39 M Reaction time ¼ 6 h	Modification of catalyst with HA enhances the removal efficiency about 3.4 times. About total PhAC degradation was achieved after 1 h and 90 % TOC removal was reported after 6 h. The pseudo-first order rate constant for PhAC and TOC removal were 0.034 and 0.0048/min, respectively.	
[Amoxicillin] ₀ = 50 mg/L	Homogeneous	FeSO ₄ ·7H ₂ O	No AMX removal by photolysis was observed at	(Trovo et al. 2011)
	photo-Fenton	Distilled water	natural pH (6.2) after 6 h irradiation.	
	vs photolysis	pH 2.5-2.8 Temperature = 25 °C [H ₂ O ₂] = 120 mg/L [Catalyst] = 0.05 mM Reaction time = 240 min Solar radiation simulator (1100 W xenon arc lamp)	100 % removal of AMX was achieved after 5 min by FeOx and 15 min by FeSO ₄ . After 240 min, between 73 and 81 % TOC removal was reported. 73 and 81 % TOC removal was obtained in the presence of FeSO ₄ and FeOx, respectively.	

[Dipyrrone] ₀ = 50 mg/L T1	Homogeneous Fenton	(Fe(NH ₄) ₂ (SO ₄) ₂ ·6H ₂ O) Distilled water Temperature = 25 °C pH 3.5 [H ₂ O ₂] ₀ = 22.5 mM [Fe ²⁺] ₀ = 2.25 mM Reaction time = 50 min	94.1 % PhAC removal was achieved after 45 min treatment. 73.5 % PhAC removal was shown after 2.5 min of oxidation. 42.78 % TOC removal was obtained in 5 min. Biodegradability (BOD ₅ /COD) was improved from ~0.1 to 0.62 in 10 min.	(Giri et al. 2014)
[Dipyrrone] ₀ = 50 mg/L T2	Homogeneous photo-Fenton	(Fe(NH ₄) ₂ (SO ₄) ₂ ·6H ₂ O) Distilled water, Temperature = 25 °C pH 3.5 [H ₂ O ₂] ₀ = 22.5 mM [Fe ²⁺] ₀ = 2.25 mM Reaction time = 45 min UV lamp 9 W (362 nm) 12 W	83.2 % drug removal was shown at 2.5 min of oxidation. 96.4% PhAC removal was achieved after 45 min reaction. In the absences of ferrous ion, the PhAC removal was 74.4 % in 45 min. 56.0 % TOC removal was obtained in 5min. Biodegradability (BOD ₅ /COD) was improved from ~0.1 to 1.51 after 10 min of reaction.	
Metronidazole] ₀ = 1 mg/L	Homogeneous Fenton	(FeSO ₄ ·7H ₂ O) Deionized water, pH 3.5 [H ₂ O ₂] ₀ = 1 mg/L [Fe ²⁺] ₀ = 11.76 mM Reaction time = 5 min	No degradation of PhAC was observed without ferrous ions. 76 % metronidazole removal was obtained after 5 min. First order rate constant of PhAC degradation was 0.066/min and t _{1/2} was 1 min.	(Shemer et al. 2006)
[Metronidazole] ₀ = 1 mg/L	Homogeneous photo-Fenton	FeSO ₄ ·7H ₂ O Deionized water, pH 3.5 [H ₂ O ₂] ₀ = 1 mg/L [Fe ²⁺] ₀ = 11.76 mM Reaction time = 5 min LP UV (254 nm) 1.95 mW and MP UV (200-400 nm) 1.9 mW	6 % removal was obtained by direct photolysis with LP while 12 % removal was achieved by MP. For both lamps about 60 % removal was observed by adding 25 mg/L of H ₂ O ₂ after 2.5 min. 94 % removal was achieved by the photo-Fenton process under optimum conditions. First order rate constant of PhAC degradation was 0.23/min, and t _{1/2} was 0.5 min	(Shemer et al. 2006)
[Metoprolol] ₀ = 50 mg/L and [Resorcinol] ₀ = 50 mg/L	Homogeneous photo-Fenton: effect of light comparison	FeSO ₄ ·7H ₂ O Deionized water pH 6.2 (natural) Temperature = 25 °C [H ₂ O ₂] ₀ = 150 mg/L [Catalyst] ₀ = 10 mg/L Reaction time = 180 min BLB 8 W, 365 nm	Adding resorcinol (ligand iron complex) to the solution let to perform the reaction in neutral pH condition. By Fenton reaction, 100 and 92 % removal were achieved for MET and RES after 20 min respectively. By photo-Fenton reaction, 100 and 94.4 % removal were achieved for MET and RES after 3 min respectively. Biodegradability increased at the end of the processes.	(Romero et al. 2016a)

[Sulfonamides] ₀ =200 mg/L	Homogeneous photo-Fenton: light source comparison	FeSO ₄ .7H ₂ O Distilled water, pH 2.8 Temperature = 23-31 °C (not controlled) [Fe ²⁺] = 10 mg/L [H ₂ O ₂] = 400 mg/L Reaction time = 100 min LP UV lamp Hg vapor 8 × 8 W (λ = 350-400 nm)	Complete degradation of PhAC was achieved in 50 min. 56.4 % TOC removal was shown after 94 min. 82.2 % COD removal was achieved after 94 min. The energy consumption was estimated 2.5 kJ/L in this research.	(Gonzalez et al. 2009)
[Sulfonamides] ₀ =200 mg/L		FeSO ₄ .7H ₂ O Distilled water, pH 2.8 Temperature = 26 °C [Fe ²⁺] = 10 mg/L [H ₂ O ₂] = 550 mg/L Reaction time = 100 min Solar radiation (300 < λ < 500 nm) z121.6 W/m ²	87 % mineralization was achieved. 96 % COD removal was achieved after 94 min. The energy consumption was estimated 19 kJ/L.	(Gonzalez et al. 2009)
[Sulfadiazine] ₀ = 25 mg/L, [Sulfathiazole] ₀ = 25 mg/L	Homogeneous photo-Fenton	Prepared (K ₃ Fe(C ₂ O ₄) ₃ .3H ₂ O) Distilled water, pH 2.5 [Fe ³⁺ - oxalate] = 0.2 mM [H ₂ O ₂] = 5 mmol/L Reaction time = 45 min 15 W Blacklight lamp UVA (320-400 nm) 19 W	The degradation was observed only when three key components of photo- Fenton were present (Light, Fe and H ₂ O ₂). 92 and 90 % mineralization was achieved after 42 min of reaction in the case of sulfadiazine and sulfathiazole, respectively.	(Batista et al. 2012)
[Diclofenac] ₀ = 0.1 mM	Heterogeneous photo-Fenton	Synthesized Fe-ZSM5 Distilled water, pH 4 [H ₂ O ₂] = 50 mM [catalyst] ₀ = 2 mM Temperature = 25 °C Reaction time ¼ 120 min UVA lamps (λ _{max} = 365 nm) 3.04 × 10 ⁷ E/s	Both adsorption (early stage) and oxidation (final stage) were contributed in the DCF and TOC removal. More than 80 % and 98.9 % of DCF was removed after 2 and 120 min reaction, respectively. 66.4 % TOC removal was achieved after 15 min. (BOD ₅ /COD) was improved significantly from 0.043 to 0.63 in 120 min.	(Perisic et al. 2016)

Combination of 11 detected drugs of abuse [TOC] ₀ = 60 mg/L	Heterogeneous photo-Fenton	Powder silica-supported iron oxide (Fe ₂ O ₃ /SBA-15) Raw river water pH 3 Temperature = 22 °C [Catalyst] = 0.1-0.6 g/L [H ₂ O ₂] = 15-60 mg/L Reaction Time = 6 h UV-Visible 150 W MP mercury Lamp (λ > 313 nm)	More than 70 % removal of all drugs were achieved using only UV-Visible light. Using 0.1 g/L of catalyst without UV-vis and H ₂ O ₂ led to strong reduction of the opioid (75-83 %), moderate reduction of benzodiazepines (32-56 %) however a strong increase of cocaine (225-159 %) and a moderate increase of ALCs (51-11 %) were observed. The best result (>75 % removal of all drugs and 86 % of TOC removal) was achieved by a combination of UV and 0.6 g/L catalyst.	(Catala et al. 2015)
ECs include PhACs and hormones [COD] ₀ = 93.9 mg/L	Heterogeneous vs homogeneous Fenton processes	MWTP [H ₂ O ₂] = 200 mg/L Reactor Type: continuous stir tank reactor Total volume: 31.34 L Temperature = 12-20 °C Natural pH residence time = 3 h	Heterogeneous Fenton process was used to remove ECs from biologically pre-treated municipal wastewater. Performing the oxidation process at the natural pH of wastewater is a major advantage compared to the homogeneous Fenton process, which is limited to pH in the range of 2-4. >90 % of the hormones and >40 % of PhACs removal were reported. BOD was reduced to less than 1 mg/L after treatment. In addition, 30 % -40 % TOC, 50 % TSS, 68-91 % turbidity and 90 % phosphate reduction were achieved. There was less than 4 % iron leachate, suggesting a good stability of the catalyst.	
Rhodamine B (RhB)/4.8 mg/L	Heterogeneous photo-Fenton vs heterogeneous Fenton	Catalyst BiFeO ₃ [H ₂ O ₂] = 340 (mg/L) [Cat] = 20 mg/L pH 5 T = 25 °C	70 % RhB removal within 40 min in the dark; 1.95 times increase in rate constants in photo-Fenton compared to Fenton.	(An et al. 2013)
Methyl Violet (MV)/12.25 mg/L	Heterogeneous photo-Fenton vs heterogeneous Fenton	Catalyst BiFeO ₃ [H ₂ O ₂] = 680 mg/L [Cat] = 50 (mg/L) pH 5 T = 25 °C	49.8 % MV removal within 120 min in the dark, increased degradation up to 92 % within 120min in presence of light; 3.47 times increase in rate constants in photo-Fenton compared to Fenton.	(An et al. 2013)
Phenol/50 mg/L	Heterogeneous photo-Fenton	Catalyst Fe-zeolites [H ₂ O ₂] = 100 mg/L [Cat] = 20 (mg/L) pH 7, T = 35 °C	100 % phenol degradation after 100 min of irradiation; 90 % DOC removal after 80 min.	(Gonzalez-Olmos 2012)

Giri et al. (2014) studied the removal of Dipyrone pharmaceutical by Fenton and photo-Fenton processes. They observed higher drug and TOC removal with higher biodegradability under photo-Fenton process with UV irradiation. Another study by Shemer et al. (2006) on the degradation of metronidazole indicated higher removal percentage and rate constants with photo-Fenton process compared to Fenton process. Based on the literature, most of the research studies done use UV lamps as a source of radiation (Esplugas et al. 2007). As an example, De la Cruz et al. (2012) compared the efficiency of UV light and sunlight in photo-Fenton process for the treatment of WWTP effluent containing 32 micropollutants of various groups (pharmaceuticals, corrosion inhibitors and biocides/pesticides). Fenton/UV254 displayed much higher degradation efficiency (100 % degradation) compared with Fenton/sunlight (47 % degradation) (Luo et al. 2014). It is important to mention that the achievement of light enhancement effect necessitates the presence of Fenton reagent as reported in several studies (Luo et al. 2014, Rodriguez-Narvaez et al. 2017a). As an example, the degradation of oxacillin by UV-visible light and Fenton reagents was studied. It was observed that the UV-visible radiation alone was unable to degrade oxacillin, while the combination of radiation with the Fenton reagents was able to completely degrade oxacillin in the reaction mixture achieving overall degradation as high as 90 % (Rodriguez-Narvaez et al. 2017a).

The photo-Fenton process can be homogeneous or heterogeneous. Homogeneous process requires the reaction between Fe^{2+} and H_2O_2 at optimum pH around 2.5-3 (Park et al. 2018). The major disadvantage of this process is the need for high concentration (50-80 ppm) of Fe^{2+} ions to remove effectively the micropollutants. This iron amount which is significantly larger than the acceptable concentration in the water treatment effluent (about 2 ppm) to be discharged into the environment (Mirzaei et al. 2017). Moreover, the generation of iron oxide sludge due to post treatment process, limited pH range, high iron discharge into the environment and the difficulty in iron ion recovery limit the use of the homogeneous process (Arzate-Salgado et al. 2016, Sreeja et al. 2016, Mirzaei et al. 2017, Park et al. 2018). Heterogeneous Fenton process (or Fenton-like reaction based on Fe^{3+}) overcomes these disadvantages by using a solid support catalyst. In this process, less iron is produced and the catalyst is separated easily from the solution (Sreeja et al. 2016). Also the process can be operated at neutral pH and ambient temperature with no need to neutralize the effluent after treatment (Mirzaei et al. 2017). For example, Chi et al. (2013) performed homogeneous and heterogeneous Fenton processes on ECs including pharmaceuticals and hormones. They concluded that the oxidation of the selected compounds at neutral pH of wastewater was the major advantage of heterogeneous Fenton process compared to homogeneous process that was limited to pH range between 2-4. Moreover, Noorjahan et al. (2005) reported higher reaction rate and less

irradiation time for the complete degradation of phenol under Fe(III)-HY UV heterogeneous photo-Fenton process compared to homogeneous photo-Fenton.

Based on this, recent studies have been carried out to develop heterogeneous catalysts with high activity, long-term stability, and low cost Fenton oxidations in wastewater treatment (Mirzaei et al. 2017). Due to the presence of catalyst in heterogeneous Fenton reactions, not only the chemical reactions, but also the physical processes (surface reactions, adsorption and desorption) that take place on the surface of catalysts control the overall yield of the process (Mirzaei et al. 2017). For example, Peristic et al. (2016) concluded that both adsorption and oxidation contribute in the diclofenac and TOC removal under heterogeneous photo-Fenton process with Fe-ZSM5 and UVA lamp. Also, Singh et al. (2016) reported that the faster rate and higher degradation efficiency of Congo dye under heterogeneous Fenton-like process is attributed to the synergic effect between adsorption and Fenton-like catalysis.

Several materials have been already used as catalyst supports in heterogeneous Fenton process such as Pillared clay, activated carbon and synthetic zeolite (Arimi 2017, Mirzaei et al. 2017). Activated carbon and synthetic zeolites adsorbents are the most used heterogeneous support materials due to their high effectiveness. Activated carbon can be used as a promising support for the heterogeneous Fenton reaction due to its large surface area, high stability in acidic or alkaline environments and wide availability (Jaafarzadeh et al. 2015, Lan et al. 2015). These factors provide a simultaneous adsorption and catalytic oxidation of soluble pollutants (Mirzaei et al. 2017). However, the use of activated carbon catalyst is limited by its high costs as well as the production of large amount of sludge (Arimi 2017). Also, the hydroxyl radicals produced by bare activated carbon need a long reaction time for the oxidation of contaminants to achieve sufficient removal (Mirzaei et al. 2017).

9.1 Zeolites catalyst for heterogeneous photo-Fenton process

Zeolites are hydrated aluminosilicate materials that can occur naturally and can be synthesized by a reaction between aluminate source (such as sodium aluminate) with silicate source (such as sodium silicate) (Arimi 2017). Zeolites are characterized by the presence of high external and internal surface areas up to several hundred square meters per gram, cage-like structures, porous structure, and high cation exchange capacity. Due to these appealing characteristics, zeolites can be used as ion exchange resins, adsorbent to remove organic contaminants from aquatic media (Kasiri et al. 2008), and a catalyst support in heterogeneous photo-Fenton processes. The Table 10 lists some

of the zeolite-based heterogeneous Fenton systems that display high removal efficiency toward the removal and degradation of different organic pollutants (Mirzaei et al. 2017).

Table 10. Selected studies on application of zeolite-based heterogeneous Fenton systems in the removal of organic pollutants.

Pollutant	Process	Experimental conditions	Results	Ref.
Orange II azo dye	Heterogeneous Fenton-like process using zeolite-Fe catalyst	5 wt. % iron loading [OH] ₀ = 0.1 mM [H ₂ O ₂] ₀ = 6 mM pH = 3, T = 30 °C	Complete oxidation of orange II after 2 h	(Rache et al. 2014)
Molasses distillery wastewater (MDW).	Heterogeneous Fenton process using modified natural zeolite	150 g/L pellet catalyst [H ₂ O ₂] ₀ = 2 g/L T = 25 °C	90 % color removal 60 % TOC removal Improvements in biodegradability of anaerobic effluent from 0.07 to 0.55	(Arimi 2017)
Acid red 1 azo dye (AR1)	Fe-zeolite Y type catalyst	0.8 wt. % iron loading [catalyst] = 2.5 g/L [H ₂ O ₂] ₀ = 16 mM [AR1] ₀ = 50 mg/L pH = 2.5, T = 30 °C	99 % of decolorization within 60 min of reaction time	(Hassan et al. 2011)
Phenol	Photo-Fenton process with immobilized Fe(III)-HY under UV light: Comparison to homogeneous photo-Fenton process	0.25 wt. % Fe(III)-HY [catalyst] = 0.5 g/L [H ₂ O ₂] ₀ = 10 ⁻³ M [Phenol] ₀ = 10 ⁻⁴ M pH = 5.6	Total degradation of phenol but with higher reaction rate, less irradiation time and wider pH range in heterogeneous photo-fenton process. 5-10 % degradation under photolysis (UV only) and 25-30 % with catalyst and UV. Complete degradation after 60 min with heterogeneous photo-Fenton system, with no change in the concentration with catalyst and H ₂ O ₂ only.	(Noorjah an et al. 2005)
Congo dye	Heterogeneous Fenton-like process based on Cu-impregnated zeolite Y: Comparison to homogeneous Fenton process.	7.5 wt. % Cu loading [catalyst] = 1 g/L [H ₂ O ₂] ₀ = 52.24 m M [Congo dye] ₀ = 0.143 mM pH = 7 T = 60 °C	93.58 % degradatio after 2.5 h 95.34 % decolorization after 2 h 79.52 % mineralization after 4 h No removal with H ₂ O ₂ alone while 4 % removal with catalyst and H ₂ O ₂ . 20% removal after 120 min with homogeneous Fenton process and 98 % removal with heterogeneous Fenton-like process.	(Rivera-Utrilla et al. 2013c)

By using zeolites as a support catalyst in the heterogeneous photo-Fenton processes, the organic pollutants can be adsorbed on the surface of the catalyst which enhances their removal. Thus there is a role for the adsorption process that should be taken into consideration beside the Fenton reaction (reaction between iron ions and hydrogen peroxide) or the direct photolysis of H_2O_2 and contaminants (Kušić et al. 2006). Another advantage for zeolites is the presence of a strong electrostatic field inside their pores that slows down the leaching of iron from Fe-zeolite catalyst during the reaction (Kasiri et al., 2008, Mirzaei et al. 2017).

Comparing natural and synthetic zeolites, even though the former are cheap, abundant and used before for the removal of dyes in wastewater effluents, but they did not show great results in the removal. Moreover, their main limitation in Fenton process is their low effectiveness especially when the wastewater is loaded with high amounts of organic matter. Synthetic zeolites have been used as heterogeneous catalyst for Fenton oxidation in wastewater treatment due to their high effectiveness (> 80 % TOC and 100 % color removal. They are able to work well at pH 5 and the accumulation of heavy metals in the treated wastewater effluent decreases by 17 fold compared to homogeneous Fenton process. Faujasite are a type of aluminosilicate zeolites combining a 3-dimensional network of accessible micropores (0.74 nm) with an organic-free synthesis (Verboekend et al. 2016). The ratio of silica to the alumina in synthetic zeolites determines the type (X or Y) of the zeolite used named Faujasite (Arimi 2017). Faujasite with Si/Al ratio lower than 1.5 corresponds to Faujasite X while Faujasite Y has a value higher than this value (Lutz 2014). The low Si/Al ratio of Faujasite X offers a large-exchange capacity governed by the high aluminum content (Neamu et al. 2004b) making it usable as ion exchange, molecular sieve and adsorbent. But its usage in catalysis is limited due to the instability of its protonic form (Verboekend et al. 2016). As a result, a more stable less-acidic Faujasite Y is the most commonly applied in preparation of heterogeneous Fenton (Arimi 2017) due to its improved catalytic and hydrothermal stability as observed in numerous petrochemical applications (Verboekend et al. 2016).

To produce heterogeneous Fenton catalyst from synthetic zeolite, ion exchange method and wet impregnation method can be used. The preparation of Fe-zeolite catalyst by ion exchange method is relatively simple due to the zeolite's cation exchange capability (Mirzaei et al. 2017) where sodium content is replaced with iron ions (Arimi 2017). It works by suspending the zeolite several times in the aqueous solution of the metal salt, followed by filtration, washing, drying, and activation at high temperature. This method is associated with several limitations such as the need of high solvent volume, high metallic content in the solvent and slow rate and poor control of metallic

loading. The wet impregnation method comes to solve some of the limitations of the aqueous ion exchange (AIE) due to its faster operating time, absence of residual solvent and additional filtration steps and finally better control of metal loading. By this method, zeolite is mixed with small volume of the iron salt solution in water or ethanol, where the solvent is continuously evaporated for the metal ions to substitute into the pores by capillary forces ([Singh et al. 2016](#)).

10 Analytical methodology for analysis, detection and quantification of micropollutants in water

10.1 Solid phase extraction (SPE)

The pre-concentration of the water samples by using solid phase extraction is an important analytical step to be considered especially when dealing with micropollutants in water at very low concentration. Most studies reported the use of liquid-liquid extraction (LLE), but the recent studies focus on the use of solid phase extraction (SPE, Fig. 9) due to several advantages over LLE including simplicity, reproducibility and applicability ([Rodriguez-Narvaez et al. 2017a](#)).



Fig. 9. Solid phase extraction machine.

The main importance of pre-concentration of the water samples before the final quantification is to lower the detection limits (LOD) and quantification limits (LOQ) of the quantification method, and thus to enhance the efficiency of the detection and quantification of the compounds. As an example, this is confirmed by one of the studies done by Miralles-Cuevas et al. ([2014](#)) who compared the LOQ and LOD for some micropollutants with and without SPE treatment as shown in Table 11. Beside pre-concentration, this method is also used to remove the interfering components of the complex matrices in order to obtain a cleaner extract containing the analytes of interest for easier and efficient quantification ([Zwir-Ferenc et al. 2006](#)).

Table 11. LOQ and LOD in (µg/L) of some micropollutants with and without SPE treatment.

Micropollutants	Without SPE		With SPE	
	LOQ (µg/L)	LOD (µg/L)	LOQ (µg/L)	LOD (µg/L)
Carbamazepine	6.0	2.0	0.4	0.1
Flumequine	3.0	1.0	0.2	0.06
Ibuprofen	6.0	1.9	0.4	0.1
Ofloxacin	3.0	1.0	0.2	0.06
Sulfamethoxazole	3.0	0.99	0.2	0.06

The applicability of SPE is mainly determined by the type of sorbent used in the extraction column. Solid phase extraction is performed mostly using either silica-based or organic resin-based sorbents, with specific physical and chemical properties. The choice of the sorbent to be used depends on the nature of the compounds of interest needed to extract (Zwir-Ferenc et al. 2006). Several papers reported on the evaluation of a number of sorbent material (stationary phases) for solid phase extraction (SPE) in case of micropollutants especially pharmaceuticals. Some indicated C18 silica sorbents for acidic non-steroidal anti-inflammatory drugs, and others reported Oasis MCX mixed mode sorbent for the polar to medium-polar pharmaceuticals. High recoveries were obtained by the polymeric Oasis HLB cartridges. Beside their high recoveries, Oasis HLB cartridges can exceptionally work at neutral pH range even when working with compounds (such as non-steroidal anti-inflammatory drugs) that need acidic pH regulation of the sample in order to achieve reproducible and high recoveries. This is due to their chemical composition that is formed of lipophilic divinylbenzene and the hydrophilic N-vinylpyrrolidone (Zwir-Ferenc et al. 2006).

The choice of an eluting solvent is determined by the relationship of strength of adsorption on silica ϵ° and the polarity of the analyte. Methanol, with high ϵ° (0.73) is mostly used as an eluate due to its unique interaction with both nonpolar and polar groups (Zwir-Ferenc et al. 2006).

The mechanism of the extraction process is achieved through the interaction of the three components: the sorbent, the analyte and the solvent. The analytes of interest are partitioned between a liquid (sample matrix or solvent with analytes) and a solid (sorbent) phase where they must be attracted more strongly to the sorbent material. Fig. 10. shows the main steps of the solid phase extraction process including (Zwir-Ferenc et al. 2006) :

- 1) loading a solution onto the SPE solid phase,
- 2) Washing away undesired components,
- 3) Washing off the desired analytes with another solvent into a collection tube.

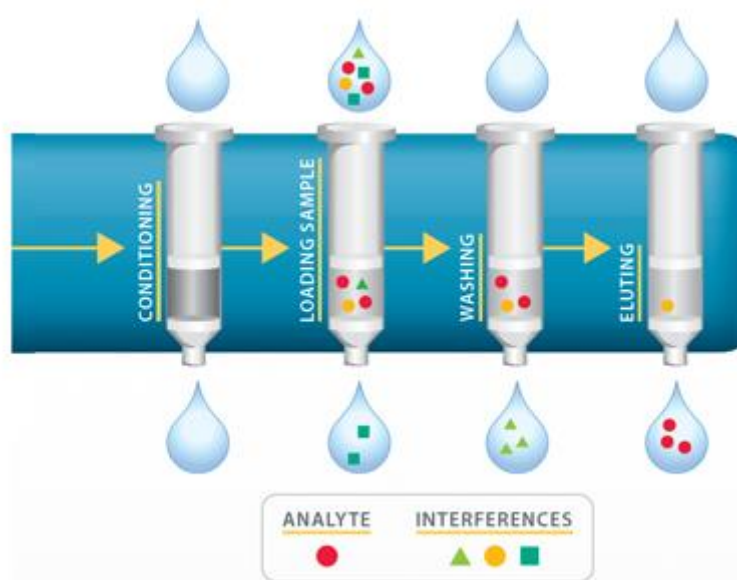


Fig. 10. Solid Phase Extraction steps.

10.2 Liquid chromatography coupled to double mass spectrometry (LC-MS/MS)

Due to the increasing discovery of PPCPs and EDCs in environmental matrices, different analytical techniques for the detection and quantification of persistent organic contaminants have been developed within the last 10–15 years (Tijani et al. 2013b). The identification and quantification of these compounds requires highly sophisticated multi-residue analytical methodologies which are able to detect and quantify micropollutants from different classes with different chemical structures and physical-chemical properties presenting at low concentrations of nanograms per liter level (ng/L) (Rodriguez-Narvaez et al. 2017a). Thus, a compromise in the selection of experimental conditions is required to determine all the present compounds accurately (Petrović et al. 2005). Table 12 lists some examples of recent advances in analytical tools available for emerging contaminants analysis in surface and groundwater and wastewater samples (Rodriguez-Narvaez et al. 2017a). Based on the table, the main multi-residue analytical method used for ECs is solid-phase extraction as a sample preparation method and almost exclusively liquid

chromatography coupled to mass spectrometry with double MS systems (LC-MS/MS) using mainly electrospray ionization for separation and quantification of up to 30 compounds on C18 column ([Kasprzyk-Hordern et al. 2007](#), [Rodriguez-Narvaez et al. 2017a](#)). It has allowed the detection and quantification of around 3000 biologically active compounds at low concentration levels ($\mu\text{g-ng/L}$) in very complex matrixes as in wastewater and in surface and ground waters ([Richardson 2012](#), [Rivera-Utrilla et al. 2013c](#)).

The coupling of MS to liquid chromatography in such analysis allow accurate identification and quantification of specific pollutants even in complex matrices ([Rodriguez-Narvaez et al. 2017a](#)) due to its selectivity, sensitivity and specificity that lease to significant advancements reported in recent years studies. Although it has been demonstrated that HPLC, a low cost technology, with diode array UV absorbance and fluorescence detection can be suited in some cases for micropollutants analysis in surface and wastewater, the coupling with MS detection is state-of-the-art and out of question for trace analysis of micropollutants ([Buchberger 2011](#)).

According to literature, different advanced mass analyzer types can be used in MS such as triple quadrupole (QqQ) and ion trap (IT) that allow ECs quantification in the ng/L level and linear ion traps (LITs) quadrupole, triple quadrupole, quadrupole time of flight (QqTOF) and quadrupole-linear ion trap (QqLIT) more specifically used for transformation products structure elucidation ([Rodriguez-Narvaez et al. 2017a](#)). Moreover, the increasing availability of chromatographic separation columns with improved hardware also plays a role in improving the separation of micropollutants of different groups.

Table 12. Advanced analytical methodologies used for analysis and quantification of micropollutants (Rodriguez-Narvaez et al. 2017a).

Micropollutants	Pre-treatment method	Quantification method	Sample type and recoveries
27 ECs including Phs, sunscreens, fragrances, antiseptics, fire retardants	Methylation of carboxyl groups with trimethylsulfonium hydroxide at 270 °C	Gas chromatography-Mass spectrometry (GC-MS) with electron impact mode (70 eV ionization energy) using a TRB5-MS column (5 % diphenyl-95 % dimethylpolisoxane)	Wastewater. LOD and LOQ in the range 1-40 and 3-80 ng/L, respectively. Recoveries and repeatability were greater than 80 %
105 Phs and life-style products, 21 drugs of abuse, metabolites	SPE using polymeric cartridges	Liquid chromatography electrospray time-of-flight mass spectrometry in positive and negative modes	Surface and wastewater. LOQ ranged 0.2-777.9 mg/L
8 artificial sweeteners	Reverse phase SPE extraction for sample pre-concentration and clean-up	LC-MS and LC-MS/MS with electrospray interface (ESI)	Surface and drinking water. LOD in the range of 0.82 and 2.8 µg/L
44 Phs and 13 EDCs	Pressurized liquid extraction, SPE purification	Ultra-performance liquid chromatograph coupled to a mass spectrometer (UPLC-MS/MS)	River water and biofilms. LOD in the range 0.2-2.4 ng/g for EDCs and 0.07-6.7 ng/g for Phs.
90 ECs including Phs and estrogens	Microwave assisted extraction (MAE) protocol followed by SPE	UPLC-MS/MS with ESI and using an Acquity BEH C18 column for both positive and negative modes	Recoveries in the range 40-152 %. LOQ from 0.1 to 24.1 ng/L
8 ECs including PFCs and Phs	Polar organic chemical integrative samples (POCIS) for in-situ pre-concentration	Fast LC-MS/MS with ESI and using a Zorbax XBD-C18 column	Drinking water. Concentration in the range 4.2-15.9 ng/L

11 Selected compounds studied

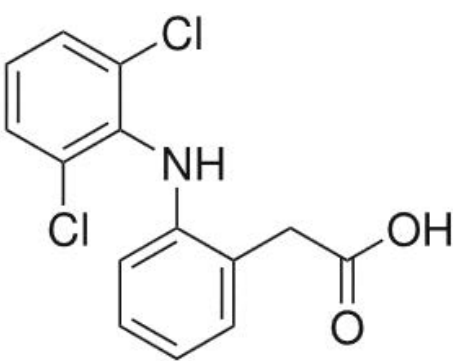
In the following part, we describe more precisely the 2 pollutants phenol and diclofenac, that will be used in our experimental work to test the efficiency of our removal process and optimize the different parameters.

11.1 Diclofenac

Diclofenac (2-(2-(2,6-dichlorophenylamino)phenyl)acetic acid)(DCF) is a common arylacetic non-steroidal anti-inflammatory drug (NSAID) (Zhang et al. 2008). It is taken as oral tablets or used as a topical gel to reduce inflammation, relieve pain (menstrual pain), also it works as an analgesic in the cases of arthritis or acute injury. It is sold under the commercial names of Acoflam, Antiflam, Diclomex, Jutafenac, Monoflam, Voltaren (Vieno et al. 2014).

Diclofenac is a polar compound with high water solubility and low potential to volatilize. It is a weak acid with pKa values ranging from 4.15 to 4.91. Table 13 shows some of its physical-chemical properties.

Table 13: Structure and physical-chemical properties of diclofenac (Mongeot 2013, Vieno et al. 2014).

Diclofenac	Parameter	Value
	Molecular weight	296.2 g/mol
	Water solubility	2.37 mg/L at 25 °C
	Henry's law constant	4.73×10^{-12} atm.m ³ /mol
	Acid/Base	Acid
	pka	4.15
	Log K _{ow}	4.51
	LogK _{oc}	2.20-3.42
	LogK _d	1.26-2.18

Diclofenac is detected in WWTP influents and effluents, surface water and ground water. In general, concentrations of NSAIDs are reported in the range of several hundred nanograms per liter in European rivers (Pérez-Estrada et al. 2005). Diclofenac is classified as the second most studied substance of the watch list in the last 10 years employing conventional processes, membrane technologies and AOPs (Barbosa et al. 2016a).

It was observed to have harmful effects on aquatic living things at environmental concentrations (Barbosa et al. 2016a). Diclofenac can bioaccumulate in the tissues of organisms ($\log K_{ow} = 4.51$) and recent studies suggested that it has the potential to cause the extinction of some organisms. Even at an extremely low concentration of 10 ng/L, diclofenac was reported to impair osmoregulatory ability of a green shore crab *Carcinusmaenas* (Vieno et al. 2014). Mehinto and co-workers emphasized that the exposure of rainbow trout species to diclofenac can change the biochemical functions of the fish damaging the tissue and affecting its gene expression even at the lowest observed effect concentration (LOEC) of 5 $\mu\text{g/L}$. Beside the parent diclofenac itself, it is reported to photo-transform producing several transformation products that themselves may pose a risk to the aquatic organisms. Although it has been proven to rapidly degrade by direct photolysis under normal environmental conditions, it is still one of the most frequently detected compounds in the water at concentrations up to 1.2 $\mu\text{g/L}$ (Pérez-Estrada et al. 2005) which indicates its persistence in the WWTP effluents. Therefore studies to implement efficient removal processes in the WWTP have been widely made to decrease its discharge into different water bodies (Vieno et al. 2014).

The removal of diclofenac is studied in different articles and reviews in the last few years (Fatta-Kassinos et al. 2011, Petrie et al. 2013, Barra Caracciolo et al. 2015). As a summary, diclofenac is poorly biodegradable and can be partially adsorbed on sludge, thus low removal rates are obtained during biological wastewater treatment (Vieno et al. 2014). The removal by membrane technologies have been used, but more research is needed. Using AOPs, the removal of diclofenac is mostly studied with heterogeneous photocatalysis and/or photo-Fenton.

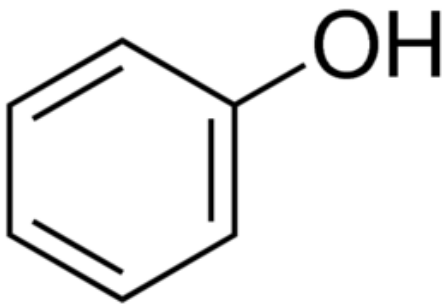
11.2 Phenol

Phenol is an aromatic organic pollutant found in industrial effluent especially in effluents from coal conversion plants, resin-manufacturing plants, oil refineries, pharmaceuticals and fruit processing industries (Khalid et al. 2004, Edalatmanesh et al. 2008). It has received a great attention because of its toxicity even at low concentration (Barakat et al. 2005). The Table 14 shows some of

the chemical and physical properties of phenol. It is a hygroscopic crystalline solid at ambient temperature and pressure with white color when pure (mostly colored due to presence of impurities). It has a limited solubility in water where it behaves as a weak acid. It is highly soluble in ethyl alcohol, ether, polar solvents and hydrocarbons. In recent days, phenol is produced at a rate of about 6 million ton/year worldwide with a significantly increasing trend (Busca et al. 2008). It is a natural constituent of many substances such as smoked food, wine and tea. It is used as a raw material in many chemical, petrochemical and pharmaceutical industries (Barakat et al. 2005). It is used in the preparation of cream and shaving soap (due to its germicidal and local anesthetic properties), primary petrochemical intermediate, peptizing agent in glue, building block for the synthesis of pharmaceuticals such as aspirin, and many other uses (Busca et al. 2008). Phenol reacts with acetone to form bisphenol A.

The sterilizing activity of phenol was discovered by the English surgeon Joseph Lister in 1865 (Busca et al. 2008). When present in wastewater and water bodies, it can cause antibacterial actions even at small concentrations. Also it can slow down or inhibit the degradation of other presenting organic compounds. The limiting concentration for which phenolic compounds have no inhibitory effects was determined to be between 400 and 600 mg/L (Edalatmanesh et al. 2008). Phenol has a germicidal activity due to its protein denaturing ability. In cases of exposure, it is rapidly absorbed through the skin and inside the eyes causing comas, convulsions and death in cases of overexposure (for example ingestion of 1 g phenol). Moreover, it can affect the liver, kidneys, lungs and vascular system (Edalatmanesh et al. 2008). In addition, phenol is considered as an intermediate product that result from the oxidation of some micropollutants. Due to all these reasons, its effective removal from wastewater is of great interest (Khalid et al. 2004), and it is taken as a model compound in advanced wastewater treatment studies with great data available on its removal especially in wastewater treatment (Edalatmanesh et al. 2008). Several methods were reported for phenol degradation including catalytic wet oxidation, heterogeneous photocatalysis, and advanced oxidation processes (Barakat et al. 2005). In recent studies, heterogeneous photo-Fenton degradation of phenolic compounds has been considered as an effective technology.

Table 14. Some of physical and chemical properties of phenol.

Phenol	Parameter	Value
	Molecular weight	94.11 g/mol
	T _{melt}	40.9 °C
	T _{boiling}	181.75 °C
	Water solubility	9.3 g _{phenol} /100 ml H ₂ O
	pKa	9.89

References

- Zwir-Ferenc A, Biziuk M (2006) Solid Phase Extraction Technique - Trends, Opportunities and Applications. 15 edition, sect. 5.
- Adeleye A. (2016) Perfluorinated compounds, bishenol A and acetaminophen in selected waste water treatment plants in and around Cape Town, South Africa. Faculty of Applied Sciences: Cape Peninsula University of Technology.
- Ahmed M.B, Zhou J, Ngo H.H, Guo W (2015) Adsorptive Removal of Antibiotics from Water and Wastewater: Progress and Challenges. *Sci. Total. Environ* 532 (novembre): 112-26.
- Al Aukidy M, Verlicchi P, Jelic A, Petrovic M, Barcelò D (2012) Monitoring Release of Pharmaceutical Compounds: Occurrence and Environmental Risk Assessment of Two WWTP Effluents and Their Receiving Bodies in the Po Valley, Italy. *Sci. Total. Environ* 438 (novembre): 15-25.
- Alaton I. A, Dogruel S, Baykal E, Gerone G (2004) Combined Chemical and Biological Oxidation of Penicillin Formulation Effluent. *J. Environ. Manag.* 73 (2): 155-63.
- An J, Zhu L, Zhang Y, Tang H (2013) Efficient visible light photo-fenton-like degradation of organic pollutants using in situ surface-modified BiFeO₃ as a catalyst. *J. Environ. Sci.* 25(6): 1213-25
- Andreozzi R, Canterino M, Marotta R, Paxeus N (2005) Antibiotic Removal from Wastewaters: The Ozonation of Amoxicillin. *J. Hazard. Mater.* 122 (3): 243-50.
- Arimi M (2017) Modified natural zeolite as heterogeneous Fenton catalyst in treatment of recalcitrants in industrial effluent. *Prog. Nat. Sci-Mater.* 27 (2): 275-82.
- Barakat M. A, Tseng J. M, Huang C. P (2005) Hydrogen peroxide-assisted photocatalytic oxidation of phenolic compounds. *Appl. Catal. B-Environ.* 59 (1): 99-104.
- Barbosa M.O, Moreira N.F.F, Ribeiro A, Pereira M, Silva A (2016a) Occurrence and Removal of Organic Micropollutants: An Overview of the Watch List of EU Decision 2015/495. *Water Res.* 94 (may): 257-79.
- Barbosa M.O, Moreira N.F.F, Ribeiro A, Pereira M, Silva A (2016b) Occurrence and Removal of Organic Micropollutants: An Overview of the Watch List of EU Decision 2015/495. *Water Res.* 94 (may): 257-79.
- Barra C.A, Topp E, Grenni P (2015) Pharmaceuticals in the Environment: Biodegradation and Effects on Natural Microbial Communities. A Review. *J. Pharmaceut. Biomed.* 106 (march): 25-36.

- Batista A.P.S, Nogueira R.F.P (2012) Parameters affecting sulfonamide photo-Fenton degradation e iron complexation and substituent group. *J. Photochem. Photobiol. A Chem.* 232: 8-13.
- Bell K.Y, Wells M.J.M, Traexler K.A, Pellegrin M.L, Morse A, Bandy J (2011) Emerging Pollutants. *Water Environ. Res.* 83 (10): 1906-84.
- Buchberger W (2011) Current Approaches to Trace Analysis of Pharmaceuticals and Personal Care Products in the Environment. *J. Chromatogr. A* 1218 (4): 603-18.
- Busca G, Berardinelli S, Resini C, Arrighi L (2008) Technologies for the Removal of Phenol from Fluid Streams: A Short Review of Recent Developments. *J. Hazard. Mater.* 160 (2-3): 265-88.
- Carbonaro S, Sugihara M, Strathmann T (2013) Continuous-Flow Photocatalytic Treatment of Pharmaceutical Micropollutants: Activity, Inhibition, and Deactivation of TiO₂ Photocatalysts in Wastewater Effluent. *Appl. Catal. B-Environ.* 129 (january): 1-12.
- Catala M, Domínguez-Morueco N, Migens A, Molina R, Martínez F, Valcarcel Y, Mastroianni N, Lopez de Alda M, Barcelo D, Segura Y (2015) Elimination of drugs of abuse and their toxicity from natural waters by photo-Fenton treatment. *Sci. Total Environ.* 520: 198-205.
- Choi J, Lee H, Choi Y, Kim S, Lee S, Lee S, Choi W, Lee J (2014) Heterogeneous Photocatalytic Treatment of Pharmaceutical Micropollutants: Effects of Wastewater Effluent Matrix and Catalyst Modifications. *Appl. Catal. B-Environ.* 147 (april): 8-16.
- Cortes Munoz J. E, Calderon Molgora C. G, Martin A, Espino de la O E. E, Gelover Santiago S. L, Hernandez Martinez C. L, Moeller Chavez G. E (2013) Endocrine Disruptors in Water Sources: Human Health Risks and EDs Removal from Water Through Nanofiltration. In *International Perspectives on Water Quality Management and Pollutant Control*, edited by Quinn N.W.T. InTech.
- Crane M, Watts C, Boucard T (2006) Chronic Aquatic Environmental Risks from Exposure to Human Pharmaceuticals. *Science of The Total Environment* 367 (1): 23-41.
- Das S, Mitra Ray N, Wan J, Khan A, Chakraborty T, B. Ray M (2017a) Micropollutants in Wastewater: Fate and Removal Processes. In *Physico-Chemical Wastewater Treatment and Resource Recovery*, edited by Robina Farooq et Zaki Ahmad. InTech.
- Das S, Mitra Ray N, Wan J, Khan A, Chakraborty T, B. Ray M (2017a) Micropollutants in Wastewater: Fate and Removal Processes. In *Physico-Chemical Wastewater Treatment and Resource Recovery*, edited by Farooq R. and Ahmad Z. InTech.
- Daughton C. G (2010) Pharmaceutical Ingredients in Drinking Water: Overview of Occurrence and Significance of Human Exposure. In *Contaminants of Emerging Concern in the Environment*:

- Ecological and Human Health Considerations, edited by Halden R.U, 1048: 9-68. Washington, DC: American Chemical Society.
- Daughton C.G, Ternes T.A (1999) Pharmaceuticals and personal care products in the environment: agents of subtle change? *Environ. Health. Persp* 107 (Suppl 6): 907-38.
- De Luca A, Dantas R.f, Simões A. S. M, Toscano I. A. S, Lofrano G, Cruz A, Esplugas S (2013) Atrazine Removal in Municipal Secondary Effluents by Fenton and Photo-Fenton Treatments. *Chem. Eng. Technol.* 36 (12): 2155-62.
- Deblonde T, Cossu-Leguille C, Hartemann P (2011) Emerging Pollutants in Wastewater: A Review of the Literature. *Int. J. Hyg. Envir. Heal.* 214 (6): 442-48.
- Diamanti-Kandarakis E, Bourguignon JP, Giudice L.C, Hauser R, Prins G.S, Soto A.M, Zoeller R.T, Gore A.C (2009) Endocrine-Disrupting Chemicals: An Endocrine Society Scientific Statement. *Endocr. Rev.* 30 (4): 293-342.
- Directive, 2000. 2000/60/EC of the European Parliament and of the Council of 23 October 2000 establishing a framework for Community action in the field of water policy. *Off. J. Eur. Commun.* L327, 1-72.
- Directive, 2008. 2008/105/EC of the European Parliament and of the Council of 16 December 2008 on environmental quality standards in the field of water policy, amending and subsequently repealing Council Directives 82/176/EEC, 83/513/EEC, 84/156/EEC, 84/491/EEC, 86/280/EEC and amending Directive 2000/60/EC of the European Parliament and of the Council. *Off. J. Eur. Union* L348, 84-97.
- Directive, 2013. 2013/39/EU of the European Parliament and of the Council of 12 August 2013 amending Directives 2000/60/EC and 2008/105/EC as regards priority substances in the field of water policy. *Off. J. Eur. Union* L226, 1-17.
- Doll T.E, Frimmel F.H (2005) Photocatalytic Degradation of Carbamazepine, Clofibric Acid and Iomeprol with P25 and Hombikat UV100 in the Presence of Natural Organic Matter (NOM) and Other Organic Water Constituents. *Water Res.* 39 (2-3): 403-11.
- Du Z, Deng S, Bei Y, Huang Q, Wang B, Huang J, Yu G (2014) Adsorption Behavior and Mechanism of Perfluorinated Compounds on Various Adsorbents—A Review. *J. Hazard. Mater.* 274 (june): 443-54.
- Edalatmanesh M, Dhib R, Mehrvar M (2008) Kinetic Modeling of Aqueous Phenol Degradation by UV/H₂O₂ Process. *Int. J. Chem. Kinet.* 40 (1): 34-43.
- Elmolla E, Chaudhuri M (2009a) Improvement of biodegradability of synthetic amoxicillin wastewater by photo-Fenton process. *World Appl. Sci. J.* 5: 53-58.

- Elmolla E, Chaudhuri M (2009) Optimization of Fenton Process for Treatment of Amoxicillin, Ampicillin and Cloxacillin Antibiotics in Aqueous Solution. *J. Hazard. Mater.* 170 (2-3): 666-72.
- Elmolla E, Chaudhuri M (2010c) Photocatalytic degradation of amoxicillin, ampicillin and cloxacillin antibiotics in aqueous solution using UV/TiO₂ and UV/ H₂O₂/TiO₂ photocatalysis. *Desalination* 252: 46-52.
- Environmental Protection Agency (2014) Emerging Contaminants – Perfluorooctane Sulfonate (PFOS) and Perfluorooctanoic Acid (PFOA) .
- Esplugas S, Bila D.M, Krause L.G.T, Dezotti M (2007) Ozonation and Advanced Oxidation Technologies to Remove Endocrine Disrupting Chemicals (EDCs) and Pharmaceuticals and Personal Care Products (PPCPs) in Water Effluents. *J. Hazard. Mater.* 149 (3): 631-42.
- Fatta-Kassinos D, Vasquez M.I, Kümmerer K (2011) Transformation Products of Pharmaceuticals in Surface Waters and Wastewater Formed during Photolysis and Advanced Oxidation Processes – Degradation, Elucidation of Byproducts and Assessment of Their Biological Potency. *Chemosphere* 85 (5): 693-709.
- Feng L, Hullebusch E, Rodrigo M.A, Esposito G, Oturan M.A (2013) Removal of Residual Anti-Inflammatory and Analgesic Pharmaceuticals from Aqueous Systems by Electrochemical Advanced Oxidation Processes. A Review. *Chem. Eng. J.* 228 (july): 944-64.
- Fenton H. J. H (1894) LXXIII.—Oxidation of Tartaric Acid in Presence of Iron. *J. Chem. Soc. Trans.* 65 (0): 899-910.
- Field J. A, Annette Johnson C, Rose J.B (2006) What Is “Emerging”? *Environ. Sci. Technol.* 40 (23): 7105-7105.
- Futran Fuhrman V, Tal A, Arnon S (2015) Why Endocrine Disrupting Chemicals (EDCs) Challenge Traditional Risk Assessment and How to Respond. *J. Hazard. Mater.* 286 (april): 589-611.
- Giri A.S, Golder A.K (2014) Fenton, photo-fenton, H₂O₂ photolysis, and TiO₂ photocatalysis for dipyrone oxidation: drug removal, mineralization, biodegradability, and degradation mechanism. *Ind. Eng. Chem. Res.* 53: 1351-1358.
- Gonzalez O, Sans C, Esplugas S, Malato S (2009) Application of solar advanced oxidation processes to the degradation of the antibiotic sulfamethoxazole. *Photochem. Photobiol. Sci.* 8: 1032-1039.
- Gonzalez-Olmos R, Martin M.J, Georgi A, Kopinke F.D, Oller I, Malato S (2012) Fe-Zeolites as Heterogeneous Catalysts in Solar Fenton-Like Reactions at Neutral pH. *Appl. Catal. B-Environ.* 125: 51-58.

- Grassi M, Rizzo L, Farina A (2013a) Endocrine Disruptors Compounds, Pharmaceuticals and Personal Care Products in Urban Wastewater: Implications for Agricultural Reuse and Their Removal by Adsorption Process. *Environ. Sci. Pollut. Res.* 20 (6): 3616-28.
- Grassi M, Rizzo L, Farina A (2013b) Endocrine Disruptors Compounds, Pharmaceuticals and Personal Care Products in Urban Wastewater: Implications for Agricultural Reuse and Their Removal by Adsorption Process. *Environ. Sci. Pollut. Res.* 20 (6): 3616-28.
- Grassi M, Rizzo L, Farina A (2013b) Endocrine disruptors compounds, pharmaceuticals and personal care products in urban wastewater: implications for agricultural reuse and their removal by adsorption process. *Environ. Sci. Pollut. Res.* 20 (6): 3616-28.
- Hassan H, Hameed B. H (2011) Oxidative decolorization of Acid Red 1 solutions by Fe-zeolite Y type catalyst . *Desalination* 276 (1): 45-52.
- Heberer T (2002) Occurrence, Fate, and Removal of Pharmaceutical Residues in the Aquatic Environment: A Review of Recent Research Data. *Toxicol. Lett.* 131 (1-2): 5-17.
- Hecker M, Giesy J.P (2008) Novel Trends in Endocrine Disruptor Testing: The H295R Steroidogenesis Assay for Identification of Inducers and Inhibitors of Hormone Production. *Anal. Bioanal. Chem.* 390 (1): 287-91.
- Homem V, Santos L (2011) Degradation and Removal Methods of Antibiotics from Aqueous Matrices – A Review . *J. Environ. Manag.* 92 (10): 2304-47.
- Hou J, Pan B, Niu X, Chen J, Xing B (2010a) Sulfamethoxazole Sorption by Sediment Fractions in Comparison to Pyrene and Bisphenol A. *Environ. Pollut.* 158 (9): 2826-32.
- Hou J, Pan B, Niu X, Chen J, Xing B (2010a) Sulfamethoxazole Sorption by Sediment Fractions in Comparison to Pyrene and Bisphenol A. *Environ. Pollut.* 158 (9): 2826-32.
- Iglesias A, Nebot C, Vázquez B.I, Miranda J.M, Franco Abuín C.M, Cepeda A (2014) Detection of Veterinary Drug Residues in Surface Waters Collected Nearby Farming Areas in Galicia, North of Spain. *Environ. Sci. Pollut. Res.* 21 (3): 2367-77.
- Jaafarzadeh N, Kakavandi B, Takdastan A, Kalantary R, Azizi M, Jorfi S (2015) Powder Activated Carbon/Fe Hybrid Composite as a Highly Efficient Heterogeneous Catalyst for Fenton Oxidation of Tetracycline: Degradation Mechanism and Kinetic. *RSC Advances* 5 (103): 84718-28.
- Jelic A, Gros M, Ginebreda A, Cespedes-Sánchez R, Ventura F, Petrovic M, Barcelo D (2011) Occurrence, Partition and Removal of Pharmaceuticals in Sewage Water and Sludge during Wastewater Treatment. *Water Res.* 45 (3): 1165-76.

- Jjemba P.K (2006) Excretion and Ecotoxicity of Pharmaceutical and Personal Care Products in the Environment. *Ecotox. Environ. Safe.* 63 (1): 113-30.
- Margot J (2015) Micropollutant removal from municipal wastewater - From conventional treatments to advanced biological processes. *École Polytechnique Fédérale De Lausanne.*
- Justo A, González O, Aceña J, Pérez S, Barceló D, Sans C, Esplugas S (2013) Pharmaceuticals and Organic Pollution Mitigation in Reclamation Osmosis Brines by UV/H₂O₂ and Ozone. *J. Hazard. Mater.* 263 (december): 268-74.
- Justo A, González Ó, Aceña J, Mita L, Casado M, Pérez S, Piña B, Sans C, Barceló D, Esplugas S (2014) Application of Bioassay Panel for Assessing the Impact of Advanced Oxidation Processes on the Treatment of Reverse Osmosis Brine: Toxicity and Pharmaceuticals Removal from Reverse Osmosis Brine by AOPs. *J. Chem. Technol. Biot.* 89 (8): 1168-74.
- Justo A, González Ó, Sans, Esplugas S (2015) BAC Filtration to Mitigate Micropollutants and EfOM Content in Reclamation Reverse Osmosis Brines. *Chem. Eng. J.* 279 (november): 589-96.
- Kabir E.R, Rahman M.S, Rahman I (2015) A Review on Endocrine Disruptors and Their Possible Impacts on Human Health. *Environ. Toxicol. Phar.* 40 (1): 241-58.
- Kasprzyk-Hordern B, Dinsdale R.M, Guwy A.J (2007) Multi-Residue Method for the Determination of Basic/Neutral Pharmaceuticals and Illicit Drugs in Surface Water by Solid-Phase Extraction and Ultra Performance Liquid Chromatography–positive Electrospray Ionisation Tandem Mass Spectrometry. *J. Chromatogr. A* 1161 (1-2): 132-45.
- Khalid M, Joly G, Renaud A, Magnoux P (2004) Removal of Phenol from Water by Adsorption Using Zeolites. *Ind. Eng. Chem. Res.* 43 (17): 5275-80.
- Kidd K. A, Blanchfield P. J, Mills K. H, Palace V. P, Evans R. E, Lazorchak J. M, Flick R. W (2007) Collapse of a Fish Population after Exposure to a Synthetic Estrogen. *P. Natl. A. Sci.* 104 (21): 8897-8901.
- Klamerth N, Rizzo L, Malato S, Maldonado M.I, Agüera A, Fernández-Alba A.R (2010) Degradation of Fifteen Emerging Contaminants at mg L⁻¹ Initial Concentrations by Mild Solar Photo-Fenton in MWTP Effluents. *Water Res.* 44 (2): 545-54.
- Kosma C.I, Lambropoulou D.A, Albanis T.A (2010) Occurrence and Removal of PPCPs in Municipal and Hospital Wastewaters in Greece. *J. Hazard. Mater.* 179 (1-3): 804-17.

- Kušić H, Koprivanac N, Selanec I (2006) Fe-Exchanged Zeolite as the Effective Heterogeneous Fenton-Type Catalyst for the Organic Pollutant Minimization: UV Irradiation Assistance. *Chemosphere* 65 (1): 65-73.
- Lai, W.W.P, Lin Y.C, Tung H.H, Lo S.L, Yu-Chen Lin A (2016) Occurrence of Pharmaceuticals and Perfluorinated Compounds and Evaluation of the Availability of Reclaimed Water in Kinmen. *Emerging Contaminants* 2 (3): 135-44.
- Lan H, Wang A, Liu R, Liu H, Qu J (2015) Heterogeneous Photo-Fenton Degradation of Acid Red B over Fe₂O₃ Supported on Activated Carbon Fiber. *J. Hazard. Mater.* 285 (march): 167-72.
- Lapworth D.J, Baran N, Stuart M.E, Ward R.S (2012) Emerging Organic Contaminants in Groundwater: A Review of Sources, Fate and Occurrence. *Environ. Pollut.* 163 (april): 287-303.
- Liu Z, Kanjo Y, Mizutani S (2009) Removal Mechanisms for Endocrine Disrupting Compounds (EDCs) in Wastewater Treatment -Physical Means, Biodegradation, and Chemical Advanced Oxidation: A Review. *Sci. Total. Environ.* 407 (2): 731-48.
- Luo Y, Guo W, Ngo H.H, Nghiem L.D, Hai F, Zhang J, Liang S, Wang X.C (2014) A Review on the Occurrence of Micropollutants in the Aquatic Environment and Their Fate and Removal during Wastewater Treatment. *Sci. Total. Environ.* 473-474 (march): 619-41.
- Lutz W (2014) Zeolite Y: Synthesis, Modification, and Properties-A Case Revisited. *ADV. MATER. SCI. ENG.* 2014 : 20 pages
- Machulek A, Vautier-Giongo C, Moraes J.E.F, Nascimento C.A.O, Quina F.H (2006) Laser Flash Photolysis Study of the Photocatalytic Step of the Photo-Fenton Reaction in Saline Solution†. *Photochemistry and Photobiology* 82 (1): 208.
- Maletz S, Floehr T, Beier S, Klümper C, Brouwer A, Behnisch P, Higley E, et al. (2013) In Vitro Characterization of the Effectiveness of Enhanced Sewage Treatment Processes to Eliminate Endocrine Activity of Hospital Effluents. *Water Res.* 47 (4): 1545-57.
- Martín J, Santos J.L, Aparicio I, Alonso E (2015) Pharmaceutically Active Compounds in Sludge Stabilization Treatments: Anaerobic and Aerobic Digestion, Wastewater Stabilization Ponds and Composting. *Sci. Total. Environ.* 503-504 (january): 97-104.
- Matthiessen P, Arnold D, Johnson A.C, Pepper T.J, Pottinger T.G, Pulman K.G.T (2006) Contamination of Headwater Streams in the United Kingdom by Oestrogenic Hormones from Livestock Farms. *Sci. Total. Environ.* 367 (2-3): 616-30.

- Méndez-Arriaga F, Esplugas S, Giménez J (2010) Degradation of the Emerging Contaminant Ibuprofen in Water by Photo-Fenton. *Water Res.* 44 (2): 589-95.
- Michael I, Hapeshi E, Michael C, Fatta-Kassinos D (2010) Solar Fenton and Solar TiO₂ Catalytic Treatment of Ofloxacin in Secondary Treated Effluents: Evaluation of Operational and Kinetic Parameters. *Water Res.* 44 (18): 5450-62.
- Migliore L, Cozzolino S, Fiori M (2003) Phytotoxicity to and Uptake of Enrofloxacin in Crop Plants. *Chemosphere* 52 (7): 1233-44.
- Miralles-Cuevas S, Oller I, Ruiz Aguirre A, Sánchez Pérez J. A, Malato Rodríguez S (2014a) Removal of pharmaceuticals at microg L⁻¹ by combined nanofiltration and mild solar photo-Fenton. *Chem. Eng. J.* 239 (Supplement C): 68-74.
- Miralles-Cuevas S, Oller I, Ruiz Aguirre A, Sánchez Pérez J. A, Malato Rodríguez S (2014b) Removal of pharmaceuticals at microg L⁻¹ by combined nanofiltration and mild solar photo-Fenton. *Chem. Eng. J.* 239 (march): 68-74.
- Mirzaei A, Chen Z, Haghighat F, Yerushalmi L (2017) Removal of Pharmaceuticals from Water by Homo/Heterogenous Fenton-Type Processes – A Review. *Chemosphere* 174 (may): 665-88.
- Möder M, Braun P, Lange F, Schrader S, Lorenz W (2007) Determination of Endocrine Disrupting Compounds and Acidic Drugs in Water by Coupling of Derivatization, Gas Chromatography and Negative-Chemical Ionization Mass Spectrometry. *Clean – Soil, Air, Water* 35 (5): 444-51.
- Mongeot E, Potier O (2013) Veille bibliographique et mise au point d'une methode de pre-concentration de composes pharmaceutiques. Laboratoire Réactions et Génie des Procédés, ENSIC, Nancy, France.
- Muir, D.C. G., H. Howard P (2006) Are There Other Persistent Organic Pollutants? A Challenge for Environmental Chemists. *Envir. Sci. Tech.* 40 (23): 7157-66.
- Nakada N, Tanishima T, Shinohara H, Kiri K, Takada H (2006) Pharmaceutical Chemicals and Endocrine Disrupters in Municipal Wastewater in Tokyo and Their Removal during Activated Sludge Treatment. *Water Res.* 40 (17): 3297-3303.
- Nakashima T, Ohko Y, Tryk D.A, Fujishima A (2002) Decomposition of Endocrine-Disrupting Chemicals in Water by Use of TiO₂ Photocatalysts Immobilized on Polytetrafluoroethylene Mesh Sheets. *J. Photoch. Photobio. A* 151 (1-3): 207-12.

- Neamu M, Catrinescu C, Kettrup A (2004) Effect of dealumination of iron(III)-exchanged Y zeolites on oxidation of Reactive Yellow 84 azo dye in the presence of hydrogen peroxide. *APPL. CATAL. B-ENVIRON.* 51 (3): 149-57.
- Niu H, Zhang D, Zhang S, Zhang X, Meng Z, Cai Y (2011) Humic acid coated Fe₃O₄ magnetic nanoparticles as highly efficient Fenton-like catalyst for complete mineralization of sulfathiazole. *J. Hazard. Mater.* 190: 559-565.
- Noorjahan M, Durga Kumari V, Subrahmanyam M, Panda L (2005) Immobilized Fe(III)-HY: an efficient and stable photo-Fenton catalyst. *APPL. CATAL. B-ENVIRON.* 57 (4): 291-98.
- Nowotny N, Epp E, Sonntag C.V, Fahlenkamp H (2007) Quantification and Modeling of the Elimination Behavior of Ecologically Problematic Wastewater Micropollutants by Adsorption on Powdered and Granulated Activated Carbon. *Environ. Sci. Technol.* 41 (6): 2050-55.
- Ohko Y, Ando I, Niwa C, Tatsuma T, Yamamura T, Nakashima T, Kubota Y, Fujishima A (2001) Degradation of Bisphenol A in Water by TiO₂ Photocatalyst. *Environ. Sci. Technol.* (11): 2365-68.
- Ohko Y, Iuchi K.I, Niwa C, Tatsuma T, Nakashima T, Iguchi T, Kubota Y, Fujishima A (2002) 17β-Estradiol Degradation by TiO₂ Photocatalysis as a Means of Reducing Estrogenic Activity. *Environ. Sci. Technol.* 36 (19): 4175-81.
- Olujimi O.O, Fatoki O.S, Odendaal J.P, Okonkwo J.O (2010) Review: Endocrine disrupting chemicals (phenol and phthalates) in the South African environment: a need for more monitoring. *Water SA* 36 (5).
- Ortiz de García S, Pinto P.P, Encina P.G, Mata R.I (2013) Consumption and Occurrence of Pharmaceutical and Personal Care Products in the Aquatic Environment in Spain. *Sci. Total Environ.* 444 (february): 451-65.
- Oulton R.L, Kohn T, Cwiertny D.M (2010) Pharmaceuticals and Personal Care Products in Effluent Matrices: A Survey of Transformation and Removal during Wastewater Treatment and Implications for Wastewater Management. *J. Environ. Monitor.* 12 (11): 1956.
- Park J.H, Wang J.J, Xiao R, Tafti N, DeLaune R.D, Seo D.C (2018) Degradation of Orange G by Fenton-like Reaction with Fe-Impregnated Biochar Catalyst. *Bioresource Technol* 249 (february): 368-76.
- Pedersen J.A, Soliman M, Suffet I. H (Mel) (2005) Human Pharmaceuticals, Hormones, and Personal Care Product Ingredients in Runoff from Agricultural Fields Irrigated with Treated Wastewater. *J. AGR. FOOD. CHEM.* 53 (5): 1625-32.

- Pedersen J.A, Yeager M.A, Suffet I. H. (Mel) (2003) Xenobiotic Organic Compounds in Runoff from Fields Irrigated with Treated Wastewater. *J. AGR. FOOD. CHEM.* 51 (5): 1360-72.
- Pérez-Estrada L.A, Malato S, Gernjak W, Agüera A, Thurman E.M, Ferrer I, Fernández-Alba A.R (2005) Photo-Fenton Degradation of Diclofenac: Identification of Main Intermediates and Degradation Pathway. *Environ. Sci. Technol.* 39 (21): 8300-8306.
- Perisic D.J, Gilja V, Stankov M.N, Katancic Z, Kusic H, Stangar U.L, Dionysiou D.D, Bozic A.L (2016) Removal of diclofenac from water by zeolite assisted advanced oxidation processes. *J. Photochem. Photobiol. A Chem.* 321: 238-247.
- Petrovic M, de Alda M. J. L, Diaz-Cruz S, Postigo C, Radjenovic J, Gros M, Barcelo D (2009) Fate and Removal of Pharmaceuticals and Illicit Drugs in Conventional and Membrane Bioreactor Wastewater Treatment Plants and by Riverbank Filtration. *PHILOS. T. ROY. SOC. A* 367 (1904): 3979-4003.
- Petrović M, Hernando M.D, Díaz-Cruz M.S, Barceló D (2005) Liquid Chromatography–tandem Mass Spectrometry for the Analysis of Pharmaceutical Residues in Environmental Samples: A Review. *J. Chromatogr A* 1067 (1-2): 1-14.
- Post G.B, Cohn P.D, Cooper K.R (2012) Perfluorooctanoic Acid (PFOA), an Emerging Drinking Water Contaminant: A Critical Review of Recent Literature. *Environ. Res.* 116 (july): 93-117.
- Potter J.M, Donnelly A (1998) Carbamazepine-10,11-epoxide in therapeutic drug monitoring. *Ther. Drug Monit.* 20 (6): 652-7.
- Prieto-Rodríguez L, Oller I, Klammerth N, Agüera A, Rodríguez E.M, Malato S (2013) Application of Solar AOPs and Ozonation for Elimination of Micropollutants in Municipal Wastewater Treatment Plant Effluents. *Water Res.* 47 (4): 1521-28.
- Pruden A, Pei R, Storteboom H, Carlson K.H (2006) Antibiotic Resistance Genes as Emerging Contaminants: Studies in Northern Colorado. *Environ. Sci. Technol.* 40 (23): 7445-50.
- Quinn B, Gagne F, Blaise C (2009) Evaluation of the Acute, Chronic and Teratogenic Effects of a Mixture of Eleven Pharmaceuticals on the Cnidarian, *Hydra Attenuata*. *Sci. Total Environ.* 407 (3): 1072-79.
- Rache M.L, García A.R, Zea H.R, Silva A.M.T, Madeira L.M, Ramírez J.H (2014) Azo-Dye Orange II Degradation by the Heterogeneous Fenton-like Process Using a Zeolite Y-Fe Catalyst-

- Kinetics with a Model Based on the Fermi's Equation. *Appl. Catal. B-Environ.* 146 (march): 192-200.
- Radjenović, J, Petrović M, Barceló D (2009) Fate and Distribution of Pharmaceuticals in Wastewater and Sewage Sludge of the Conventional Activated Sludge (CAS) and Advanced Membrane Bioreactor (MBR) Treatment. *Water Res.* 43 (3): 831-41.
- Radjenović J, Sirtori C, Petrović M, Barceló D, Malato S (2009) Solar Photocatalytic Degradation of Persistent Pharmaceuticals at Pilot-Scale: Kinetics and Characterization of Major Intermediate Products. *Appl. Catal. B-Environ.* 89 (1-2): 255-64.
- Ribeiro A.R, Nunes O.C, Pereira M.F.R, Silva A.M.T (2015a) An Overview on the Advanced Oxidation Processes Applied for the Treatment of Water Pollutants Defined in the Recently Launched Directive 2013/39/EU. *Environ. Int.* 75 (february): 33-51.
- Ribeiro A.R, Nunes O.C, Pereira M.F.R, Silva A.M.T (2015b) An Overview on the Advanced Oxidation Processes Applied for the Treatment of Water Pollutants Defined in the Recently Launched Directive 2013/39/EU. *Environ. Int.* 75 (february): 33-51.
- Richardson S.D (2012) Environmental Mass Spectrometry: Emerging Contaminants and Current Issues. *Anal. Chem.* 84 (2): 747-78.
- Rivera-Utrilla J, Sánchez-Polo M, Ferro-García M.A, Prados-Joya G, Ocampo-Pérez R (2013a) Pharmaceuticals as Emerging Contaminants and Their Removal from Water. A Review. *Chemosphere* 93 (7): 1268-87.
- Rivera-Utrilla J, Sánchez-Polo M, Ferro-García M.A, Prados-Joya G, Ocampo-Pérez R (2013b) Pharmaceuticals as Emerging Contaminants and Their Removal from Water. A Review. *Chemosphere* 93 (7): 1268-87.
- Rivera-Utrilla J, Sánchez-Polo M, Ferro-García M.A, Prados-Joya G, Ocampo-Pérez R (2013c) Pharmaceuticals as Emerging Contaminants and Their Removal from Water. A Review. *Chemosphere* 93 (7): 1268-87.
- Rizzo L, Manaia C, Merlin C, Schwartz T, Dagot C, Ploy M.C, Michael I, Fatta-Kassinos D (2013) Urban Wastewater Treatment Plants as Hotspots for Antibiotic Resistant Bacteria and Genes Spread into the Environment: A Review. *Sci. Total Environ* 447 (march): 345-60.
- Rizzo L, Meric S, Guida M, Kassinos D, Belgiorno V (2009) Heterogenous Photocatalytic Degradation Kinetics and Detoxification of an Urban Wastewater Treatment Plant Effluent Contaminated with Pharmaceuticals. *Water Res.* 43 (16): 4070-78.

- Rizzo L, Meric S, Kassinos D, Guida M, Russo F, Belgiorno V (2009) Degradation of Diclofenac by TiO₂ Photocatalysis: UV Absorbance Kinetics and Process Evaluation through a Set of Toxicity Bioassays. *Water Res.* 43 (4): 979-88.
- Rodriguez-Narvaez O.M, Peralta-Hernandez J.M, Goonetilleke A, Bandala E.R (2017a) Treatment Technologies for Emerging Contaminants in Water: A Review. *Chem. Eng. J.* 323 (september): 361-80.
- Rodriguez-Narvaez O.M, Peralta-Hernandez J.M, Goonetilleke A, Bandala E.R (2017b) Treatment Technologies for Emerging Contaminants in Water: A Review. *Chem. Eng. J.* 323 (september): 361-80.
- Roh H, Subramanya N, Zhao F, Yu C.P, Sandt J, Chu K.H (2009) Biodegradation Potential of Wastewater Micropollutants by Ammonia-Oxidizing Bacteria. *Chemosphere* 77 (8): 1084-89.
- Romero V, Acevedo S, Marco P, Gimenez J, Esplugas S (2016a) Enhancement of Fenton and photo-Fenton processes at initial circumneutral pH for the degradation of the b-blocker metoprolol. *Water Res.* 88: 449-457.
- Santos L, Araújo A.N, Fachini A, Pena A, Delerue-Matos C, Montenegro M.C.B.S.M (2010) Ecotoxicological Aspects Related to the Presence of Pharmaceuticals in the Aquatic Environment. *J. Hazard. Mater.* 175 (1-3): 45-95.
- Schug T.T, Janesick A, Blumberg B, Heindel J.J (2011) Endocrine Disrupting Chemicals and Disease Susceptibility ». *The Journal of Steroid Biochemistry and Molecular Biology* 127 (3-5): 204-15.
- Schwaiger J, Ferling H, Mallow U, Wintermayr H, Negele R.D (2004) Toxic Effects of the Non-Steroidal Anti-Inflammatory Drug Diclofenac. *Aquat. Toxicol.* 68 (2): 141-50.
- Schwarzenbach R. P (2006) The Challenge of Micropollutants in Aquatic Systems. *Science* 313 (5790): 1072-77.
- Shemer H, Kunukcu Y.K, Linden K.G (2006) Degradation of the pharmaceutical Metronidazole via UV, Fenton and photo-Fenton processes. *Chemosphere* 63: 269-276.
- Shin J, Moon H.j, Kang H, Kim T.S, Lee S.J, Ahn J.Y, Bae H, Jeung E.B, Han S.Y (2007) OECD Validation of the Rodent Hershberger Assay Using Three Reference Chemicals; 17 α -Methyltestosterone, Procymidone, and p,P'-DDE. *Arch. Toxicol.* 81 (5): 309-18.

- Silva A.K, Amador J, Cherchi C, Miller S.M, Morse A.N, Pellegrin M.L, Wells M.J.M (2013) Emerging Pollutants – Part I: Occurrence, Fate and Transport. *Water Environ. Res.* 85 (10): 1978-2021.
- Singh L, Rekha P, Chand S (2016) Cu-impregnated zeolite Y as highly active and stable heterogeneous Fenton-like catalyst for degradation of Congo red dye. *Sep. Purif. Technol.* 170 (Supplement C): 321-36.
- Sotelo J. L, Rodríguez A.R, Mateos M.M, Hernández S.D, Torrellas S.A, Rodríguez J.G (2012) Adsorption of Pharmaceutical Compounds and an Endocrine Disruptor from Aqueous Solutions by Carbon Materials. *J. Environ. Sci. Health, Part B* 47 (7): 640-52.
- Sreeja P.H, Sosamony K.J (2016) A Comparative Study of Homogeneous and Heterogeneous Photo-Fenton Process for Textile Wastewater Treatment. *Procedia Technol.* 24: 217-23.
- Sudhakaran S, Maeng S.K, Amy G (2013) Hybridization of Natural Systems with Advanced Treatment Processes for Organic Micropollutant Removals: New Concepts in Multi-Barrier Treatment. *Chemosphere* 92 (6): 731-37.
- Tambosi J.L, Sena R.F, Favier M, Gebhardt W, José H.J, Schröder H.F, Moreira R.F.P.M (2010) Removal of Pharmaceutical Compounds in Membrane Bioreactors (MBR) Applying Submerged Membranes. *Desalination* 261 (1-2): 148-56.
- Thomas A.T (2010) Occurrence and fate of emerging organic micropollutants in biological wastewater treatment. Koblenz-Landau university.
- Tijani J.O, Fatoba O.O, Petrik L.F (2013a) A Review of Pharmaceuticals and Endocrine-Disrupting Compounds: Sources, Effects, Removal, and Detections. *Water, Air, & Soil Pollution* 224 (11).
- Tijani J.O, Fatoba O.O, Petrik L.F (2013b) A Review of Pharmaceuticals and Endocrine-Disrupting Compounds: Sources, Effects, Removal, and Detections. *Water, Air, & Soil Pollution* 224 (11).
- Tran N.H, Gin K.Y.H (2017a) Occurrence and Removal of Pharmaceuticals, Hormones, Personal Care Products, and Endocrine Disrupters in a Full-Scale Water Reclamation Plant. *Sci. Total Environ.* 599-600 (december): 1503-16.
- Tran N.H, Gin K.Y.H (2017b) Occurrence and Removal of Pharmaceuticals, Hormones, Personal Care Products, and Endocrine Disrupters in a Full-Scale Water Reclamation Plant. *Sci. Total Environ.* 599-600 (december): 1503-16.

- Trovó A.G, Nogueira R.F.P, Agüera A, Fernandez-Alba A.R, Malato S (2012) Paracetamol Degradation Intermediates and Toxicity during Photo-Fenton Treatment Using Different Iron Species. *Water Res.* 46 (16): 5374-80.
- Trovo A.G, Pupo Nogueira R.F, Agüera A, Fernandez-Alba A.R, Malato S (2011) Degradation of the antibiotic amoxicillin by photo-Fenton process e chemical and toxicological assessment. *Water Res.* 45: 1394-1402.
- Velasquez M, Santander I.P, Contreras D.R, Yanez J, Zaror C, Salazar R.A, Perez-Moya M, Mansilla H.D (2014) Oxidative degradation of sulfathiazole by Fenton and photo-Fenton reactions. *J. Environ. Sci. Health, Part A* 49: 661-670.
- Verboekend D, Nuttens N, Locus R, Aelst J.V, Verolme P, Groen J. C, Pérez-Ramírez J, Sels B. F (2016) Synthesis, Characterisation, and Catalytic Evaluation of Hierarchical Faujasite Zeolites: Milestones, Challenges, and Future Directions. *Chem. Soc. Rev.* 45 (12): 3331-52.
- Veronica D (2013) Heterogeneous TiO₂ Photocatalysis - Fundamental Chemical Aspects and Effects of Solid Phase Alterations. *Université Paris-Sud* 11.
- Vieno N, Sillanpää M (2014a) Fate of Diclofenac in Municipal Wastewater Treatment Plant — A Review. *Environ. Int.* 69 (august): 28-39.
- Vieno N, Sillanpää M (2014b) Fate of Diclofenac in Municipal Wastewater Treatment Plant — A Review. *Environ. Int.* 69 (august): 28-39.
- Wolf L, Zwiener C, Zemann M (2012) Tracking Artificial Sweeteners and Pharmaceuticals Introduced into Urban Groundwater by Leaking Sewer Networks. *Sci. Total Environ.* 430 (july): 8-19.
- Yang K, Yu J, Guo Q, Wang C, Yang M, Zhang Y, Xia P, Zhang D, Yu Z (2017) Comparison of Micropollutants' Removal Performance between Pre-Ozonation and Post-Ozonation Using a Pilot Study. *Water Res.* 111 (march): 147-53.
- Yu Z, Peldszus S, Huck P.M (2007) Optimizing Gas Chromatographic–mass Spectrometric Analysis of Selected Pharmaceuticals and Endocrine-Disrupting Substances in Water Using Factorial Experimental Design. *J. Chromatogr. A* 1148 (1): 65-77.
- Zhang Y, Geißen S.U, Gal C (2008) Carbamazepine and Diclofenac: Removal in Wastewater Treatment Plants and Occurrence in Water Bodies. *Chemosphere* 73 (8): 1151-61.

Chapter II

Detection and Quantification of Micropollutants at Very Low Concentrations from River Water

In this chapter, we will discuss the detection and quantification of 21 micropollutants belonging to 4 different groups present in 2 rivers in Nancy city. Through the analysis, we will be able to specify the best conditions needed to choose the good water sample for applying the removal treatment on real water. Several sampling factors are studied in addition to the calculation of the fluxes and estimation of the mass balance at the confluence between the 2 rivers.

Abstract

The efficiency of heterogeneous photo-Fenton process under UV light using Faujasite Y zeolite as a catalyst in the removal of a cocktail of 21 micropollutants of different groups in real water matrix is the main goal of our study. To achieve this goal, real water samples are taken from different positions on the Meurthe river and Moselle river during three periods: September 2015, January 2016 and October 2016. The presence of 21 micropollutants including 17 pharmaceutical compounds were identified and quantified in a range of ng/L. using a multi-residual analytical technique based on a preconcentration step followed by Liquid Chromatography/Mass Spectrometry analysis (LC-MS/MS). Bisphenol A, Carbamazepine, Clarithromycin, Diclofenac, Erythromycin, Estrone, Ibuprofen, Ketoprofen, Lidocaine, Naproxen, PFOA, PFOS, Sulfamethoxazole and Triclosan were detected and quantified in all the sites. Conversely, Carbamazepine-10,11-epoxide, Cyclophosphamide, Estradiol-beta, Ethynylestradiol, Sulfadimethoxine, Sulfadimidine and Sulfathiazole were below the limit of quantification. The variation of the concentration of each micropollutant in the water river depends on the period of the year and the sampling position. The pollutant content is affected by 2 factors: (i) the variation of the drug medication and the drug treatment during the year, and (ii) the flow rate change of the river between the seasons. This was reflected by studying the flux variation which takes these 2 factors into consideration.

Moreover, the fluxes are used to estimate the mass balance at the confluence between the 2 rivers. The values obtained for the mass balance measurements during the three sampling periods were a good indication for the precision, reliability and the good quality of the values obtained, confirming the ability of applying the real water treatment tests based on the measurement methodology used. In addition, the effect of some other factors on the quantification of micropollutants in real river water is studied. These include the weather conditions, the position of the sampling, and the flow rate of the river on specific site, the efficiency of the WWTP in the treatment of micropollutants and the best location suitable for real water treatment analysis. Results shows that Moulin Noir located on the Meurthe river downstream the WWTP is the best sampling site to take water to be used in the treatment experiments due to the large variety in the type and number of micropollutants it contains. After identifying the range of concentration at which micropollutants are present and the most suitable sampling point, heterogeneous photo-Fenton reactions were applied in the laboratory reactor and the results are discussed in the next chapter.

1 Introduction

Heterogeneous photo-Fenton treatment using Faujasite Y catalyst proved to be the method of interest for the removal of micropollutants present in rivers and lakes including pharmaceuticals, personal care products, endocrines disruptors and perfluorinated compounds, found at low concentrations in the picogram per liter to microgram per liter range (König et al. 2017) (Schwientek et al. 2016, Tousova et al. 2017). This is due to its high removal efficiency examined by several studies in the last few years.

In order to evaluate the real removal efficiency of the chosen removal method in the degradation of micropollutants, it is important to perform the treatment tests on real water that contain a mixture of micropollutants presenting together at low concentration, and not only on synthetic water solution that contain one or more compound which is the case in most of the studies (Miren Blanco et al. 2014, Fard et al. 2017, Wu et al. 2017). The work with real water samples makes the analysis more realistic and gives clearer picture about the ability to implement such treatment method in WWTPs. Moreover, even though the main target of the treatment method is the degradation of micropollutants, but this does not ignore or eliminate matrix effect by different wastewater components. Organic and inorganic pollutants are present in the treated water such as fulvic acids, humic substances, inorganic ions as carbonates and nitrates and much more. These compounds interfere greatly and have a high effect on the degradation of micropollutants in wastewater (Wang et al. 2017). For this reason, it is important to perform the removal analysis and quantification on real sample water. Furthermore, the release and quantification of micropollutants in water is affected by some environmental factors related to the place where the river water samples were taken and studied. This includes the location, the flow rate of the water, the flux, the nature and concentration of the micropollutants released by human and industrial activities, the efficiency of the WWTP in the removal of micropollutants, and the effect of the weather conditions and the urban life. These factors are rarely taken into considerations in the studies done before.

The aim of this chapter is to analyze and quantify the presence of 21 micropollutants among them pharmaceuticals, personal care products, endocrine disruptors and perfluorinated compounds in river water samples from Meurthe river and Moselle river in Nancy, France. To examine the effect of different factors, three sampling campaigns were performed during 13 months: September 2015, January 2016 and October 2016 to study the effect of time and weather conditions on the presence and quantification of micropollutants. The goal is to identify “the best” location from where river water will be taken to be used in heterogeneous photo-Fenton treatment experiments that are

discussed in the next chapter. This identified location is the place where the variety and the number of micropollutants are the highest. During each sampling, samples were taken at five sites across the two rivers. It also allows studying the efficiency of the WWTP located across the Meurthe river, the effect of the confluence between the two rivers, and the efficiency of the drinking water treatment plant (DWTP) in removal of micropollutants. The flow rate of the river water at each sampling site during each sampling period was examined and used to calculate the fluxes of the studied micropollutants. This allows applying a mass balance approach to identify the main reasons behind the measured effects and evaluate quantitatively their relative contribution to the overall factors effect. The mass balance at the confluence of the 2 rivers is also a way to check the repeatability of our experimental procedure. The detection and quantification of the micropollutants in all the samples was done by the SPE-LS-MS/MS-ESI multi-residual methodology for its sensitivity and high quantification ability as discussed before.

2 Materials and Methods

2.1 River system and Sampling

River waters were collected from the 2 rivers, the Meurthe river and the Moselle river, close to the city of Nancy in France. The samples were taken from five different sites located on the 2 rivers with specific positions: Belleville, Pompey, Messein, Moulin Noir and Malzéville as shown in Fig. 1 with the characteristics of each position for each site listed in Table 1. Three sampling campaigns were performed on 11 September 2015, 5 January 2016 and 14 October 2016. The weather conditions are presented in Table 2. Samples at each site were collected from the middle of a bridge from above the rivers to ensure the good mixing of the water content. The samples were collected using brown glass bottle surrounded by iron cover, to avoid its breakage, using a thick long ribbon that was dropped from the bridge into the river to take the water samples. Samples were placed in 1 L dark glass bottles and transported to the laboratory.

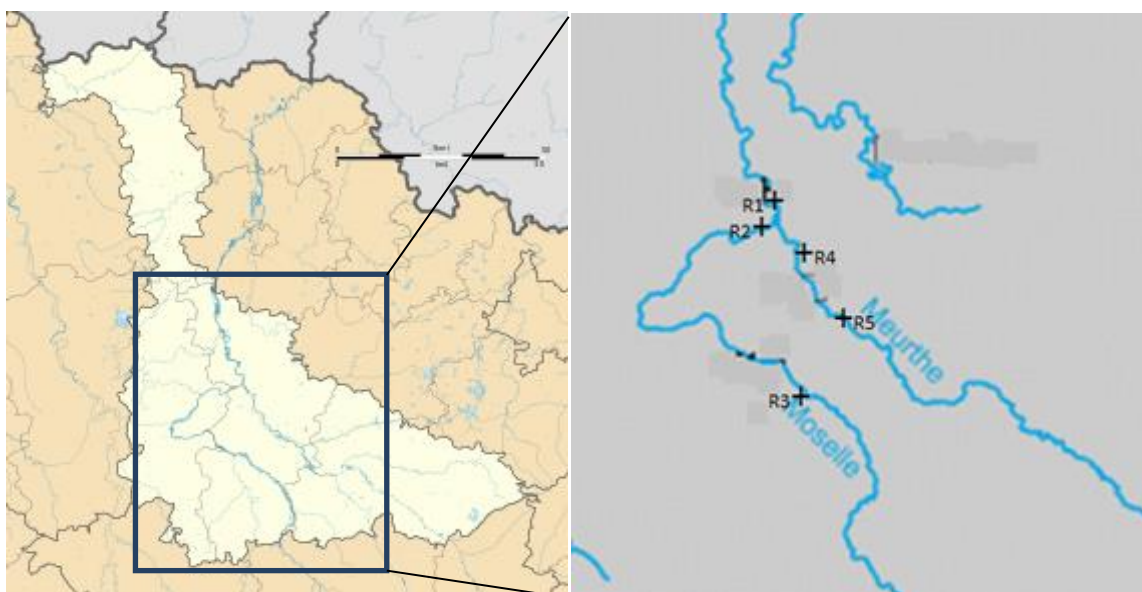


Fig. 11. Sampling sites located on the Meurthe and Moselle rivers. The notation R1 refers to Belleville, R2 Pompey, R3 Messein, R4 Moulin Noir and R5 Malzéville.

Table 15. Sampling sites and their main characteristics.

Site symbol	Site name	Location	Coordination
R1	Belleville	On the Moselle river, downstream the confluence of the Meurthe river and Moselle rivers	Latitude : 48°48.514'N Longitude : 6°7.075'E
R2	Pompey	On the Moselle river, upstream of the confluence	Latitude : 48°46.639'N Longitude : 6°8.191'E
R3	Messein	On the Moselle river, place of water catchment (to produce drinking water)	Latitude : 48°36.123'N Longitude : 6°9.219'E
R4	Moulin Noir	On the Meurthe river, downstream the wastewater treatment plant and upstream the confluence	Latitude : 48°44.605'N Longitude : 6°10.865'E
R5	Malzéville	On the Meurthe river, upstream the wastewater treatment plant	Latitude : 48°42.556'N Longitude : 6°10.833'E

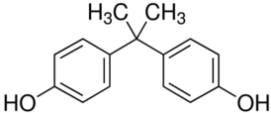
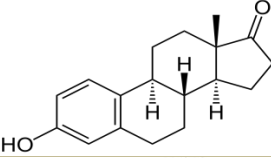
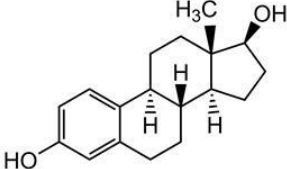
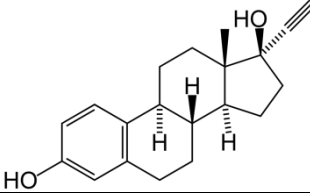
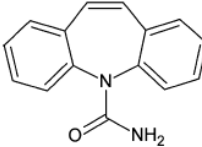
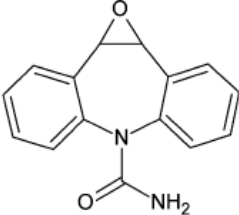
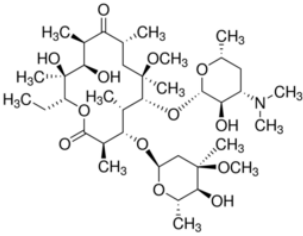
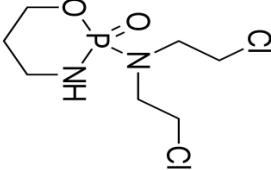
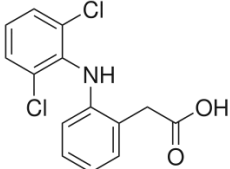
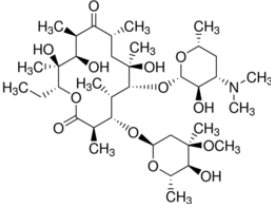
Table 2. Weather conditions during the three sampling periods.

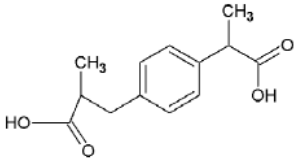
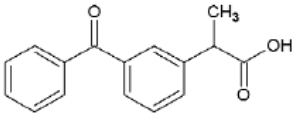
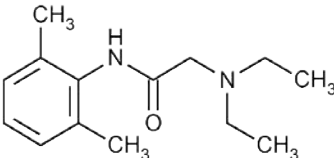
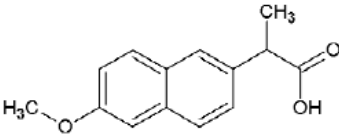
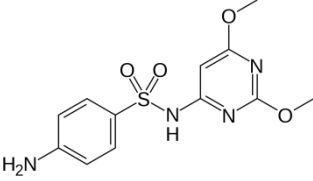
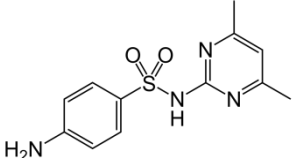
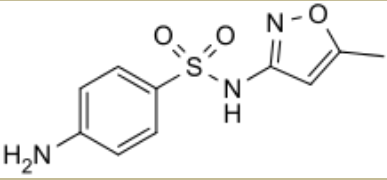
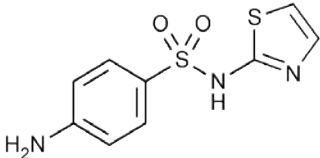
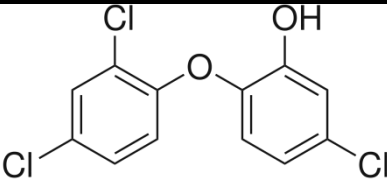

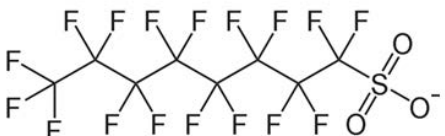
Conditions	Sampling 1	Sampling 2	Sampling 3
Date	11 September 2015	5 January 2016	14 October 2016
Weather	Sunny	Rainy in some sites	, nuol C, rael C
Weather days before	Sunny	Cold but not raining	Some rain
Temperature	22°C	7°C	8 °C

2.2 Compounds selection

The selection of the micropollutants to be studied was based on the advice of Christophe Rosin deputy director of the ‘Laboratoire d’Hydrologie’ of ANSES, taking into account some factors such as the usage (pharmaceuticals, hormones, industrial compounds), occurrence in the municipal wastewater and water systems and different physical-chemical properties. Then, 21 micropollutants from different classes including pharmaceuticals, endocrine disruptors, personal care products and some perfluorinated compounds were selected. The list of the target compounds is presented in Table 3.

Table 3. List of the studied micropollutants and their corresponding classes.

Family	Class	Compound	Structure	Ionization mode
EDCs	Endocrine disruptor	Bisphenol A		Negative
	Hormone	Estrone		Negative
	Hormone	Estradiol-beta		Negative
	Hormone	Ethinylestradiol		Negative
Phs	Anti-epileptic	Carbamazepine		Positive
	Anti-epileptic	Carbamazepine-10,11-epoxide		Positive
	Antibiotic	Clarithromycin		Positive
	Chemotherapy Drug	Cyclophosphamide		Positive
	Anti-inflammatory	Diclofenac		Positive
	Antibiotic	Erythromycin		Positive

	Anti-inflammatory	Ibuprofen		Negative
	Anti-inflammatory	Ketoprofen		Positive
	Anesthetic	Lidocaine		Positive
	Anti-inflammatory	Naproxen		Positive
	Antibiotic	Sulfadimethoxine		Positive
	Antibiotic	Sulfadimidine		Positive
	Antibiotic	Sulfamethoxazole		Positive
	Antibiotic	Sulfathiazole		Positive
PCP	Antiseptic (PCP)	Triclosan		Negative
PFCs	Perfluorinated compound	PFOA		Negative
	Perfluorinated compound	PFOS		Negative

2.3 Preparation and analytical processes

Samples preparation

After bringing the river sampled waters to the laboratory, they were directly filtrated by 2 processes. The first one employs funnel and filter paper to remove the bulk materials. The second one uses successively a glass filter of 1.2 μm porosity followed by a cellulose acetate filter with a porosity of 0.45 μm . After filtration, the samples were stored in dark bottles in the refrigerator at a temperature of 4 °C before processing.

Solid phase extraction

The preconcentration of the river water samples were done using Solid Phase Extraction (SPE). The preconcentration of the samples was based on the adsorption of the required components on the adsorbent, then their elution using an appropriate solvent to obtain the final concentrated solution. After filtration, the samples were acidified to pH 4 with pure sulfuric acid. A total volume of 500 mL of the sample was extracted by SPE using an Auto trace SPE Workstation (Thermo Fisher Scientific, Waltham USA). The SPE cartridge (Oasis HLB 200 mg/6mL, Waters, Milford USA) was previously conditioned with methanol then water at pH 4. After the sample loading, the cartridge was washed with water/methanol 95/5 (v/v), dried under nitrogen during 15 minutes and eluted with 10 mL of methanol. To enhance the concentration factor, the extract was evaporated under vacuum at 50 °C to near dryness and recovered in 500 μL of water/methanol 90/10, the same starting conditions as the initial LC-MS/MS mobile phase. The initial samples are pre-concentrated with a ratio of 1000. A total volume of 10 mL is obtained at the end. All the eluents used for SPE were of ultra-pure or LC-MS grade.

Quantification of micropollutants by LC-MS/MS

After SPE, the samples were kept at -20 °C in half-filled glass bottles stored in a horizontal position until quantification analysis. Then, they were sent to the Luxembourg Institute of Science and Technology (LIST) in Luxembourg for analysis. For the quantification of micropollutants, the final extract was analyzed by Liquid Chromatography (1260 Series, Agilent, Santa Clara USA) coupled to triple-quadrupole Mass Spectrometry (QTRAP 4500, AB Sciex, Framingham USA). The chromatographic separation was achieved on a Zorbax Eclipse Plus C18 column, 150 x 2.1 mm ID, 3.5 μm particle size (Agilent). The flow rate of the mobile phase was kept constant at 0.25 mL/min and the oven at 40 °C. The nature of the mobile phases and the eluent programs are given in the

Table 4. According to the target compounds, the mass spectrometer was operated in positive/negative electrospray ionization (Table 3). The MS/MS was operated in Multiple Reaction Monitoring (MRM) mode. Two MRM transitions were used for each compound on interest, for quantification and confirmation, respectively. Quantitative results were provided thanks to internal calibrations.

Table 4. Conditions of the instrument used in LC-MS/MS measurements including the mobiles phases used and eluent programs. The notation “min” corresponds to minutes.

	Positive mode	Negative mode
Column	Zorbax Eclipse Plus C18 (Agilent)	
Oven temperature	40 °C	
Flow	0.25 mL/min	
Injection	25 µL	
Eluents	A2: Water + 0.1 % formic acid B2: Methanol + 0.1 % formic acid	A1: Water + 2.5 mM ammonium acetate B1: Acetonitrile
Eluent program	0 min 10 % B – 2 min 10 % B – 10 min 30 % B – 14 min 95 % B – 16 min 95 % B – 17 min 10 % B – 28 min 10 % B	0 min 30 % B – 1 min 30 % B – 3 min 50 % B – 8 min 80 % B – 9 min 95 % B – 11 min 95 % B – 12 min 30 % B – 15 min 30 % B

2.4 Flux and mass balance calculations

For flux and mass balance calculations, the flow rate data at each sampling site on the two rivers during the three sampling periods were provided by the “Ministère de l’écologie, du développement durable et de l’énergie” (Site address: <http://www.hydro.eaufrance.fr/>).

For flux calculation of each micropollutant at each site, the flow rate during the selected sampling day was multiplied by the concentration of the selected micropollutants according to Eq. (1).

$$F_{ij} = Q \times C_{ij} \quad (1)$$

where i represents the micropollutant type and j represents the location and time.

and:

F the flux in g/day, Q the flow rate in L/day, and C the concentration of micropollutants in g/L.

Then for the estimation of the mass balance upstream and downstream the confluence, the total flux upstream the confluence is the sum of all the 2 fluxes according to Eq. (2):

$$F(\text{upstream}) = F(\text{Pompey}) + F(\text{Moulin Noir}) \quad (2)$$

The calculated $F(\text{upstream})$ was compared to the real flux downstream the confluence at Belleville represented by $F(\text{downstream})$. The mass balance precision factor ($f\%$) for each micropollutant during each sampling day was calculated according to the Eq. (3):

$$f\% = \frac{F(\text{upstream}) - F(\text{downstream})}{F(\text{upstream})} \times 100 \quad (3)$$

2.5 Characterizations of macropollutants

For the water samples, the total organic carbon (TOC) including non-purgeable organic carbon (NPOC), total nitrogen (TN) and inorganic carbon (IC) were measured using TOC analyzer TOC-VCSH (Shimadzu). The UV/Visible absorbance spectrum was recorded using a spectrophotometer (Cary 5G UV-Vis-NIR) in wavelength range between 190 nm and 900 nm using quartz cuvette. For the fluorescence measurement, spectrum was recorded using F-2500 fluorescence spectrophotometry in synchronous fluorescence mode excitation wavelength ranging from 230 nm to 600 nm with $\Delta\lambda (\lambda_{em} - \lambda_{ex}) = 50$ nm.

3 Results and Discussion

3.1 Macropollutants analysis

3.1.1 Total Organic Carbon (TOC)

First the variation of the flow rate between the sampling periods at the five sampling sites is shown in Fig. 2. The flow rate follows an increase in its trend from September to January which is due to the normal increase of precipitation in winter seasons (January) compared to the other seasons

(September and October). The highest flow rate is recorded at Belleville since it is located after the confluence between the 2 rivers.

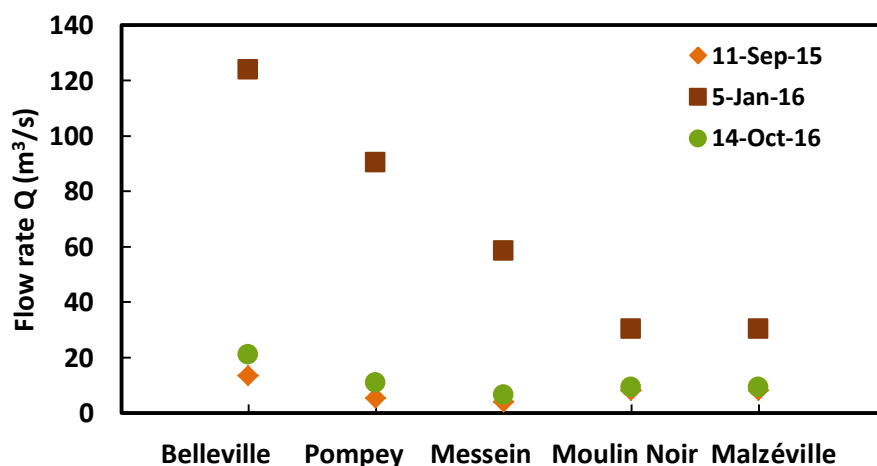


Fig. 12. The variation of the flow rate in September 2015, January 2016 and October 2016 at the five sampling sites.

The Fig. 3 shows the amounts of non-purgeable organic carbon, total nitrogen and inorganic carbon measured in the five different sites on the Meurthe river and Moselle river during the three sampling periods: September 2015, January 2016 and October 2016.

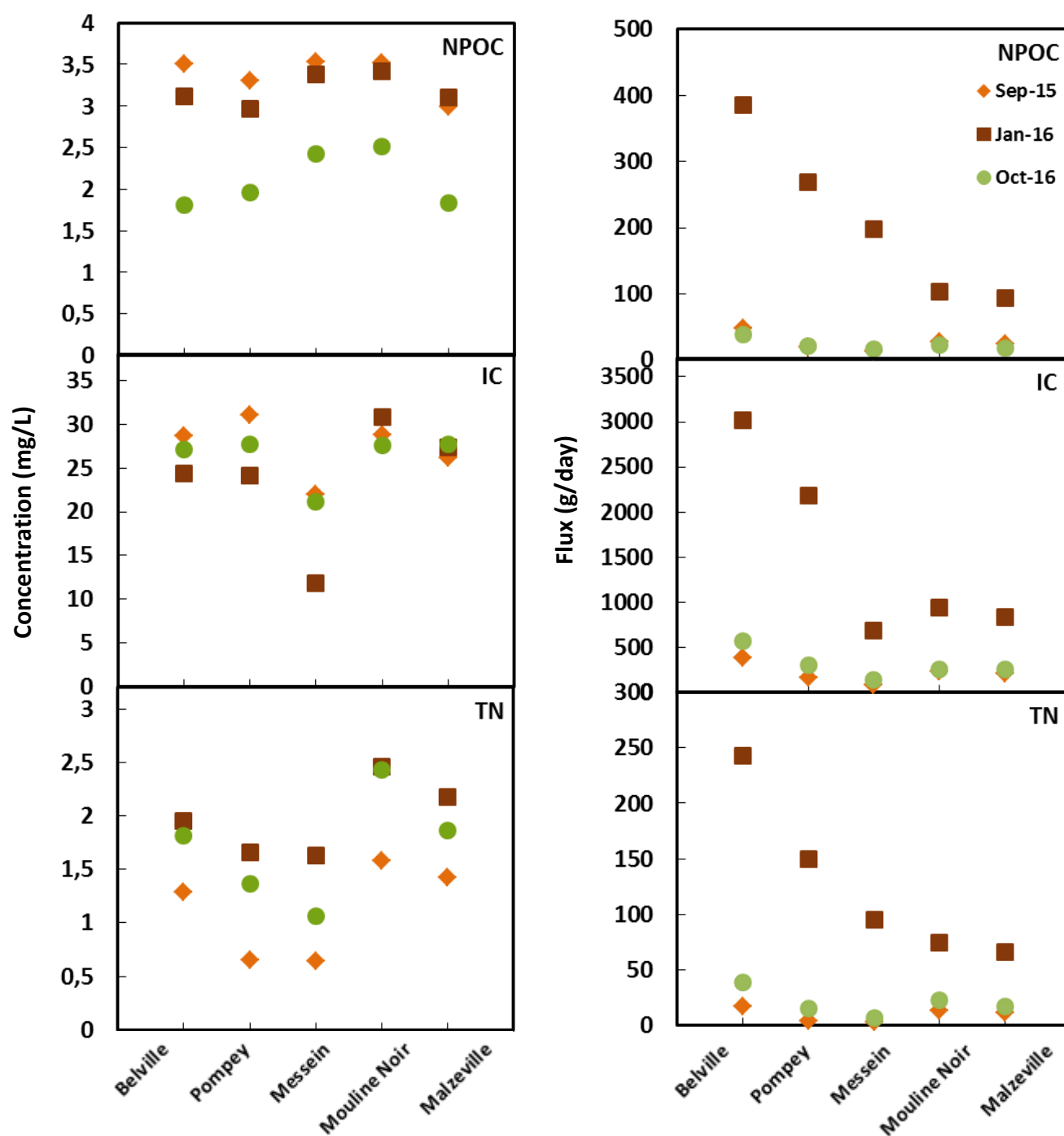


Fig. 13. The concentrations in mg/L and the fluxes in g/day of non-purgeable organic carbon (NPOC), inorganic carbon (IC) and total nitrogen (TN) in the five studied sites on the Meurthe river and Moselle river on September 2015, January 2016 and October 2016.

➤ **Non-Purgeable Organic Carbon (NPOC)**

The amount of organic carbon is in the order of 3-3.5 mg/L in September 2015 and January 2016, and is lower in October 2016 with a maximum of 2.5 mg/L. In the two first sampling periods, no large variation is observed between the different sites in each month with the highest organic carbon concentration measured in Moulin Noir. Literature data ([Niemirycz et al. 2006](#)) give the following values of TOC content in natural waters: in ground waters about 0.7 mg/L, ground waters with high amounts of humic substances 6-15 mg/L, seas with about 2 mg/L and rivers and lakes ranging from a few to above 10 mg/L. Consequently, the amount detected in the rivers water in a normal range. Usually organic carbon is released from both natural and man-made sources including sewage treatment plants, farm slurry, silage run-off, leachate from waste disposal landfills, fish farm and food processing effluents and spillage of food stuffs, excretion and eventual decomposition. Soils and peat also release TOC into water bodies ([Scottish Environment Protection Agency, s. d.](#)).

➤ **Inorganic Carbon (IC)**

The concentration of inorganic carbon is the lowest in Messein while it is slightly higher in Belleville, Pompey, Moulin Noir and Malzéville with a maximum concentration of 31.0 mg/L. The detection of inorganic carbon in the rivers is mainly due to presence of carbonate (CO_3^{2-}) and hydrocarbonate (HCO_3^-) species with carbonic acid in some quantitative proportions. The sources of CO_3^{2-} and HCO_3^- are usually the various carbonate rocks (limestones, dolomites, magnesites), where dissolution occurs in the presence of carbon dioxide. Based on literature data, HCO_3^- content in surface fresh water does not exceed 250 mg/L (not the case of soda alkaline waters where HCO_3^- and CO_3^{2-} content can reach grams and even dozens of grams per kilogram) ([Nikanorov et al.](#)). This amount is much higher than the maximum amount of inorganic carbon detected in both rivers (31.0 mg/L).

➤ **Total Nitrogen (TN)**

The highest concentration of nitrogen was measured in January 2016 (between 1.6 and 2.5 mg/L) compared to the concentration analyzed in September 2015 (0.6 mg/L and 1.5 mg/L) and October 2016 (1.1 mg/L and 2.4 mg/L). For the 3 months, the highest concentrations were detected in Moulin Noir and Malzéville located on the Meurthe river. They are followed by Belleville located after the confluence and the last are Pompey and Messein located on the Moselle river. The amounts detected are acceptable based on the acceptable range of total nitrogen (2 mg/L to 6 mg/L)

mentioned in the literature (Nordin et al. 2009). Total nitrogen includes nitrate, nitrite, ammonia, and organic nitrogen. Organic nitrogen includes natural materials such as proteins, peptides, urea, nucleic acids and other synthetic organic materials (Walker).

➤ Flux and Mass Balance

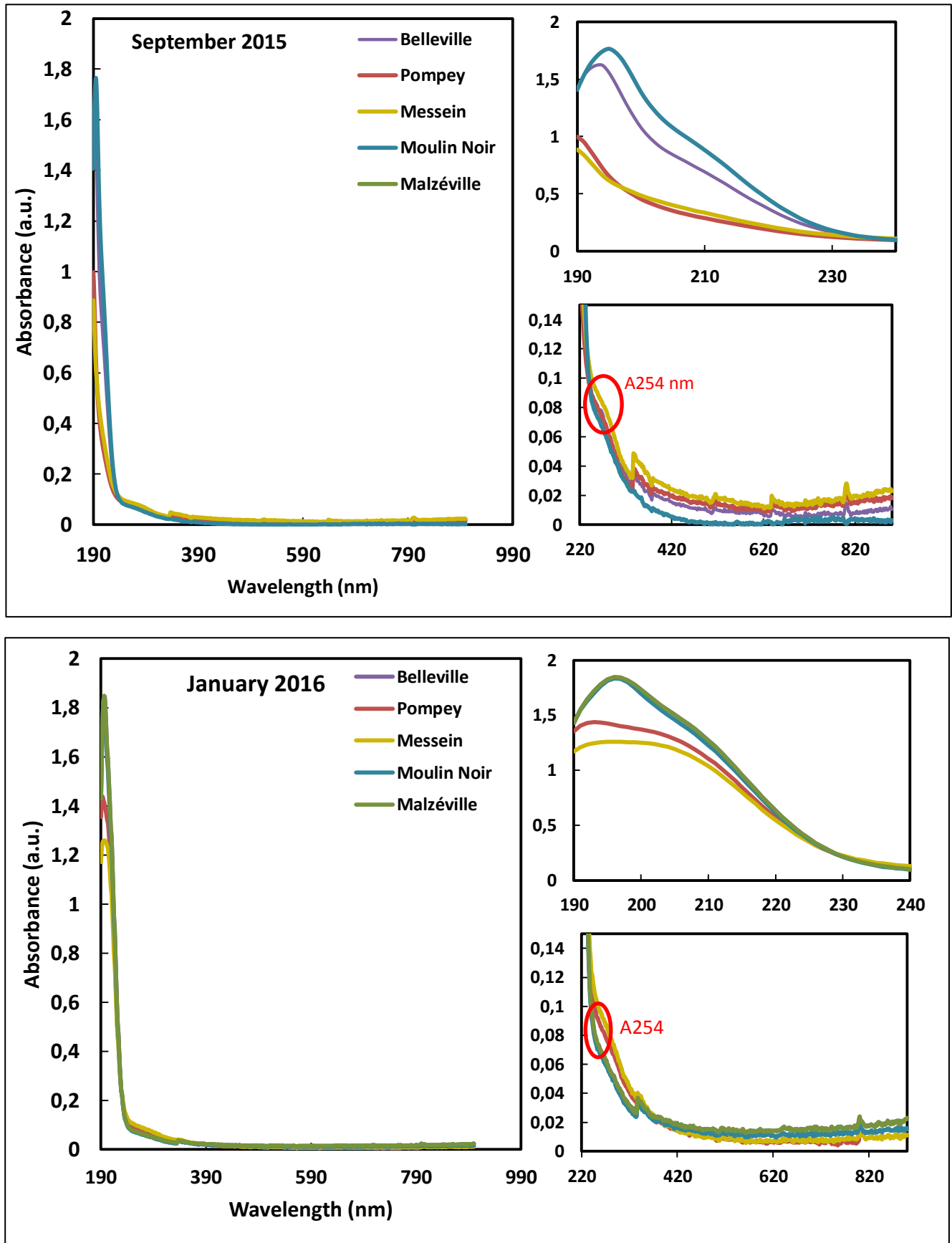
The fluxes of NPOC, TN and IC were calculated upstream (Pompey and Moulin Noir) and downstream (Belleville) the confluence to verify the mass balance. As shown in Table 5, the mass balance precision factor ($f_{\%}$) for the NPOC, TN and IC measurements is low ranging between -7.6 % and 13.6 % which is relatively good, confirming the precision and reliability of our measurements.

Table 5. Flux and mass balance for NPOC, TN and IC.

	Flux (g/s)	$F_{\text{Pompey, Upstream}}$	$F_{\text{Moulin Noir, Upstream}}$	$F_{\text{Sum, Rivers 1+2}}$	$F_{\text{Belleville, Downstream}}$	$f_{\%} (\%)$
September 2015	NPOC	19	27	46	48	-4.3
	TN	4	13	16	17	-6.3
	IC	168	233	400	387	3.3
January 2016	NPOC	269	104	372	386	-3.8
	TN	150	75	225	242	-7.6
	IC	2184	936	3119	3023	3.1
October 2016	NPOC	21	23	44	38	13.6
	TN	15	23	37	38	-2.7
	IC	300	257	556	569	-2.3

3.1.2 UV-Visible Spectroscopic analysis

Fig. 4. shows the UV absorbance spectra for the 3 sampling periods for all the sites using 3 scales for each sampling.



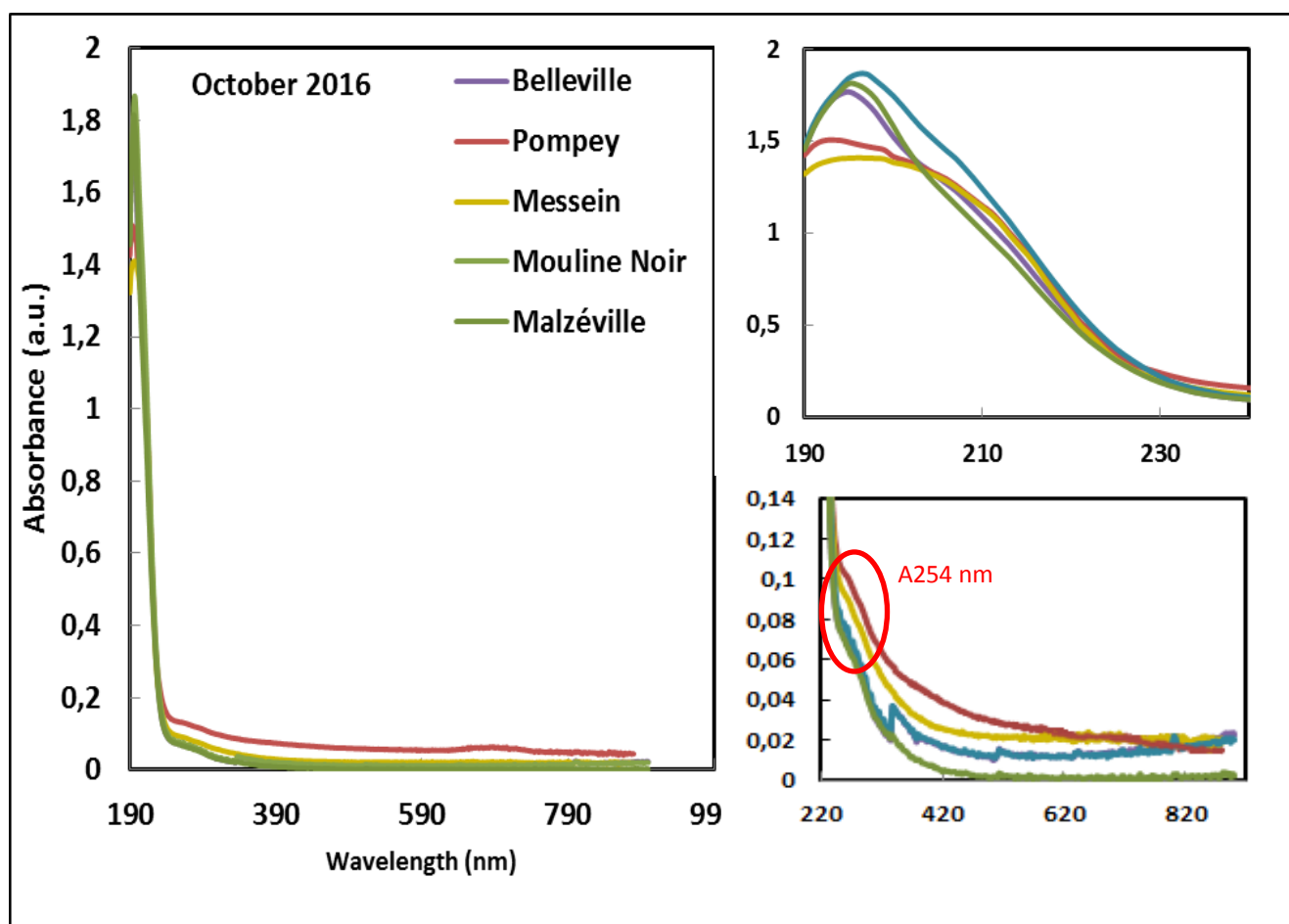


Fig. 14. UV-Visible absorption spectrum for water samples in the five sites in the Meurthe river and the Moselle river in September 2015, January 2016, and October 2016 under different scales.

All the samples exhibit similar absorption spectra curve shape irrespective of location and sampling period. Usually the shape of the curve is related to the relative mixing of industrial, agricultural and domestic wastes, and the social–economical profile of the society. These factors affect the composition of domestic wastewater (Pons et al. 2004).

For the 3 periods and in all the sites, a maximum absorbance peak is observed at around 190-200 nm as shown in Fig. 4 in the first zoomed part. Higher absorbance intensity is observed for the sites Moulin Noir, Malzéville and Belleville reaching absorbance intensity of 1.8. The absorbance at this wavelength range is related mainly to nitrate and nitrite species that exhibit absorption peak around 200 nm (Ianoul et al. 2002) thus, confirming the presence of these ions in the studied river water. The second zoomed part of the graphs in Fig. 4. is an indication for the color of the samples. Consequently, all the water samples have the same color regardless of the sites and the period.

The UV absorbance at around 254 nm (A_{254}) has been found by most authors to be correlated to the dissolved organic matter (Ahmad et Reynolds 1999). Also correlations between the absorbance at 254 nm (A_{254}), the Chemical Oxygen Demand (COD) and the Total Organic Carbon have been already established (Pons et al. 2005). The Table 6 shows the absorbance of the samples at 254 nm. In the present study, Messein and Pompey have the highest absorbance A_{254} . This indicates that the 2 sites have the largest COD and TOC content among all the other sites investigated.

Table 6. Absorbance at 254 nm and NPOC values in the 2 months.

	September 2015		January 2016		October 2016	
	A_{254}	NPOC(mg/L)	A_{254}	NPOC(mg/L)	A_{254}	NPOC(mg/L)
Belleville	0.08	3.6	0.07	3.1	0.07	2.1
Pompey	0.08	3.5	0.09	3	0.06	3.5
Messein	0.09	3.5	0.10	3.4	0.07	2.5
Moulin Noir	0.07	3.3	0.07	3.4	0.07	2.8
Malzéville	0.06	3	0.07	3.1	0.07	2.2

A pseudo-flux can be then calculated on the fact that A_{254} is proportional to COD (Pons et al. 2005), according to Eq. (4) (where Q in is m^3/s). The results are given in Table 7.

$$F_{A_{254}} = A_{254} \times Q \quad (4)$$

Table 7. The pseudo-flux A_{254} in the five studied sites on the Meurthe river and Moselle river in September 2015, January 2016 and October 2016.

Pseudo flux $F_{A_{254}}$ (m^3/s)	September 2015	January 2015	October 2016
Belleville	1.123	9.188	1.564
Pompey	0.449	8.326	0.729
Messein	0.361	5.990	0.501
Moulin Noir	0.618	2.145	0.729
Malzéville	0.554	2.245	0.678

The pseudo flux of A_{254} is the highest for Belleville despite the fact that A_{254} is the highest in Messein, since the highest flow rate is in Belleville. Thus fluxes are significantly higher in January 2016.

3.1.3 Synchronous fluorescence spectroscopy

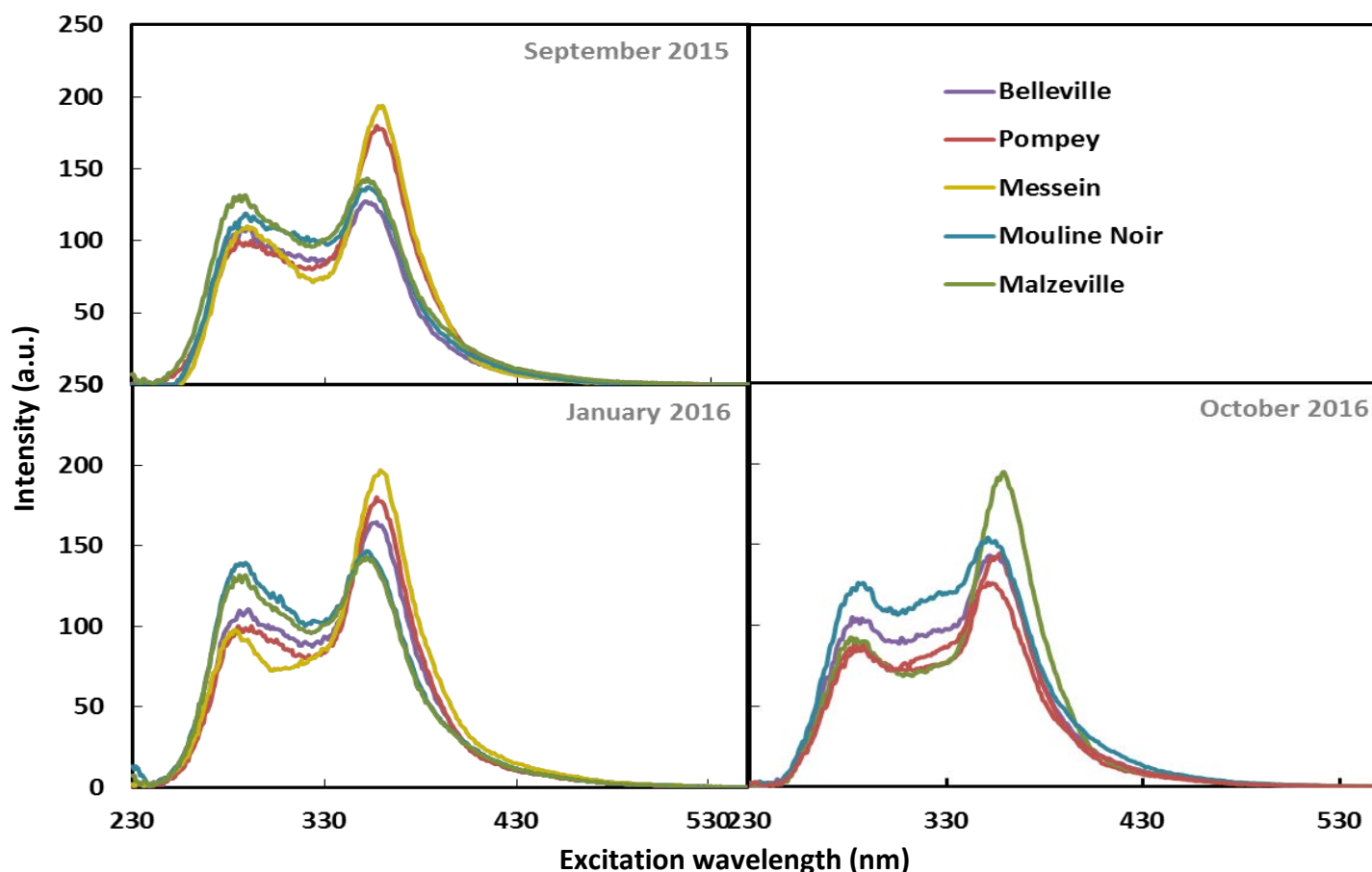


Fig. 15. Synchronous fluorescence spectra with $\Delta\lambda = 50$ nm for the five studied sites in the Meurthe and Moselle rivers.

All the fluorescence spectra displayed in Fig. 5 are similar irrespective of its location and nature (domestic/industrial). Only their respective intensities vary depending on the location, nature and period of the sampling. Two peaks were recorded for all the sites in the 3 sampling periods: the first at an excitation wavelength (λ_{ex}) around $\lambda_{ex} = 290$ nm where Mouline Noir has the highest intensity in January and October 2016, and the second at around $\lambda_{ex} = 355$ nm with a higher intensity and with Messein the highest in September 2015 and January 2016.

To discuss the presence of these 2 peaks, Fig. 6. shows the localization of excitation-emission zones for some biological substances.

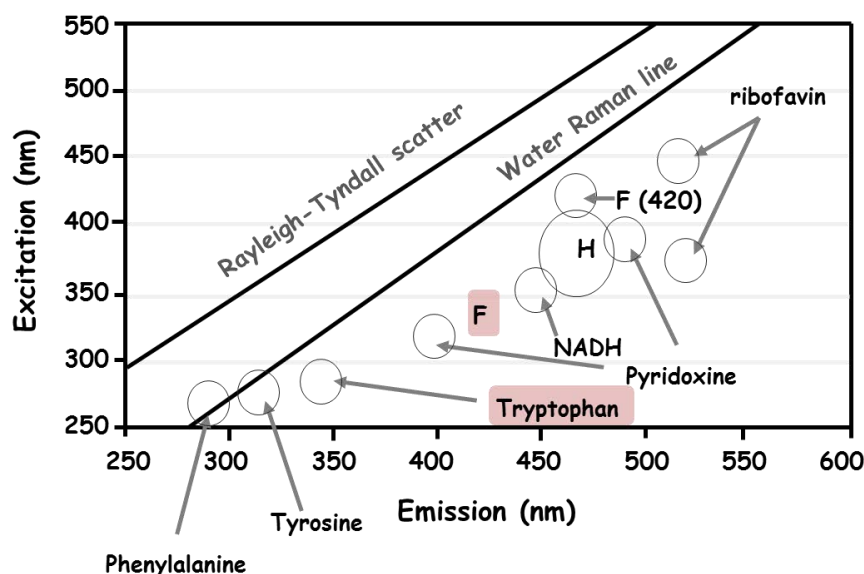


Fig. 16. Localization of excitation-emission zones. Note that F refers to fulvic.

By comparing our spectra to the localization zones in Fig. 6.; it can be deduced that the water samples of Meurthe river and Moselle river contain mainly tryptophan-like compounds ($\lambda_{ex} = 290$ nm, $\lambda_{em} = 350$ nm) and fulvic acids related to zone F ($\lambda_{exc} = 355$ nm, $\lambda_{em} = 405$ nm) (Pons et al. 2005). The 2 peaks are related to organic matter and organic nitrogen.

The presence of tryptophan is linked directly to the domestic and the agricultural pollution such as domestic organic nitrogen and domestic organic matter whose presence in rivers are related to the direct release of domestic wastes especially in places where there is no pretreatment sites. After their release into water some undergo transformation and treatment by wastewater treatment plant (WWTP) and some others remain in their state. The Fig. 7. shows the tryptophan-like emission in the different sites during the 3 sampling periods.

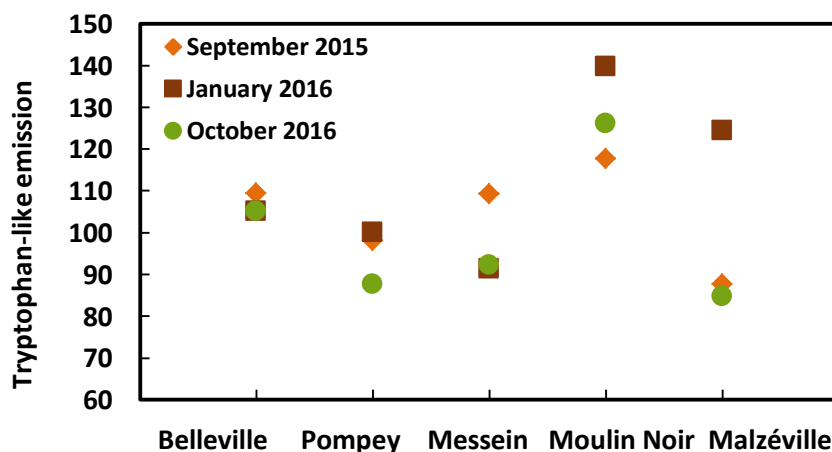


Fig. 17. Tryptophan-like fluorescence in the different sites for the 3 sampling periods.

The highest amount of organic nitrogen is detected in Moulin Noir. ‘Tryptophan-like’ fluorescence can be used as a measure of the “microbial health” of a water body and therefore can be used as an indicator of Biochemical Oxygen Demand (BOD). Good correlations (correlation coefficient > 0.9) were established between wastewater BOD and fluorescence ($\lambda_{exc} = 248$ nm or 280 nm, $\lambda_{em} = 340$ nm) by Reynolds and Ahmad (1997) and Ahmad and Reynolds (1999). This range corresponds to the tryptophan-like fluorescence (Ahmad et al. 1999, Pons et al. 2005).

The Table 8 describes the pseudo-flux, calculated according to Eq. (5), for the different sites for the 3 different periods. Moulin Noir has the highest tryptophan-like peak intensity while Belleville corresponds to the site with the highest tryptophan pseudo-flux. As mentioned before, this shows the effect of the flow rate on the measured species where Belleville has the highest flow rate in the 3 periods. Moreover, the flux of tryptophan-like is much higher in January 2016 than in September 2015 and October 2016.

Table 8. Pseudo-flux for tryptophan-like fluorescence in the 3 sampling periods.

Site	September 2015			January 2016			October 2016		
	Tryptophan-like emission intensity	Flow rate (m ³ /s)	Pseudo Flux (m ³ /s)	Tryptophan-like emission intensity	Flow rate (m ³ /s)	Pseudo Flux (m ³ /s)	Tryptophan-like emission intensity	Flow rate (m ³ /s)	Pseudo Flux (m ³ /s)
Belleville	109	13.5	1477	105	124	13032	105	21	2207
Pompey	98	5.4	530	100	90.5	9059	87	10.8	947
Messein	109	3.9	426	91	58.5	5347	92	6.46	596
Moulin Noir	117	8.08	951	139	30.3	4233	126	9.28	1170
Malzéville	87	8.08	708	124	30.3	3772	84	9.28	787

$$F_{\text{Trypto}} = \text{Tryptophan}_{(\text{intensity})} \times Q_{(\text{m}^3/\text{s})} \quad (5)$$

Concerning fulvic acids, they corresponds to an important fraction of Dissolved Organic Matter (DOM) in waters (McKnight et al. 2001). Fig. 8 displays the fulvic acid in different sites in the 3 sampling periods.

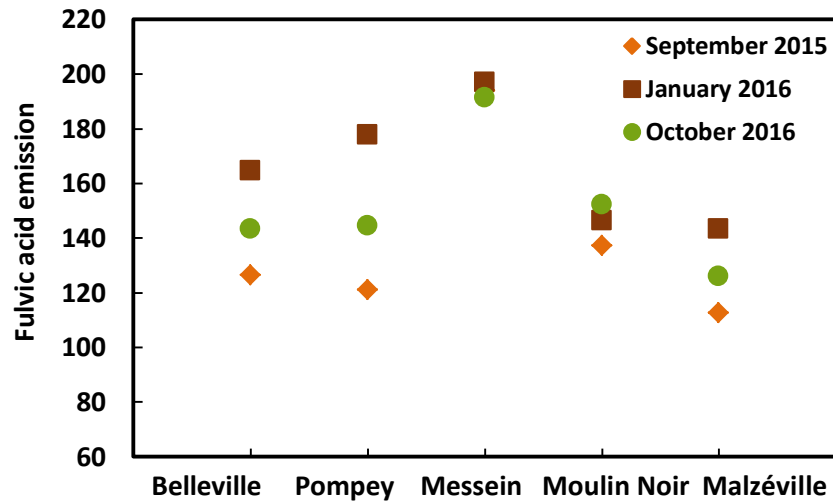


Fig. 18. Fulvic acid emission intensity in the five sites during the 3 sampling periods.

The highest amount of fulvic acids is found in Messein and it is approximately the same for the 3 months (Emission intensity = 197). For the other sites, the emission intensity is the highest in January 2016. Fulvic acid is a naturally occurring organic substance. It is part of the humic structure in a rich composting soil. It is produced in very small amounts by the action of million numbers of beneficial microbes, that work on decaying plant matter in a soil environment with adequate oxygen and released by paper mills.

As with tryptophan-like emission fluorescence, the pseudo-flux for fulvic emission is estimated in Eq. (6) for the studied sites in the 3 sampling periods. The results are presented in Table 9. Messein has the highest fulvic emission intensity (between 191.5 and 197) with the highest value obtained during January 2016. In terms of pseudo-fulvic flux, Belleville corresponds to the site with the highest. As a comparison of the fulvic pseudo-flux between the 3 sampling periods, the highest values are obtained in January 2016.

$$F_{\text{Fulvic}} = \text{Fulvic}_{(\text{intensity})} \times Q_{(\text{m}^3/\text{s})} \quad (6)$$

Table 9. Pseudo-flux for fulvic emission fluorescence during the 3 sampling periods.

	September 2015			January 2016			October 2016		
Site	Fulvic emission intensity	Flow rate (m ³ /s)	Pseudo-flux (m ³ /s)	Fulvic emission intensity	Flow rate (m ³ /s)	Pseudo-flux (m ³ /s)	Fulvic emission intensity	Flow rate (m ³ /s)	Pseudo-flux (m ³ /s)
Belleville	126	13.5	1708	164	124	20410	143.3	21	3009
Pompey	121	5.4	654	177	90.5	16091	144.6	10.8	1562
Messein	193	3.9	756	197	58.5	11530	191.5	6.46	1237
Moulin Noir	137	8.08	1109	146	30.3	4436	152.2	9.28	1412
Malzéville	112	8.08	911	143	30.3	4345	126	9.28	1169

3.2 Quantification of micropollutants in river water

The presence of 21 micropollutants were studied, detected and quantified at five different sites on Meurthe river and Moselle river during the same three periods between 2015 and 2016. Table 10 summarizes the concentration of each compound analyzed in the river water, its flux and the flow rate during every sampling period at the studied sites in September 2015, January 2016 and October 2016. Among these, the 2 hormones estradiol-beta and ethynylestradiol, and the 3 antibiotics sulfadimethoxine, sulfadimidine and sulfathiazole were below the limit of quantification (LOQ) at all sites and in the 3 samplings. Whereas, bisphenol A, carbamazepine, ibuprofen, PFOS and sulfamethoxazole were quantified at all sites and in the 3 samplings. The other compounds were differently quantified depending on the sampling site and the sampling period.

Table 10. The concentration in ng/L and the flux in g/day of the 21 studied micropollutants analyzed in the different sites during the 3 sampling periods. Note that F refers to flux in g/day and C refers to concentration in ng/L.

Compound	Value	Belleville	Pompey	Messein	Moulin Noir	Malzéville
September 2015	Q (m³/s)	13.5	5.4	3.9	8.08	8.08
Bisphenol A	F	155	15	15	165	48
	C	133	31.7	44.3	236	69.1
Estradiol-beta	F	-	-	-	-	-
	C	n.q	n.q	n.q	n.q	n.q
Estrone	F	-	-	-	-	-
	C	n.q	n.q	n.q	n.q	n.q
Ethinylestradiol	F	-	-	-	-	-
	C	n.q	n.q	n.q	n.q	n.q
Carbamazepine	F	58	10	8	38	15
	C	49.2	21	23.1	54.1	21.8
Carbamazepine-10,11-epoxide	F	-	-	-	-	-
	C	n.q	n.q	n.q	2.99	n.q
Clarithromycine	F	97	-	-	103	19
	C	83.5	n.q	n.q	148	27.3
Cyclophosphamide	F	-	-	-	-	-
	C	n.q	n.q	n.q	2.04	n.q
Diclofenac	F	33	-	2	61	5
	C	28.6	n.q	7.06	87.4	6.86
Erythromycin	F	-	-	-	-	-
	C	n.q	n.q	n.q	n.q	n.q
Ibuprofen	F	9	2	2	7	6
	C	7.63	5	5.7	9.33	8.18
Ketoprofen	F	-	-	-	12	-
	C	n.q	n.q	n.q	16.9	n.q
Lidocaine	F	44	12	14	40	13
	C	37.4	25.6	41	57.2	18.3
Naproxen	F	19	-	-	21	11
	C	16.4	n.q	n.q	29.6	15.2
Sulfadimethoxine	F	-	-	-	-	-
	C	n.q	n.q	n.q	n.q	n.q
Sulfadimidine	F	-	-	-	-	-
	C	n.q	n.q	n.q	n.q	n.q
Sulfamethoxazole	F	52	4	2	45	11
	C	44.6	8.96	6.63	64.6	15.8
Sulfathiazole	F	-	-	-	-	-
	C	n.q	n.q	n.q	n.q	n.q
Triclosan	F	-	-	-	-	-
	C	n.q	n.q	n.q	n.q	n.q
PFOA	F	-	-	-	-	-
	C	n.q	8.52	n.q	n.q	n.q
PFOS	F	19	7	7	10	9
	C	15.9	16	21.9	14.1	12.3

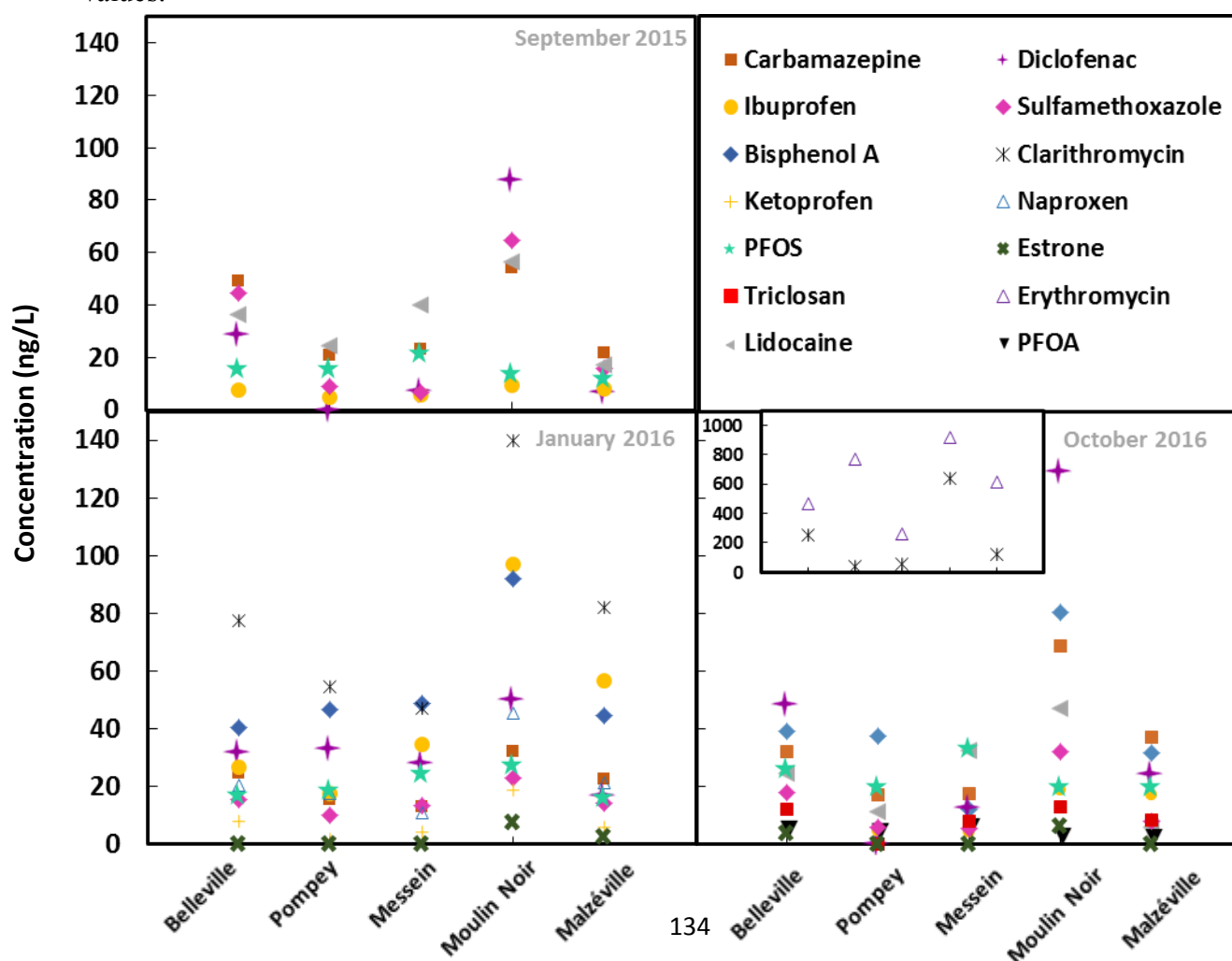
Compound	Value	Belleville	Pompey	Messein	Moulin Noir	Malzéville
January 2016	Q (m ³ /s)	124	90.5	58.5	30.3	30.3
Bisphenol A	F	435	366	246	241	117
	C	40.6	46.8	48.7	92.1	44.5
Estradiol-beta	F	-	-	-	-	-
	C	n.q	n.q	n.q	n.q	n.q
Estrone	F	-	-	-	-	-
	C	n.q	n.q	n.q	7.55	2.8
Ethinylestradiol	F	-	-	-	-	-
	C	n.q	n.q	n.q	n.q	n.q
Carbamazepine	F	264	123	66	84	59
	C	24.6	15.7	13	32.2	22.5
Carbamazepine-10,11-epoxide	F	-	-	-	-	-
	C	n.q	n.q	n.q	n.q	n.q
Clarithromycine	F	825	426	237	367	214
	C	77	54.5	46.9	140	81.6
Cyclophosphamide	F	-	-	-	-	-
	C	n.q	n.q	n.q	n.q	n.q
Diclofenac	F	340	257	142	131	43
	C	31.7	32.9	28	50	16.6
Erythromycin	F	-	-	-	-	-
	C	n.q	n.q	n.q	n.q	n.q
Ibuprofen	F	287	138	174	255	148
	C	26.8	17.6	34.5	97.3	56.7
Ketoprofen	F	83	13	19	49	15
	C	7.71	1.63	3.79	18.7	5.69
Lidocaine	F	268	315	194	-	-
	C	25	40.3	38.3	n.q	n.q
Naproxen	F	216	136	53	118	55
	C	20.2	17.4	10.4	45	21.1
Sulfadimethoxine	F	-	-	-	-	-
	C	n.q	n.q	n.q	n.q	n.q
Sulfadimidine	F	-	-	-	-	-
	C	n.q	n.q	n.q	n.q	n.q
Sulfamethoxazole	F	168	80	69	61	37
	C	15.7	10.2	13.7	23.2	14.2
Sulfathiazole	F	-	-	-	-	-
	C	n.q	n.q	n.q	n.q	n.q
Triclosan	F	903	-	-	157	186
	C	84.3	n.q	n.q	59.8	71.2
PFOA	F	77	112	79	-	-
	C	7.19	14.3	15.7	n.q	n.q
PFOS	F	185	146	124	73	43
	C	17.3	18.7	24.6	27.8	16.5

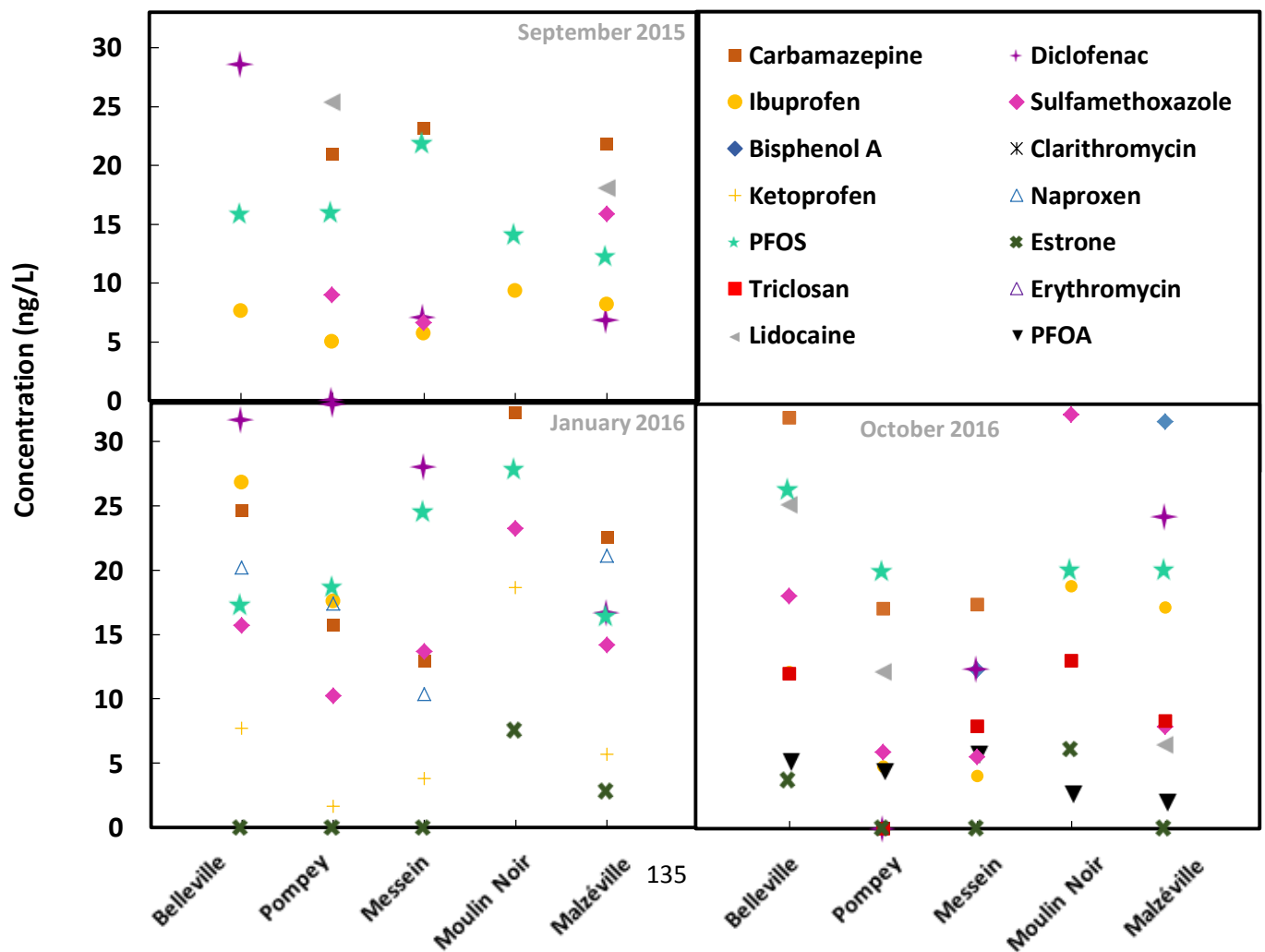
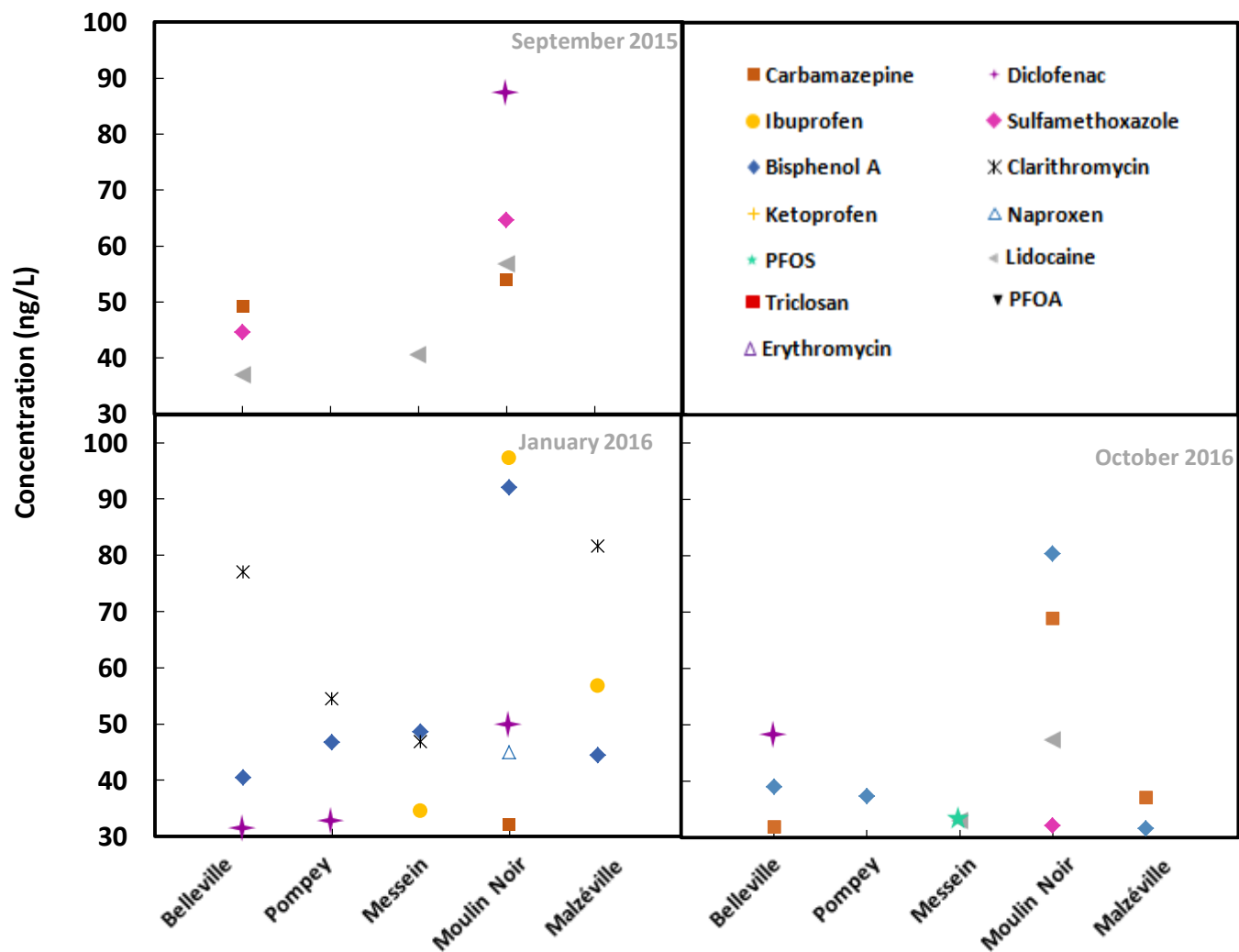
Compound	Value	Belleville	Pompey	Messein	Moulin Noir	Malzéville
October 2016	Q (m³/s)	21	10.8	6.46	9.28	9.28
Bisphenol A	F	71	35	7	64	25
	C	39.1	37.4	12.3	80.3	31.6
Estradiol-beta	F	-	-	-	-	-
	C	n.q	n.q	n.q	n.q	n.q
Estrone	F	7	-	-	5	-
	C	3.8	n.q	n.q	6.18	n.q
Ethinylestradiol	F	-	-	-	-	-
	C	n.q	n.q	n.q	n.q	n.q
Carbamazepine	F	58	16	10	55	30
	C	31.96	17.1	17.4	68.92	37.2
Carbamazepine-10,11-epoxide	F	-	-	-	-	-
	C	n.q	n.q	n.q	3.1	n.q
Clarithromycine	F	495	34	32	512	95
	C	253	36.23	57.49	639	118.2
Cyclophosphamide	F	-	-	-	-	-
	C	n.q	n.q	n.q	n.q	n.q
Diclofenac	F	88	-	7	104	19
	C	48.5	n.q	12.4	129	24.27
Erythromycin	F	847	717	148	734	494
	C	467	768.8	264.37	914.9	615.7
Ibuprofen	F	22	5	2	15	14
	C	12.2	4.9	4.1	18.8	17.2
Ketoprofen	F	-	-	-	6	-
	C	n.q	n.q	n.q	6.99	n.q
Lidocaine	F	46	12	19	38	5
	C	25.4	12.4	33.4	47.8	6.7
Naproxen	F	-	-	-	11	11
	C	n.q	n.q	n.q	13.7	13.6
Sulfadimethoxine	F	-	-	-	-	-
	C	n.q	n.q	n.q	n.q	n.q
Sulfadimidine	F	-	-	-	-	-
	C	n.q	n.q	n.q	n.q	n.q
Sulfamethoxazole	F	33	6	3	26	6
	C	18.1	5.9	5.58	32.2	7.92
Sulfathiazole	F	-	-	-	-	-
	C	n.q	n.q	n.q	n.q	n.q
Triclosan	F	22	-	5	11	7
	C	12.1	n.q	8	13.1	8.4
PFOA	F	9	4	3	2	2
	C	5.2	4.47	5.8	3	2.1
PFOS	F	47	19	19	16	16
	C	26	20	34	20	20

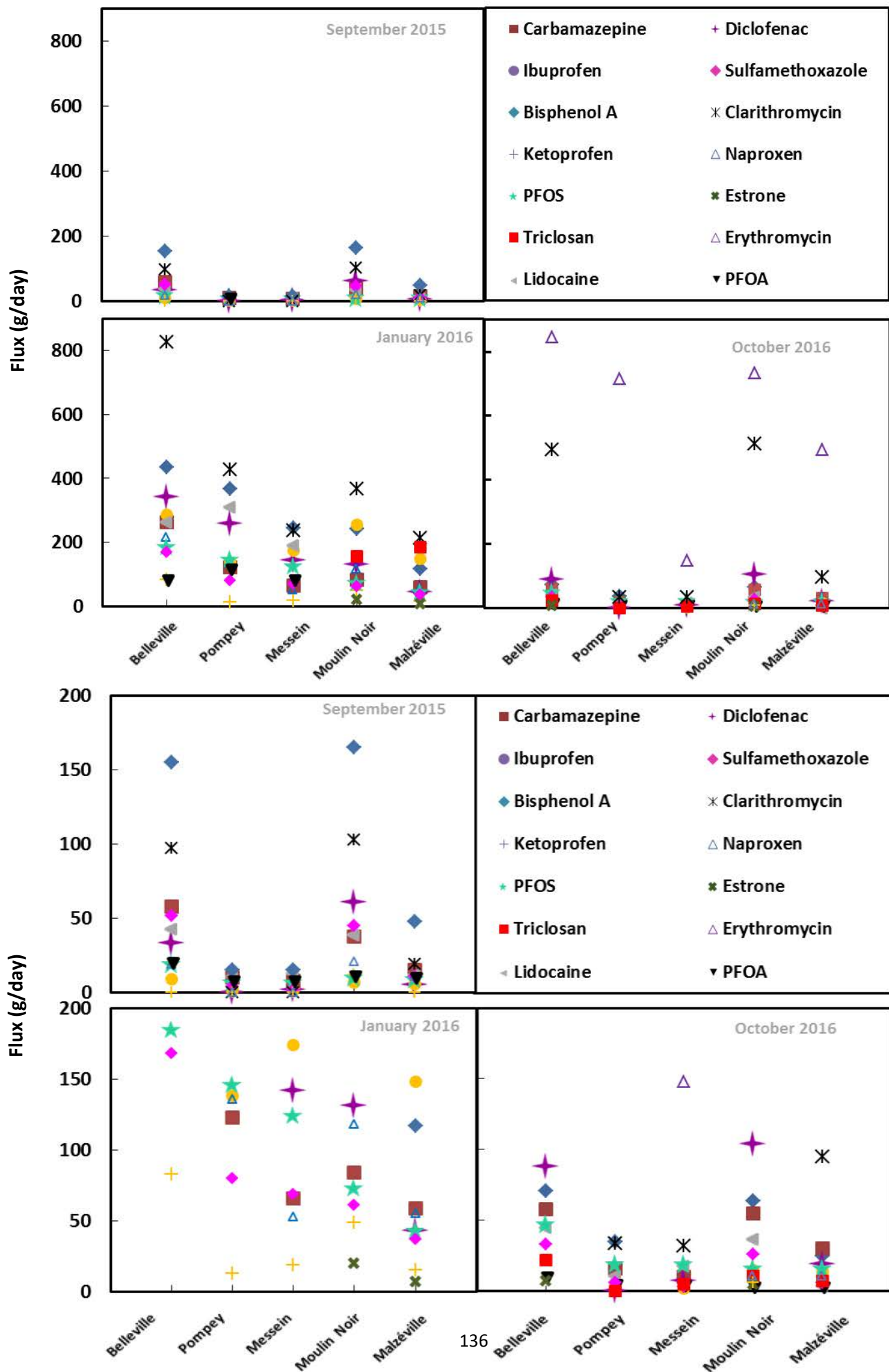
Referring to Tables 10, the concentrations of the micropollutants range from few ng/L to hundreds ng/L. Some compounds are poorly quantified such as Carbamazepine-10, 11-epoxide, cyclophosphamide, and estrone. Carbamazepine-10,11-epoxide is quantified in Moulin Noir in September 2015 and October 2016 only, and cyclophosphamide is quantified only in Moulin Noir in September 2015. Erythromycin is quantified only in October 2016 with relatively high concentrations ranging between 260 ng/L and 900 ng/L, while its concentration is below LOQ in September 2015 and January 2016. This wide gap in the quantified concentration is possibly due to the instability of the erythromycin molecule in solutions during the analysis and the storage of the sample (Brisaert et al. 1996). Estrone is the only ED hormone that is quantified in some sites. Its concentration is below the LOQ in September 2015 while its concentration is quantified at Moulin Noir (7.55 ng/L) and Malzéville (2.8 ng/L) in January 2016, and at Belleville (3.8 ng/L) and Moulin Noir (6.18 ng/L) in October 2016 with relatively low concentrations.

3.2.1 Site position effect

Fig. 9. shows the concentrations and the fluxes of the mostly quantified compounds at the five sampling sites for the 3 sampling periods using 3 different scales for more clear reading of the values.







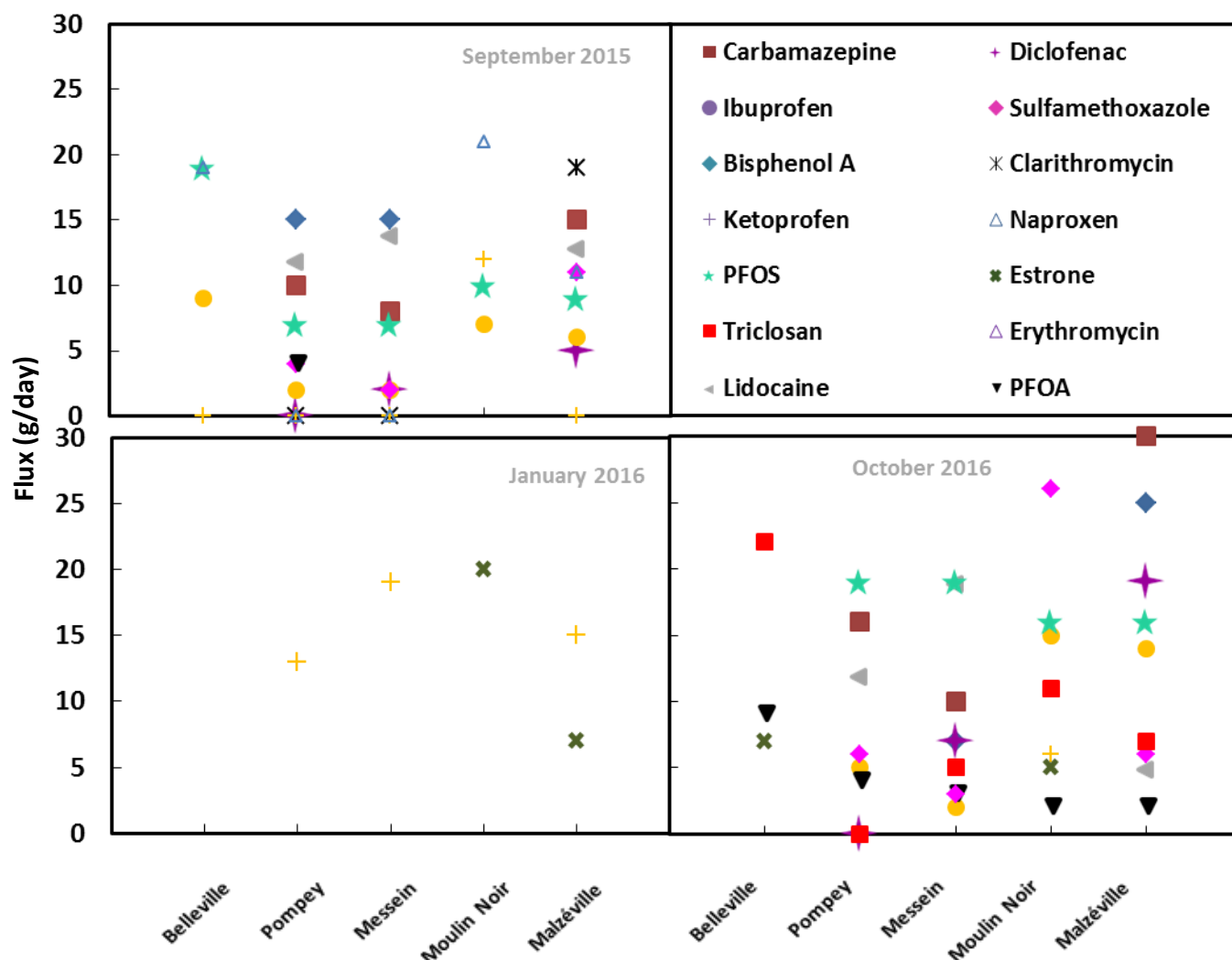


Fig. 19. The concentrations and fluxes of the mostly quantified micropollutants at the five sampling sites in the 3 sampling periods.

The highest concentrations of different micropollutants are quantified in October 2016. To explain the site position effect, Fig. 10 and Table 11 shows the location of the five sampling sites across the 2 rivers and their characteristics. Moulin Noir, downstream the WWTP, has generally the highest concentration for most of the micropollutants whereas the lowest concentrations is quantified in Messein and Pompey. It can be also mentioned that the concentration of micropollutants downstream the confluence, i.e. Belleville, is between the concentration of the two rivers, Meurthe and Moselle rivers, upstream the confluence. Consequently, its flux is, on average, the sum of the two fluxes upstream the confluence normally Pompey and Moulin Noir.

Moulin Noir and Malzéville are located on the Meurthe river, and Pompey and Messein on the Moselle river. The largest city in the region, Nancy, is located on the Meurthe river (River 2). Its wastewater is treated in a WWTP and released in the Meurthe river between Malzéville and Moulin Noir. It corresponds to about 300,000 inhabitants. In comparison to the release into the Moselle river

where there is the far smaller cities of Epinal with an average population of about 35 800 and Toul with 16300 (Fig. 10).

Messein has the lowest concentration for most of micropollutants among all the other sites. Water from Messein Lake is pumped for appropriate treatment before being distributed to the city as drinking water. The low concentration of micropollutants in Messein is a good indication for the quality of the water used for drinking.

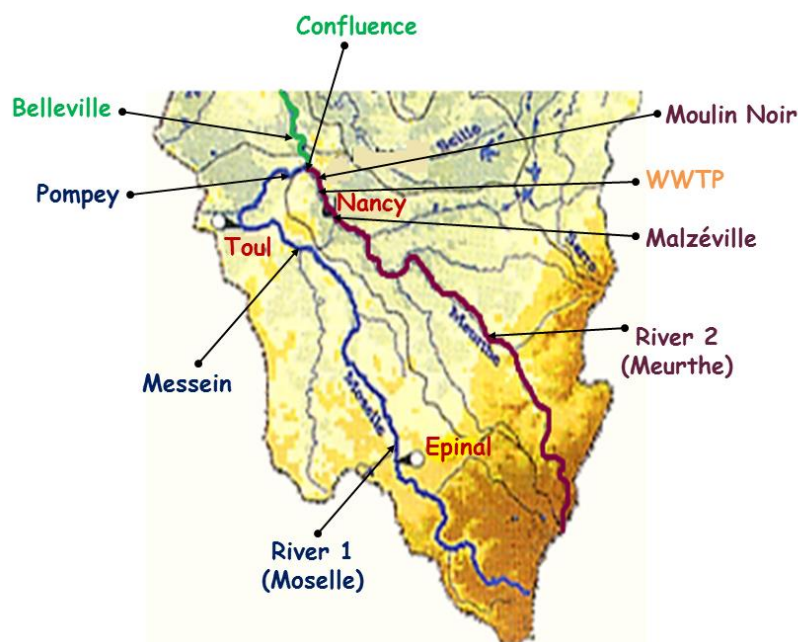


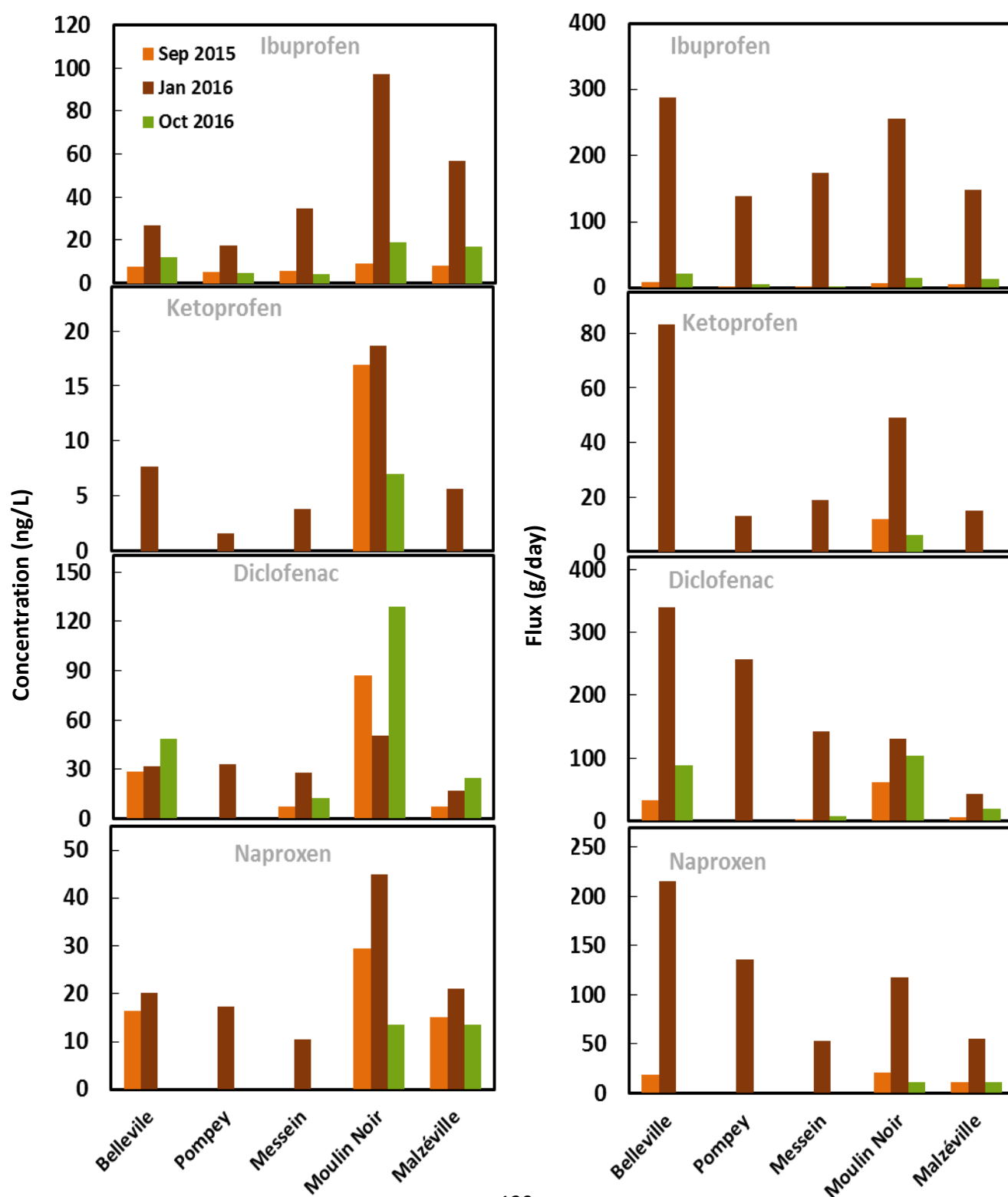
Fig. 20. Corresponding cities located across the Meurthe river and Moselle river.

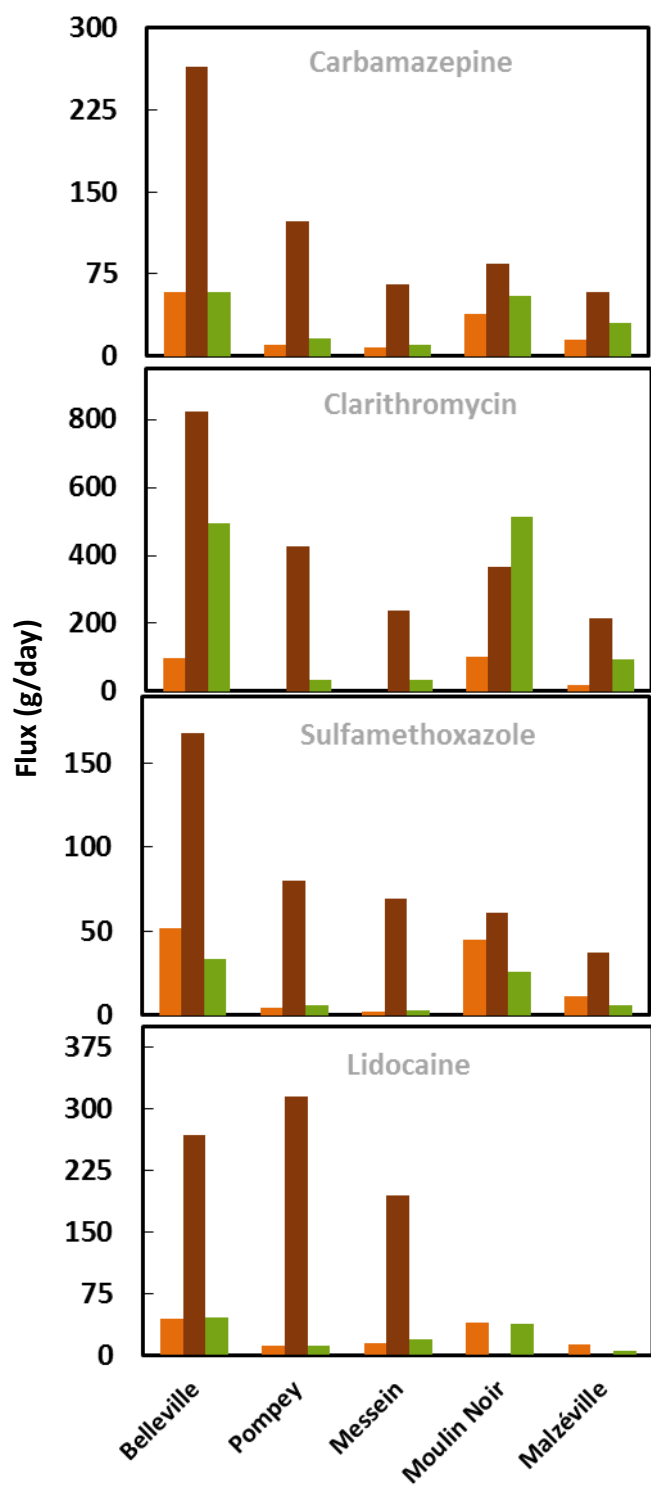
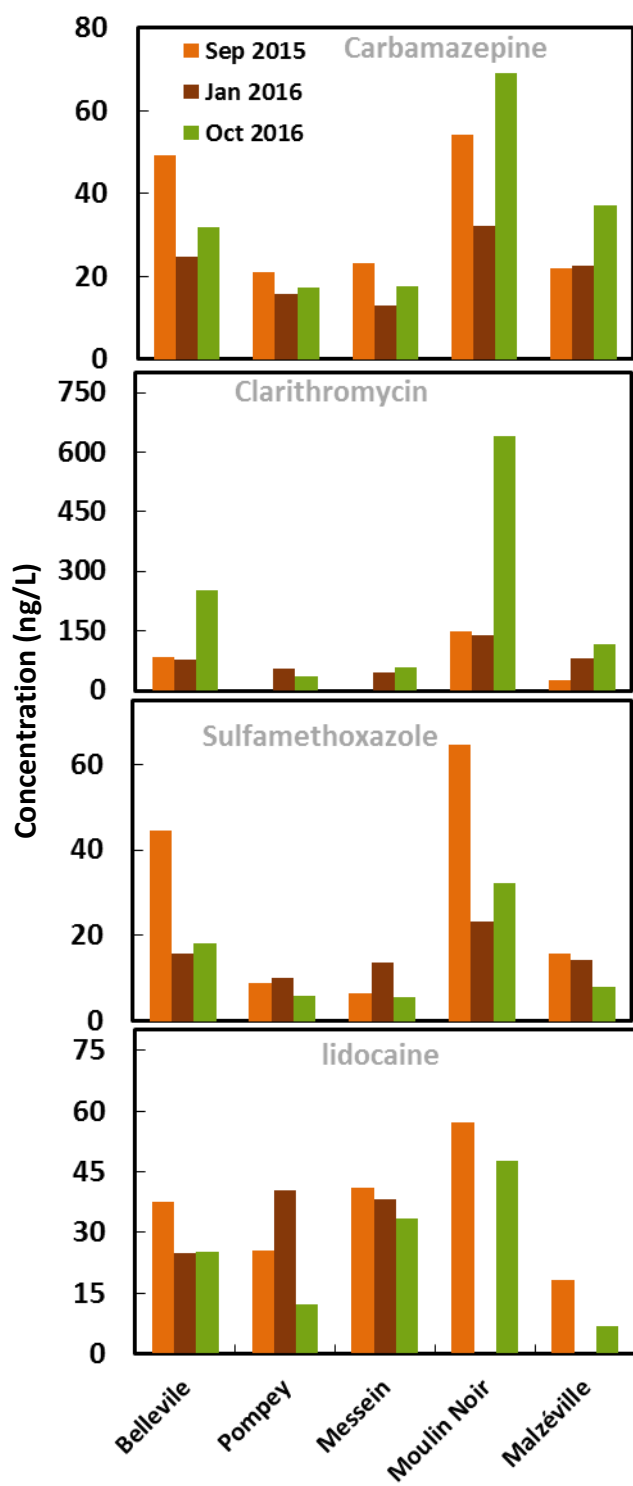
Table 11. The characteristics of the five sampling sites on Meurthe river and Moselle river.

Site name	Location
Belleville	Downstream of the confluence of river 1 and river 2.
Pompey	River 1 (Moselle river), upstream of the confluence.
Messein	River 1 (Moselle river), catchment area for drinking water.
Moulin Noir	River 2 (Meurthe river), upstream of the confluence and downstream of the WWTP.
Malzéville	River 2 (Meurthe river), upstream of the WWTP.

3.2.2 Variation with the time

Then, we study the variation of the concentration of micropollutants with time. To this aim, the concentration of each of the quantified compounds is shown in Fig. 11. for the 3 sampling dates: September 2015, January 2016 and October 2016.





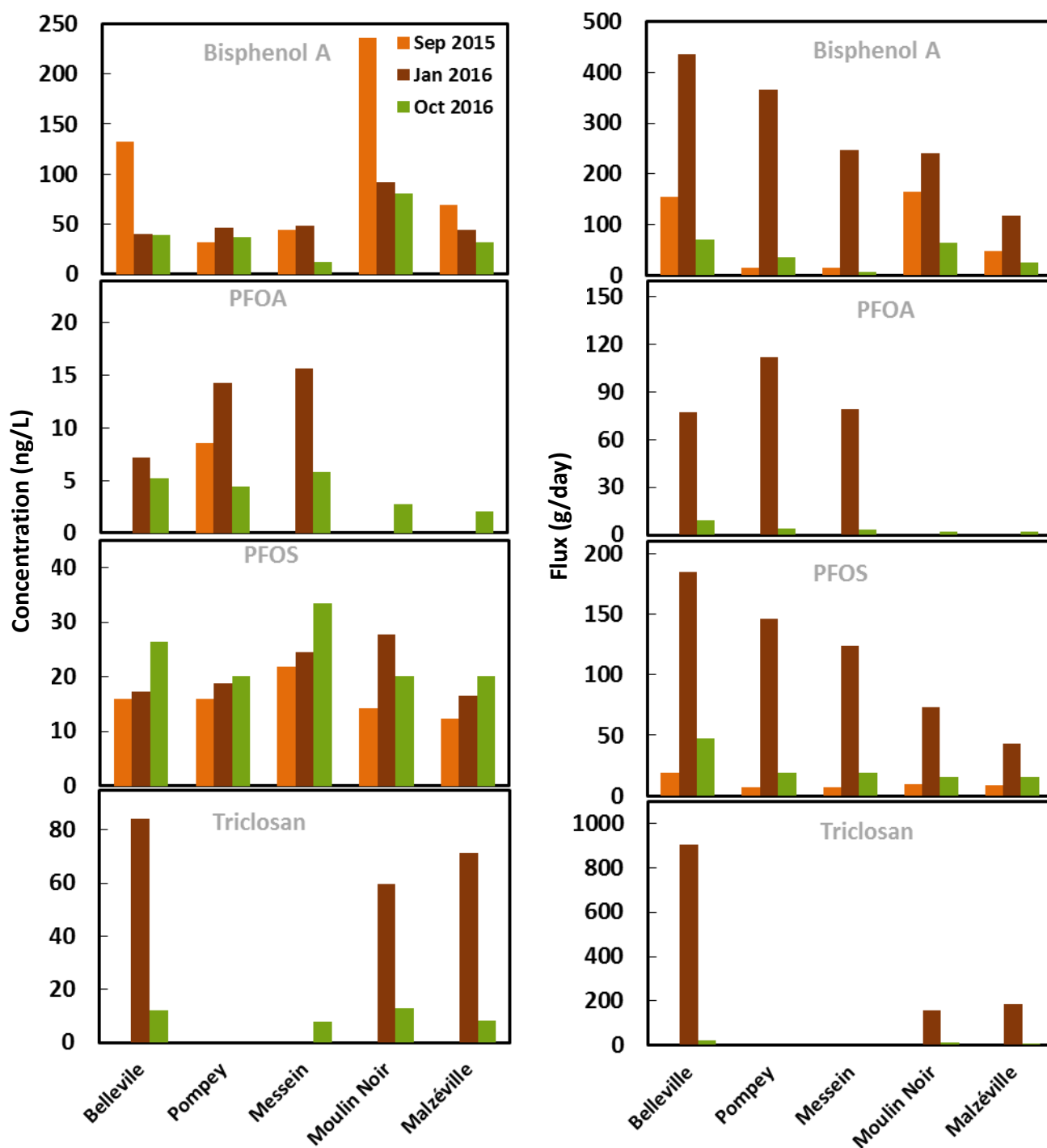


Fig. 21. Concentration and flux of each of the quantified micropollutants at different sites in the 3 sampling periods.

The fluxes are the highest in January 2016. Ketoprofen, Naproxen and Ibuprofen are more quantified in January with the highest concentration in Moulin Noir with 18.65 ng/L, 45.0 ng/L and 97.3 ng/L respectively. Ibuprofen is present all the year and at all positions, ketoprofen is present all the year in Moulin Noir, Naproxen is detected in Moulin Noir and Malzéville. The three drugs are non-steroidal anti-inflammatory drugs (NSAID). More specifically, they are used to treat inflammation or pain caused by many conditions such as arthritis, menstrual cramps, bursitis, and tendinitis. Ibuprofen has higher concentration than the other two drugs since it is more commonly used by people especially for being also used to reduce fever, headache and back pain. All these inflammatories and pains are more prominent in winter where people suffer from joints pain, fever, and flu. Diclofenac is another NSAID with higher and unstable variation between January and October. This is due to the fact that it is used all the year as a pain removal so it is difficult to have a precise comparison. Carbamazepine is quantified everywhere and all the time. It is due to its wide usage as antiepileptic drug to prevent and control seizures. Then, this compound needed during all the year. Clarithromycin and sulfamethoxazole are both antibiotics. Clarithromycin is mostly quantified in October with a very high concentration of 639 ng/L compared to the other 2 samplings and the other quantified compounds. The reason for this high concentration is the widespread use of this compound to treat some bacterial infections, such as bronchitis (infection of the tubes leading to the lungs), and infections of the skin, ears, throat and sinuses that increase with the beginning of the cold weather in October. Sulfamethoxazole is most quantified in September with the highest concentration in Moulin Noir (64.6 ng/L). Moreover, the concentration is much less than that of clarithromycin. This is due to the fact that it is abandoned as a single effective agent today due to the development of bacterial resistance to its effect and its brands and generic formulations have been discontinued according to the FDA database ([Raymond et al. 2010](#)). Lidocaine has a close concentration in the 3 samplings with the highest at Moulin Noir in September 2015 with 57.3 ng/L. Its flux is present in Moselle river in January 2016 only. This comes maybe from Epinal and Toul cities and not from Nancy city. Lidocaine is a local anesthetic that is used to stop pain and itching of the skin by causing temporary loss of skin feeling. This action is independent of the weather and used in all seasons. Bisphenol A is most quantified in January 2016. It is a chemical contained in polycarbonate plastics and epoxy resins which is included in various products used in industry. Concerning the perfluorinated compounds, PFOS is quantified with similar concentrations in all the sampling dates at all the sites. The largest concentration is quantified at Messein in October 2016 with 31 ng/L. PFOA is mostly quantified at Messein in January with 15.69 ng/L. Low concentration and flux are present on the Meurthe river (river 2) with nothing in January 2016 and September 2015. It could be released by a factory located on Moselle river. Concerning triclosan, it is quantified

at Belleville, Moulin Noir and Malzéville in October 2016 and January 2015 with a maximum concentration of 84.3 ng/L at Belleville in January. There is nothing in the Moselle river (river 1) upstream the confluence. So, there is probably a factory upstream the WWTP on the Meurthe river and another one just before Belleville (between Pompey and Belleville or between Moulin Noir and Belleville).

3.3 Release of micropollutants by the wastewater treatment plant

To study the release of micropollutants by WWTP, we will follow more particularly the micropollutants analyzed in Moulin Noir, that is located downstream the WWTP, and Malzéville, that is located upstream the WWTP. Table 12 shows the concentrations and fluxes of the quantified micropollutants upstream (Malzéville) and downstream (Moulin Noir) the WWTP during the 3 sampling dates. In addition, the table presents the flux coming from the WWTP released into the city river (F_{city} in g/day) where its variation during the 3 sampling periods is shown in Fig. 12. F_{city} can be calculated from its relation with the fluxes upstream (Malzéville) and downstream (Moulin Noir) the WWTP illustrated in Eq. (7) and Eq. (8).

$$F_{city} + F_{upstream} = F_{downstream} \quad (7)$$

Where F is in g/day. Then

$$F_{city} = F_{downstream} - F_{upstream} \quad (8)$$

Table 12. The concentrations in ng/L, the fluxes in g/day of the quantified micropollutants and the flux coming from the WWTP in g/day during September 2015, January 2016 and October 2016 upstream and downstream the WWTP. The letter F refers to flux and C to concentration.

The micropollutants that are not mentioned in Table 12 which are estradiol-beta, ethynyl estradiol, carbamazepine-10,11-epoxide, cyclophosphamide, sulfadimethoxine, sulfadimidine, sulfathiazole, triclosan, and PFOA are not quantified downstream the WWTP during the three sampling periods. The concentration of the different groups of micropollutants increased after the WWTP. This emphasizes the relative inefficiency of the WWTP in the removal of the micropollutants due to the use of conventional treatments that are not specified for the removal of micropollutants. Then, in Moulin Noir, micropollutants coming from both river water and water from the WWTP lead to this increase in the concentration.

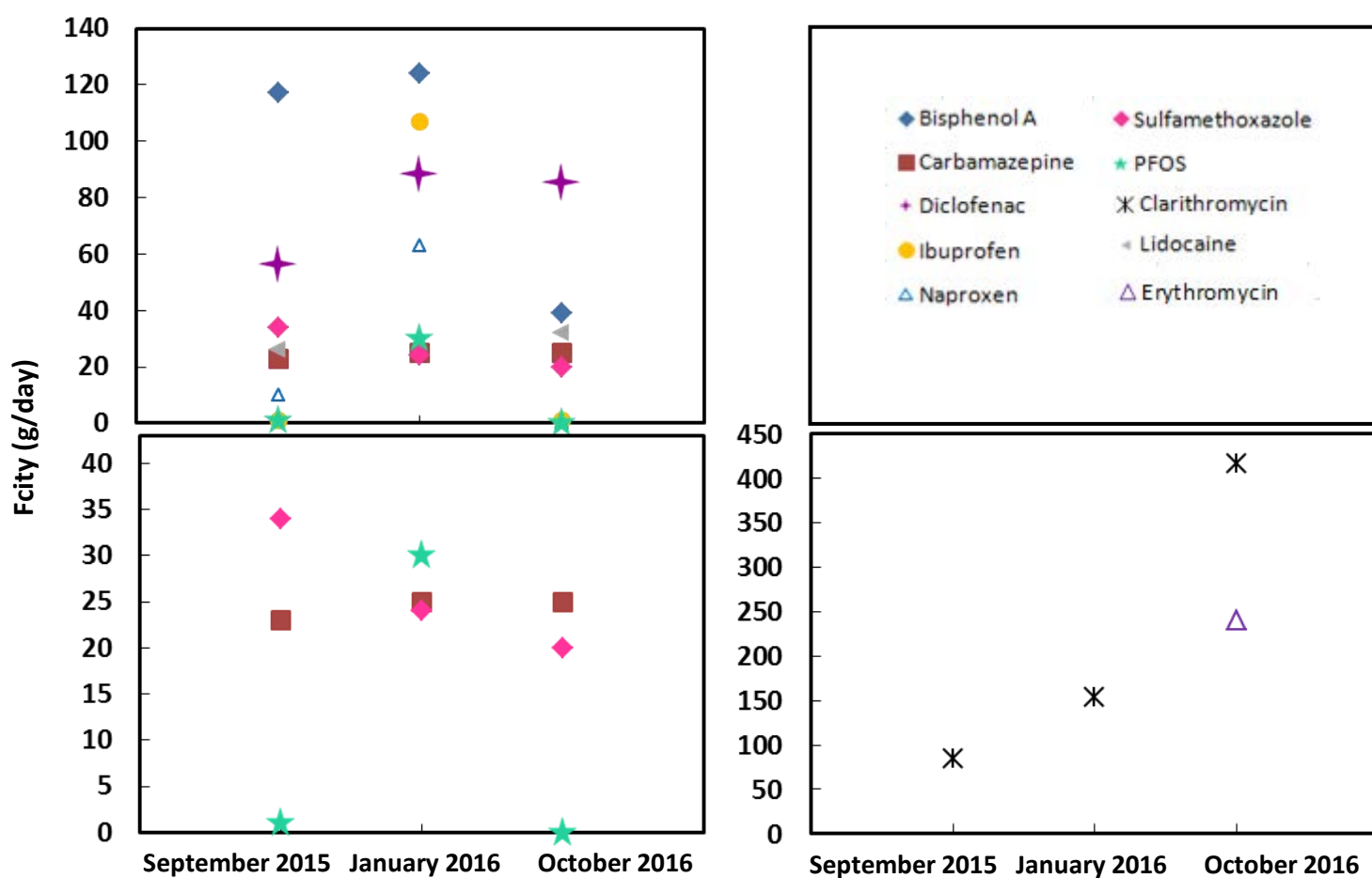


Fig. 22. The variation of the fluxes from the WWTP, F_{city} in g/day, during the 3 sampling periods.

The variation of the F_{city} between the 3 sampling periods differs from one micropollutant to another (Fig. 12). It appears also that F_{city} of carbamazepine and lidocaine are somehow constant between the 3 sampling periods. For carbamazepine, it is not surprising to have the same values during the 3 sampling periods since it is an anti-epileptic that people use every day with the same amounts as a long term treatment. The change in F_{city} of sulfamethoxazole is not significant which is

an indication for having fluxes of same proportion all the time. PFOS, clarithromycin and Naproxen show great variation in the F_{city} between the 3 periods. Bisphenol A has close F_{city} values in September 2015 (117 g/day) and January 2016 (124 g/day) that decrease sharply in October 2016 (39 g/day). This is probably due to the fact that bisphenol A is becoming forbidden in France recently. As a consequence, its use as a raw material by industry and thus by people is decreasing. Diclofenac displays an increase in F_{city} from September 2015 (56 g/day) to January 2016 and October 2016 that have similar F_{city} of around 85-88 g/day due to its increased usage as a pain removal at cold weather. F_{city} of ibuprofen remains the same in September 2015 and October 2016 (1 g/day) while it increases sharply to 107 g/day in January 2016 since it is used against fever, pain and flu that people suffer from during winter season starting from December.

3.4 Mass balance study

The study of the mass balances upstream and downstream the confluence between Meurthe river and Moselle river could be a way to control the quality of the measurements. For this goal, the sum of the fluxes was compared to the real flux downstream the confluence (Belleville), in order to calculate the mass balance precision percentage ($f_{\%}$). The Table 13 presents the $f_{\%}$ for the quantified micropollutants upstream and downstream the confluence in September 2015, January 2016 and October 2016. The average $off_{\%}$ in the 3 sampling periods for each micropollutant is calculated using the absolute values of $f_{\%}$ according to Eq. (9).

$$\text{Average } f_{\%} (i) = \frac{f_{\%} (i)(\text{September}) + f_{\%} (i)(\text{January}) + f_{\%} (i)(\text{October})}{3} \quad (9)$$

where (i) is the selected micropollutant.

Table 13. Mass balance precision percentage ($f_{\%}$) of the confluence between Meurthe and Moselle rivers for the quantified micropollutants during the 3 sampling periods.

Date/ $f_{\%}$	11-Sep-15	5-Jan-16	14-Oct-16	Average
Clarithromycine	-	-4	9	6.5
Sulfamethoxazole	-6	-20	-6	10.7
Lidocaine	15	-	8	11.5
Diclofenac	-	12	-	12.0
Naproxen	-	15	-	15.0
Ibuprofen	-13	27	-10	16.7
PFOS	-12	16	-34	20.7
Carbamazepine	-19	-28	18	21.7
Bisphenol A	14	28	28	23.3
Ketoprofen	-	-34	-	34.0
Erythromycine	-	-	42	42.0
PFOA	-	-	-50	50.0

The absolute values of the mass balance precision percentage for the first ten micropollutants range between 24 % as a minimum and 34 % as a maximum. As for the average $f_{\%}$, it is below 34 % with the $f_{\%}$ for the first five compounds below 15 %. Such values are relatively good taking into consideration the difficulty of quantifying such low concentration in ng/L. The results of $f_{\%}$ were below 25 % in the cases when it was possible to calculate an average for 3 sampling periods where the percentage error of the chemical analysis ranges between 10 % and 20 %. Thus this is an important indication for the good quality of the measurements and their precision and reliability.

3.5 Detection of micropollutants in drinking water

Two drinking water samples are taken from LRGP laboratory in Nancy, France on 05 January 2016 and 14 October 2016 to be analyzed. The concentrations of all the analyzed micropollutants were below the limits of quantification. By comparing this result to the concentration of the micropollutants in Messein, the water catchment for drinking water, that are shown in Table 14, we can conclude that the drinking water treatment plant (DWTP) has the ability to remove micropollutants that are analyzed at ng/L. This is reflected from the concentrations of

micropollutants, listed in Table 14, that were quantified in Messein and their concentration become below the limit of quantification in the analyzed drinking water. After the treatment of drinking water by DWTP, it is used by the city which then goes to the WWTP for treatment before discharging it into the rivers. Consequently, all the pollutants released in the rivers are coming from the activity of the city (some part is not removed by the WWTP) since the concentration of micropollutants in drinking water is below the LOQ.

Table 14. Concentration of micropollutants in Messein on January 2016 and October 2016.

Micropollutant concentration (ng/L)	January 2016	October 2016
Bisphenol A	48.7	12.3
Estradiol-beta	n.q	n.q
Estrone	n.q	n.q
Ethinylestradiol	n.q	n.q
Carbamazepine	13.0	17.4
Carbamazepine-10,11-epoxide	n.q	n.q
Clarithromycin	46.9	57.49
Cyclophosphamide	n.q	n.q
Diclofenac	28.0	12.4
Erythromycin	n.q	264.37
Ibuprofen	34.5	4.1
Ketoprofen	3.79	n.q
Lidocaine	38.3	33.4
Naproxen	10.4	n.q
Sulfadimethoxine	n.q	n.q
Sulfadimidine	n.q	n.q
Sulfamethoxazole	13.7	5.58
Sulfathiazole	n.q	n.q
Triclosan	n.q	8.0
PFOA	15.7	5.8
PFOS	24.6	34

4 Conclusion

The detection and quantification of 21 micropollutants (pharmaceuticals, endocrine disruptors, personal care products) present in the Meurthe river and Moselle river were performed using a multi-residual SPE-LC-MS/MS system based on electro-spray ionization method. Samples were taken from five sites during three sampling periods between September 2015 and October 2016. The concentrations of the studied micropollutants present in the two rivers vary according to the sampling site, sampling period and the type of micropollutants. Quantification at a concentration of ng/L, the concentration of some compounds was eye-catching such as the unusual concentrations of triclosan quantified in Meurthe river, and PFOA in Moselle river that could be due to presence of specific factories on specific locations causing the presence of these compounds in certain sites only.

The fluxes of the analyzed micropollutants and their change were calculated based on the variation of the flow rate of the two rivers at each site during the three sampling periods. It is showed that, as a function of concentration, the change in fluxes can be very different depending on the flow rate of the rivers. Also this depends on what is released by the different area and on the kind of use of micropollutants during the year such that if the use is permanent or temporary. As an example, carbamazepine is an anti-epileptic used every day to treat seizures independent of the time and weather. Its flux is approximately the same during the year, as well as bisphenol A which is found in different home stuff materials and that is always used along the year. Contrary to diclofenac that has flux change during time since its release depends on the activity of people.

The release of micropollutants by the wastewater treatment plant is studied. The concentrations and fluxes of micropollutants upstream (Malzéville) and downstream (Moulin Noir) the WWTP are compared allowing the calculation of the release of micropollutants at the outlet of WWTP and quantification of their fluxes. Results demonstrate that the WWTP is not completely efficient in the removal of micropollutants due to the use of conventional treatment methods.

The mass balance at the confluence between the Meurthe and Moselle rives is evaluated. Taking into account the difficulty of measuring the very low concentration of micropollutants, the results are relatively good with an average $f_{\%}$ below 25 % for most of the micropollutants that we were able to calculate their $f_{\%}$. This is a good value especially when compared to the percentage of the error of the chemical analysis ranging between 10 % and 20 %. Thus, it is an important indication for the good quality of the analytical procedure and measurements and their precision and reliability of our methods.

The concentrations of micropollutants present in drinking water samples taken directly from the tap are examined to be below the limit of quantification. This is an important indication for the good quality of the drinking water. If we compare this result to the quantified concentrations in Messein, we can see that the concentration of some micropollutants in the later is significantly larger than the limit of quantification. This emphasizes the efficiency of the drinking water treatment plant DWTP in the removal of micropollutants.

It was not surprising to identify Moulin Noir, the location downstream the WWTP, as the place with the highest number of different kinds of micropollutants. This observation was the same for the three sampling periods. Then, we conclude that river water to be used in the laboratory experiments for the removal of pollutants by heterogeneous photo-Fenton process, should be taken at the location of Moulin Noir (on the Meurthe river, downstream the WWTP). This aspect will be presented in the next chapter.

References

- Ahmad S.R., Reynolds D.M (1999) Monitoring of Water Quality Using Fluorescence Technique: Prospect of on-Line Process Control. *Water Res.* 33 (9): 2069-74.
- Blanco M, Martinez A, Marcaide A, Aranzabe E, Ana Aranzabe A (2014) Heterogeneous Fenton Catalyst for the Efficient Removal of Azo Dyes in Water. *Am. J. Anal. Chem.* 5 (8): 490-499
- Brisaert M, Heylen M, Plaizier-Vercammen J (1996) Investigation on the Chemical Stability of Erythromycin in Solutions Using an Optimization System. *Pharm. World Sci.* 18 (5): 182-86.
- Fard M.A, Barkdoll B, Vosoogh A, Aminzadeh B (2017) Using polymer coated nanoparticles for adsorption of micropollutants from water. *Colloids Surface A* 531 (october): 189-97.
- Ianoul Ai, Coleman T, Asher S.A (2002) UV Resonance Raman Spectroscopic Detection of Nitrate and Nitrite in Wastewater Treatment Processes. *Anal. Chem.* 74 (6): 1458-61.
- König M, Escher B.I, Neale P.A, Krauss M, Hilscherová K, Novák J, Teodorović I, et al (2017) Impact of Untreated Wastewater on a Major European River Evaluated with a Combination of in Vitro Bioassays and Chemical Analysis. *Environ. Pollut.* 220 (january): 1220-30.
- McKnight D.M, Boyer E.W, Westerhoff P.K, Doran P.T, Kulbe.T, Andersen D.T (2001) Spectrofluorometric Characterization of Dissolved Organic Matter for Indication of Precursor Organic Material and Aromaticity. *Limnol. Oceanogr.* 46 (1): 38-48.
- Nikanorov A.M, Brazhnikova L.V. *Water Chemical Composition Of Rivers, Lakes And Wetlands. Encyclopedia of Life Support Systems (EOLSS).*
- Niemirycz E, Gozdek J, Koszka-Maróń D (2006) Variability of Organic Carbon in Water and Sediments of the Odra River and Its Tributaries. *Polish J. of Environ.* 15 (4): 557-563
- Nordin R.N, Pommen L.W (2009) *Water Quality Guidelines for Nitrogen (Nitrate, Nitrite, and Ammonia).* Water Stewardship Division Ministry of Environment Province of British Columbia.
- Pons M.N, Le Bonté S, Potier O (2004) Spectral Analysis and Fingerprinting for Biomedica Characterisation. *J. Biotechnol.* 113 (1-3):211-30.
- Pons M.N, Jing W, Potier O (2005) Chemometric Estimation of Wastewater Composition for the On-line Control of Treatment Plants. *IFAC Proceedings Volumes* 38 (1): 49-54.
- Raymon J, Lamarque D, Kalach N, Chaussade S, Burucoa C (2010) High Level of Antimicrobial Resistance in French *Helicobacter Pylori* Isolates. *Helicobacter* 15 (1): 21-27.

- Schwiente M, Guillet G, Rügner H, Kuch B, Grathwohl P (2016) A High-Precision Sampling Scheme to Assess Persistence and Transport Characteristics of Micropollutants in Rivers . Science of The Total Environment 540 (january): 444-54.
- Tousov Z, Oswald P, Slobodnik J, Blaha L, Muz M, Hu M, Brack W, et al (2017) European Demonstration Program on the Effect-Based and Chemical Identification and Monitoring of Organic Pollutants in European Surface Waters. Sci. Total Environ. 601-602 (december): 1849-68.
- Walker K « Total Nitrogen Analysis: A New Perspective on TOC ».
- Wang Y, Roddick F.A, Fan L (2017) Direct and indirect photolysis of seven micropollutants in secondary effluent from a wastewater lagoon. Chemosphere 185 (Supplement C): 297-308.
- Wu Z, Guo K, Fang J, Yang X, Xiao H, Hou S, Kong X, et al (2017) Factors affecting the roles of reactive species in the degradation of micropollutants by the UV/chlorine process. Water Res. 126 (Supplement C): 351-60.

Chapter III

Iron impregnated zeolite catalyst for efficient removal of micropollutants at very low concentration from Meurthe river: Comparison with heterogeneous TiO₂ photocatalysis

After succeeding in the quantification of different micropollutants at ng/L concentration level in river water, this chapter studies the efficiency of the heterogeneous photo-Fenton in the removal of 21 micropollutants present in real water. The preparation and characterization of the catalyst are performed. Process removal efficiency and optimization of the different experimental factors are done using two model macropollutants: phenol and diclofenac. Tests are then applied on real river water to study the removal of different micropollutants. The efficiency of our chosen process is compared to the removal efficiency of TiO₂ in photocatalysis.

Abstract

In this paper, for the first time, Faujasite Y zeolite impregnated with iron (III) was employed as a catalyst to remove a real cocktail of micropollutants inside real water samples from the Meurthe river by the means of the heterogeneous photo-Fenton process. The catalyst was prepared by the wet impregnation method using iron (III) nitrate nonahydrate as iron precursor. First, an optimization of the process parameters was conducted using phenol as model macro-pollutant. The hydrogen peroxide concentration, the light wavelength (UV and visible) and intensity, the iron loading immobilized, as well as the pH of the solution were investigated. Complete photo-Fenton degradation of the contaminant was achieved using Faujasite containing 20 wt. % of iron, under UV light, and in the presence of 0.007 mol/L of H_2O_2 at pH 5.5. In a second step, the optimized process was used with real water samples from the Meurthe river. Twenty-one micropollutants (endocrine disruptors, pharmaceuticals, personal care products, and perfluorinated compounds) including 17 pharmaceutical compounds were specifically targeted, detected, and quantified. All the initial concentrations remained in the range of ng/L (2 – 88 ng/L). The majority of the micropollutants had a large affinity for the surface of the iron-impregnated Faujasite. Our results emphasized the very good efficiency of the photo-Fenton process with a cocktail of a minimum of 21 micropollutants. Except for sulfamethoxazole and PFOA, the concentrations of all the other micro contaminants (bisphenol A, carbamazepine, carbamazepine-10,11-epoxide, clarithromycin, diclofenac, estrone, ibuprofen, ketoprofen, lidocaine, naproxen, PFOS, triclosan, etc.) became lower than the limit of quantification of the LC-MS/MS after 30 minutes or 6 hours of photo-Fenton treatment depending on their initial concentrations. The photo-Fenton degradation of PFOA can be neglected. The photo-Fenton degradation of sulfamethoxazole obeys first order kinetics in the presence of the cocktail of the other micropollutants.

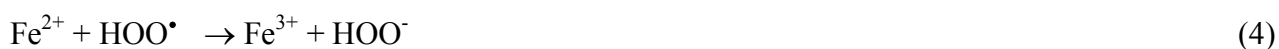
1 Introduction

Numerous contaminants, *e.g.* endocrine disruptors, pharmaceuticals and personal care products, have been detected in the outlet of conventional wastewater treatment plant (WWTP) at trace level, *i.e.* in the range of ng/L to µg/L (Fatta-Kassinos et al. 2011; Igos et al. 2012; Richardson et al. 2016). Even at such low concentrations, many studies highlight the potential toxicity of these micropollutants for the environment and the human health (Kovalova et al. 2013; Mariangela et al. 2013; Trapido et al. 2014). Being bio-recalcitrant, most of these emerging pollutants cannot be totally eliminated by conventional biological treatment (Rodriguez et al. 2011). Therefore, the development of an advanced physical-chemical complementary treatment becomes a promising alternative. Advanced oxidation processes (AOPs) have been proposed as they rely on the production of very strong oxidizing agent such as hydroxyl radicals ($\cdot\text{OH}$) having a high standard reduction potential ($E^\circ = 2.80 \text{ V vs SHE}$), second only after fluorine that is ruled out for this application (de Witte et al. 2011; Ghatak 2014; Oturan et al. 2014). Among these nascent technologies, photo-Fenton depicted high removal rates and yields of xenobiotic pollutants, thanks to the formation of $\cdot\text{OH}$ through Fenton and Fenton-like reactions from initial addition of hydrogen peroxide (H_2O_2) with ferrous ion (Fe^{2+}) and ferric ions (Fe^{3+}) in the effluent (Hartmann et al. 2010; Xavier et al. 2016):

Fenton:



Fenton-like:



Two additional $\cdot\text{OH}$ sources can be obtained through (i) the photolysis of iron-hydroxy complexes such as $\text{Fe}(\text{OH})^{2+}$, the predominant Fe(III) species at pH 3 (Eq. (8)), and (ii) the photolysis of H_2O_2 under UVA irradiation (Eq. (9)) (Loaiza-Ambuludi et al. 2014; Xavier et al. 2016):

Photo-Fenton:



However, homogeneous photo-Fenton process has been proven to have several disadvantages. This process leads to formation of sludge containing Fe ions costly removed at the end of wastewater treatment and needs a large amount of chemicals (Feng et al. 2003). Moreover, the need to continuously adjust to acidic pH (around pH 3) makes photo-Fenton process not convenient enough to be operated for wastewater application. These drawbacks limit the use of homogeneous photo-Fenton reaction in wastewater treatment. The development of heterogeneous photo-Fenton is being considered to face this issue (Nidheesh 2015). For these purposes, many supports such as nafion, zeolite, silica, clay, and activated carbon have been suggested in heterogeneous Fenton oxidation processes (Kim et al. 2015). Several factors such as pore volume, pore size distribution, surface area, effectiveness, and cost play a role in choosing the appropriate material to be used as a support (Blanco 2014). Most of the suggested materials have low effectiveness or high cost. Activated carbon, one of the most studied heterogeneous catalyst, is limited by its high cost and sludge formation (Arimi 2017). The use of zeo-type catalysts is very promising due to their unique properties (Kasiri et al. 2008) and less severe experimental conditions (mild temperature and pressure) that improve the efficiency and lower the formation of by-products compared to the other advanced oxidation treatments (Neamu et al. 2004a).

Zeolites are microporous, microcrystalline aluminosilicate materials (Neamu et al. 2004b) with a three dimensional structure and four-connected framework built from tetrahedral of $[\text{SiO}_4]^{4-}$ and $[\text{AlO}_4]^{5-}$, bonded together via the oxygen atoms. Al^{3+} can replace Si^{4+} resulting in a negatively charged framework (Blanco 2014). Zeolites are capable of complexing or adsorbing small and medium-sized organic molecules that give them an advantage over other carriers (such as clay, activated carbon, laponite, bentonite, etc.) (Neamu et al. 2004a) due to their molecular sieve structure and unique framework that generates a high internal surface area. They are characterized by their temperature stability, well-defined uniform pore and crystal structure, and easy ion-exchange method (Turapan et al. 2012).

Faujasite are a type of aluminosilicate zeolites combining a 3-dimensional network of accessible micropores (0.74 nm) with an organic-free synthesis (Verboekend et al. 2016). The ratio

of silica to the alumina determines the type (X or Y) of the synthetic zeolite (Arimi 2017). A more stable less-acidic Faujasite Y is more commonly applied in preparation of heterogeneous Fenton catalyst (Arimi 2017) due to its improved catalytic and hydrothermal stability as observed in numerous petrochemical applications (Verboekend et al. 2016). Recently, metal containing zeolites have been proven to be efficient and promising catalysts for the oxidation of different groups of organic pollutants with hydrogen peroxide (Kasiri et al. 2008, Barreca et al. 2014, 2015, Arimi 2017). More particularly, zeolite-based Fe catalysts were reported to have high degradation efficiency which could be similar as homogeneous Fe ions (Noorjahan et al. 2005).

The photo-Fenton degradation of micropollutants has been studied before but most of the research has been conducted using synthetic waters (Lam and Mabury 2005, Jiang et al. 2014, Huang et al. 2017, Natali Sora and Fumagalli 2017) or real waters (WWTP effluents or real natural water) but spiked with solutions of model micropollutants (Klamerth et al. 2012; Sanches et al. 2016). At the same time, the concentrations of micropollutants are generally high, *i.e.* from $\mu\text{g/L}$ to mg/L . Only very few studies work with micropollutants in real water. For example, Miralles-Cuevas et al. (2014) have reported the photo-Fenton removal of micropollutants in real municipal effluents. They studied 9 pharmaceuticals micropollutants of the same family with concentrations between 20.200 $\mu\text{g/L}$ and 0.86 $\mu\text{g/L}$. In addition, the photo-Fenton degradation of some specific micropollutants, such as PFCs, has been barely evaluated due to the carbon-fluorine bond that makes them environmentally persistent (Arvaniti et al. 2015).

It appears, then, relevant to work with real water containing different families of compounds. In this article, Faujasite zeolite impregnated with iron has been applied to remove a cocktail of micropollutants inside real water samples from the Meurthe river (France) by the means of the heterogeneous photo-Fenton process. These contaminants belong to 4 different families which are pharmaceuticals, personal care products, endocrine disruptors and perfluorinated compounds having different chemical structures. For the first time, the detection and the removal at trace levels (range of ng/L) of a mixture of 21 micropollutants, in water from a river has been achieved. Moreover, working with very low concentration of micropollutants remains an analytical challenge since most of the previous studies avoid working with these low concentrations due to the complexity of the analysis on LC-MS/MS, the high number of measurement steps, and the unavailability of the needed analytical instruments in all the laboratories. However, the removal of micropollutants at such low concentration is representative of the emerging contaminant concentration level (ng/L) encountered at the outlet of the WWTP. Consequently, the results can be directly applied in wastewater treatment plants.

This paper intends to bring new scientific and technological insights through the three following objectives: (1) manufacture a catalyst (Fe) impregnated on a sorbent (Faujasite Y) and characterize the multi-functional material, (2) optimize the performance of the material in synthetic medium with a representative pollutant, *e.g.* phenol, by varying the main impacting operating parameters of heterogeneous photo-Fenton process, and (3) test the efficiency of the materials in the treatment of real water samples containing a real cocktail of micropollutants from the Meurthe river.

2 Materials and methods

2.1 Chemicals

The Faujasite used in our study was an industrial zeolite supplied by zeolyst international. The zeolite was dealuminated. Consequently, the ratio of Si/Al increased till 19. The Table 1 of the Supporting information shows the main characteristics of this zeolite. Iron (III) nitrate nonahydrate ($\text{Fe}(\text{NO}_3)_3 \cdot 9\text{H}_2\text{O}$) salt was purchased from Sigma Aldrich. Hydrogen peroxide (H_2O_2 , 30 or 50 wt. % aqueous) was obtained from Sigma Aldrich. Concerning the model pollutant, phenol was purchased from Merck.

Table 1. Characteristics of the faujasite Y used in this study.

Zeolite	Formula	Pore size	Si/Al	S_{BET} (m^2/g)	Pore volume (cm^3/g)	
		(\AA)			micropore	mesopore
HFAU ₁₉	$\text{H}_{9.6}\text{Al}_{9.6}\text{Si}_{182.5}\text{O}_{384}$	7.4	19	930	0.245	0.11

2.2 Catalyst preparation

Iron-impregnated Faujasite was prepared by the wet impregnation method with 3 different impregnation percentages: 10, 20 and 30 wt. %. For this purpose, a given amount of iron (III) nitrate nonahydrate was dissolved in 50 mL of deionized water, and 1 g of Faujasite was added under continuous magnetic stirring. The obtained slurries were heated slowly to 90 °C and kept at this temperature until nearly all the water had evaporated. The wet solid obtained was then dried at 100 °C for 24 h.

The synthesis of free Fe_2O_3 particles was performed using the same procedure as for the immobilized systems but in the absence of the Faujasite. To this aim, 16 mg of iron (III) nitrate nonahydrate were introduced in 80 mL of deionized water in order to have the same amount of iron than that we used to prepare the 20 wt. % impregnated Faujasite.

2.3 Catalyst characterizations

Different techniques were used to characterize the Faujasite before and after the iron impregnation: scanning electron microscope (SEM) coupled with energy dispersive X-ray spectroscopy (EDS), X-ray powder diffraction (XRD), diffuse reflectance UV/visible spectroscopy, and zeta potential measurements.

The impregnated zeolites were observed with a scanning electron microscope coupled with energy dispersive X-ray spectroscopy (JEOL-JSM-6490LV) after being coated with a gold/palladium alloy deposited by low-vacuum sputter coating. Powder X-ray diffraction (XRD) measurements were recorded by means of a D8 Discover BRUKER diffractometer equipped with $\text{Cu K}\alpha$ radiation. The solid samples were scanned over 2θ range of 5° to 80° at a step size of 0.02° . The nature of the Fe species in the catalyst structure was identified by diffuse reflectance UV/Visible spectrophotometry. The absorption spectra were recorded on a UV-3600 UV/visible double beam spectrophotometer (SHIMADZU) in the 200-800 nm wavelength range. The zeta potential of the particles was determined using a Zetasizer NanoZS (Malvern) equipped with a He-Ne laser at 633 nm. The nanoparticles were dispersed in milliQ water and diluted in an aqueous solution of NaCl (0.01 M) adjusted to the required pH through the addition of NaOH or HCl. The nitrogen adsorption-desorption isotherms were recorded, at 77 K, on a Micromeritics TRISTAR 3000 instrument. The samples were outgassed overnight at 300°C under residual pressure of 0.001 Pa. Specific surface area and pore volume were obtained by measuring volume adsorbed at different P/P_0 values and by applying different methods. The specific surface area was evaluated by applying the Brunauer-Emmet-Teller (BET) equation to the adsorption data. T-plot method plot method was used to calculate the micropore surface area and volume distribution.

2.4 Photo-Fenton reactions with model pollutant

The activity of the catalyst was studied and the optimization of the different experimental conditions was done by using phenol and diclofenac as the model pollutants. The photo-Fenton tests were performed, at room temperature (20°C), inside a glass crystallizer. On the one hand, the UV

irradiation was provided by a mercury lamp (low pressure mercury arc, 18 W) emitting in the near-UV. The emission of the lamp indicated a spectral response centered at 254 nm with a half bandwidth of 12 nm. The lamp was positioned outside the reactor and was parallel to it. The distance between the lamp and the top of the crystallizer was 3.5 cm, while the height of the solution amounted to 2.5 cm. The incident light intensity reaching the top of the reacting suspension was equal to 10^{-6} Einstein/L s. On the other hand, for the photo-Fenton tests under visible light irradiation, a different lamp was employed. The source of visible light was an OmniCure[®] S2000 platform equipped with a 200 W lamp with an emission wavelength ranging from 250 to 500 nm. The UV emission of the lamp (below 400 nm) was filtered out by a polycarbonate plate placed between the light source and the reaction medium. The optical fiber was placed at a distance of 16.2 cm from the crystallizer containing the reaction mixture, and the height of the solution was equal to 2.5 cm. The power of the lamp was adjusted to 497 mW/cm² with 18 % of light emerging percentage.

Phenol was utilized as the representative organic pollutant since it is an aromatic compound, as most of the organic micropollutants, widely present in water. The concentration of phenol studied was in mg/L and not in ng/L as the micropollutants present in real water, because most of the studies performed on phenol work in this range of concentration. Thus, it became easy to compare with the literature data to validate the results in order to optimize the process. Moreover, it was easier to analyze, quantify and optimize the different experimental conditions using mg/L concentrations rather than ng/L. In certain cases, the pH of the aqueous solutions was adjusted before the introduction of the catalyst through NaOH or HCl addition. For all the experiments, the catalyst (Fe/Faujasite) content and the initial pollutant concentration were equal to 1 g/L and 10 mg/L, respectively. Note that depending on the nature of the light used, the size of the reactor was different but the catalyst amount/solution volume ratio was maintained constant whatever the reactor configuration. For the experiments under UV light, the photo-Fenton oxidation was carried out in solution containing 80 mg of the catalyst in 80 mL of pollutant solution. Conversely, when using visible light, 40 mg of solid catalyst was introduced inside a volume of the pollutant solution equal to 40 mL. In addition, a study was also conducted with diclofenac because it was present among the 21 micropollutants analyzed.

In a typical experiment, the dispersion containing the zeolite and the pollutant was stirred for 1 hour under dark condition. After that period, a known concentration of H₂O₂ was introduced into the suspension. The occurrence of an optimum concentration of H₂O₂ corresponding to a maximum degradation at H₂O₂ concentration between 0.01-0.02 M was observed experimentally in several

instances (Ghaly et al. 2001; Neamu et al. 2004a; Barakat et al. 2005; Kasiri, et al. 2008). Thus, the concentrations of H_2O_2 selected were below (0.0048, 0.007 M), between (0.0156 M) and above (0.06 M) this range. Just after the H_2O_2 addition, the lamp (UV or visible) was turned on. Liquid samples were taken at different time intervals. The liquid was separated from the solid by the means of 0.45 μm filters. The phenol concentration remaining in the supernatant was analyzed by both UV/Visible spectrophotometry (Cary 5G UV-Vis-NIR) at absorption wavelength of $\lambda = 269 \text{ nm}$ and by HPLC (Shimadzu SPD-20A UV-Vis detector) equipped with a classical C-18 column. The total organic carbon content (TOC) at the end of the experiments was measured using a TOC analyzer TOC-V_{CSH} (Shimadzu). The amount of iron species leached from the catalyst during the photo-Fenton degradation tests was measured at the end of the process using a flame atomic absorption (Thermo Electron Corporation) with a Fe-lamp and standard solutions of Fe in 3 v. % acidified HNO_3 deionized water.

It appeared important to perform blank experiments in the absence of catalyst. First, under UV light irradiation but in the absence of iron impregnated Faujasite and H_2O_2 , the results indicated no photolysis of phenol (Fig. 1). Second, in the presence of UV light irradiation and H_2O_2 , the degradation of phenol remains also negligible (Fig. 1).

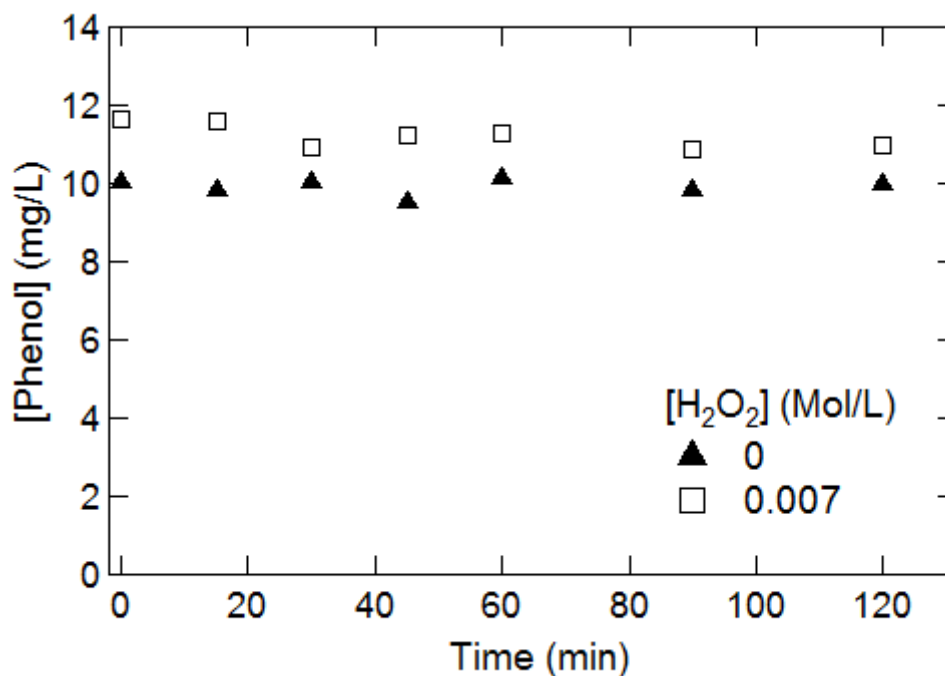


Fig. 1. Blank experiments in the absence of catalyst. Degradation of phenol under UV light irradiation in the presence ($[\text{H}_2\text{O}_2] = 0.007 \text{ mol/L}$) and in the absence ($[\text{H}_2\text{O}_2] = 0 \text{ mol/L}$) of H_2O_2 but without iron impregnated Faujasite.

2.5 Catalyst reusability

The reusability of the impregnated zeolite was also evaluated. Two main parameters were tested: the iron content immobilized onto the zeolite (10 and 20 wt. %) and the recycling protocol. The photo-Fenton experiment was conducted with 80 mg of the catalyst in 80 mL of 10 mg/L phenol aqueous solution in the presence of 0.007M H₂O₂. After 4 hours under UV irradiation, the reaction solution was centrifuged for 30 min at 4000 rpm. The catalyst remaining was washed with 100 mL of deionized water for 1 hour. Then, the mixture was centrifuged (30 min at 4000 rpm), and the catalyst remaining was kept at room temperature for the next day to dry. On the next day, the solid catalyst was weighed and then dispersed again in the phenol solution to proceed to the second photo-Fenton experiment under the same conditions as for the first run. Note that the amounts of impregnated zeolite employed in the successive cycle experiments were lower than 80 mg due to the loss of product during the washing procedure. The zeolite contents were successively 50, and 30-25 mg, for the second, and third photo-fenton experiments, respectively. To test the effect of washing of the catalyst between the runs, the reusability test was studied using the same approach as above but no without washing the catalyst with deionized water after the centrifugation. Between each photo-Fenton tests, the zeolite was only centrifuged.

2.6 Photo-Fenton tests with real water

Photo-Fenton tests were carried out with real water samples taken from the Meurthe river. This river was located close to Nancy in France as shown in Fig. 2. The samplings were conducted in a site named Moulin Noir from the Meurthe river. This location was chosen in order to ensure a sufficiently large amount of micropollutants in terms of both concentration (in a range of ng/L) and nature. Twenty-one micropollutants including 17 pharmaceutical compounds were targeted. In details, bisphenol A, carbamazepine, carbamazepine-10,11-epoxide, clarithromycin, cyclophosphamide, diclofenac, erythromycin, estradiol-beta, estrone, ethynylestradiol, ibuprofen, ketoprofen, lidocaine, naproxen, PFOA, PFOS, sulfadimethoxine, sulfadimidine, sulfamethoxazole, sulfathiazole, and triclosan were specifically detected and quantified. The Table S1 the Supporting information gives more information about the 21 micropollutants.

The sampling was carried out from the middle of the bridge to ensure the good mixing of the micropollutants in water samples (Fig. 2B). A glass bottle surrounded by iron cover to avoid its breakage with a thick long ribbon was dropped from the bridge into the river to take a water sample. After sampling, the water samples were filtrated by 2 processes. First, funnel and filter paper were

employed to remove the bulk materials. Then, the water was filtrated using successively a glass filter of 1.2 μm porosity followed by a cellulose acetate filter with a porosity of 0.45 μm . After those filtration steps, the samples water were kept inside dark bottles in the fridge at a temperature of 4 $^{\circ}\text{C}$.



Fig. 2. Map showing (A) the location of Moulin Noir and Nancy, and (B) Moulin Noir site under the bridge.

Concerning the photo-Fenton degradation tests, 600 mL of water sample was used. This large volume was necessary for the micropollutants analysis. Actually, a final volume of 500 mL appeared necessary for the micropollutant quantification. For practical reasons, the initial volume of water was split into 3 crystallizers of 200 mL each in order to use the same UV lamp as described previously. For each crystallizer reactor, 0.2 g of the 20 wt. % Fe impregnated Faujasite was added into 200 mL of water. No modification of the pH or the temperature was performed. Blank experiments were undertaken. To this aim, experiments were conducted in the absence of iron-impregnated Faujasite under UV illumination in the presence or in the absence of H_2O_2 . The duration of the experiments was fixed to 30 minutes or 6 hours. To evaluate the adsorption capacity of the Fe/Faujasite towards the 21 micropollutants, the suspensions were stirred for 2 hours in the dark and in the absence of H_2O_2 . The photo-Fenton tests were carried out during 30 minutes or 6 hours under UV irradiation

and in the presence of hydrogen peroxide. The same experiments were performed in the dark but in the presence of H_2O_2 to evaluate the Fenton activity of the iron-impregnated Faujasite. The H_2O_2 concentration was fixed to 0.007 M while the Fe/Faujasite content equaled 1 g/L, unless stated otherwise. The Faujasite containing 20 wt. % of iron was used as catalyst. It is also important to note that only one sampling was carried out at the end of the experiment. The treated water was centrifuged for 25 minutes at 4000 rpm.

For the micropollutants detection and quantification, a concentration step by Solid-Phase Extraction (SPE) was followed. The samples were filtrated under 1.2 μm glass fiber and 0.45 μm cellulose acetate filters and adjusted to pH 4 with sulfuric acid. 550 mL of sample were concentrated and purified by SPE (Autotrace SPE Workstation, Thermo Fisher Scientific, Waltham USA). The SPE cartridge (Oasis HLB 200mg/6mL, Waters, Milford USA) was formerly conditioned with methanol, and then water at pH 4. After the sample loading, the cartridge was washed with water/methanol 95/5 (v/v), dried under nitrogen and eluted with 10 mL of methanol. To enhance the concentration factor, the extract was evaporated under vacuum at 50 °C to the drop and recovered in 500 μL of water/methanol 90/10, the same starting conditions as those employed for the analysis. The eluents were all of ultra-pure grade. The final extract was analyzed by Liquid Chromatography (1260 Series, Agilent, Santa Clara USA) coupled to triple-quadrupole Mass Spectrometry (QTRAP 4500, AB Sciex, Framingham USA). The chromatographic separation was realized on a Zorbax Eclipse Plus C18 column, 150 x 2.1 mm ID, 3.5 μm particle size (Agilent). The flow rate of the mobile phase was kept constant at 0.25 mL/min and the oven at 40 °C. The nature of the mobile phases and the eluent programs are given in the Table S2 of the Supporting information. According to the target compounds, the mass spectrometer was operated in positive or negative electrospray mode. Two transitions were saved in Multiple Reaction Monitoring mode for quantification and confirmation of each target compound. Quantitative results were provided thanks to internal calibrations.

3 Results and discussion

3.1 Characterization of the Fe impregnated Faujasite

Fig. 3. shows the SEM images for the raw and Fe impregnated Faujasite. As we can see in Fig. 3a, the raw Faujasite appears as fine particles. The morphology of the Faujasite is not modified by the iron impregnation. From the pictures, the possible presence of iron oxide particles (Fe_2O_3) cannot be observed.

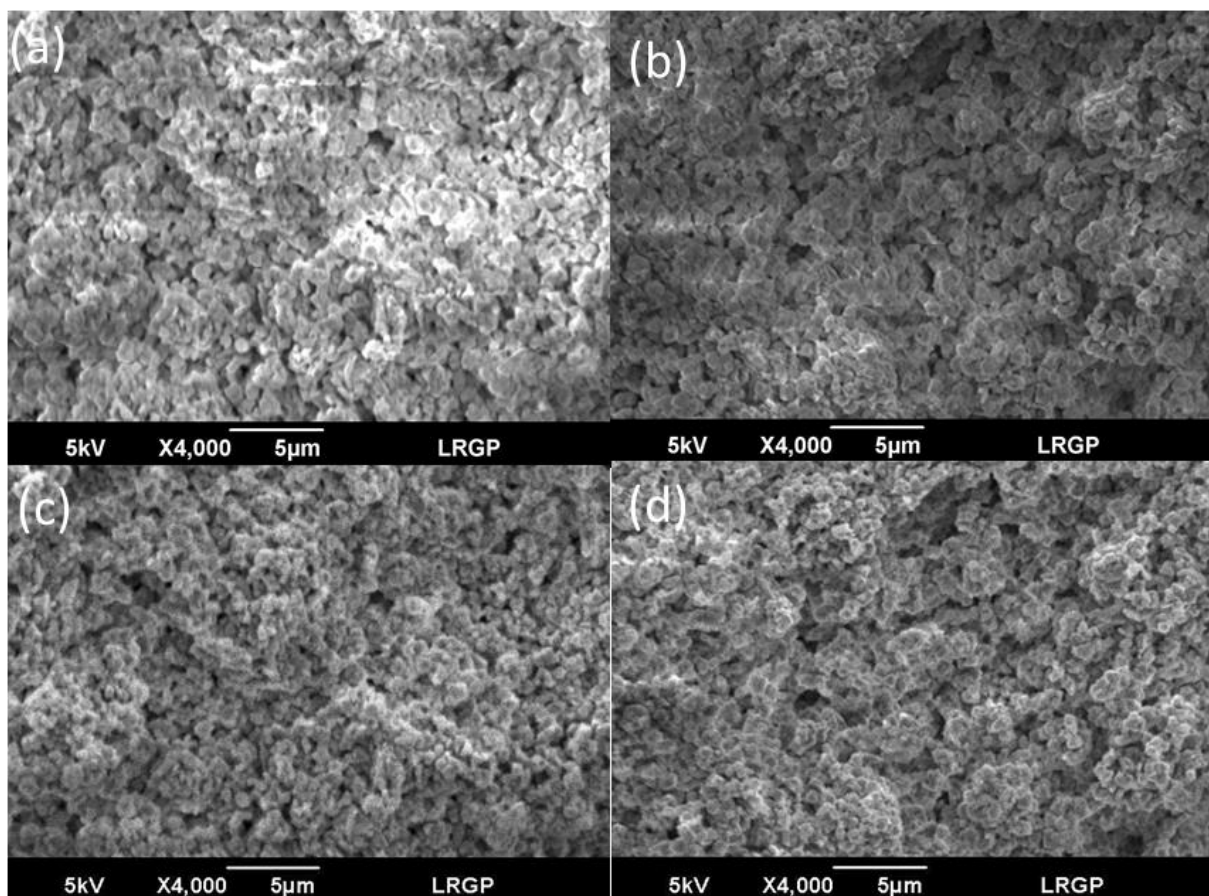


Fig. 3. SEM pictures of (a) raw Faujasite, and Fe impregnated Faujasite prepared with initial masses of iron (III) nitrate nonahydrate of: (b) 10 wt.%, (c) 20 wt.%, and (d) 30 wt.%.

In addition, EDS is used to detect the presence of iron onto the impregnated samples (Fig. 2). For the analysis, we concentrate on the quantification of the Fe, Si and Al elements. The amount of iron increases with the initial concentration of iron nitrate in solution. This confirms the immobilization of iron onto the zeolite for all the mixtures. The iron content is directly connected to the initial concentration of iron nitrate but is also sensitive to the zeolite amount. To estimate semi-quantitatively the amount of iron-impregnated onto the Faujasite, the ratio of the atomic percentages of iron and silicon (Fe/Si) is calculated for various iron nitrate initial concentrations (Fig. 4). Note that the atomic percentage of Si is used as quantitative reference of the zeolite amount. The ratio increases continuously with the initial iron concentration.

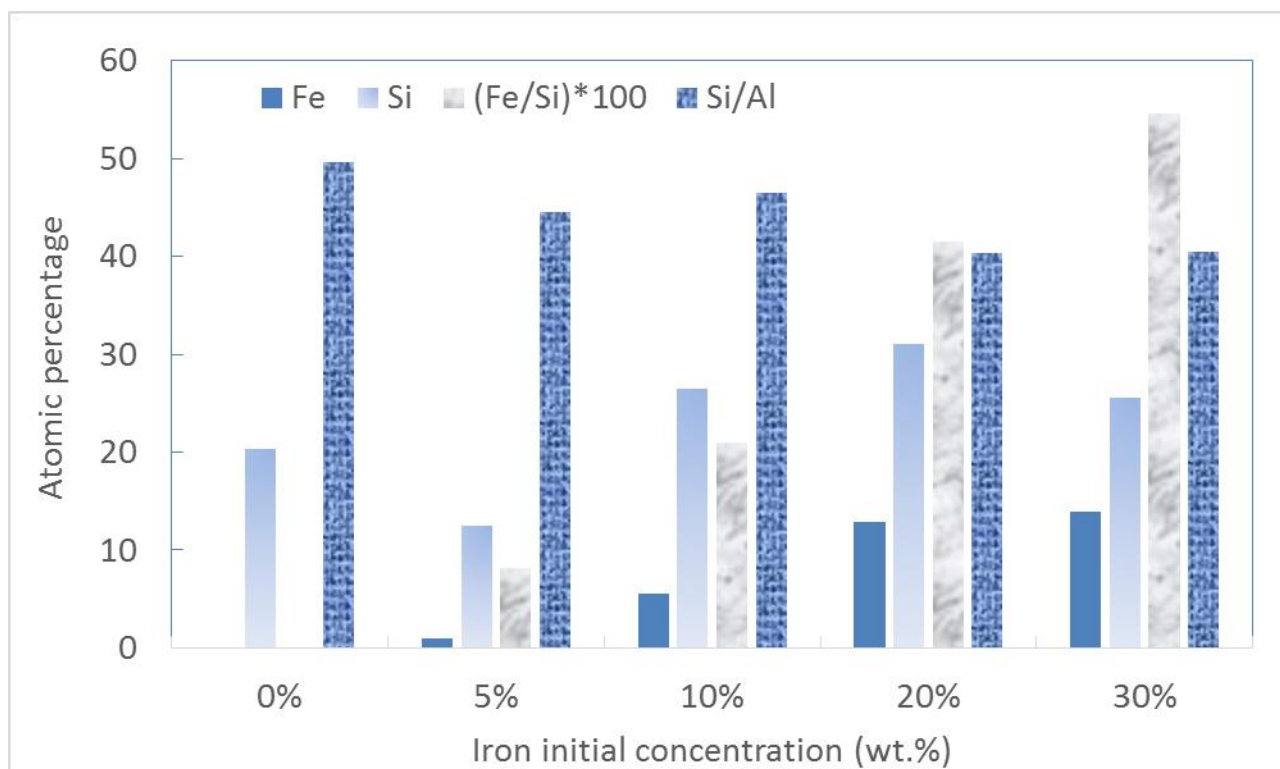


Fig. 4. Influence of the iron initial concentration on the atomic percentages and atomic ratios, obtained from EDS emitted by the elements (Fe, Si, and Al) encountered on the surface of bare and modified Faujasite.

The influence of the initial concentration of iron nitrate on the XRD patterns of the impregnated Faujasite samples is depicted in Fig. 5A. The XRD pattern of the raw Faujasite fits well with the one mentioned in the literature (Cejka 2005; Treacy et al. 2007). In details, the values of the 2θ of the different peaks and their corresponding hkl indices in brackets are: $2\theta = 6.19^\circ$ (111), 10.36° (220), 12.18° (311), 15.8° (331), 19.1° (511), 20.7° (440), 22.02° (420), 23.9° (533), 27.4° (642), 30.16° (660), 31.32° (555), and 32.5° (840) (Cejka 2005). For all the impregnated samples, no peak corresponding to iron oxide can be detected. However, all the reflection peaks related to the Faujasite are observed. Actually, in the presence of iron, the height of the peaks of the zeolite decreases in comparison to those of pure Faujasite. The height of the peaks diminishes with the impregnated iron content. The absence of detectable peak corresponding to iron may arise from two causes. First, this occurs when the Fe species are well dispersed or framework-incorporated in the zeolite. This aspect was already reported in the literature (Yue et al. 2015). However, it seems more logical that the absence of diffraction lines of Fe_2O_3 in the XRD might be due to the formation of amorphous Fe_2O_3 .

This certainly occurs because the heat treatment performed during the synthesis was realized at low temperature (100 °C, 24 hours).

Diffuse reflectance UV/Visible spectroscopy is employed to characterize the optical properties of the powder materials and also to determine the nature of the iron species in the zeolite structure (Fig. 5B). The spectrum recorded with the non-immobilized Fe₂O₃ particles is also represented in the figure. The raw Faujasite displays a strong absorption in the UV-spectral range, between 250 and 350 nm. Conversely, no absorbance can be detected in the visible range between 400 and 800 nm. The spectrum of pure Fe₂O₃ particles appears different. It displays a plateau between 350 and 550 nm, and the absorbance decreases for larger wavelengths. More remarkably, in the presence of iron onto the Faujasite, the absorbance data seems to be a mix of the spectra of raw Faujasite and pure Fe₂O₃. The maximum in absorbance is obtained at a wavelength of 260 nm. This peak corresponds to isolated Fe²⁺ and Fe³⁺ ions (Kowalska-Kuś et al. 2013). In addition, for larger wavelengths, the absorbance decreases continuously up to 600-650 nm. This indicates that the photoresponse of the modified zeolite is successfully extended to the visible region of light. A peak in the UV range 300-400 nm appears for 20 wt. % and 30 wt. % impregnated Faujasite while it is less intense for 10 wt. % impregnated form. This peak corresponds to the small oligonuclear Fe_x³⁺O_y in zeolite channels (Rutkowska et al. 2014). Another peak with a maximum intensity at about 500 nm is observed for the pure Fe₂O₃ particles and the impregnated Faujasite. This peak is attributed to the bulky Fe₂O₃ aggregates located on the external surface of the Faujasite (Li et al. 2008; Rutkowska et al. 2014). It has a higher intensity for 20 wt. % and 30 wt. % impregnated Faujasite compared to the 10 wt. %. Additionally, the appearance of this peak for the impregnated Faujasite confirms the presence of Fe species, mainly under the form of Fe₂O₃, in the zeolite.

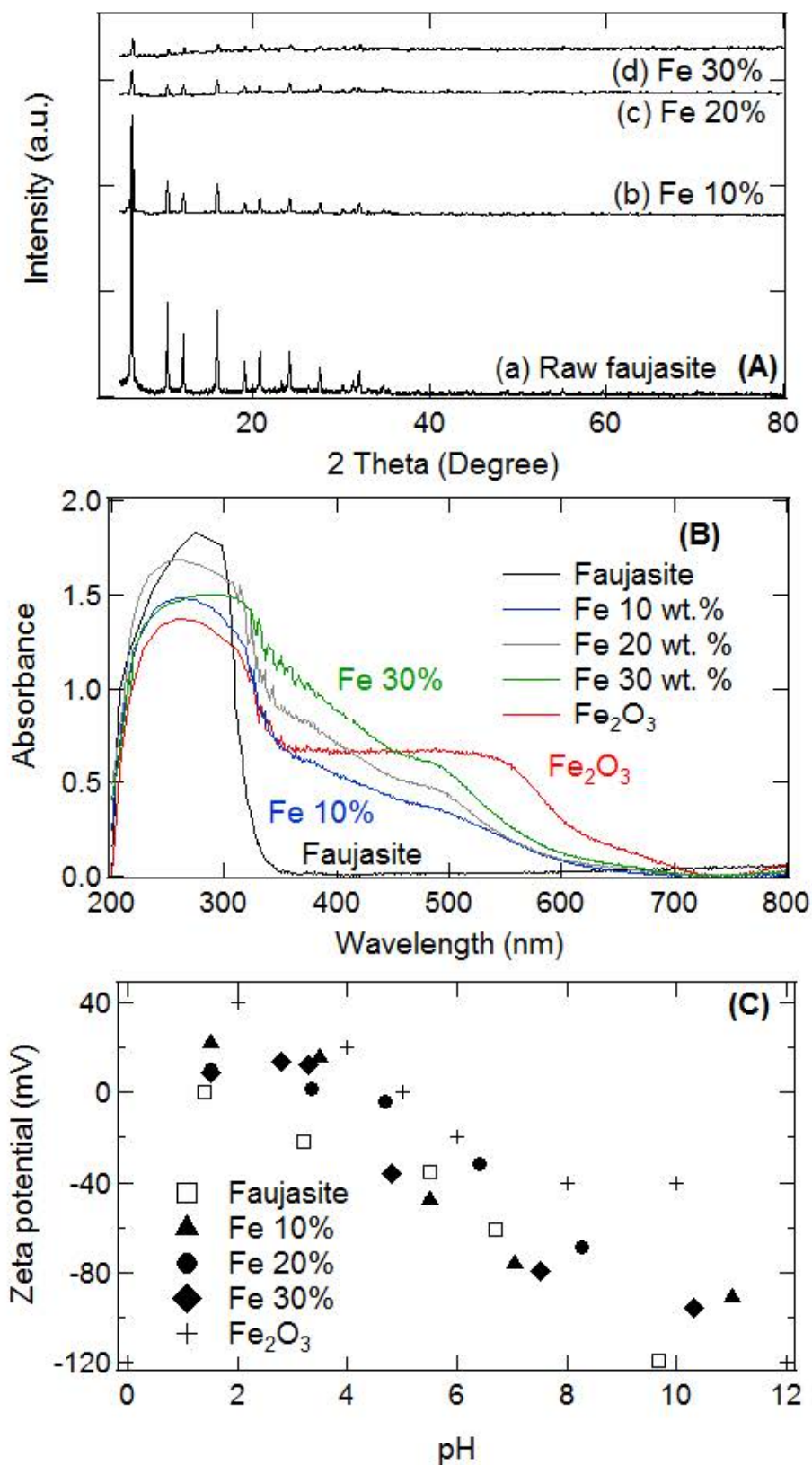


Fig. 5. Characterization of the Fe impregnated Faujasite. (A) XRD patterns of Fe impregnated Faujasite prepared with initial masses of iron nitrate of: (a) 0 %, (b) 10 wt. %, (c) 20 wt. %, and (d) 30 wt. %. (B) Solid absorbance UV/visible spectra for raw Faujasite, and zeolite impregnated with

various amounts of iron. (C) Zeta potential of bare and iron-covered Faujasite samples as a function of the pH.

Zeta potential-pH curves are obtained to investigate the surface character of the original zeolite and the iron-coated Faujasite (Fig. 5C). The raw Faujasite is negative in the whole range of pH. There is a significant increase in the negative charge with the pH. The zeta potential is zero at pH 1-1.5 and it decreases up to pH 10. These values correspond perfectly to the ones mentioned in the literature (Basumatary et al. 2016). The impregnation of iron over Faujasite impacts the surface charge behavior. The zeta potential decreases with the pH from positive values in acidic medium (pH < 1.5-4) to negative values at higher pH. The presence of iron onto the zeolite causes a shift of the point of zero charge (PZC) towards larger pH values between 3 and 4. The zeta potential-pH of the composites follows the same trend as compared to that reported for the non-immobilized iron oxide Fe_2O_3 particles but with a shift of the PZC (Erdemoğlu et al. 2006, Andrade et al. 2009). The similarity between zeta potential data on the iron-impregnated Faujasite and the pure Fe_2O_3 particles suggests that iron oxide particles are deposited onto the surface. An alternative explanation can be also discussed. The impregnation of iron over Faujasite hides some Al sites from the surface, thus the PZC shifts to higher pH, and the zeta potential to larger values due to higher acidic strength of the Al atoms (Kuzniatsova et al. 2007).

N_2 adsorption isotherm at 77 K of the bare Faujasite and Fe impregnated Faujasite are shown in Fig. 6. The isotherm of bare Faujasite displays a larger hysteresis loop starting at P/P_0 0.4 indicating that this material has a combination of micropores and mesopores, with a predominance of microporous structure. The hysteresis loop becomes smaller for the Fe-Faujasite and the volume of N_2 adsorbed at low values of P/P_0 decreased, suggesting a reduction in the available microporosity. This is confirmed by the decrease in BET surface area and micropore surface and volume after the impregnation where the values are given in Table 2. Therefore, properties like specific surface area and pore volume are greatly affected by the iron impregnation on Faujasite, which is consistent with the decrease of crystallinity of the impregnated Faujasite that was concluded also from the XRD analysis (Rache et al. 2014)

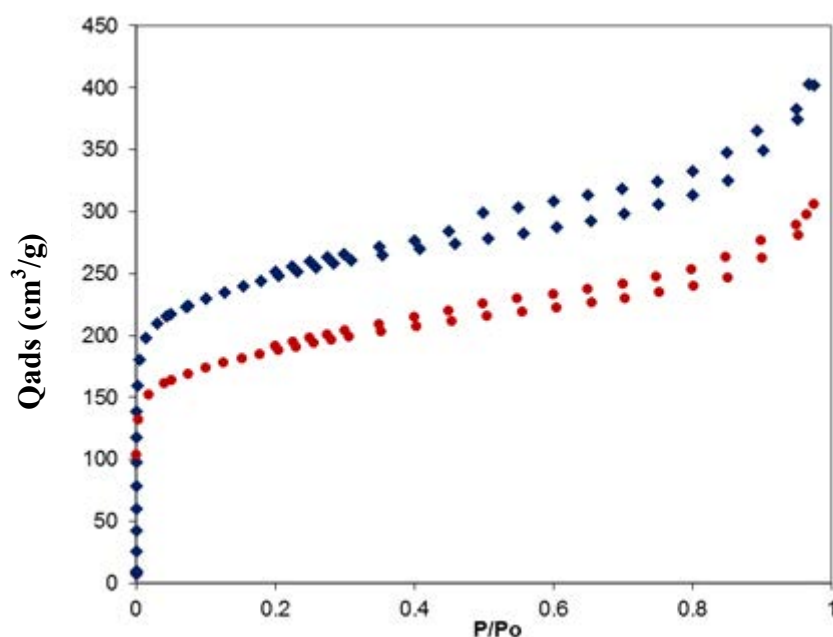


Fig. 6. N₂ adsorption isotherm of non-exchanged zeolite (blue curve), and exchanged zeolite (red curve).

Table 2. specific surface area and micropore calculations of bare and impregnate Faujasite Y.

Samples	BET method		T-plot method		
	Constant C	Specific surface area (m ² /g)	Micropores surface (m ² /g)	Non micropores surface (m ² /g)	Micropores volume (cm ³ /g)
Faujasite Y	874	930	553.8	432.8	0.20
Fe-Faujasite Y	795	640	400.9	344.4	0.14

3.2 Photo-Fenton degradation of phenol pollutant

The photo-Fenton activity of the iron-impregnated zeolite samples has been tested on the photodegradation of phenol. The kinetics of the phenol degradation is analyzed in detail to optimize the performance of both the material and the process. The effect of some physicochemical parameters such as H₂O₂ concentration, incident light nature and intensity, amount of iron deposited onto the Faujasite, and pH have been varied. Prior to analyze the degradation results, it seems interesting to discuss the adsorption capability of the modified zeolites (results not shown). A very weak adsorption of phenol onto bare and Fe impregnated faujasite is obtained. The pollutant uptake

does not significantly vary with the iron surface concentration. This low adsorption is mainly due to the hydrophilic nature of phenol bearing a hydroxyl OH group that makes its interaction with the hydrophobic zeolite negligible.

The presence of hydrogen peroxide is an important parameter required for the degradation of the pollutants in heterogeneous photo-Fenton process. The dependence of the hydrogen peroxide concentration on the time course of the UV photo-Fenton degradation of phenol is illustrated in Fig. 7a. Each curve shows the bulk concentration of phenol as a function of the time of treatment. In the absence of hydrogen peroxide, no diminution of the phenol concentration with the process time can be detected. This validates the lack of degradation in the absence of H₂O₂, and also the fact that the UV photolysis of phenol is negligible. Conversely, in the presence of H₂O₂, the bulk concentration of phenol declines over photo-Fenton process time. The total degradation is obtained using the four different concentrations of hydrogen peroxide. The degradation becomes faster as the concentration of hydrogen peroxide increases up to 0.015 M. Then, H₂O₂ concentrations of 0.015 M and 0.06 M give very similar removal efficiency. The presence of hydrogen peroxide allows the production of hydroxyl radicals through the mechanisms given in Eqs. (1)-(9) (Ghaly et al. 2001). At low concentration of hydrogen peroxide, the production of hydroxyl radicals remains low, thus, resulting in slow oxidation rate. When the concentration of H₂O₂ becomes higher, the amount of hydroxyl radicals used for phenol oxidation increases (Kasiri et al. 2008). This enhances the probability of reaction between the pollutant molecules and the oxidizing species leading to a rise of the degradation rate. However, there is an optimum in the H₂O₂ concentration, *i.e.* 0.015 M, since larger hydrogen peroxide concentrations do not lead to higher removal rate. Actually, as soon as all the Fe²⁺ and Fe³⁺ have reacted with the H₂O₂, whatever the hydrogen peroxide content remaining in the solution, they will not be able to produce supplementary hydroxyl radicals by the Fenton reaction (Eqs. (1-6)).

The variation of the phenol concentration (C) with respect to the time of the process (t) corresponds to an exponential decay shape, which is characteristic of a first-order kinetic reaction regardless of the hydrogen peroxide content:

$$C = C_0 \exp(-k \times t) \quad (10)$$

Note that C₀ stands for the initial pollutant concentration in the bulk solution at the beginning of the photo-Fenton process. The Table 3 of the Supporting information illustrates the effect of the H₂O₂ content on the values of the reaction rate constant k.

Table 3. The effect of the concentration of H₂O₂ on the reaction rate constant (k), the total organic carbon content (TOC), and the iron concentration ([Fe]) in the solutions at the end of the UV photo-Fenton process. R² represents the correlation coefficient of the linear transform of ln(C₀/C) versus time.

[H ₂ O ₂] (mol/L)	TOC (mg C/L)	[Fe] (mg/L)	k (min ⁻¹)	R ²
0	8.709	6.37	-	-
0.0048	1.733	5.73	0.025	0.9567
0.0070	2.177	3.96	0.039	0.9924
0.0156	3.378	-	0.147	0.9886
0.06	-	-	0.135	0.9981

The phenol mineralization is examined by TOC analysis at the end of the photo-Fenton process, *i.e.* when the phenol concentration becomes equal to zero (Table 3). In the presence of H₂O₂, the TOC value increases with the concentration of H₂O₂. A weak carbon content remains in solution ([TOC] = 1.7-2.1 mg C/L) for H₂O₂ concentrations of 0.007 and 0.0048 M. It seems now established that a TOC value lower than or equal to 2.5 mg C/L indicates the quasi-complete mineralization of the pollutant. No organic by-product is produced during the degradation and the quasi-complete mineralization of phenol takes place for H₂O₂ concentrations of 0.007 and 0.0048 M. To investigate the most efficient H₂O₂ content to be used, the rate constants of phenol degradation of the different tests are compared to the H₂O₂ concentration. The system with the highest rate constant and the lowest H₂O₂ concentration used is the most efficient. For this reason, the ratios of the rate constant are normalized by the concentration of H₂O₂, *i.e.* the [H₂O₂]/k ratios are calculated. The calculated ratios for the tests with H₂O₂ concentrations of 0.0048 M, 0.007 M, 0.0156 M, and 0.06 M are equal to 0.192, 0.179, 0.106 and 0.444 mol minutes/L, respectively. As seen from the ratios obtained, H₂O₂ concentrations of 0.007 M and 0.0156 M lead to the lowest ratio with close values. Based on all these data, a concentration of hydrogen peroxide of 0.007 M was chosen to be used in all the experiments.

Incident light nature and intensity can affect the degradation efficiency of the iron-impregnated Faujasite. Series of experiments are carried out in the absence of illumination (“Dark”), under UV and visible irradiations (Fig. 7b). The complete phenol degradation is achieved in the absence of illumination, under UV and visible light irradiation. The TOC analysis is employed to support this interpretation. The TOC values of the solutions at the end of the degradation process range between 1.9 and 2.1 mg C/L (Table 4) confirming the quasi-complete mineralization of the contaminants and also the absence of by-products. However, the nature and the intensity of the light affects the kinetics of degradation. The phenol solutions become fully degraded within 60 minutes under visible light, 90 minutes under UV light, and 240 minutes in the absence of light. Faster degradation occurs under irradiation. The presence of UV radiations enhances the photolysis of hydrogen peroxide and thus the amount of hydroxyl radicals produced (Eq. (9)). Another consequence could be the photo-reduction of Fe(III) to Fe(II) ions, in the presence of illumination. The produced Fe(II) can react with hydrogen peroxide molecules and leads to the production of additional hydroxyl radicals through Fenton reaction, *i.e.* Eqs. (7) and (8) (Kasiri et al. 2008).

Table 4. The effect of the light nature on the reaction rate constant (k), the total organic carbon content (TOC), and the iron concentration ($[Fe]$) in the solutions at the end of the photo-Fenton process. R^2 represents the correlation coefficient of the linear transform of $\ln(C_0/C)$ versus time.

Light nature	TOC (mg C/L)	[Fe] (mg/L)	k (min^{-1})	R^2
Dark	1.929	5.93	0.019	0.8871
UV	2.177	3.96	0.039	0.9924
Visible	-	-	0.05	0.9634

To compare the efficiency of both UV and visible light, the rate constants for the catalytic tests under both light illuminations is calculated. The fit of the experimental data by a first order exponential decay function of the form $A \exp(-k t)$ confirms a first-order degradation mechanism independently of the light nature. The deduced rate constants k are reported in the Table 4. Recall that the size of the reactor is affected by the type of illumination source, *i.e.* for the experiments under UV light, volume of solution up to 200 mL can be used, while the volume remains limited to

40 mL when performing degradation under visible light because of the optical fiber. For this reason, the volume of the reaction mixture treated has to be taken into consideration. This is done by normalizing the rate constants (k) by the volume (V) of the reaction mixture used, *i.e.* the test with higher rate constant and larger volume of reaction mixture treated shows better efficiency. Under UV light, $k \times V$ factor is 3.152 mL/minutes which is greater than under visible light where $k \times V = 2$ mL/minutes. Therefore, the following experiments will be carried out under UV light illumination.

The effect of the iron content immobilized onto the zeolite on the kinetics of the UV photo-Fenton degradation of phenol is illustrated in Fig. 7c. In the absence of iron deposited onto the Faujasite, no change in the concentration of phenol during the treatment can be detected. So we can conclude that the Faujasite alone does not have any degradation effect on phenol. In the presence of iron onto the Faujasite, an increase of the degradation rate with the initial mass of iron nitrate nonahydrate from 10 wt. % to 20 wt. % is observed. The kinetic constant k increases from 0.016 min^{-1} to 0.039 min^{-1} (Table 5). Another interesting feature is that the degradation rate reaches a constant value at iron concentrations larger than or equal to 20 wt. % ($k = 0.03\text{-}0.039 \text{ minutes}^{-1}$). It appears more suitable to discuss the relationship between the degradation rate and the real iron amount deposited onto the zeolite, derived from the EDS data (Fig. 2). A substantial enhancement in the amount of Fe deposited onto the Faujasite surface between 10 wt.% (Fe = 5.56 wt.%) and 20 wt.% (Fe = 12.89 wt.%) is demonstrated. The increase in the degradation rate is mainly due to the greater loading of iron onto the zeolite surface that are involved in the photo-Fenton heterogeneous process, thus, improving the quantity of hydroxyl radicals. At higher iron dose, *i.e.* when the initial concentration of iron in solution increases beyond 20 wt. %, the deposited uptakes remain constant and equal to ca. 12-13%. In this range of iron content, no difference in the temporal evolution of the phenol degradation can be observed. In order to analyse the data more deeply, the TOC and Fe concentrations at the end of the heterogeneous photo-Fenton process are given in Table 5. The TOC decreases with the amount of iron deposited from 2.3 to 1.0 mg C/L. These low carbon contents confirm the quasi-complete mineralization of the phenol regardless of the iron loading deposited onto the zeolite. At the same time, the iron concentration in solution increases, from 0.7 mg/L to 4.4 mg/L, with the amount of iron immobilized. The sample containing theoretically 20 wt. % of iron seems sufficient to reach quickly total phenol degradation while maintaining a fair amount of lixiviated iron. Consequently, this sample has been selected for the next experiments.

Table 5. The effect of the initial masses of iron nitrate nonahydrate used to prepare the iron/Faujasite composites on the reaction rate constant (k), the total organic carbon content (TOC), and the iron

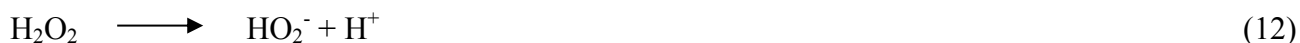
concentration ([Fe]) in the solutions at the end of the UV photo-Fenton process. R^2 represents the correlation coefficient of the linear transform of $\ln(C_0/C)$ versus time.

Initial mass of iron nitrate (wt. %)	TOC (mg C/L)	[Fe] (mg/L)	k (min ⁻¹)	R ²
10	2.300	0.79	0.016	0.9451
20	2.177	3.96	0.039	0.9924
30	1.006	4.44	0.030	0.9852

The effect of the pH on the photo-Fenton degradation of phenol is examined in amplitude pH of 3–12 in the presence of 20 wt. % Fe impregnated Faujasite catalyst. The results are depicted in Fig. 7d and Table 6 of the Supporting information. The maximum degradation efficiency is obtained at pH 5.5 (natural pH of the phenol solution) and pH 7. The pH value 5.5 is generally considered as the optimum pH in heterogeneous Fenton process using Fe-zeolite systems in the literature (Neamu et al. 2004a , Kasiri et al. 2008). We notice also lower degradation efficiency at pH 3 and a lack of degradation activity at pH 12. The optimum activity of the catalyst at pH 5.5 is related to the nature of the environment of the iron cations inside the pore structure of the zeolite even though the distribution of the iron species in this environment has not been elucidated yet. A strong electrostatic interaction is present between the positively charged Fe cations and the negatively charged zeolite framework. This interaction can prevent or slow down the precipitation of iron hydroxides even at quasi-neutral pH values (Neamu et al. 2004b). Moreover, other parameters can explain the change of the catalyst activity with pH. On the one hand, the pH of the solution is regulated from pH 5.5 to pH 3 using hydrochloric acid. Consequently, a high amount of Cl⁻ ions was added to the phenol solution. The chloride ions have the ability to deactivate the hydroxyl radicals (Eq. (11)). This causes a decline in the degradation efficiency since the formed inorganic radical anions present a very low reactivity compared to that of •OH (Kasiri et al. 2008).



On the other hand, at very basic pH (pH 12), the hydrogen peroxide decomposition becomes favored, increasing the amount of conjugate base HO_2^- in the solution (Eq. (12))



The formed conjugate base (HO_2^-) produces a double scavenging effect. First, it can react with the H_2O_2 molecules (Eq. (13)) restricting the production of hydroxyl radicals. Second, it can also deactivate the hydroxyl radicals (Eq. (14)).

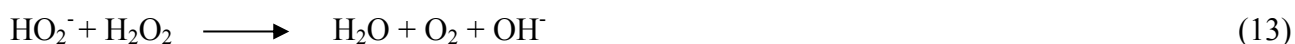


Table 6. The effect of the pH on the reaction rate constant (k), the total organic carbon content (TOC), and the iron concentration ([Fe]) in the solutions at the end of the photo-Fenton process. R^2 represents the correlation coefficient of the linear transform of $\ln(C_0/C)$ versus time.

pH	TOC (mg C/L)	[Fe] (mg/L)	k (min^{-1})	R^2
3	4.711	7.83	0.0129	0.9626
5.5	2.177	3.96	0.039	0.9924
7	3.861	4.82	0.027	0.8894
12	14.01	4.14	0.0003	0.8639

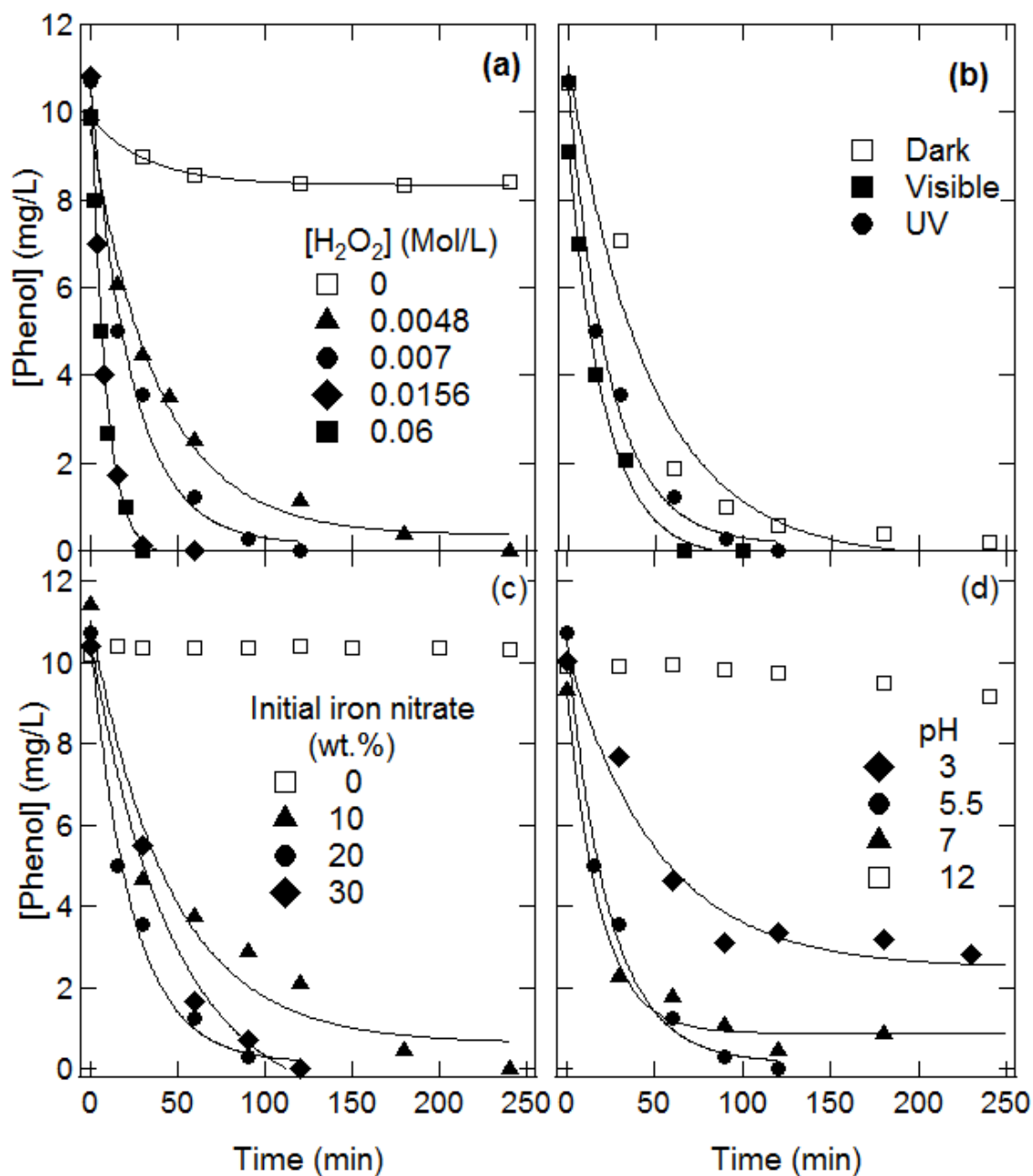


Fig. 7. Optimization of the experimental parameters during the photo-Fenton degradation of phenol using Fe impregnated Faujasite. (a) Effect of the concentration of H_2O_2 . Experimental conditions: catalyst concentration = 1 g/L, UV light, and pH 5.5. (b) Influence of the light nature. Experimental conditions: catalyst concentration = 1 g/L, 0.007 M H_2O_2 , and pH 5.5. (c) Effect of the initial masses of iron nitrate nonahydrate used to prepare the iron/Faujasite composites. Experimental conditions: catalyst concentration = 1 g/L, 0.007 M H_2O_2 , UV light and pH 5.5. (d) Influence of pH. Experimental conditions: catalyst concentration = 1 g/L, 0.007 M H_2O_2 , and UV light. The lines correspond to the fit of the experimental data by a first order exponential decay function of the form $A \exp(-k t)$ consistent with a first order kinetics.

The formed oxygen anion radical has a very low reactivity with organic pollutants in comparison with that of H_2O_2 and $\cdot\text{OH}$ (Li et al. 2006).

For an optimal choice of the pH, it seems also relevant to discuss the remaining TOC and the lixiviated iron at the end of the heterogeneous photo-Fenton process (Table 6). The minimum TOC content (2.1 mg C/L) and iron concentration (3.9 mg/L) are obtained at the natural pH of the phenol solution, *i.e.* pH 5.5. Consequently, the pH will be set at 5.5 for all the experiments with real water.

3.3 Study of the catalyst reusability

The reusability of the catalyst is evaluated by using the same iron impregnated Faujasite system several times for the phenol degradation under similar experimental conditions. For this purpose, three kind of measurement procedures were utilized in terms of catalyst washing and sampling. For the protocol denoted “washing”, the particles were washed with water between each photo-fenton cycles and a sampling was conducted each 30 minutes during the process. The protocol denoted “no washing” follow the same sampling procedure while no rinsing of the catalyst with water is performed. For the last process called “no washing 10%”, no washing was conducted and the sampling is only carried out at the end of the photo-fenton process. To investigate the long-term stability of the photo-fenton properties of the iron impregnated Faujasite, we compare the degradation of phenol using fresh and reused samples. Fig. 8 and Table 7 show the reproducibility of the Fe/Faujasite systems during three different photo-fenton cycles. The figure presents all the data, including the measurements using freshly prepared Fe/Faujasite.

Regardless of the iron amount impregnated (10% or 20%) and the protocol utilized (washing or no washing), fresh and reused Faujasite do not behave similarly. Reactions performed with fresh catalyst show the greatest rates of degradation. A substantial decline in the performance of the catalyst is detected during the first three cycles. This was already reported by others groups. They attributed this irreversibility to the iron leaching from the zeolite. In the present study, the diminution of the photo-Fenton activity with respect to the number of cycles depends significantly on both the iron amount impregnated and the washing steps. Consequently, the lack of long-term stability and reusability can be mainly attributed to the iron leaching. The lixiviation of the metal ions occurs preferentially with 20 % iron/Faujasite and is also favored by the washing of the catalyst. Under these particular conditions, the largest irreversibility is detected (Fig. 8, washing). After one cycle, the photo-Fenton activity drops significantly since a diminution of 65 % from the starting degradation yield is reported. For the third cycle, the quite complete loss of degradation activity

takes place. In the absence of washing of the Faujasite at the end of the degradation runs, a slight difference is obtained between the degradation data during the first and the second cycles (Fig. 8, no washing). On the contrary, a higher discrepancy takes place during the third cycle, and a diminution of 50 % of the degradation yield is reported compared to that obtained with the original catalyst (first cycle). To reduce the iron leaching from the Faujasite, the reusability of the catalyst is tested in consecutive cycles using the 10 % iron impregnated Faujasite (Table 7). The degradation percentage of phenol is complete in the first cycle, but it decreases by about 30 % in both the second and the third cycles after the same treatment duration (5 h). This indicates that the catalyst loses a part of its activity after the first cycle, and then it tends to stabilize in terms of efficiency for the other consecutive experiments.

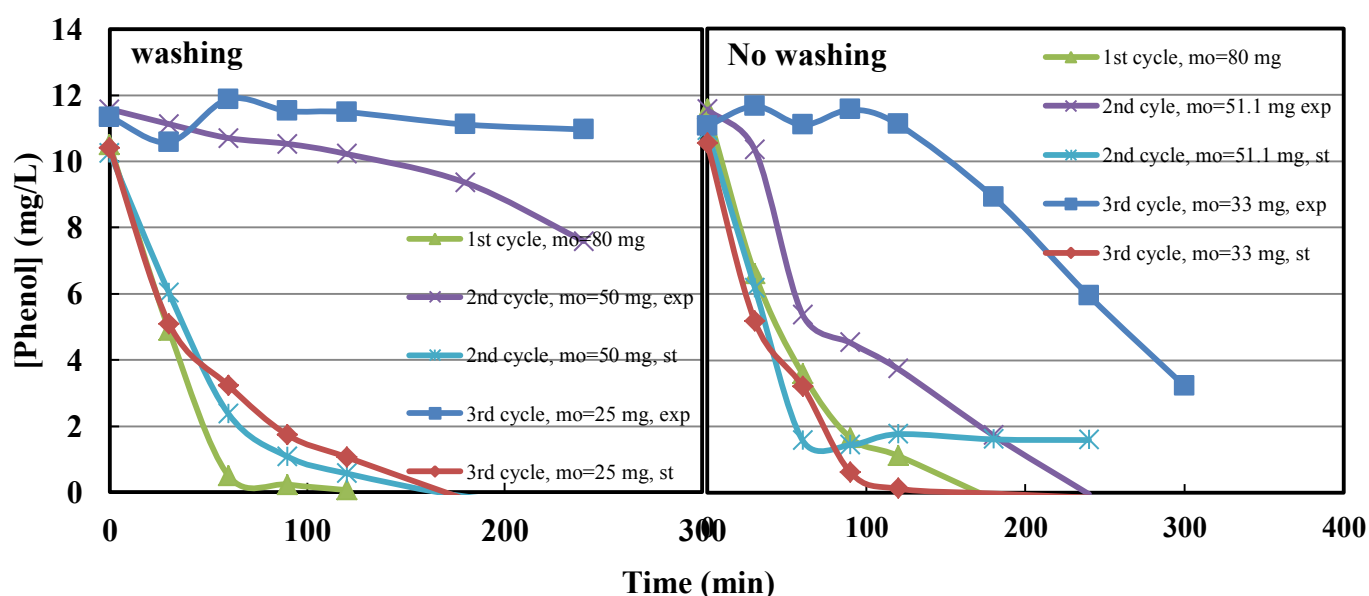


Fig. 8. The reusability of the 20 % Fe impregnated Faujasite catalyst is evaluated by using the same composite several times for the phenol degradation under similar experimental conditions. The catalyst (Fe+Faujasite) amounts are successively 80, 50, and 30-25 mg, for the first, second, and third photo-Fenton experiments, respectively (“Exp”). The direct experiments using freshly prepared 20 % Fe impregnated Faujasite catalyst are also shown for comparison (“St”). The measurement procedures are: Washing Catalyst, No catalyst washing. Experimental conditions: 0.007 M H_2O_2 , pH = 5.5, and UV light.

Table 7. Degradation of phenol over 10 % impregnated Faujasite, catalyst concentration 1g/L, 0.007 M H₂O₂ and under UV light.

Cycles	Degradation %
First cycle	100
Second cycle	69.6
Third cycle	67.6

3.4 Photo-Fenton removal of diclofenac

The photo-Fenton degradation of diclofenac is studied because it is found to be among the 21 micropollutants present in real river water. The main part of the decomposition processes is expected to occur onto the surface of the catalyst. Consequently, the adsorption features could be one of the factors that drive the photo-Fenton performance. To explore in detail the adsorption of diclofenac onto the raw Faujasite, the adsorption isotherm is measured (Fig. 9).

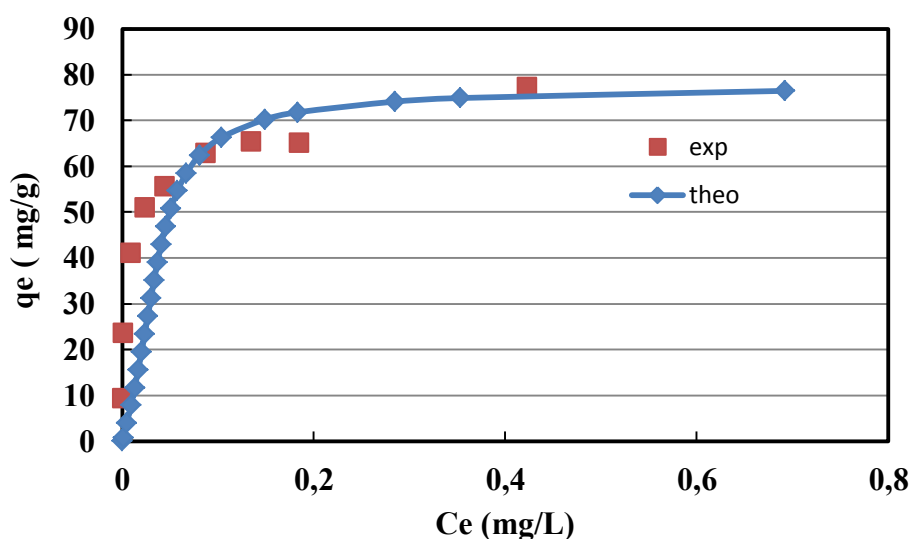


Fig. 9. Adsorption isotherm of diclofenac onto bare Faujasite. Comparison of the experimental (symbols) and calculated according to the Langmuir model (line) adsorption isotherms. Experimental conditions: Faujasite content = 2 g/L.

The diclofenac adsorbed amount initially increases with the pollutant concentration up to an equilibrium concentration of 0.24 mg/L. At higher diclofenac doses, the adsorbed uptakes remain

constant and the maximum surface coverage equals 70-80 mg/g. This seems to correspond to the saturation of the surface since no further adsorption takes place. The solid line in the figure is calculated using the Langmuir approach, and the model fits the data within experimental errors.

Fig. 10 shows the temporal evolution of the diclofenac concentration during the adsorption followed by the photo-Fenton process using iron impregnated Faujasite in an example which is representative of the other results and which has been selected to illustrate the trends. The data at irradiation time 0 corresponds to the remaining pollutant concentration after one hour of stirring in the dark. Consequently, it gives access to the adsorption capability of the samples.

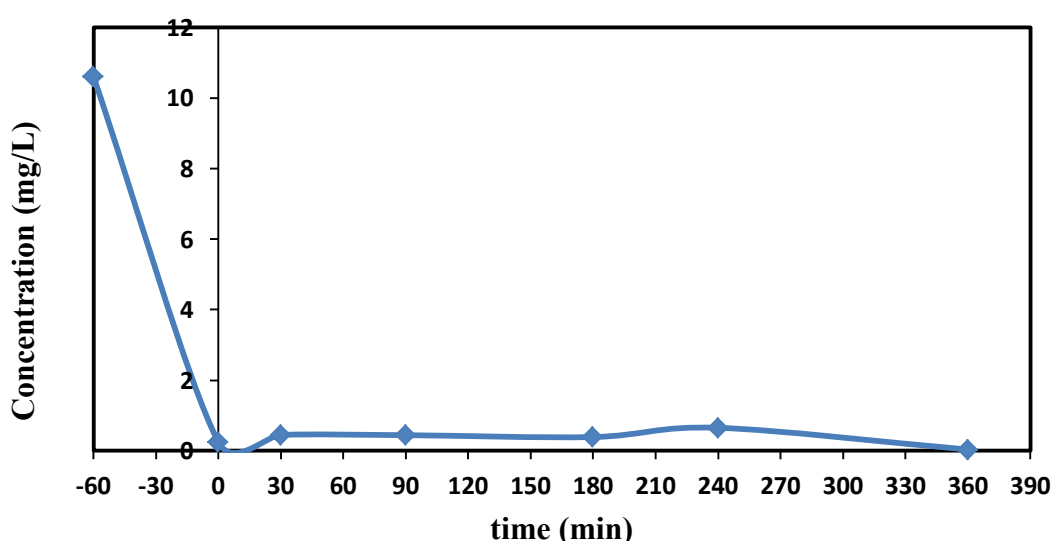


Fig. 10. Variation of the concentration of diclofenac during the adsorption followed by the photo-Fenton process using 10 % impregnated Faujasite. Experimental conditions: catalyst concentration 1g/L, 0.007 M H_2O_2 , and UV light.

Under our experimental conditions, the diclofenac concentration becomes very low after one hour of adsorption. This indicates that a total adsorption of the contaminant takes place onto the Faujasite. The TOC values of the solutions at the end of the adsorption process (irradiation time = 0 min) is equal to 2.6 mg C/L (Table 8). This confirms the total adsorption of the diclofenac onto the catalyst and the absence of pollutant into the solution. The TOC values of the solutions after 6 hours of photo-Fenton process remains equal to 2.6 mg C/L (Table 8). However, we are aware that, during the photo-Fenton process, a large percentage of contaminant could remain adsorbed onto the material without being degraded. The absence of diclofenac molecules onto the catalyst at the end of the photo-Fenton process was evaluated by measuring both the concentration of diclofenac and also the

amount of total organic carbon in the liquid after the washing of the catalyst. In fact, the physisorbed pollutant molecules or by-products can be removed by contact with water for several hours at room temperature. We used the following washing procedure: washing with pure deionized water with $V(\text{water}) = 100 \text{ mL}$ during 1 h and 1 night. At the end of the rinsing step, the particles were centrifuged. The possible presence of diclofenac molecules and by-products in the supernatant, *i.e.* desorbed from the Faujasite surface, was measured by organic carbon titration (Table 8) and by UV/visible spectroscopy (Fig. 11).

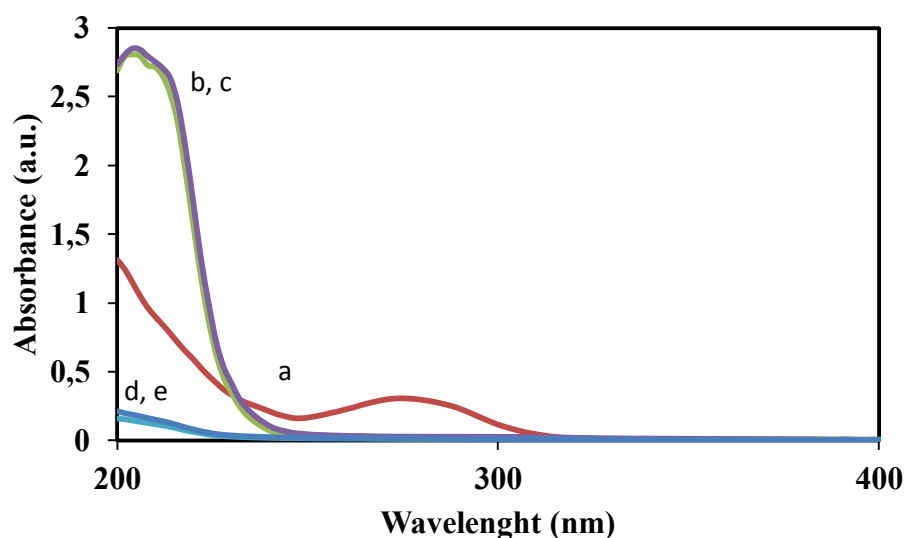


Fig. 11. UV/Visible absorption spectrum for: (a) initial diclofenac solution containing 10 mg/L of diclofenac, (b) the solution after 1 h of adsorption, (c) the solution at the end of the photo-Fenton process, and (d,e) the water after washing of the catalyst for (d) 1 h, and (e) overnight.

The UV/visible spectra (Fig. 11) reveal the absence of diclofenac in the solution after the washing of the catalyst. The TOC data (Table 8) indicates that a non-negligible small amount of carbon remains in the washing solution after one night ($[\text{TOC}] = 4.3 \text{ mg C/L}$). These results imply that the desorption of some species containing carbons occur. In other words, at the end of the photo-Fenton process some molecules remain onto the surface. These adsorbed molecules are not pure diclofenac but by-products. Consequently, there are still some by-products onto the surface which are desorbed during the washing. We then consider the degradation of the diclofenac, and also the presence of by-products onto the catalyst.

Table 8. TOC measurements for different solutions.

Experiment	NPOC mg Carbon/L
Diclofenac solution after 1 h of adsorption	2,670
Diclofenac solution at the end of the photo-Fenton process	2,568
Water solution after the washing of the catalyst for 1 h	1,998
Water solution after the washing of the catalyst overnight	4,329

4 Photo-Fenton degradation of micropollutants from real water

The photo-Fenton process is used with real water samples from the Meurthe river. The Faujasite containing 20 wt. % of iron was used as catalyst. All the results are listed in the Table S3 of the Supporting information.

First, it is interesting to analyze the initial concentration of the micropollutants before the water treatment process (Fig. 12). All the concentrations remain in the range of ng/L. The maximum concentration measured is equal to approximately 50 ng/L. It is recorded for diclofenac and bisphenol A. On the one hand, the presence of carbamazepine-10,11-epoxide, cyclophosphamide, erythromycin, estradiol-beta, ethynylestradiol, sulfadimethoxine, sulfadimidine, and sulfathiazole is detected. However, their concentrations fall under the limit of quantification of the LC-MS/MS apparatus. On the other hand, the micropollutants initial concentrations decrease from 54 ng/L to 1 ng/L in the following order: bisphenol A (54 ng/L), diclofenac (51 ng/L), ibuprofen (22 ng/L), naproxen (20 ng/L), carbamazepine (19 ng/L), clarithromycin (16 ng/L), triclosan (13 ng/L), lidocaine (7 ng/L), ketoprofen (7 ng/L), PFOS (6 ng/L), sulfamethoxazole (6 ng/L), estrone (4 ng/L) and PFOA (0.8 ng/L).

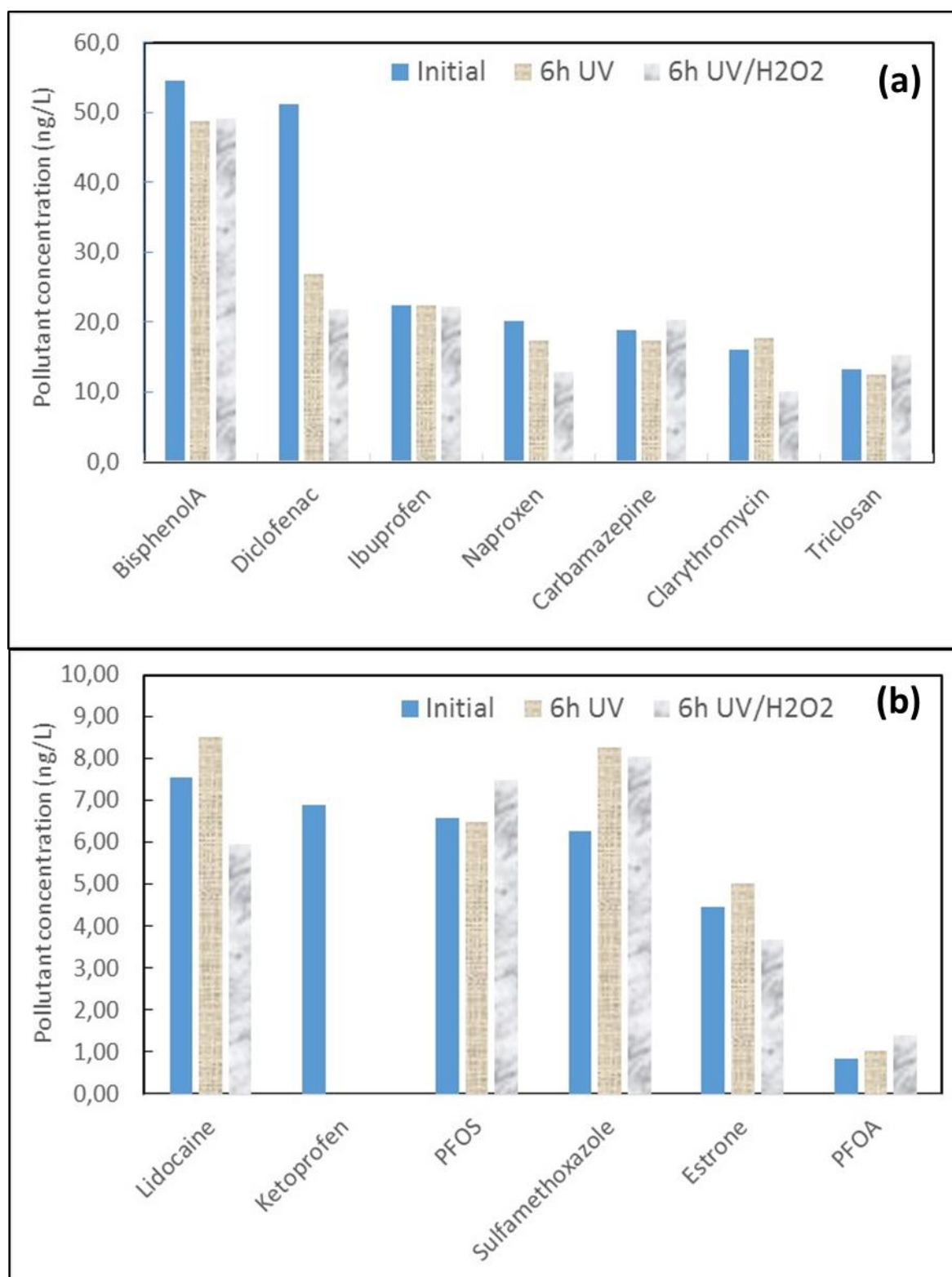


Fig. 12. Blank experiments in the absence of the iron-impregnated Faujasite under UV illumination (“6 h UV”) or in the simultaneous presence of UV and H₂O₂ (6h UV/H₂O₂). The notation “Initial” indicates the initial micropollutants concentration before the treatment.

It appears also necessary to perform blank experiments in the absence of the iron-impregnated Faujasite under UV illumination and in the presence of H_2O_2 (Fig. 12). For the majority of the micropollutants, the photolysis of the contaminants can be neglected since the pollutants concentrations do not vary after 6 h under UV irradiation. At the same time, the degradation remains also negligible in the presence of hydrogen peroxide. However, the concentration of ketoprofen after 6 h of UV becomes lower than the quantification limit of the analytical system regardless of the presence of H_2O_2 . For this reason, this pollutant cannot be considered in the photo-Fenton analysis. It is also important to note that the photolysis and the effect of hydrogen peroxide cannot be neglected with diclofenac. The contaminant concentration drops from 51 ng/L to 27-22 ng/L after 6 h of irradiation. In addition, a weak degradation occurs for bisphenol A (from 54 ng/L to 49 ng/L), naproxen (from 20 ng/L to 17-13 ng/L), and clarithromycin (from 16 ng/L to 10 ng/L).

The main part of the decomposition processes is expected to take place onto the surface of the catalyst. Consequently, the adsorption features could be one of the factors that drive the photo-Fenton performance. To explore in detail the adsorption of the micropollutants onto the iron-impregnated Faujasite, the contaminants concentration is analyzed after 2 hours of contact between the water and the catalyst (Fig. 13). The data correspond to the remaining pollutant concentration after 2 hours of stirring in the dark and in the absence of H_2O_2 . Consequently, they give access to the adsorption capability of the samples. For bisphenol A, diclofenac, naproxen, carbamazepine, triclosan, lidocaine, PFOS, and estrone, the concentrations after 2 hours in the dark appear below the limit of quantification of the LC-MS/MS system. This indicates a large and substantial adsorption of these contaminants onto the Fe/Faujasite. For instance, in the presence of all the other micropollutants, the adsorption of the diclofenac from an initial solution of 50 ng/L appears significant due to the high affinity of this pollutant for the Faujasite surface. These results emphasize also that all these micropollutants can be efficiently removed from the water by the adsorption process. Oppositely, for ibuprofen, clarithromycin, and ketoprofen a non-negligible adsorption takes place after 2 h of contact with the modified Faujasite in the dark. However, it remains some of these micropollutants in the water. At the same time, the absence of adsorption of sulfamethoxazole and PFOA onto the iron-impregnated zeolite has to be mentioned.

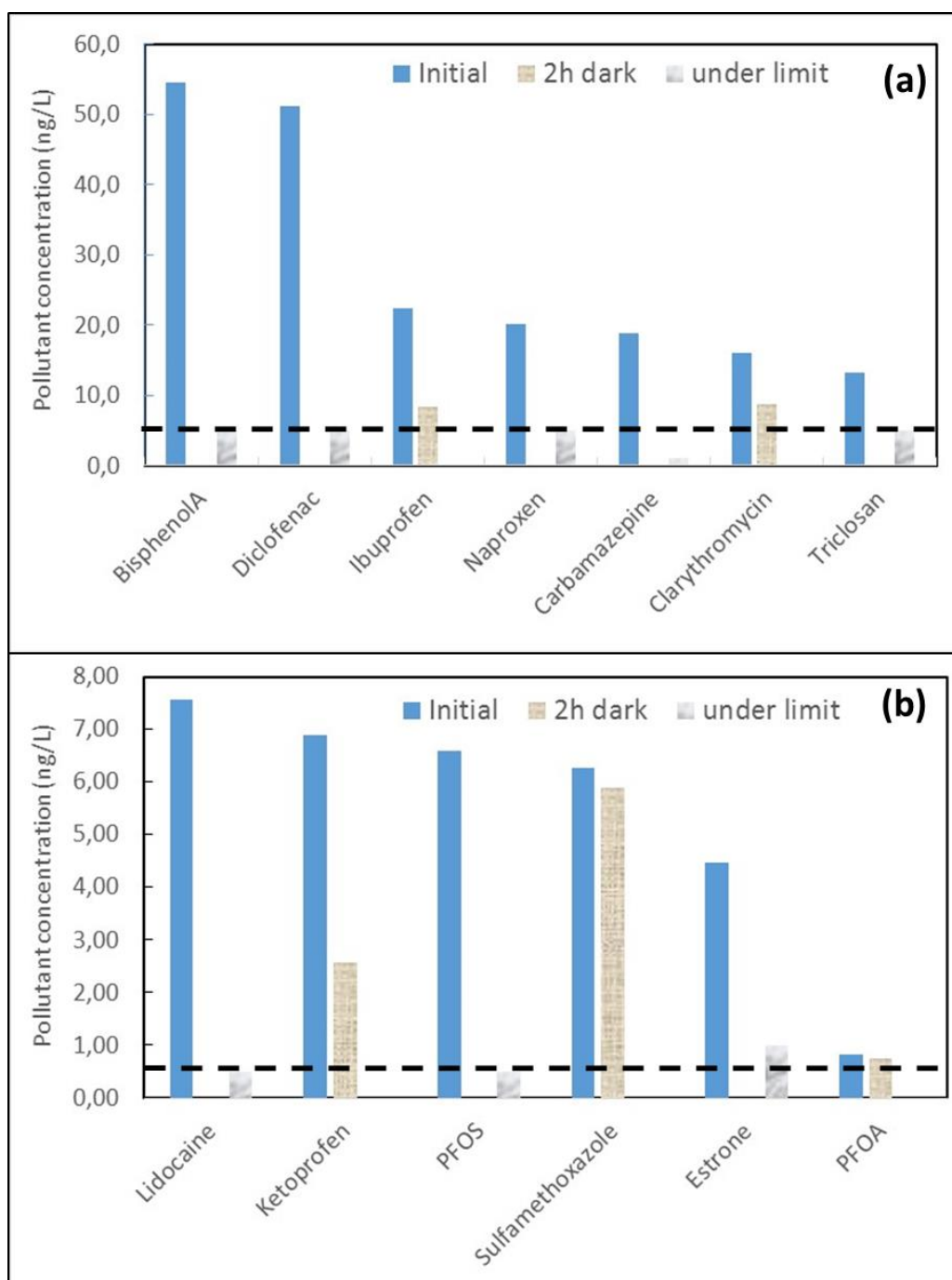


Fig. 13. Adsorption of the micropollutants onto the iron-impregnated Faujasite. The notation “Initial” indicates the initial micropollutants concentration before the treatment, while “2h dark” corresponds to the micropollutants concentration remaining in solution after 2 hours of contact between the water and the catalyst in the dark and in the absence of H_2O_2 . The specific legend “under limit” indicates that the concentration remains lower than the limit of quantification of the LC-MS/MS. The dotted lines give also the limit of quantification of the LC-MS/MS. Experimental conditions: catalyst concentration = 1 g/L, and pH 5.5.

We move now to the case of the photo-Fenton treatment of the water (Fig. 14). Except for sulfamethoxazole and PFOA, the concentration of all the other micro-contaminants becomes lower than the limit of quantification of the LC-MS/MS after 30 minutes of photo-Fenton treatment. This does not necessary demonstrate a total degradation of the pollutants but this emphasizes that; at least, a very low concentration of these micropollutants remains in the solution. This indicates the good efficiency of the photo-Fenton process using iron-impregnated Faujasite with a cocktail of a minimum of 21 micropollutants. We can also stress the quicker degradation with the mixture of the micropollutants (30 minutes) compared to the time necessary to degrade a larger concentration of phenol (10 mg/L), which takes 100 minutes. However, the comparison of the initial TOC values of the solutions, *i.e.* 2.8 mg C/L for the water containing the micropollutants and 6.8 mg C/L for the phenol solution, demonstrates that a greater amount of phenol macro-pollutant has to be degraded in comparison to the sum of all the micropollutants present inside the real water. However, the complete degradation of sulfamethoxazole does not occur. The initial concentration of 6.2 ng/L decreases to 3.7 ng/L after 30 minutes of process, and then to 1.6 ng/L after 6 hours of photo-Fenton treatment. This indicates that the kinetic of degradation is slower than for the other micropollutants. In addition, the degradation of PFOA can be neglected since the micropollutant concentration does not vary after 6 h of the process.

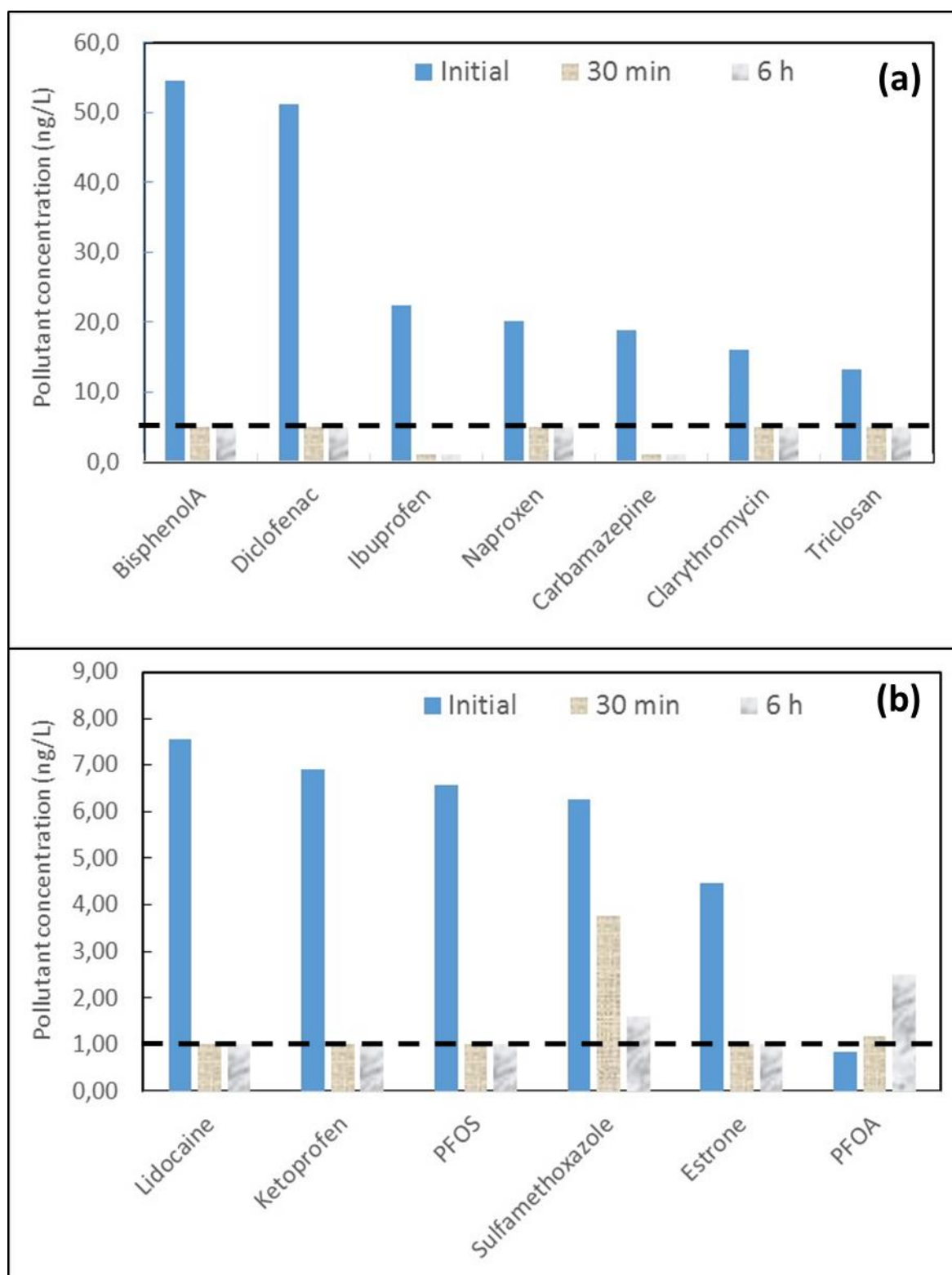


Fig. 14. Photo-Fenton treatment of the water using iron-impregnated Faujasite. The notation “Initial” indicates the initial micropollutants concentration before the treatment, while “30 min” and “6 h” correspond to the micropollutants concentrations remaining in the solution after 30 min and 6 hours of photo-Fenton process. The dotted lines give the limit of quantification of the LC-MS/MS. Experimental conditions: catalyst concentration = 1 g/L, 0.007 M H₂O₂, UV light and pH 5.5.

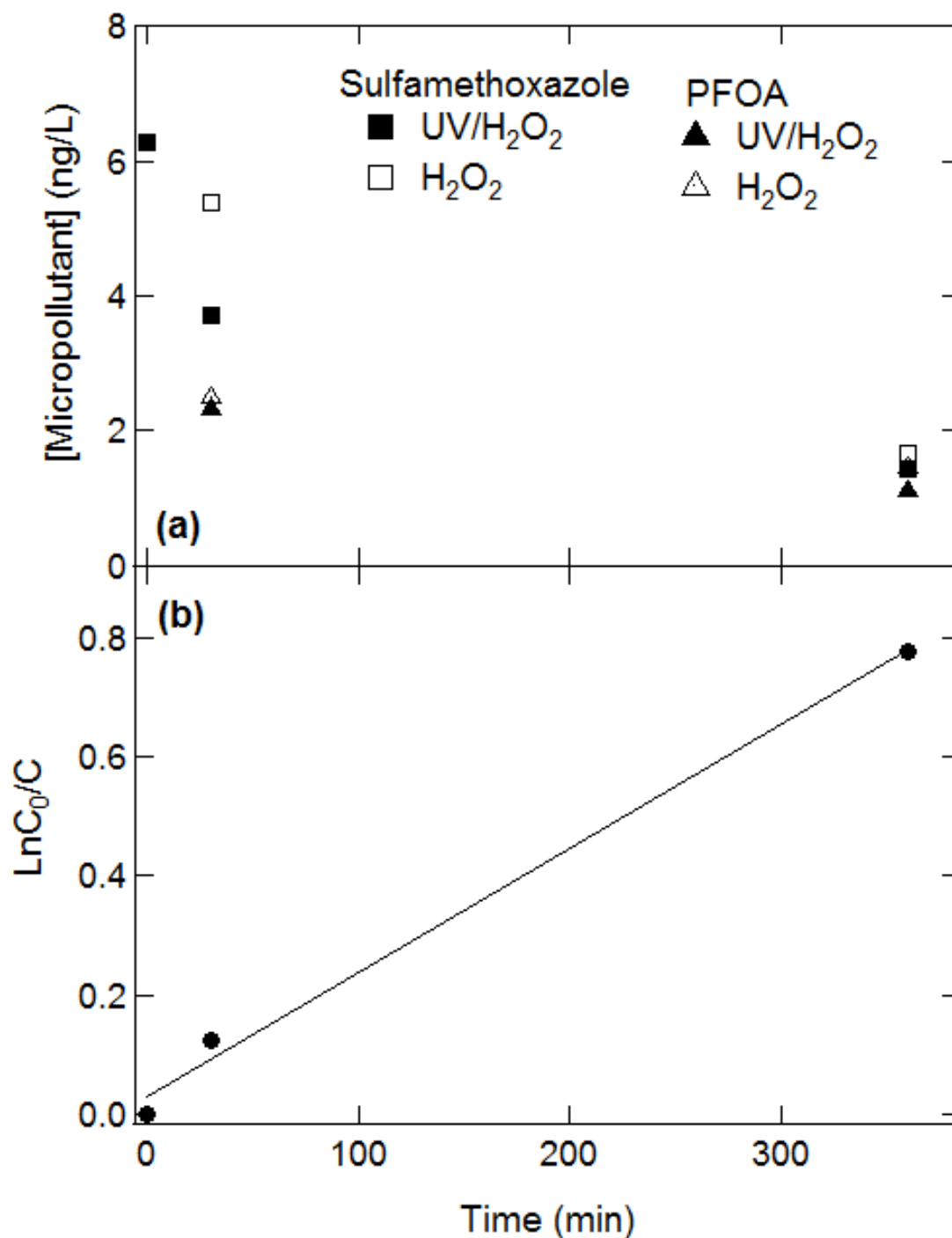


Fig. 15. (a) Effect of the illumination on the degradation performances. The photo-Fenton data (“UV/H₂O₂”) are compared to the Fenton results in the dark (“H₂O₂”) for sulfamethoxazole and PFOA micropollutants. (b) Kinetics of sulfamethoxazole photo-Fenton degradation by the iron-impregnated Faujasite (20 wt. % Fe). Linear transform: $\ln(C_0/C)$ versus time. The line represents the best linear fit given by $\ln(C_0/C) = 0.0021 \text{ Time} + 0.029$ ($R^2 = 0.9947$). Experimental conditions: catalyst concentration = 1 g/L, 0.007 M H₂O₂, and pH 5.5.

It appears relevant to address the effect of the illumination on the degradation performances. In that respect, the photo-Fenton data (“UV/H₂O₂”) are compared to the Fenton results in the dark (“H₂O₂”) in the Fig. 15a. As previously reported during the degradation of the model phenol macro-pollutant, a weak effect of the UV irradiation is observed. A slight improvement of the degradation efficiency of the micropollutants occurs in the presence of UV in comparison to that reported in the dark. For instance, the concentration of sulfamethoxazole after 30 minutes of treatment becomes equal to 5.3 ng/L in the absence of illumination (Fenton) while it drops to 3.7 ng/L under UV illumination (photo-Fenton). The same trend is reported for PFOA. Nevertheless, it is interesting to note that for all the other micropollutants, 30 minutes of Fenton process in the dark is sufficient to reach concentrations below the limit of quantification of the analytical apparatus (Table S3 of the Supporting information). The same behavior was also observed in the presence of UV illumination.

Finally, to test the effect of the micropollutant concentration, additional data corresponding to photo-Fenton experiments performed with new water are discussed (Fig. 16 and Table S4 of the Supporting information). The water was sampled from the same location in the Meurthe river but at a different period. The sampling was performed in October 2016 while it was carried out in March 2017 for the previous experiments. The initial concentration of the micropollutants is higher inside the water taken in October. This allows us to evaluate the efficiency of the photo-Fenton process in the presence of larger contaminant content. Consequently, the degradation of new molecules such as carbamazepine-10,11-epoxide and erythromycin can be tested since their initial concentrations become larger than the limit of quantification of the LC-MS/MS. After 30 minutes of photo-Fenton treatment, the total abatement of lidocaine, naproxen, triclosan, carbamazepine, carbamazepine-10,11-epoxide, diclofenac and estrone occurs. These results corroborate our previous measurements obtained during the first sampling (March 2017) despite the larger micropollutants concentrations. After 6 hours of photo-Fenton process, the clarithromycin disappears. In addition, bisphenol A, erythromycin, ibuprofen, and PFOS are not completely removed after 6 hours of treatment but their initial concentrations have been reduced by a factor larger than or equal to 10.

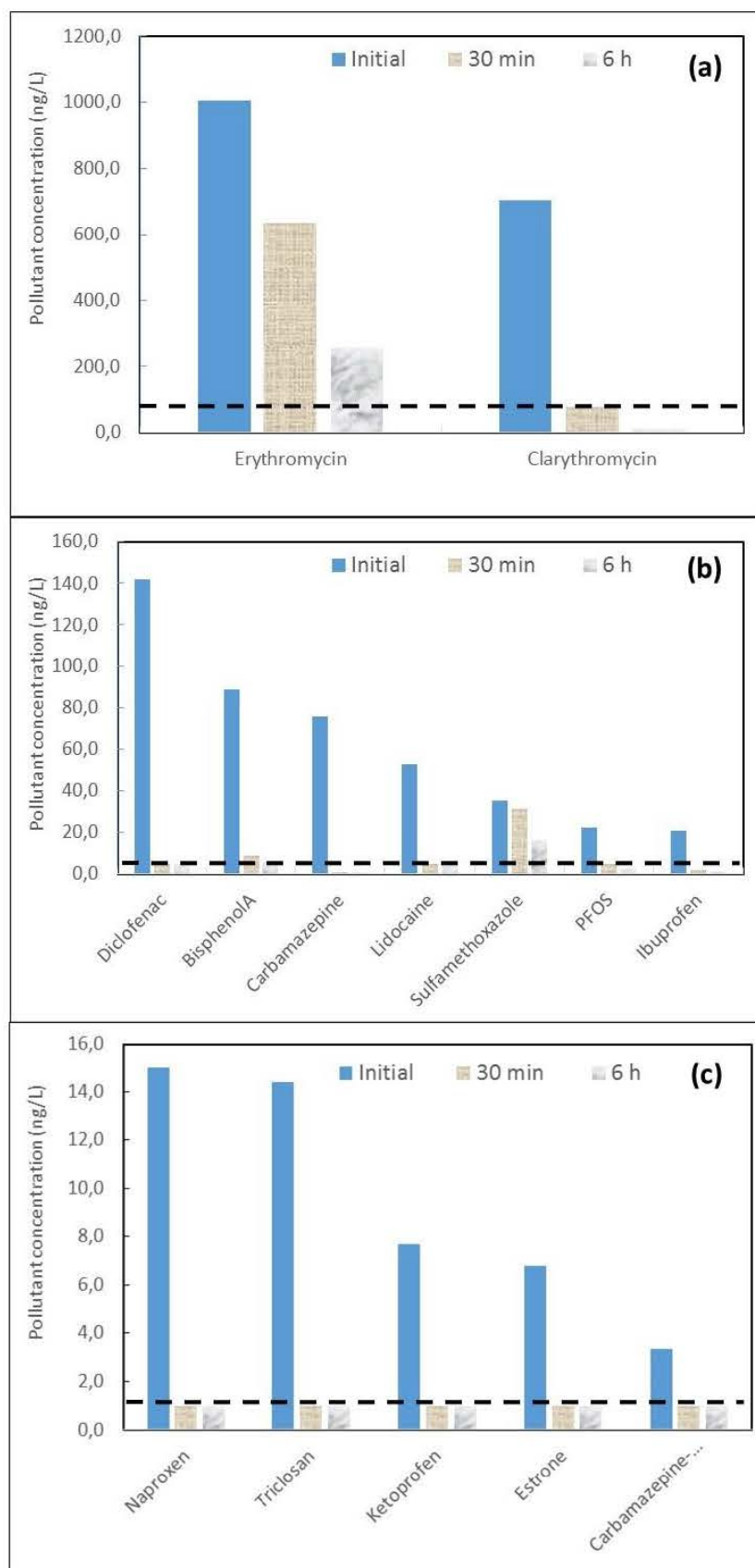


Fig. 16. Photo-Fenton treatment of the water using iron-impregnated Faujasite. The sampling was performed in October 2016. The notation “Initial” indicates the initial micropollutants concentration before the treatment, while “30 min” and “6 h” correspond to the micropollutants concentrations

remaining in the solution after 30 min and 6 hours of photo-Fenton process. The dotted lines give the limit of quantification of the LC-MS/MS. Experimental conditions: catalyst concentration = 1 g/L, 0.007 M H₂O₂, UV light and pH 5.5.

For ibuprofen, ketoprofen, and triclosan, the initial concentrations are similar between the two samplings. These data can be analyzed in order to have an idea of the reproducibility of the measurements and the degradation process. In both cases, the photo-Fenton treatment leads to the disappearance of triclosan after 30 minutes. The adsorbed amount of ketoprofen onto the Fe/Faujasite remains very close. In the special case of ibuprofen, the kinetic of degradation does not quantitatively differ from the first result and the trends are similar.

Using the new data obtained at larger initial concentrations, it becomes possible to examine the kinetics of the photo-Fenton degradation for some micropollutants. Particularly, the temporal evolution of the concentration of sulfamethoxazole gives a lot of relevant information. Based on our previous experiments with phenol (macro-pollutant, 10 mg/L), the photo-Fenton degradation is expected to follow a first-order kinetics with respect to the sulfamethoxazole concentration in the bulk solution (C). A plot of $\ln(C_0/C)$ versus the time is shown in Fig. 15b. Note that C_0 stands for the initial micropollutant concentration in the bulk solution (at time = 0). The linear increase of $\ln(C_0/C)$ as a function of time confirms that the photo-Fenton degradation of sulfamethoxazole obeys first order kinetics in the presence of the cocktail of the other micropollutants. The linearization gives a kinetic constant k of 0.0021 minutes⁻¹. We stress that great care has to be taken with the value of this constant because it was obtained with only 3 experimental data, which do not ensure a great accuracy. However, the k value can be compared with the kinetic constant already obtained with phenol. We found a constant of 0.0394 min⁻¹ for the photo-Fenton degradation of an initial solution containing 10 mg/L of phenol. The lower value obtained with the sulfamethoxazole from the real water can be explained by the competition between all the micropollutants for the iron catalysts active sites of the Faujasite surface.

It seems also interesting to discuss the relative importance of the photo-Fenton and the adsorption effects to remove the micropollutants from the real water using iron-impregnated Faujasite. For this purpose, the remaining microcontaminants concentrations are analyzed after 2 hours of adsorption and after 30 minutes of photo-Fenton treatment. For carbamazepine, carbamazepine-10,11-epoxide, triclosan, estrone and lidocaine, the two concentrations are similar and lower than the limit of quantification of the LC-MS/MS. For these contaminants, it is impossible to discriminate between the effect of the adsorption and the photo-Fenton degradation. In other

words, it is not possible to conclude that the micropollutant concentrations decrease due to adsorption or/and photo-Fenton effect with radicals production. It appears more relevant to address the other micropollutants for which the concentrations after the adsorption process and the photo-Fenton treatment are different. The results are depicted in Figs. 17 for the waters sampled in March 2017 (Fig. 17a) and October 2016 (Fig. 17b,c). For clarithromycin, ibuprofen, ketoprofen, sulfamethoxazole, bisphenol A, and naproxen, the microcontaminants concentrations after 30 minutes of photo-Fenton are lower than those after 2 hours of adsorption. Consequently, the photo-Fenton treatment shows superior degradation efficiency than the adsorption process. These results confirm that photo-Fenton degradation could be one of the main causes of the high activity during the removal of these micropollutants using iron-impregnated Faujasite. This is not surprising since the heterogeneous photo-Fenton process can be viewed as the sum of the adsorption and radicals generation. In other words, the high contaminant surface concentration provides a large amount of molecules to react with the hydroxyl radicals generated by the light and the iron.

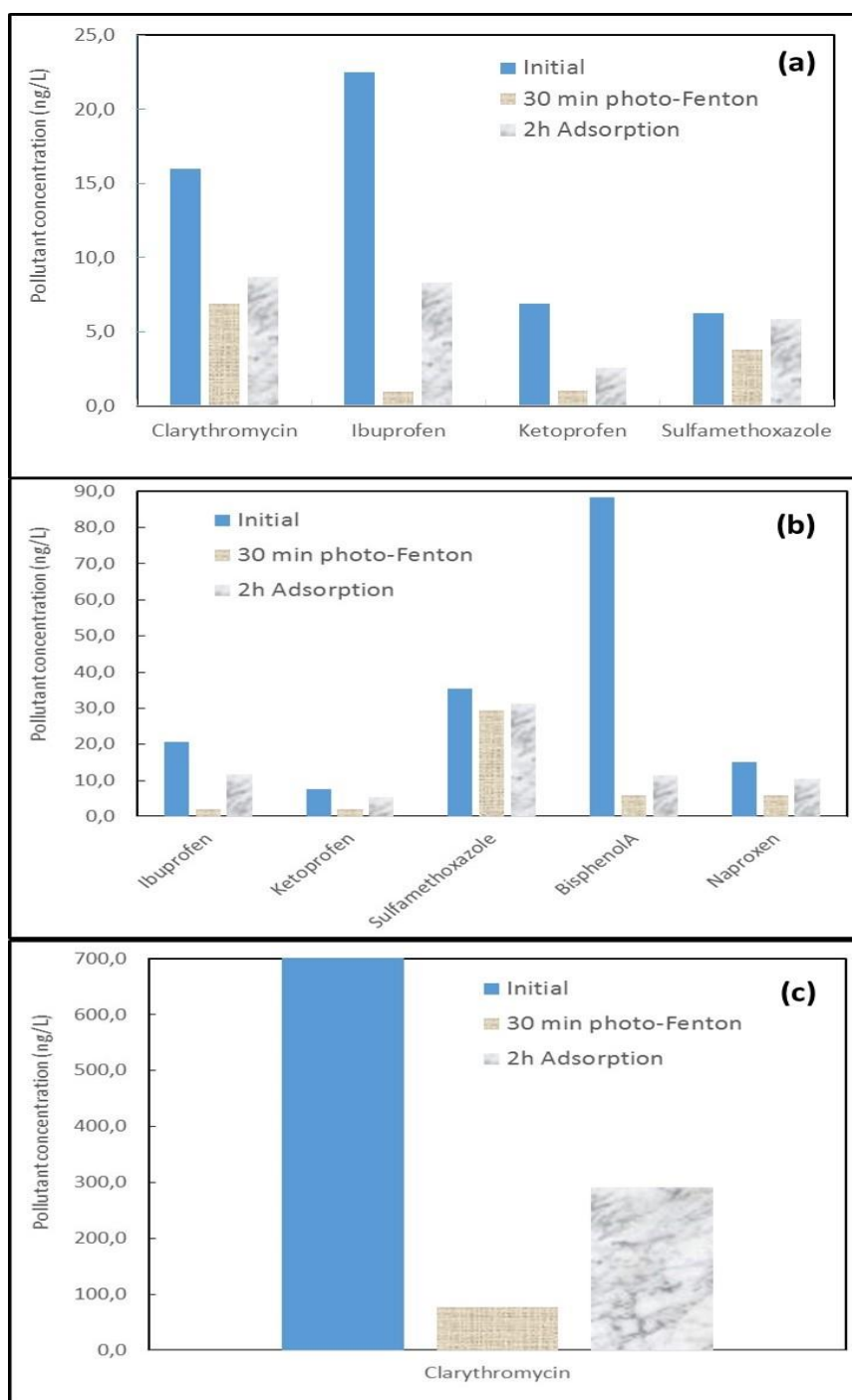


Fig. 17. Comparison between the photo-Fenton and the adsorption effect to remove the micropollutants from the real water using iron-impregnated Faujasite. The sampling was performed in (a) March 2017, and (b,c) October 2016. The notation “Initial” indicates the initial micropollutants concentration before the treatment, while “30 min photo-Fenton” correspond to the micropollutants concentrations remaining in the solution after 30 min of photo-Fenton process. The notation “2h Adsorption” corresponds to the micropollutants concentration remaining in solution after 2 hours of contact between the water and the catalyst in the dark and in the absence of H_2O_2 . Experimental conditions: catalyst concentration = 1 g/L, 0.007 M H_2O_2 , UV light and pH 5.5.

5 Heterogeneous photocatalysis of pollutants using TiO₂

5.1 Photocatalytic degradation of model macropollutants

The photocatalytic degradation of phenol and diclofenac in the presence of titania particles is illustrated in Fig. 18. In the figure, the negative time (from -120 min to 0 min) corresponds to the adsorption period in the absence of illumination. Consequently, the remaining pollutant concentration at irradiation time 0 gives access to the adsorption capability of the sample.

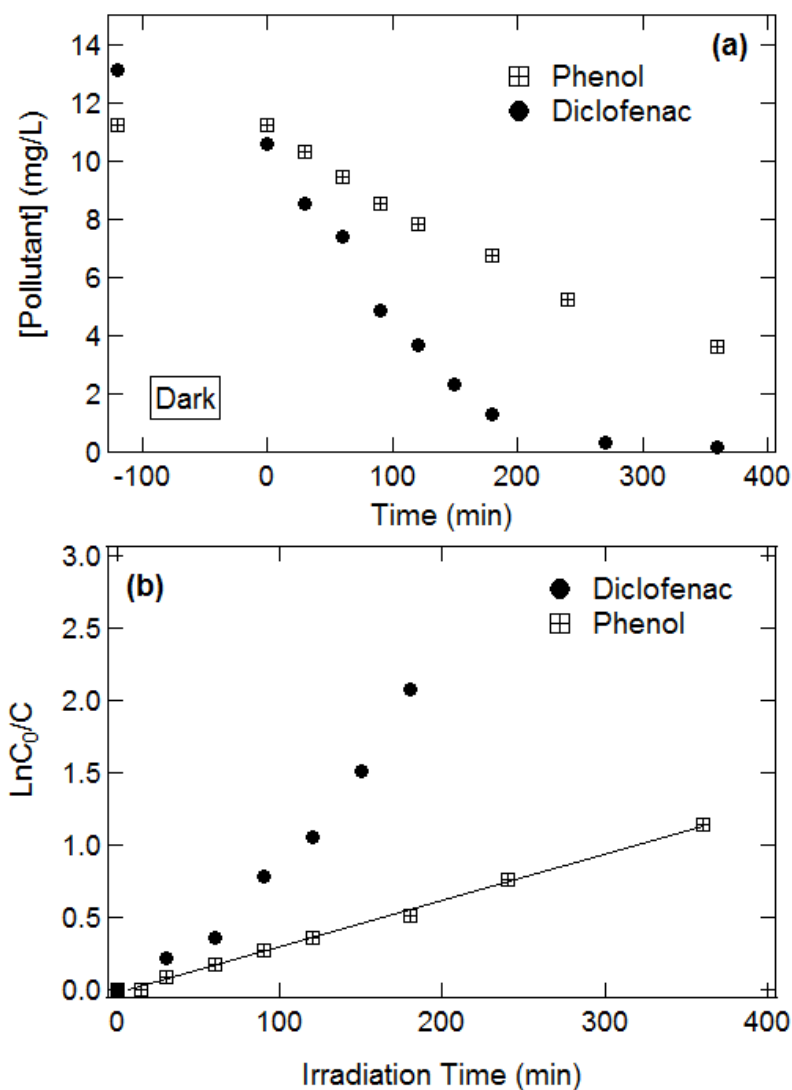


Fig. 18. (a) Photocatalytic degradation of diclofenac and phenol as a function of the time of irradiation for the titania photocatalyst. (b) Linear transform: $\ln(C_0/C)$ versus time. The line represents the best linear fit given by $\ln(C_0/C) = 0.0032 \text{ Time} + 0.0215$ ($R^2 = 0.9966$) for the degradation of phenol. C_0 is the initial micropollutant concentration (at irradiation time = 0) while C is the micropollutant concentration at a given time.

Each curve shows a similar trend. The bulk concentration of macropollutants decreases with the reaction time. Both the adsorption and the photocatalytic performance depend on the nature of the contaminant. The adsorption and photodegradation of diclofenac proceed more favorably than that of phenol. A very weak adsorption of phenol onto TiO₂ is reported. The adsorbed amount is equal to 0.0068 mg/g. In the presence of diclofenac, the titania adsorption capacity becomes larger and the adsorbed diclofenac uptake amounts to 2.53 mg/g. The photocatalytic efficiency of TiO₂ towards diclofenac removal is superior to that with phenol. For phenol, there is some degradation but it remains a non-negligible amount of pollutant after 360 min of irradiation. On the contrary, in the presence diclofenac, the complete degradation of the pollutant phenol takes place within 270 min of irradiation.

It appears relevant to study in details the kinetics of the reactions. The degradation experiments by UV irradiation of macropollutants by TiO₂ photocatalyst is expected to follow a first-order kinetics ($r = k C$ or $C = C_0 \exp(-k \times t)$) with respect to the contaminant concentration in the bulk solution (C). A plot of $\ln(C_0/C)$ versus the time t is shown in Fig. 18b. Note that C_0 stands for the initial pollutant concentration in the bulk solution (at time = 0). The linear increase of $\ln(C_0/C)$ as a function of t attests/confirms that the photocatalytic degradation of phenol obeys first order kinetics. Conversely, for diclofenac, there is a non-linear increase of the $\ln(C_0/C)$ with the irradiation time.

5.2 Photocatalytic degradation of micropollutants

The photocatalytic decomposition of the micropollutants from real river water is studied in the presence of TiO₂ catalyst. Two series of sampled water are treated. The sampling was performed in October 2016 and March 2017. All the results are listed in the Table S5 of the Supporting information.

Adsorption is the first mechanism that could drive the removal of the different micropollutants. To explore in detail the adsorption of the micropollutants onto the titania, the contaminants concentration is analyzed after 2 hours of contact between the water and the photocatalyst (Figs. 19 and 20). The data correspond to the remaining pollutant concentration after 2 hours of stirring in the dark. Consequently, they give access to the adsorption capability of the samples. To discuss in details the adsorption capacity of the titania towards the micropollutants, it appears relevant to use the whole data recorded with the two samplings performed at different

periods (Figs. 19 and 20). This allows us to emphasize the impact of the nature and the initial concentration of micropollutants on the adsorbed amounts.

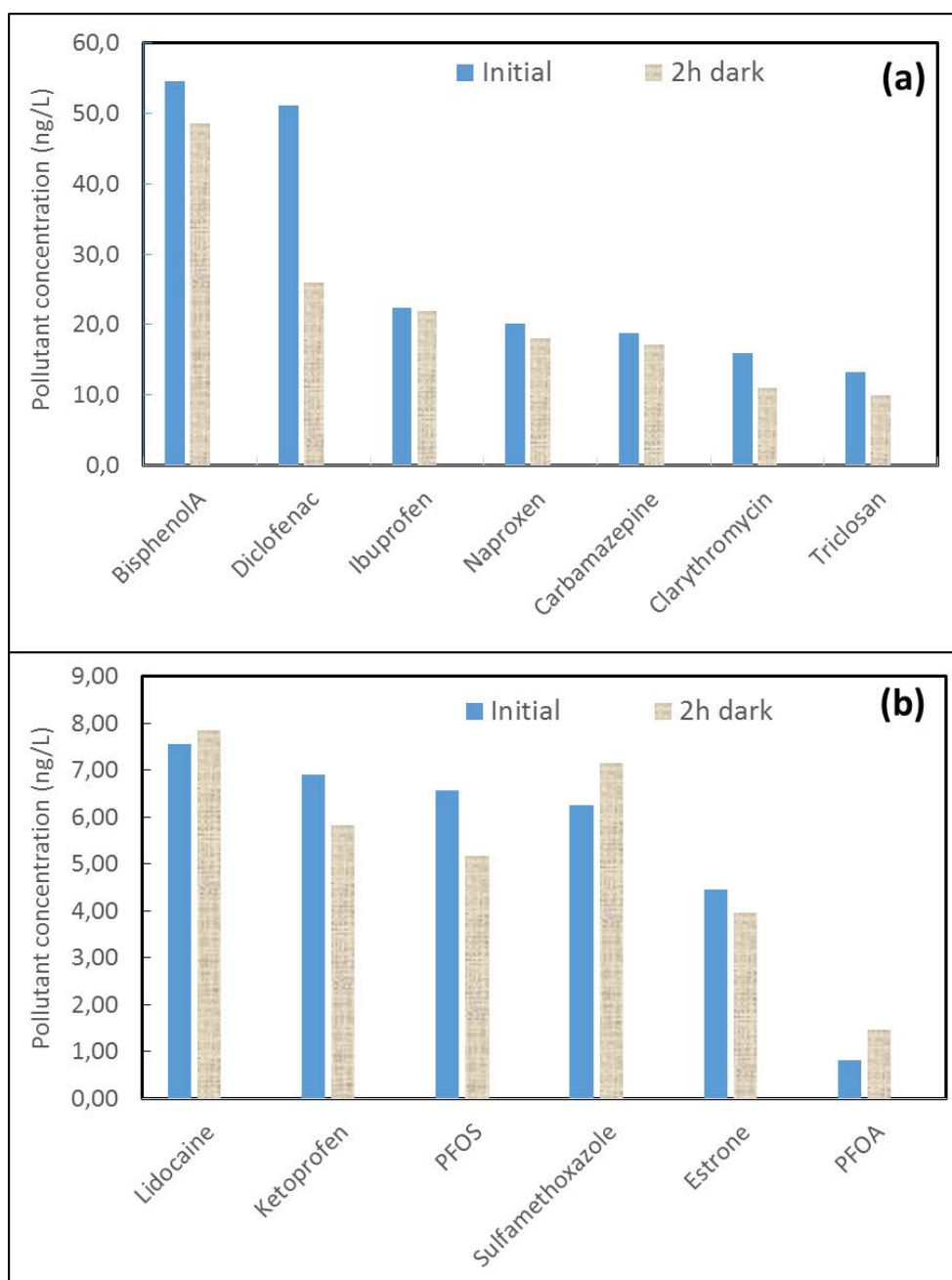


Fig. 19. Adsorption of the micropollutants onto the titania. The sampling was performed in March 2017. The notation “Initial” indicates the initial micropollutants concentration before the treatment, while “2h dark” corresponds to the micropollutants concentration remaining in solution after 2 hours of contact between the water and the catalyst in the dark.

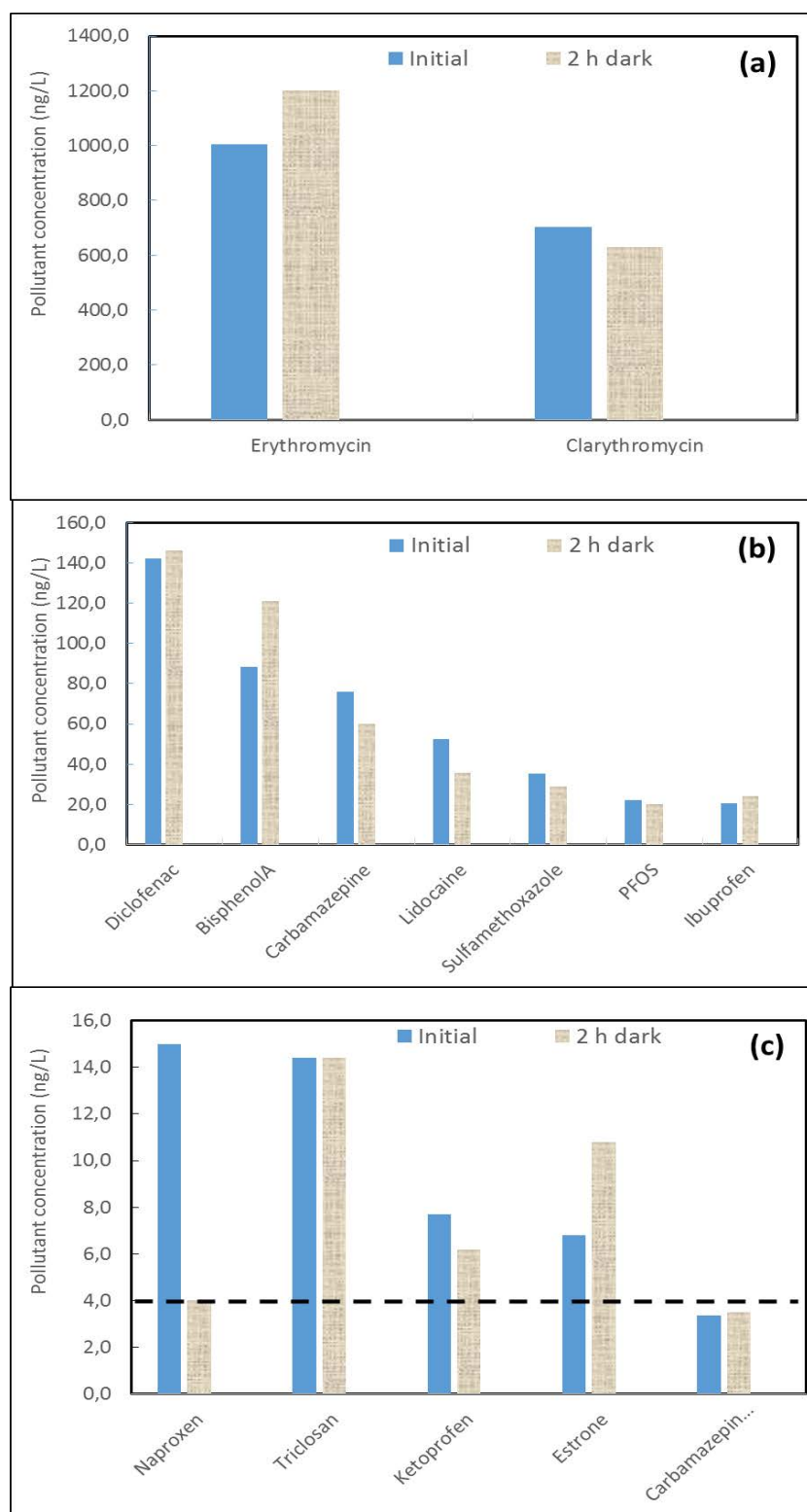


Fig. 20. Adsorption of the micropollutants onto the titania. The sampling was performed in October 2016. The notation “Initial” indicates the initial micropollutants concentration before the treatment, while “2h dark” corresponds to the micropollutants concentration remaining in solution after 2 hours of contact between the water and the catalyst in the dark. The dotted line gives the limit of quantification of the LC/MS-MS.

Among all the quantified micropollutants, only carbamazepine-10,11-epoxide and naproxen fall below their limit of quantification after 2 h of stirring in the dark for the water sampled in October 2016. The initial concentration of carbamazepine-10,11-epoxide in water is already low (3.3 ng/L) and close to its limit of quantification given as 3.0 ng/L. For naproxen, the initial concentration of 15 ng/L falls to a value lower than 7.9 ng/L. Note also that in some cases, the remaining content after two hours of adsorption ($C(2\text{hours})$) becomes larger than the initial micropollutant concentration (C_0). This happens for lidocaine, sulfamethoxazole, and PFOA for the water sampled in March 2017 where the concentrations are low. On the other hand, this occurs also for erythromycin, diclofenac, bisphenol A, ibuprofen, estrone, PFOA, and carbamazepine for larger initial micropollutant concentrations when treating the water withdrawn in October 2016. This may indicate experimental artifacts during the adsorption process, water separation from the titania, and/or the analytical procedures during the micropollutant analysis. However, when this phenomenon takes place for the two sampling, it might indicate the lack of adsorption of the micropollutant. For instance, we consider the absence of adsorption of ibuprofen onto the titania. For PFOA and erythromycin, it is difficult to conclude. Actually, the remaining content of PFOA after two hours of adsorption becomes larger than the initial micropollutant concentration in the two studies. For erythromycin, the concentration was too low to be evaluated for the first sampling and the final concentration was larger than the initial ones. For the other micropollutants, *i.e.* lidocaine, sulfamethoxazole, diclofenac, bisphenol A, estrone, and carbamazepine this configuration ($C_0 < C(2\text{hours})$) occur only once and generally during the adsorption with the water sampled in October 2016. We then consider that the adsorption of these micropollutants occur onto titania but we evaluate the adsorbed amount only when $C_0 > C(2\text{hours})$.

From the adsorption results, it can be concluded that the micropollutants cannot be efficiently removed by adsorption over TiO_2 catalyst surface. This is not surprising since the titania used in this study possesses a low specific surface area (around $59 \text{ m}^2/\text{g}$) and no apparent porosity (Kassir et al. 2015). This result appears coherent with the results of adsorption experiments of the model macropollutants that resulted in the absence of adsorption of phenol onto TiO_2 . To evaluate the impact of the nature and the initial micropollutant concentration on the adsorption, it seems relevant to express the adsorption data in terms of adsorbed amount:

$$\Gamma = \frac{(C_0 - C(2\text{hours})) \times V}{m_{\text{TiO}_2}} \quad (11)$$

where C_0 and $C(2\text{hours})$ represent the initial micropollutant concentration and the pollutant concentration remaining after 2 hours of adsorption, respectively. In addition, m_{TiO_2} is the mass of titania and V is the volume of the solution.

The Fig. 21 describes the evolution of the micropollutants adsorbed amounts versus the initial pollutant concentration. For all the micropollutants, the contaminant adsorbed amount increases with the pollutant concentration. It can be also mentioned that all the data seem to follow the same trend which can be represented onto a unique master curve.

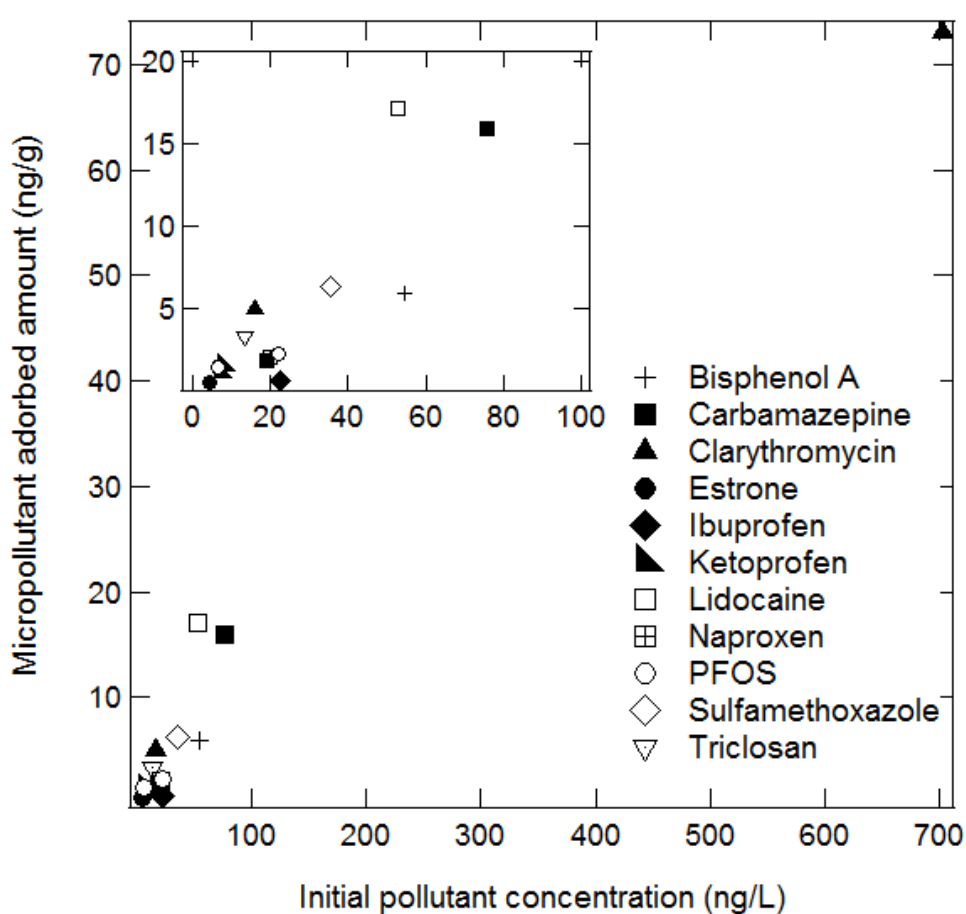


Fig. 21. Micropollutant adsorbed amount as a function of the initial pollutant concentration. The inset shows the data for initial micropollutant concentrations lower than 100 ng/L.

After that, the photocatalytic removal of the micropollutants with TiO₂ catalyst under UV light is studied. After the adsorption period (2 h of dark stirring), the concentrations of the different compounds is estimated after 30 min and 6 h under UV irradiation. The resulted are given in the Figures 22 and 23 for the sampling performed in March 2017 and October 2016, respectively.

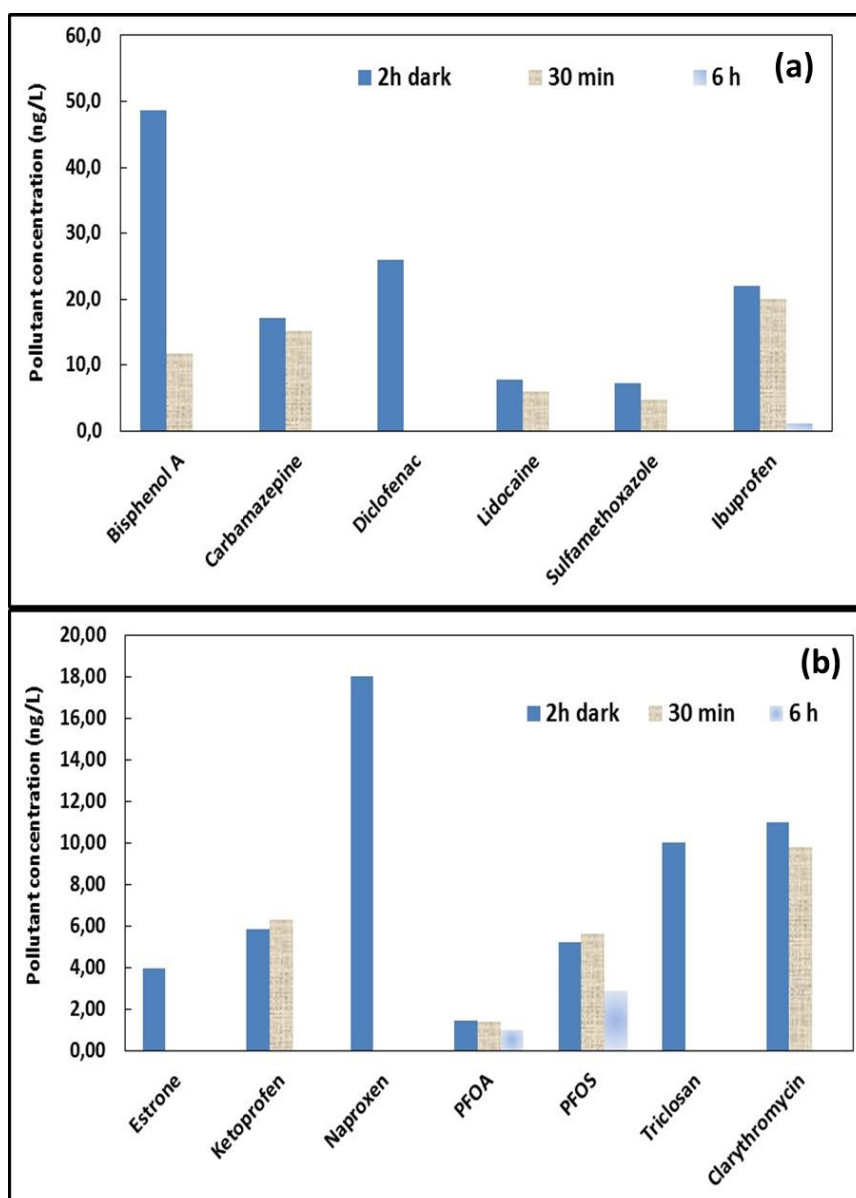


Fig. 22. Photocatalytic treatment of the water using titania. The sampling was performed in March 2017. The notation “2h dark” corresponds to the micropollutants concentration remaining in solution after 2 hours of contact between the water and the catalyst in the dark, while “30 min” and “6 h” corresponds to the micropollutants concentrations remaining in the solution after 30 min and 6 hours of photocatalysis process. The absence of bar indicates that the micropollutant concentration becomes lower than the limit of quantification of the LC/MS-MS.

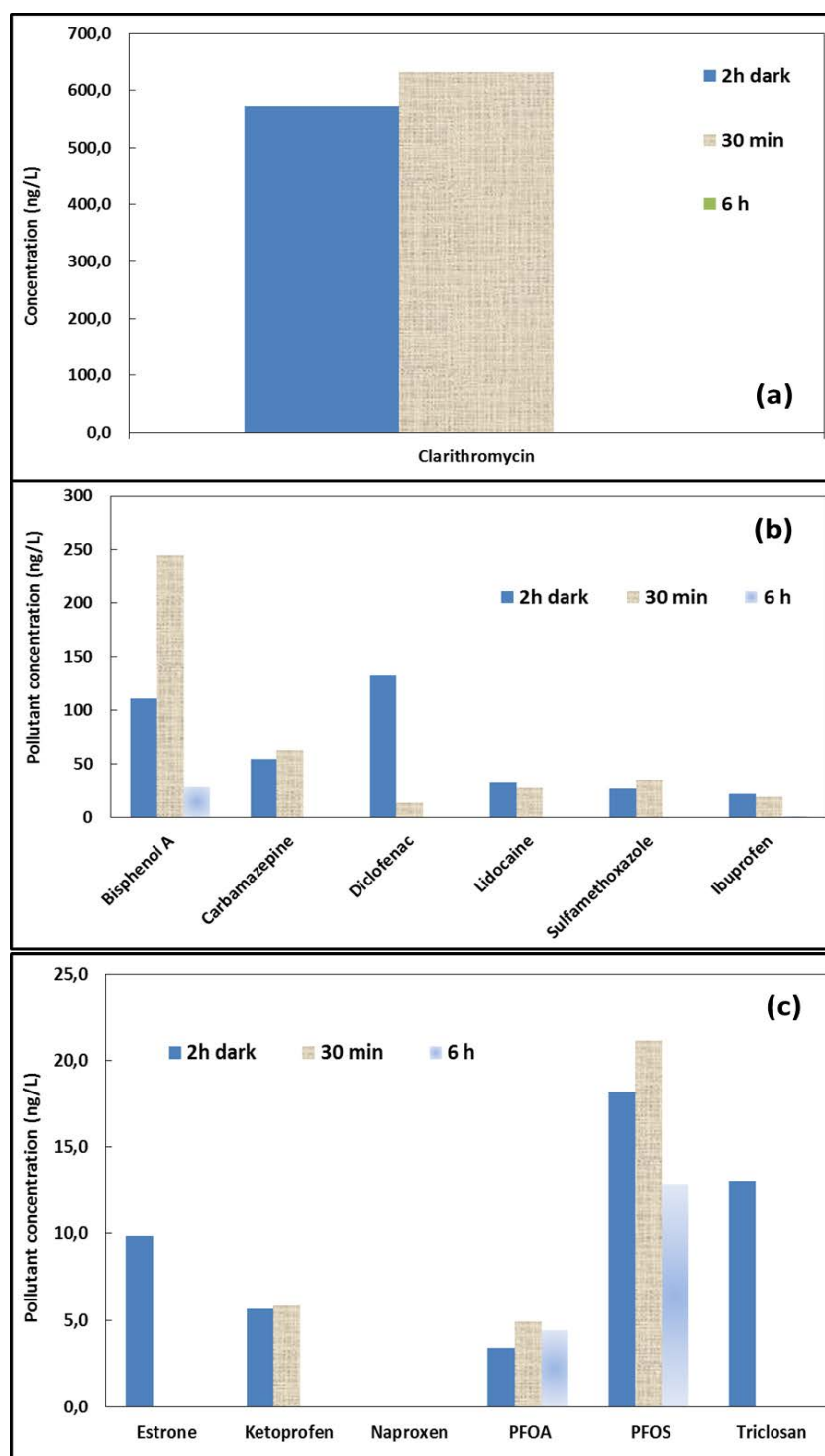


Fig. 23. Photocatalytic treatment of the water using titania. The sampling was performed in October 2016. The notation “2h dark” corresponds to the micropollutants concentration remaining in solution after 2 hours of contact between the water and the catalyst in the dark, while “30 min” and “6 h” corresponds to the micropollutants concentrations remaining in the solution after 30 min and 6 hours of photocatalysis process. The absence of bar indicates that the micropollutant concentration becomes lower than the limit of quantification of the LC/MS-MS.

For all the micropollutants, the contaminant concentration decreases with the time of irradiation. This confirms the photocatalytic activity of titania towards the cocktail of 21 micropollutants. After 6 hours of photocatalytic process, the concentrations of the majority of the micropollutants become below their limit of quantification. For the two waters, ibuprofen, PFOA and PFOS remain in the solution at the end of the process while the presence of erythromycin and bisphenol A is detected only from the water sampled in October 2017 due to their larger initial concentrations. The removal percentage can be expressed as:

$$X = \left(\frac{C_0 - C(6\text{hours})}{C_0} \right) \times 100 \quad (12)$$

Where C_0 and $C(6\text{hours})$ represent the initial micropollutant concentration and the pollutant concentration remaining after 6 hours of photocatalytic treatment.

The removal percentages are equal to 95 % for ibuprofen, 65% for bisphenol A, 56% for PFOS, and 18 % for erythromycin. The degradation percentages of PFOA cannot be evaluated since the final concentration ($C(6\text{hours})$) is larger than the initial concentration. For all the other micropollutants, the removal percentage is maximal and evaluated to 100% since the final concentration is below the limit of quantification. This attests the high photocatalytic efficiency of the titania towards the degradation of several micropollutants including diclofenac, carbamazepine, lidocaine, sulfamethoxazole, estrone, ketoprofen, naproxen, clarithromycin, and triclosan. This indicates the efficient photocatalytic degradation with TiO_2 catalyst of a mixture of micropollutants even if there is still a very low concentration of 3 micropollutants remaining in the solution.

However, the kinetics of degradation is mainly affected by the nature of the micro contaminants while the effect of the initial concentration is less pronounced. In the presence of larger micropollutant concentrations (sampled in 2016, Fig. 23), the concentrations of naproxen, estrone and triclosan fall below their limit of quantification after 30 min of UV irradiation. Conversely, the concentrations of carbamazepine, clarithromycin, diclofenac, ketoprofen, lidocaine and sulfamethoxazole become lower than their limit of quantification after 6 h of process under UV illumination. In the presence of lower micropollutants concentrations (sampled in 2017, Fig. 22), the degradation trend remains similar. Surprisingly, the time of process necessary to reach a micropollutant concentration lower than the limit of quantification of the LC/MS-MS is not affected

by the initial micro contaminant concentration for our two times scale (30 min and 6 hours). For instance, 6 hours of photocatalytic treatment lead to the total degradation of 19 ng/L and 75 ng/L of carbamazepine, 16 ng/L and 703 ng/L of clarithromycin, 6 ng/L and 35 ng/L of sulfamethoxazole. For bisphenol A, the total degradation of 54 ng/L takes place in 6 hours. For larger bisphenol A content, the initial concentration of 88 ng/L drops to 31 ng/L after 6 hours of illumination. The concentration degraded ($\Delta C = C_0 - C(6\text{hours})$) equals 57 ng/L which is similar to the amount removed at low initial concentration. This seems to indicate that a maximum degradation of 57 ng/L can be obtain in 6 hours. For diclofenac, the total degradation of an initial concentration of 51 ng/L is achieved after 30 minutes of irradiation. On the opposite, 142 ng/L of the same micropollutant are removed after 6 hours of process. Note that the concentration falls down to 14 ng/L after 30 minutes of irradiation indicating a maximum rate of degradation of 256 ng/L per hour.

We discuss the relationship between the rate of degradation after 30 minutes and the initial micropollutant concentration taking into account the nature of the emerging contaminant. An average rate of degradation r can be defined corresponding to ΔC during time t_i :

$$r = \frac{C_0 - C(30\text{minutes})}{t_i} \quad (13)$$

where t_i is fixed to 30 minutes, C_0 and $C(30\text{minutes})$ refer to the initial micropollutant concentration and the pollutant concentration remaining after 30 minutes of photocatalytic treatment.

In the Fig. 24 the reported rate of degradation from the data of the Figs. 22 and 23 are plotted against the initial pollutant concentration, for the various emerging contaminants. The rate of degradation depends on the initial pollutant concentration. For each micropollutant, r increases with the pollutant content. For instance, for lidocaine, the rate shifts from 0.05 ng/L min to 0.68 ng/L min as the concentration is increased from 7 to 47 ng/L. Similarly, the rate changes from 0.12 ng/L min to 0.19 ng/L min have been achieved when the initial carbamazepine concentration varies from 18 to 68 ng/L. Using the whole data obtained with all the micropollutants, it appears that the rate is enhanced as the pollutant concentration is increased. Despite a large scatter in the data, a linear evolution can be extracted from the data. This may indicate a first order kinetics.

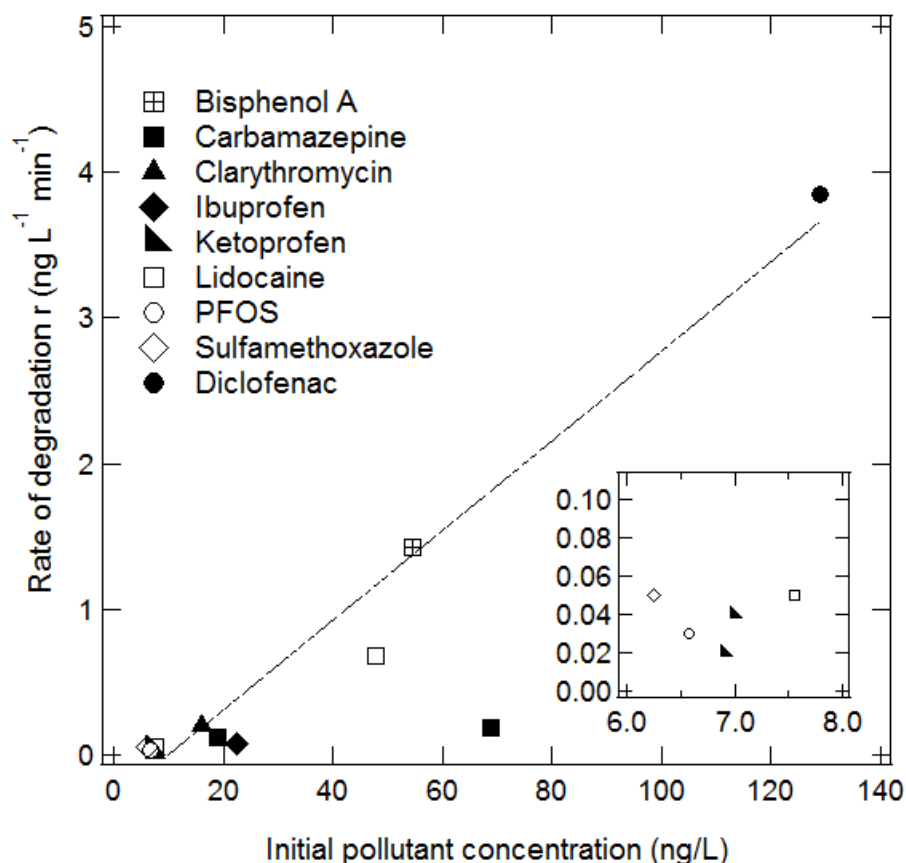


Fig. 24. The effect of the initial micropollutant concentration ($[\text{Micropollutant}]$) on the rate of degradation. The rate of degradation is expressed as the difference ΔC between the initial micropollutant concentration (C_0) and the pollutant concentration remaining after 30 minutes of photocatalytic treatment ($C(30\text{minutes})$) divided by the time of the process t_i ($\Delta C/t_i$ with $t_i = 30$ min). The line represents the best linear fit given by $r = 0.0307 [\text{Micropollutant}] - 0.3045$ ($R^2 = 0.9645$). The inset depicts a zoom of the data for initial pollutant concentrations lower than 8 ng/L.

The large amount of different pollutant having initial concentrations lower than or equal to 20 ng/L gives a lot of information. First, PFOS, lidocaine, ketoprofen and sulfamethoxazole have concentrations ranging between 6.2 and 7.6 ng/L and their rates of degradation remain similar. The maximum rate equals 0.05 ng/L min while the lower rate is 0.03 ng/L min. For larger initial pollutants concentrations, *i.e.* 15 and 18 ng/L (clarithromycin and carbamazepine), a larger scatter in the rates occur but the difference remain acceptable (from 0.13 ng/L min to 0.20 ng/L min). It can then be concluded that the rate of degradation does not depend on the nature of the contaminants but is mainly affected by the contaminant concentration. This result is understandable considering that the hydroxyl radicals are a non-selective oxidant well adapted to degrade all the organic species

without preference. This is not the case, for instance, with singlet oxygen (electrophilic $^1\text{O}_2$) which oxidizes preferentially electron-rich species such as olefins, dienes, and sulfides.

In the special case of ibuprofen, it becomes possible to follow the entire kinetic of degradation (Fig. 25_a). The decay in the bulk concentration appears linear to the irradiation time ($R^2 = 0.9978$). This seems to indicate that the kinetic of degradation follows a zero-order reaction. The slope of the linear variation gives access to the reaction rate constant k . However, based on our previous experiments with the macropollutants (phenol, Fig. 18(b)), the photocatalytic degradation is expected to follow a first-order kinetics with respect to the pollutant concentration in the bulk solution (C). A plot of $\ln(C_0/C)$ versus the time t is shown in Fig. 25_b. Note that C_0 stands for the initial pollutant concentration in the bulk solution (at irradiation time = 0). The linear increase of $\ln(C_0/C)$ as a function of t ($R^2 = 0.9988$) could also indicate that the photocatalytic degradation of ibuprofen obeys first order kinetics in the presence of the cocktails of the other micropollutants. The linearization gives a kinetic constant k of 0.0083/ min. It is important to note that we cannot conclude on the exact kinetic order because the linearization are based on only 3 experimental data which do not ensure a great accuracy. However, our previous results which indicated that the degradation rate was affected by the initial emerging pollutant concentration (Fig 24) seem to be another argument in favor of a first order kinetics.

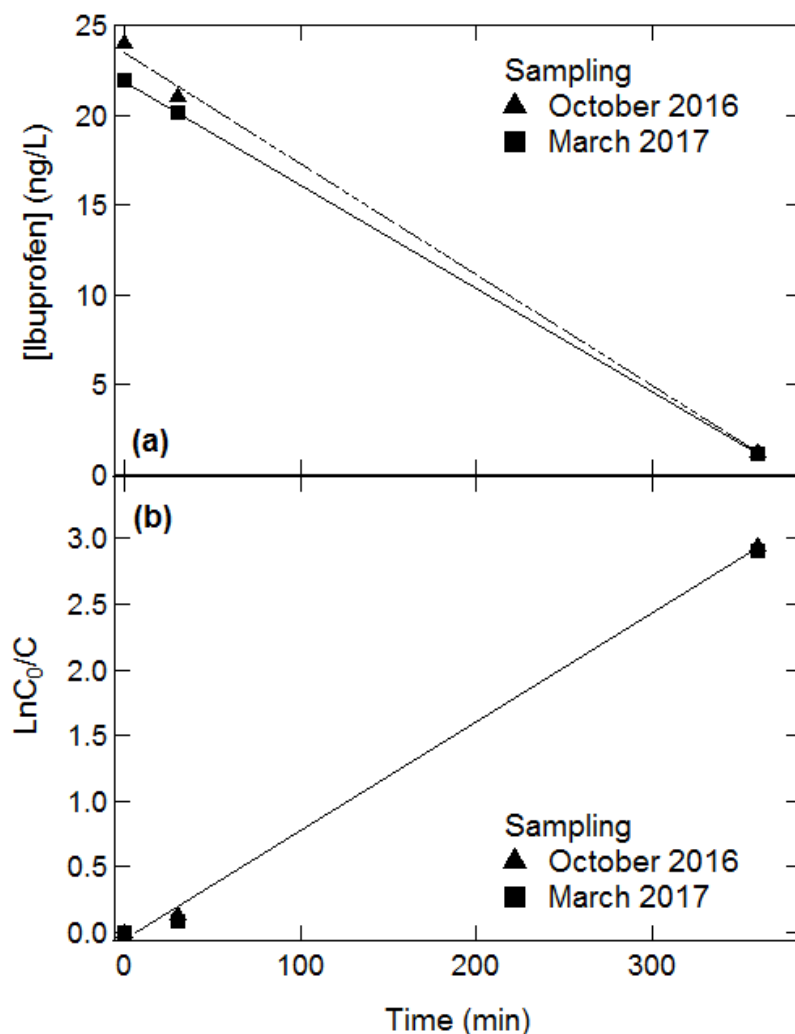


Fig. 25. (a) Photocatalytic degradation of ibuprofen as a function of the time of irradiation. The lines represent the best linear fit given by $[\text{Ibuprofen}] = -0.0574 \text{ Time} + 21.863$ ($R^2 = 1$) for the sample of March 2017, and $[\text{Ibuprofen}] = -0.0618 \text{ Time} + 23.451$ ($R^2 = 0.9978$) for the sample of October 2016. (b) Linear transform: $\ln(C_0/C)$ versus time. The lines represent the best linear fit given by $\ln(C_0/C) = 0.0083 \text{ Time} + 0.0779$ ($R^2 = 0.9976$) for the sample of March 2017 and $\ln(C_0/C) = 0.0083 \text{ Time} + 0.0553$ ($R^2 = 0.9988$) for the sample of October 2016. C_0 represents the initial micropollutant concentration (at irradiation time = 0) while C is the micropollutant concentration at a given time.

For ibuprofen, ketoprofen, and triclosan, the initial concentrations are similar between the two samplings (Fig. 22 and 23). These data can be analyzed in order to assess the matrix effect, *i.e.* the effect of the components other than the micropollutant of interest, on the adsorption and the photodegradation process. In both cases, the photocatalytic treatment leads to the disappearance of triclosan after 30 minutes of irradiation. For ketoprofen, the concentration of the micropollutant falls

below the limit of detection after 6 hours of illumination for the two samplings. More remarkably, the remaining concentration after 30 minutes of treatment is similar, *i.e.* 6,3 ng/L and 6.4 ng/L. For ibuprofen, the concentrations remain larger than the quantification limit of the analytical apparatus during all the process giving access to the temporal evolution of the micropollutant content (Fig. 21a). The 2 degradation curves follow perfectly the same trend and merge into a single curve. This emphasizes similar concentrations, in terms of dark adsorption (C(2hours)) and photocatalytic degradation (C(30minutes) and C(6hours)). It is striking that the degradation performances are not affected by the concentration of the other micropollutants. Recall that the initial concentration of the micropollutants is higher inside the water taken in October 2016 as compared to that sampled in March 2017. These results seem to point out the absence of significant matrix effect on the photocatalytic process. Considering only the 21 micropollutants analyzed here, the sum of all the micro contaminants becomes equal to 1996 ng/L for the water sampled in October 2016 and it drops to 228 ng/L for March 2017. The total micropollutant content (based on 21 contaminants) is 9 times larger inside the water withdrawn in 2016 than that in 2017.

The results obtained with the emerging contaminants can be compared with those reported during the degradation of the two model macropollutants (phenol and diclofenac at an initial concentration of 10 mg/L). Diclofenac was used in both cases while phenol macro contaminant can be compared to bisphenol A micropollutant. The variation of the adsorption and the degradation properties of the each pollutant evolves in a similar fashion when they are present in mg/L or ng/L. In both cases, the diclofenac adsorbed amounts remain much higher than those obtained with phenol based pollutants. The adsorption of phenolic pollutants onto the titania is very weak regardless of the initial concentrations (10 mg/L or 80-50 ng/L). For the two waters, the degradation efficiency is larger with diclofenac than with phenol. Surprisingly, the removal percentages are similar between the water containing the macro and the micropollutants. The diclofenac degradation efficiency equals 100% and 98% when the contaminant was present in ng/L and mg/L, respectively. For bisphenol (micropollutant), X amounts to 100% and 65% for initial pollutant concentrations of 54 ng/L and 88 ng/L, respectively. For phenol (macropollutant), the efficiency X is 68%. As far as the kinetic law is concerned, a first order kinetic was determined with phenol macropollutant. At the same time, a first order dependency towards the ibuprofen concentration was also discussed with the mixtures of the micropollutants. The k value obtained with the micropollutant cannot be easily compared with that found with the macropollutant because the former was obtained with only 3 experimental data which do not ensure a great accuracy. Recall that we found a constant of 0.0032 min^{-1} for the photocatalytic degradation of an initial solution containing 10 mg/L of phenol. The obtained k value is comparable

with that of about 0.0083 min^{-1} already reported for ibuprofen in the presence of the cocktail of micropollutants. The variation in the k values (0.0032 min^{-1} vs 0.0083 min^{-1}) is within the margin of error of the kinetic constants determination.

6 Comparison between titania photocatalytic and iron impregnated Faujasite photo-Fenton degradation of micropollutants

The comparison of the micropollutants adsorbed amounts onto titania and iron impregnated Faujasite is depicted in Figs. 26 and 27 for the waters sampled in March 2017 and October 2016, respectively.

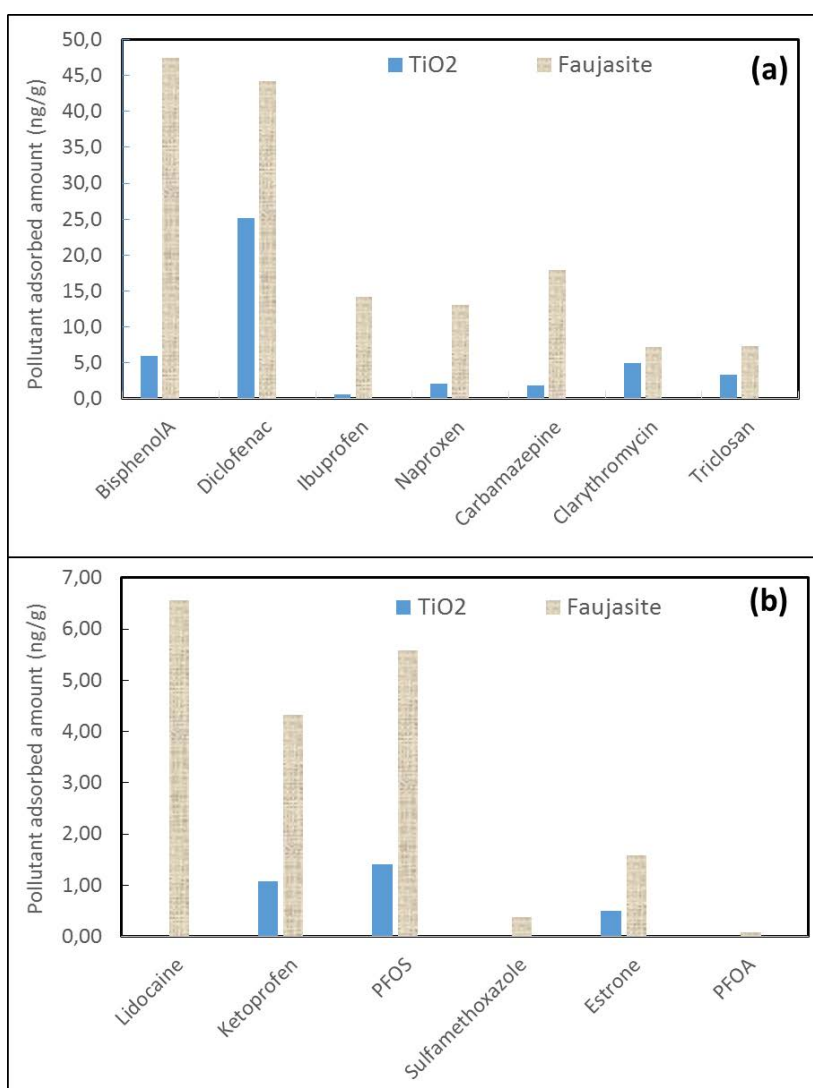


Fig. 26. Comparison of the micropollutant adsorbed amounts onto titania and Faujasite. The sampling was performed in March 2017.

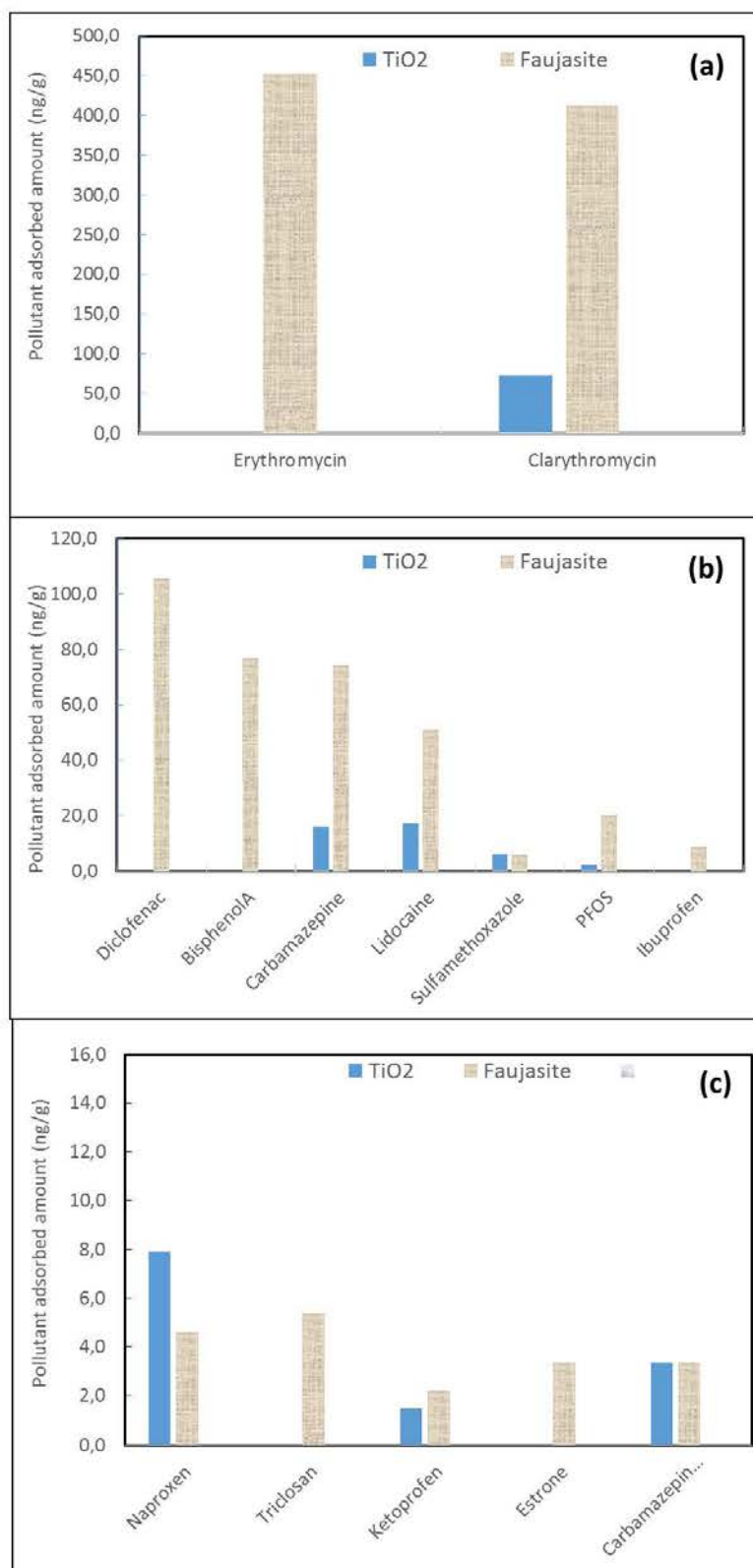


Fig. 27. Comparison of the micropollutant adsorbed amounts onto titania and Faujasite. The sampling was performed in October 2016.

The adsorption of all the micropollutants is larger onto the Faujasite zeolite compared to that onto titania. The better adsorption properties of the iron impregnated Faujasite are also confirmed by carbon analysis performed with the sample of water withdrawn in October 2016 (Table 9). The initial total organic carbon (TOC) of 4.3 mg C/L decreases to 2.9 mg C/L and 3.5 mg C/L at the end of the 2 h of adsorption in the presence of Faujasite and TiO₂, respectively. At the same time, the initial inorganic carbon content of 30.3 mg C/L drops to 16.1 mg C/L and 25.3 mg C/L after 2 h of contact with the zeolite and the photocatalyst, respectively.

Table 9. Comparison of the kinetic of degradation of the micropollutants using titania photocatalysis and iron impregnated Faujasite photo-Fenton. The sampling was performed in October 2016. The notation n.m. means not measured.

Time	TiO₂ TOC (mg C/L)	Faujasite TOC (mg C/L)	TiO₂ Inorganic carbon (mg C/L)	Faujasite Inorganic carbon (mg C/L)
Initial	4.36	4.36	30.33	30.33
0 (2 h adsorption)	3.51	2.91	25.31	16.18
30 min	3.01	2.65	n.m.	n.m.
6 hours	2.67	2.44	n.m.	n.m.

These results can be explained by the comparing the surface areas of the two solids. Generally, large surface area is likely to exhibit better adsorption activity, because a large surface area provides more active sites for adsorbing the contaminant molecules. In the present study, large surface area gives better sorption activity since the Faujasite (640 m²/g) has a greater surface area than TiO₂ (59 m²/g) as shown in Fig. 28. It seems also interesting to compare the polar and non-polar properties of the two catalysts surfaces. To this aim, the BET constant C_{BET} can be used as a method to assess the surface polarity of the surface. The parameter C_{BET} is high for polar surfaces and low for non-polar surfaces. In the present study, the large values of the parameter C_{BET} emphasize the polar character of the two surfaces. However, the reduction of the constant from 795 (Faujasite) to 200 (TiO₂) indicates the larger polar character of the Faujasite.

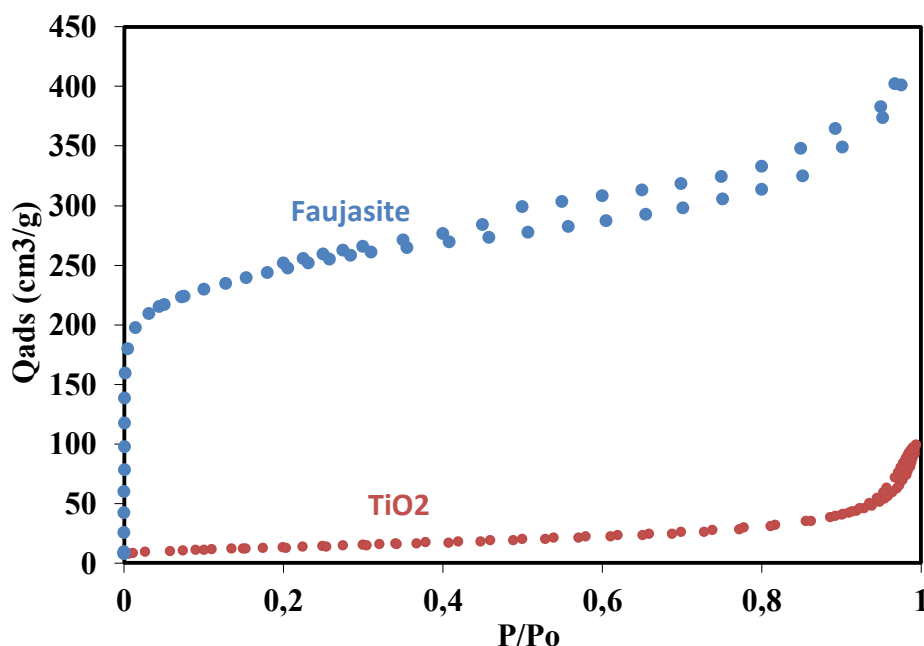


Fig. 28. N₂ adsorption isotherm of Faujasite and TiO₂.

The two catalysts and the 2 processes (photocatalysis and photo-Fenton) lead to roughly similar performances. After 6 hours of photocatalytic and photo-Fenton treatment, the majority of the micropollutants are removed. To be more accurate, the remaining pollutant concentration becomes lower than the limit of quantification of the analytical apparatus. In other words, carbamazepine, carbamazepine-10,11-epoxide, clarithromycin, diclofenac, estrone, ketoprofen, lidocaine, naproxen, and triclosan are totally removed by the two catalysts under UV irradiation for the two initial concentrations. At the end of the two processes, PFOA, PFOS, ibuprofen, bisphenol A, and erythromycin remain in solutions for all the initial concentrations. For all these micropollutants, the remaining concentration is larger after the photocatalytic process in comparison with that obtained with the photo-Fenton treatment. In order to be more quantitative, it appears interesting to discuss the results based on the removal efficiency of the process (after 6h of process). To this aim, the Fig. 29 compares the removal percentage for titania and iron impregnated Faujasite systems. Note that the X for certain micropollutants are not displayed when it goes to 100% for the two processes. The removal percentage after 6 hours of treatment is generally better using the photo-Fenton process than with the photocatalytic degradation. Significant difference in the efficiency can be noticed. For bisphenol A, erythromycin, and PFOS, X increases, respectively, from 65% to 90%, from 18% to 37%, and from 36% to 78% when the TiO₂ photocatalyst is replaced by the iron impregnated faujasite photo-Fenton catalyst. Another interesting feature is that the photocatalytic process leads to

the total degradation of initial sulfamethoxazole concentrations of 35.4 ng/L and 6.2 ng/L, while the photo-Fenton treatment leads to the partial degradation with X values of 54% and 74%, respectively.

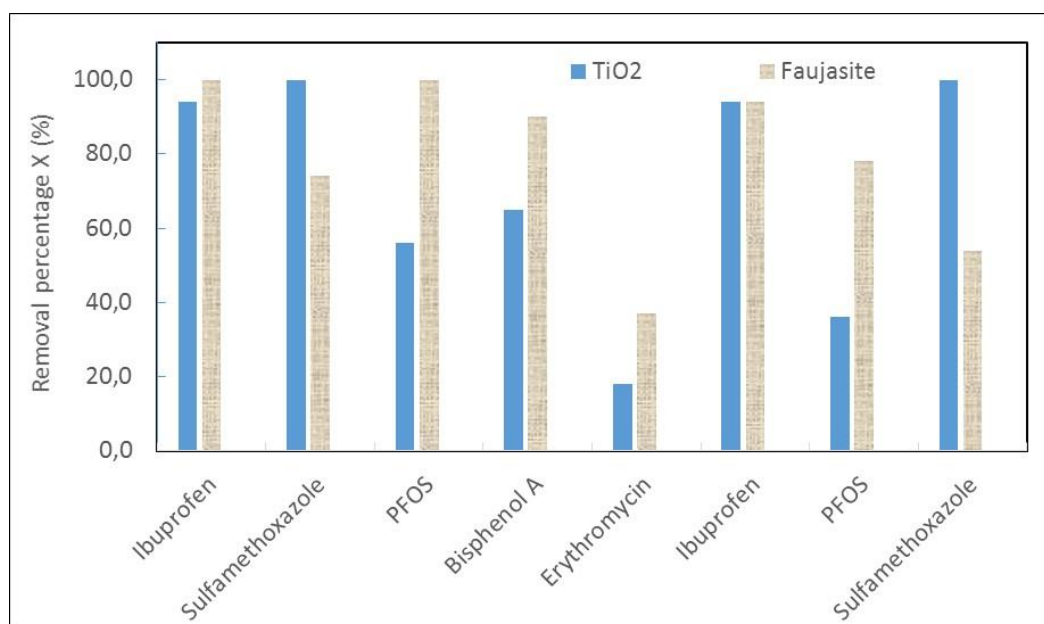


Fig. 29. Comparison of the removal percentage using titania photocatalysis and iron impregnated Faujasite photo-Fenton after 6 h of process. For ibuprofen, sulfamethoxazole, and PFOS, from the left to the right, the sampling was performed in March 2017. For the other pollutants, from the right to the left, sulfamethoxazole, PFOS, ibuprofen, erythromycin, and bisphenol A, the sampling was performed in October 2016.

In order to analyze the kinetic of degradation, it appears practical to discuss the time necessary to totally remove the contaminant. The time after which the micropollutant concentration goes below the limit of quantification of the LC/MS-MS is defined as the time necessary to totally remove the contaminant. We are aware that this not necessary means the complete mineralization of the micro contaminant since we are unable to follow the TOC values of each contaminant. In addition, recall that the micropollutant concentrations were only evaluated after 30 minutes and 6 hours of process. The comparison of the characteristic times obtained by photocatalysis and photo-Fenton for all the micropollutants are reported in the Table 10.

Table 10. Comparison of the time necessary to totally remove the contaminant by TiO₂ photocatalysis and iron impregnated Faujasite photo-Fenton. The time after which the micropollutant concentration goes below the limit of quantification of the LC-MS/MS is defined as the time

necessary to totally remove the contaminant. The notation “-” indicates that the micropollutant is not totally removed after 6 h of treatment since the concentration appears larger than the limit of quantification of the LC/MS-MS.

Time	March 2017 TiO ₂	March 2017 Faujasite	October 2016 TiO ₂	October 2016 Faujasite
Bisphenol A	6 h	30 min	-	-
Carbamazepine	6 h	30 min	6 h	30 min
Carbamazepine- 10,11-epoxide	-	-	30 min	30 min
Clarithromycin	6 h	30 min	6 h	6 h
Diclofenac	30 min	30 min	6 h	30 min
Estrone	30 min	30 min	30 min	30 min
Ibuprofen	-	30 min	-	-
Ketoprofen	6 h	30 min	6 h	30 min
Lidocaine	6 h	30 min	6 h	30 min
Naproxen	30 min	30 min	30 min	6 h
PFOS	-	30 min	-	-
Sulfamethoxazole	6 h	-	6 h	-
Triclosan	30 min	30 min	30 min	30 min

For almost all the micropollutants, the contaminants are totally removed within a short period of time with Faujasite than with titanium dioxide. Generally speaking, 30 minutes of photo-Fenton process are sufficient while 6 hours of photocatalysis appear necessary. The temporal evolution of the TOC values supports these results (Table 9). The TOC decreases with the time of process from 3.5 mg C/L to 3.0 mg C/L and 2.7 mg C/L after 30 min and 6 hours of photocatalysis. Conversely, in the presence of iron impregnated Faujasite, the TOC values of the solutions after 30 minutes and 6 hours of treatment range between 2.6 and 2.4 mg C/L. The fastest degradation in the presence of Fe/Faujasite photo-Fenton catalyst may arise from two causes: (i) the larger micropollutant adsorbed amount and/or (ii) the higher production of radicals. A correlation between the time to degrade the pollutant and the contaminant surface coverage (i) was already reported in several instances for both photocatalysis and photo-Fenton processes (Inumaru et al. 2004, Sakai et al. 2013, Kassir et al. 2015). All the previous studies indicated that a large contaminant adsorbed amount improves and

accelerates the efficiency of the degradation process. For the second explanation (ii), it can be noticed that the hydroxyl radicals have been deemed to be the major active species during the photocatalytic and photo-Fenton oxidation reactions. In general, it is assumed that iron catalyst photo-Fenton process produces a larger amount of hydroxyl radicals (OH°) than TiO_2 photocatalytic reactions. The additional formation of OH° through Fenton reaction mainly comes from the presence of hydrogen peroxide (H_2O_2). In the present study, the H_2O_2 concentration is equal to 0.007 M.

Regarding the kinetic law, a first order kinetic was determined with sulfamethoxazole photo-Fenton degradation. In addition, a first order dependency towards the ibuprofen concentration was also discussed with the mixtures of the micropollutants. The k values obtained with the 2 different micropollutant (sulfamethoxazole and ibuprofen) cannot be easily compared since the two micropollutants are different and also mainly due to the weak accuracy in the constant determination. Recall that the constant was evaluated using only 3 experimental data. However, the two constants are in the same order of magnitude. In other words k becomes equal to 0.0021 min^{-1} for the photo-Fenton degradation of sulfamethoxazole while k amounts to 0.0083 min^{-1} for the photocatalytic degradation of ibuprofen. The difference in the k values remains within the margin of error of the kinetic constants determination.

7 Conclusion

The aim of this paper was to evaluate, for the first time, the heterogeneous photo-Fenton degradation of some micropollutants inside real water samples from a river using Faujasite Y zeolite impregnated with iron. The catalyst was prepared by the wet impregnation method using iron (III) nitrate nonahydrate as iron precursor. The characterization methods such as SEM coupled with EDS, XRD, diffuse reflectance UV/visible spectroscopy, and zeta potential, confirm the presence of Fe species, mainly under the form of Fe_2O_3 , deposited onto the surface of the zeolite. The photo-Fenton activity of the iron-impregnated Faujasite samples has been optimized on the removal of 10 mg/L of phenol employed as model macro-pollutant. Complete photo-Fenton degradation of the contaminant was achieved using Faujasite containing 20 wt. % of iron, under UV light, and in the presence of 0.007 mol/L of H_2O_2 at pH 5.5.

In a second step, the process was used with real water samples from the Meurthe river. Two samplings were carried out in October 2016 and in March 2017. Twenty-one micropollutants including 17 pharmaceutical compounds were specifically targeted, detected, quantified and degraded. All the initial concentrations remained in the range of ng/L (0.8 – 88 ng/L). The majority of the micropollutants possessed a large affinity for the surface of the iron-impregnated Faujasite. The results demonstrated the good efficiency of the photo-Fenton process with the cocktail of 21 micropollutants. Except for sulfamethoxazole and PFOA, the concentrations of all the other microcontaminants (bisphenol A, carbamazepine, carbamazepine-10,11-epoxide, clarithromycin, diclofenac, estrone, ibuprofen, ketoprofen, lidocaine, naproxen, PFOS, triclosan, etc.) became lower than the limit of quantification of the LC-MS/MS after 30 minutes or 6 hours of photo-Fenton treatment depending on their initial concentrations. In the presence of the cocktail of the other micropollutants, the photo-Fenton degradation of PFOA can be neglected, while the degradation of sulfamethoxazole obeys first order kinetics.

The efficiency of the photo-Fenton process towards the degradation of the 21 micropollutants from the site of Moulin Noir was compared to that of TiO_2 photocatalysis. After h hours of treatment, the 2 processes lead to similar removal performance. However, the kinetic of photodegradation is affected by the process. Faster degradation takes place using the photo-Fenton process via the prepared iron-Faujasite system.

References

- Andrade A.L, Souza DM, Pereira M.C, Fabris JD, Domingues R.Z (2009) Synthesis and characterization of magnetic nanoparticles coated with silica through a sol-gel approach. *Ceramica* 55 (336): 420–424
- Arimi M (2017) Modified natural zeolite as heterogeneous Fenton catalyst in treatment of recalcitrants in industrial effluent. *Progress in Natural Science: Materials International* 27 (2): 275–282
- Arvaniti O, Stasinakis A (2015) Review on the occurrence, fate and removal of perfluorinated compounds during wastewater treatment. *Sci. Total Environ.* 524-525: 81-92
- Barakat M. A, Tseng JM, Huang C.P (2005) Hydrogen peroxide-assisted photocatalytic oxidation of phenolic compounds. *Appl. Catal. B.* 59 (1): 99–104
- Barreca S, Velez Colmenares J, Pace A, Orecchio S, Pulgarin C (2014) Neutral solar photo-Fenton degradation of 4-nitrophenol on iron-enriched hybrid montmorillonite-alginate beads (Fe-MABs). *J. Photochem. Photobiol. A.* 282: 33-40
- Barreca S, Velez Colmenares J, Pace A, Orecchio S, Pulgarin C (2015) Escherichia Coli inactivation by neutral solar heterogeneous photo-Fenton (HPF) over hybrid iron/montmorillonite/alginate beads. *J. Env. Chem. Eng.* 3 (1): 317–324
- Basumatary K.A, Pratim Adhikari P, Ghoshal AK, Pugazhenth G (2016) Fabrication and performance evaluation of faujasite zeolite composite ultrafiltration membrane by separation of trivalent ions from aqueous solution. *Environ. Prog. Sustain. Energy* 35 (4): 1047–1054
- Blanco M, Martinez A, Marcaide A, Aranzabe E, Aranzabe A (2014) Heterogeneous Fenton catalyst for the efficient removal of azo dyes in water. *Am. J. Analyt. Chem.* 5: 490-499
- Cejka J, Zilkova N, Nachtigall P (2005) Molecular sieves: From basic research to industrial applications. *Proceedings of the 3rd International Zeolite Symposium (3rd FEZA) Prague, Czech Republic*
- de Witte B, van Langenhove H, Demeestere K, Dewulf J (2011) Advanced oxidation of pharmaceuticals: Chemical analysis and biological assessment of degradation products. *Crit. Rev. Environ. Sci. Technol.* 41: 215-242
- Erdemoğlu M, Sarıkaya M (2006) Effects of heavy metals and oxalate on the zeta potential of magnetite. *J. Colloid Interface Sci.* 300 (2): 795–804
- Fatta-Kassinos D, Meric S, Nikolaou A (2011) Pharmaceutical residues in environmental waters and wastewater: current state of knowledge and future research. *Anal. Bioanal. Chem.* 399: 251-275

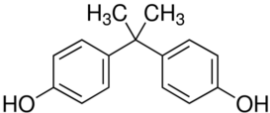
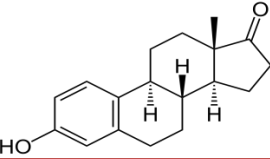
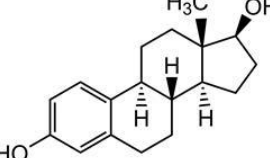
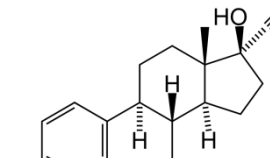
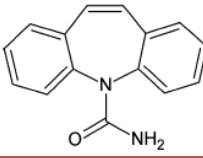
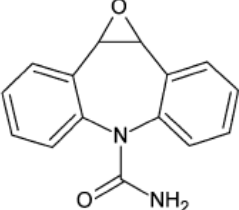
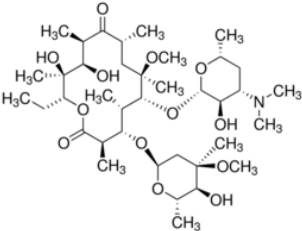
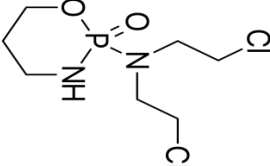
- Feng J, Hu X, Yue P.L, Zhu H.Y, Lu G.Q (2003) Discoloration and mineralization of reactive red HE-3B by heterogeneous photo-Fenton reaction. *Water Res.* 37 (15): 3776–3784
- Ghaly M.Y, Härtel G, Mayer R, Haseneder R (2001) Photochemical oxidation of P-chlorophenol by UV/H₂O₂ and photo-Fenton process. A comparative study. *Waste Manage.* 21 (1): 41–47
- Ghatak HR (2014) Advanced oxidation processes for the treatment of biorecalcitrant organics in wastewater. *Crit. Rev. Environ. Sci. Technol.* 44: 1167-1219
- Hartmann M, Kullmann S, Keller H (2010) Wastewater treatment with heterogeneous Fenton-type catalysts based on porous materials. *J. Mat. Chem.* 20 (41): 9002–9017
- Huang W, Luo M, Wei C, Wang Y, Hanna K, Mailhot G (2017) Enhanced heterogeneous photo-Fenton process modified by magnetite and EDDS: BPA degradation. *Environ. Sci. Pollut. R.* 24 (11): 10421–10429
- Igos E, Benetto E, Venditti S, Kohler C, Cornelissen A, Moeller R, Biwer A (2012) Is it better to remove pharmaceuticals in decentralized or conventional wastewater treatment plants? A life cycle assessment comparison. *Sci. Total Environ.* 438: 533-540
- Inumaru K, Murashima M, Kasahara T, Yamanaka S (2004) Enhanced photocatalytic decomposition of 4-nonylphenol by surface-organografted TiO₂: a combination of molecular selective adsorption and photocatalysis, *Appl. Catal. B.* 52: 275-280.
- Jiang C, Xu Z, Guo Q, Zhuo Q (2014) Degradation of bisphenol A in water by the heterogeneous photo-Fenton. *Environ. Technol.* 5 (8): 966–972
- Kasiri M.B, Aleboyeh H, Aleboyeh A (2008) Degradation of acid blue 74 using Fe-ZSM5 zeolite as a heterogeneous photo-Fenton catalyst. *Appl. Catal. B.* 84(1): 9–15
- Kassir M, Roques-Carmes T, Hamieh T, Toufaily J, Akil M, Barres O, Villiéras F (2015) Improvement of the photocatalytic activity of TiO₂ induced by organic pollutant enrichment at the surface of the organografted catalyst, *Colloids Surf. A* 485: 73-83.
- Kim S, Durand P, Roques-Carmes T, Eastoe J, Pasc A (2015) Metallo-solid lipid nanoparticles as colloidal tools for meso-macroporous supported catalysts. *Langmuir* 31: 1842-1849
- Klamerth N, Malato S, Agüera A, Fernández-Alba A, Mailhot G (2012) Treatment of municipal wastewater treatment plant effluents with modified photo-Fenton as a tertiary treatment for the degradation of micro pollutants and disinfection. *Environ. Sci. Technol.* 46 (5):2885–2892
- Kovalova L, Knappe DRU, Lehnberg K, Kazner C, Hollender J (2013) Removal of highly polar micropollutants from wastewater by powdered activated carbon. *Environ. Sci. Pollut. Res.* 20: 3607-3615

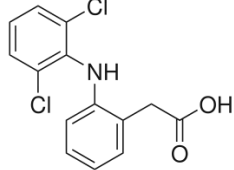
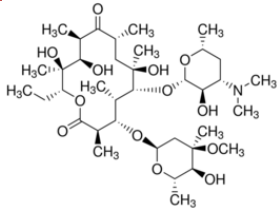
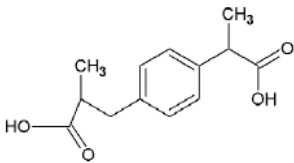
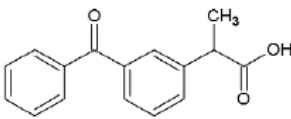
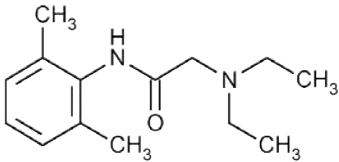
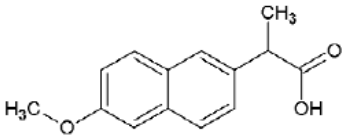
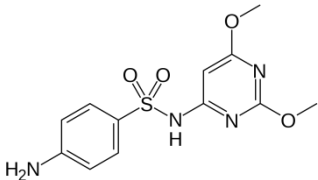
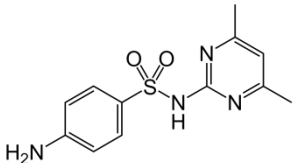
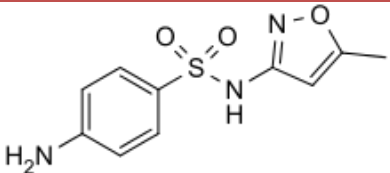
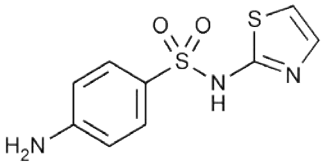
- Kowalska-Kuś J, Held A, Nowińska K (2013). Oxydehydrogenation of C₂–C₄ hydrocarbons over Fe-ZSM-5 zeolites with N₂O as an oxidant. *Catal. Sci. Tech.* 3 (2): 508–518
- Kuzniatsova T, Kim Y, Shqau K, Dutta PK, Verweij H (2007) Zeta potential measurements of zeolite Y: Application in homogeneous deposition of particle coatings. *Microporous Mesoporous Mater.* 103 (1): 102–107
- Lam M, Mabury S (2005) Photodegradation of the pharmaceuticals atorvastatin, carbamazepine, levofloxacin, and sulfamethoxazole in natural waters. *Aquat. Sci.* 67 (2): 177–188
- Li Y, Lu Y, Zhu X (2006) Photo-Fenton discoloration of the azo dye X-3B over pillared bentonites containing iron. *J. Hazard. Mater.* 132 (2):196–201
- Li L, Shen Q, Li J, Hao Z, Ping Xu Z, Max Lu GQ (2008) Iron-exchanged FAU zeolites: Preparation, characterization and catalytic properties for N₂O decomposition. *Appl. Catal. A: General* 344 (1): 131–141
- Loaiza-Ambuludi S, Panizza M, Oturan N, Oturan MA (2014) Removal of the anti-inflammatory drug ibuprofen from water using homogeneous photocatalysis. *Catal. Today* 224: 29–33
- Lutz W (2014) Zeolite Y: synthesis, modification, and properties - A case revisited. *Advances in Materials Science and Engineering* ID 724248.
- Mariangela G, Rizzo L, Farina A (2013) Endocrine disruptors compounds, pharmaceuticals and personal care products in urban wastewater: implications for agricultural reuse and their removal by adsorption process. *Environ. Sci. Pollut. Res.* 20 (6): 3616–3628
- Miralles-Cuevas S, Oller I, Ruiz Aguirre A, Sánchez Pérez JA, Malato Rodríguez S (2014) Removal of pharmaceuticals at microg L⁻¹ by combined nanofiltration and mild solar photo-Fenton. *Chem. Eng. J.* 239: 68-74
- Natali Sora I, Fumagalli D (2017) Fast photocatalytic degradation of pharmaceutical micropollutants and ecotoxicological effects. *Environ. Sci. Pollut. R.* 24(14): 12556-12561
- Neamu M, Catrinescu C, Kettrup A (2004a) Effect of dealumination of iron(III)-exchanged Y zeolites on oxidation of reactive yellow 84 azo dye in the presence of hydrogen peroxide. *Appl. Catal. B.* 51 (3): 149–157
- Neamu M, Zaharia C, Catrinescu C, Yediler A, Macoveanu M, Kettrup A (2004b) Fe-exchanged Y zeolite as catalyst for wet peroxide oxidation of reactive azo dye procion marine H-EXL. *Appl. Catal. B.* 48 (4): 287–294
- Nidheesh PV (2015). Heterogeneous Fenton catalysts for the abatement of organic pollutants from aqueous solution: A review. *RSC Adv.* 5 (51): 40552–40577
- Noorjahan M, Durga Kumari V, Subrahmanyam M, Panda L (2005). Immobilized Fe(III)-HY: an efficient and stable photo-Fenton catalyst. *Appl. Catal. B.* 57 (4): 291–298

- Oturan MA, Aaron J.J (2014) Advanced oxidation processes in water/wastewater treatment: Principles and applications. A review. *Crit. Rev. Environ. Sci. Technol.* 44 (23): 2577–2641.
- Richardson SD, Kimura SY (2016) Water analysis: Emerging contaminants and current issues. *Anal. Chem.* 88 (1): 546–582
- Rodriguez S, Aurora S, Arturo R (2011) Effectiveness of AOP's on abatement of emerging pollutants and their oxidation intermediates: nicotine removal with Fenton's reagent. *Desalination* 280 (1): 108–113
- Rutkowska M, Chmielarz L, Jabłońska M, Van Oers CJ, Cool P (2014) Iron exchanged ZSM-5 and Y zeolites calcined at different temperatures: Activity in N₂O decomposition. *J. Porous Mater.* 21 (1): 91–98
- Sakai T, Da Loves A, Okada T, Mishima S (2013) Titania/C_nTAB nanoskeleton as adsorbent and photocatalyst for removal of alkylphenols dissolved in water, *J. Hazard. Mater.* 248: 487-495.
- Sanches S, Rodrigues A, Cardoso V, Benoliel M, Crespo G, Pereira V (2016) Comparison of UV photolysis, nanofiltration, and their combination to remove hormones from a drinking water source and reduce endocrine disrupting activity. *Environ. Sci. Pollut. R.* 23 (11):11279–11288
- Trapido M, Epold I, Bolobajev J, Dulova N (2014) Emerging micropollutants in water/wastewater: growing demand on removal technologies. *Environ. Sci. Pollut. Res.* 21: 12217-12222
- Treacy MMJ, Higgins JB (2007). FAU - Faujasite. In collection of simulated XRD powder patterns for zeolites (Fifth Edition), 166–167. Amsterdam: Elsevier Science B.V.
- Turapan S, Kongkachuichay P, Worathanakul P (2012) Synthesis and characterization of Fe/SUZ-4 zeolite. *Procedia Engineering* 32: 191-197
- Verboekend DN, Nuttens R, Locus J, Van Aelst P, Verolme JC, Groen J, Pérez-Ramírez, Sels BF (2016) Synthesis, characterization, and catalytic evaluation of hierarchical faujasite zeolites: milestones, challenges, and future directions. *Chem. Rev.* 45 (12): 3331–3352
- Xavier S, Gandhimathi R, Nidheesh PV, Ramesh ST (2016) Comparative removal of magenta MB from aqueous solution by homogeneous and heterogeneous photo-Fenton processes. *Desalin. Water Treat.* 57: 12832-12841
- Yue Y, Liu H, Yuan P, Yu C, Bao X (2015) One-pot synthesis of hierarchical FeZSM-5 zeolites from natural aluminosilicates for selective catalytic reduction of NO by NH₃. *Sci. Rep.* 5: 09270

Supporting Information

Table S1. Description of the 21 micropollutants. The notation EDCs corresponds to endocrine disruptors, Phs indicates pharmaceuticals, PCPS means personal care products, and PFCs corresponds to perfluorinated compounds.

Family	Class	Compound	Structure
EDCs	Endocrine disruptor	Bisphenol A	
	Hormone	Estrone	
	Hormone	Estradiol-beta	
	Hormone	Ethynylestradiol	
Phs	Anti-epileptic	Carbamazepine	
	Anti-epileptic	Carbamazepine-10,11-epoxide	
	Antibiotic	Clarithromycin	
	Chemotherapy Drug	Cyclophosphamide	

	Anti-inflammatory	Diclofenac	
	Antibiotic	Erythromycin	
	Anti-inflammatory	Ibuprofen	
	Anti-inflammatory	Ketoprofen	
	Anesthetic	Lidocaine	
	Anti-inflammatory	Naproxen	
	Antibiotic	Sulfadimethoxine	
	Antibiotic	Sulfadimidine	
	Antibiotic	Sulfamethoxazole	
	Antibiotic	Sulfathiazole	

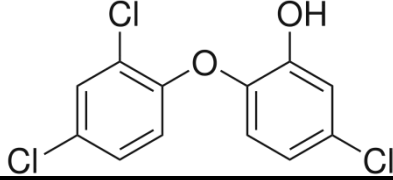
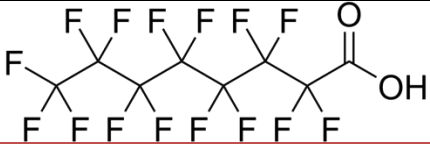
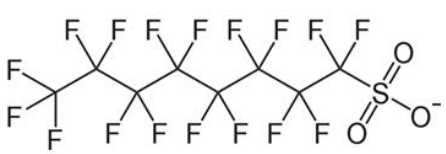
PCP	Antiseptic (PCP)	Triclosan	
PFCs	Perfluorinated compound	PFOA	
	Perfluorinated compound	PFOS	

Table S2. Conditions of the instrument used in LC-MS/MS measurements. The notation “min” corresponds to minutes.

	Positive mode	Negative mode
Column	Zorbax Eclipse Plus C18 (Agilent)	
Oven temperature	40 °C	
Flow	0.25 mL/min	
Injection	25 µL	
Eluents	A2: Water + 0.1 % formic acid	A1: Water + 2.5 mM ammonium acetate
	B2: Methanol + 0.1 % formic acid	B1: Acetonitrile
Eluent program	0 min 10 % B – 2 min 10 % B – 10 min 30 % B – 14 min 95 % B – 16 min 95 % B – 17 min 10 % B – 28 min 10 % B	0 min 30 % B – 1 min 30 % B – 3 min 50 % B – 8 min 80 % B – 9 min 95 % B – 11 min 95 % B – 12 min 30 % B – 15 min 30 % B

Table S3 Concentrations of the micropollutants after the various treatments. The notation “Initial” indicates the initial micropollutants concentration before the treatment, “Blank” corresponds to the experiments in the absence of the iron impregnated Faujasite, “Adsorption” gives the micropollutants concentration remaining in solution after 2 hours of contact between the water and the catalyst in the dark and in the absence of H₂O₂. The notations “Photo-Fenton 30 min UV/H₂O₂” and “Photo-Fenton 6 h UV/H₂O₂” correspond to the micropollutants concentrations remaining in the solution after 30 min and 6 hours of photo-Fenton process. Experimental conditions: catalyst concentration = 1 g/L, 0.007 M H₂O₂, UV light and pH 5.5.

	Initial	Blank 30min	Blank 6h UV	Blank 30min UV/H ₂ O ₂	Blank 6h UV/H ₂ O ₂	Adsorption 2h dark	Photo-Fenton 30min UV/H ₂ O ₂	Photo-Fenton 6h UV/H ₂ O ₂	Fenton 30min H ₂ O ₂ dark	Fenton 6h H ₂ O ₂ dark
Bisphenol A	54.5	56.4	48.8	39.0	49.1	< 7.01	< 7.40	15.8	< 7.53	< 7.14
Carbamazepine	18.9	17.4	27.3	13.7	20.3	< 1.00	< 1.06	< 1.04	< 1.08	< 1.02
Carbamazepine-10,11-epoxide	< 1.13	1.21	< 1.17	< 1.19	< 1.21	< 1.11	< 1.17	< 1.15	< 1.19	< 1.13
Clarithromycin	16.0	12.0	17.8	12.0	10.1	8.71	< 6.93	< 6.81	< 7.05	< 6.69
Cyclophosphamide	< 0.86	< 0.90	< 0.89	< 0.90	< 0.92	< 0.84	< 0.89	< 0.87	< 0.90	< 0.86
Diclofenac	51.2	32.6	26.9	27.9	21.7	< 7.24	< 7.64	< 7.51	< 7.78	< 7.38
Erythromycin	< 29.6	63.3	32.6	< 31.2	48.7	178	< 30.7	< 30.1	< 31.2	< 29.6
Estradiol-beta	< 2.35	< 2.47	< 2.43	< 2.47	< 2.52	< 2.30	< 2.43	< 2.39	< 2.47	< 2.35
Estrone	4.46	4.90	5.03	3.99	3.69	< 2.88	< 3.04	< 2.98	< 3.09	< 2.93
Ethinylestradiol	< 17.2	< 18.2	< 17.8	< 18.2	< 18.5	< 16.9	< 17.8	< 17.5	< 18.2	< 17.2
Ibuprofen	22.5	24.7	22.4	22.0	22.2	8.32	< 0.97	< 0.95	< 0.99	< 0.94
Ketoprofen	6.90	4.50	< 2.71	4.17	< 2.81	2.58	< 2.71	< 2.66	< 2.76	< 2.62
Lidocaine	7.56	6.60	8.53	6.57	5.94	< 0.99	< 1.05	< 1.03	< 1.06	< 1.01
Naproxen	20.1	19.3	17.3	18.8	12.9	< 7.47	< 7.88	< 7.74	< 8.02	< 7.60
PFOA	0.829	1.16	1.02	1.19	1.39	0.752	1.17	2.51	1.11	2.32
PFOS	6.58	6.69	6.48	5.89	7.50	< 1.19	< 1.26	< 1.24	< 1.28	< 1.22
Sulfadimethoxine	< 4.70	< 4.96	< 4.87	< 4.96	< 5.04	< 4.61	< 4.87	< 4.78	< 4.96	< 4.70
Sulfadimidine	< 7.36	< 7.76	< 7.63	< 7.76	< 7.89	< 7.23	< 7.63	< 7.49	< 7.76	< 7.36
Sulfamethoxazole	6.26	5.68	8.27	7.71	8.06	5.88	3.77	1.61	5.37	1.44
Sulfathiazole	< 0.84	< 0.89	< 0.87	< 0.89	< 0.90	< 0.83	< 0.87	< 0.86	< 0.89	< 0.84
Triclosan	13.3	18.4	12.5	17.5	15.2	< 6.55	< 6.92	< 6.80	< 7.04	< 6.68

Table S4 Concentrations of the micropollutants after the various treatments. The sampling was performed in October 2016. The notation “Initial” indicates the initial micropollutants concentration before the treatment, “Adsorption” gives the micropollutants concentration remaining in solution after 2 hours of contact between the water and the catalyst in the dark and in the absence of H₂O₂. The notations “Photo-Fenton 30 min UV/H₂O₂” and “Photo-Fenton 6 h UV/H₂O₂” correspond to the micropollutants concentrations remaining in the solution after 30 min and 6 hours of photo-Fenton process. Experimental Conditions: catalyst concentration = 1 g/L, 0.007 M H₂O₂, UV light and pH 5.5.

October 2016				
Micropollutant	Initial	Adsorption (2h dark)	Photo-Fenton 30 min UV/H ₂ O ₂	Photo-Fenton 6 h UV/H ₂ O ₂
Bisphenol A	88.4	11.5	5.80	8.88
Carbamazepine	75.8	< 1.37	< 1.32	< 1.32
Carbamazepine-10,11-epoxide	3.36	< 3.26	< 3.15	< 3.15
Clarithromycin	703	291	77.4	< 10.5
Cyclophosphamide	< 1.04	< 1.06	< 1.02	< 1.02
Diclofenac	142	36.1	< 9.41	< 9.41
Erythromycin	1006	554	255	635
Estradiol-beta	< 2.90	< 2.52	< 2.44	< 2.44
Estrone	6.80	< 3.45	< 3.34	< 3.34
Ethinylestradiol	< 21.7	< 22.1	< 21.3	< 21.3
Ibuprofen	20.7	11.7	2.02	1.23
Ketoprofen	7.69	5.50	< 2.44	< 2.44
Lidocaine	52.6	< 1.59	< 1.54	< 1.54
Naproxen	15.0	10.4	< 7.85	< 7.85
PFOA	2.99	1.89	3.74	10.8
PFOS	22.2	< 2.02	2.62	4.76
Sulfadimethoxine	< 3.51	< 4.97	< 4.80	< 4.80
Sulfadimidine	< 1.38	< 1.33	< 1.28	< 1.28
Sulfamethoxazole	35.4	29.4	31.3	16.3
Sulfathiazole	< 0.91	< 0.93	< 0.90	< 0.90
Triclosan	14.4	< 9.24	< 8.94	< 8.94

Table S5 Concentrations of the micropollutants after the various treatments. The sampling was performed in October 2016 and March 2017. The notation “Initial” indicates the initial micropollutants concentration before the treatment, “Adsorption” gives the micropollutants concentration remaining in solution after 2 hours of contact between the water and the catalyst in the dark and in the absence of H₂O₂. The notations “30 min UV” and “6 h UV” correspond to the micropollutants concentrations remaining in the solution after 30 min and 6 hours of TiO₂ photocatalysis. Experimental conditions: catalyst concentration = 1 g/L, UV light and pH 5.5.

October 2016				
Micropollutants	Initial	Adsorption (2h, dark)	30 min UV	6h UV
BisphenolA	88,4	121	270	31,0
Carbamazepine	75,8	59,9	69,3	<1.43
Carbamazepine-10,11-epoxide	3,36	<3.20	<3.04	<3.42
Clarithromycin	703	630	695	<11.3
Cyclophosphamide	<1.04	<1.04	<0.99	<1.11
Diclofenac	142	146	14,8	<10.2
Erythromycin	1006	1202	3632	820
Estradiol-beta	<2.90	<2.48	<2.36	<2.64
Estrone	6,80	10,8	<3.23	<3.62
Ethinylestradiol	<21.7	<21.7	<20.6	<23.1
Ibuprofen	20,7	24,2	21,1	1,27
Ketoprofen	7,69	6,20	6,40	<2.65
Lidocaine	52,6	35,5	30,0	<1.67
Naproxen	15,0	<7.98	<7.58	<8.51
PFOA	2,99	3,73	5,38	4,85
PFOS	22,2	20,0	23,2	14,1
Sulfadimethoxine	<3.51	<4.88	<4.64	<5.21
Sulfadimidine	<1.38	<1.30	<1.24	<1.39
Sulfamethoxazole	35,4	29,1	38,8	<0.91
Sulfathiazole	<0.91	<0.91	<0.86	<0.97
Triclosan	14,4	14,4	<8.64	<9.70

March 2017				
Micropollutants	Initial	Adsorption (2h, dark)	30 min UV	6h UV
BisphenolA	54,5	48,6	11,8	<7.53
Carbamazepine	18,9	17,1	15,1	<1.08
Carbamazepine-10,11-epoxide	<1.13	<1.15	<1.21	<1.19
Clarithromycin	16,0	11,0	9,79	<7.05
Cyclophosphamide	<0.86	<0.87	<0.92	<0.90
Diclofenac	51,2	26,0	<7.91	<7.78
Erythromycin	<29.6	154	217	<31.2
Estradiol-beta	<2.35	<2.39	<2.52	<2.47
Estrone	4,46	3,96	<3.14	<3.09
Ethinylestradiol	<17.2	<17.5	<18.5	<18.2
Ibuprofen	22,5	21,9	20,1	1,19
Ketoprofen	6,90	5,83	6,30	<2.76
Lidocaine	7,56	7,85	5,92	<1.06
Naproxen	20,1	18,03	<8.16	<8.02
PFOA	0,829	1,46	1,35	0,97
PFOS	6,58	5,18	5,61	2,84
Sulfadimethoxine	<4.70	<4.78	<5.04	<4.96
Sulfadimidine	<7.36	<7.49	<7.89	<7.76
Sulfamethoxazole	6,26	7,16	4,65	<0.71
Sulfathiazole	<0.84	<0.86	<0.90	<0.89
Triclosan	13,3	10,0	<7.16	<7.04

Conclusion and Perspectives

Conclusion and Perspectives

It is now widely proved that the existence of micropollutants surface water, rivers and lakes pose serious and harmful effects on both human health and environment even at extremely low concentrations. The risk is not related to the toxicity of each individual compound in distilled water only, it is proven that the observed effect is resulted from a mixture of several compounds together that display a higher toxicity than a single component. Consequently, the ongoing research studies should take this fact into consideration when applying their water treatment experiments in order to finish the process with an efficient treatment technology specially designed for the emerging contaminants.

In this thesis study, for the first time, the removal of a mixture of 21 micropollutants of different groups presenting at ng/L in the real water of Meurthe river has been achieved using heterogeneous photo-Fenton process with Faujasite Y catalyst under UV light. Faujasite-Y zeolite impregnated with iron (III) in the presence of hydrogen peroxide under UV light proved to have high removal efficiencies as discussed in our report. To achieve this goal several successive steps were necessary. First of all, the possibility of the quantification of a mixture of micropollutants of different groups at ng/L levels is evaluated. Water samples from two rivers were analyzed in 3 different periods of the year from 5 sites located on the Meurthe river and Moselle river. The micropollutants were successively quantified using a preconcentration SPE method followed by LC-MS/MS analysis. This allowed us to widen our research study. Different influential factors that affect the presence and quantification of micropollutants in river water were addressed including the site position, flow rate, weather conditions, efficiency of WWTP and the quality of water treated for drinking use. The results showed that the highest concentrations of most of the present micropollutants are observed in October at ng/L. The site so-called Moulin Noir contains the largest number and type of these pollutants. Therefore, it was chosen as the best location for taking the real water samples for the removal tests. The flow rate and the concentration of the different compounds is affected by the weather conditions and the release behavior of each type of compounds by the people. This was reflected by following the flux variation of each micropollutant which allowed us to estimate the mass balance at the confluence between the two rivers. The values obtained were in fair agreement confirming the precision and validating the analytical methodology that can thus be used in the water treatment study.

The second step was related to the development of a new kind of catalyst and the optimization of the different experimental conditions of the photo-Fenton process. The optimization of the process parameters was conducted using phenol and diclofenac as model macropollutants. The hydrogen peroxide concentration, the light wavelength (UV and visible) and intensity, the iron loading immobilized as well as the pH of the solution were varied. Complete photo-fenton degradation of phenol and diclofenac was achieved using Faujasite containing 20 wt. % of iron, under UV light, and in solution containing 0.007 mol/L of H_2O_2 at pH 5.5.

Finally, it comes to the study the efficiency of our process in the removal of micropollutants in real water. The results demonstrated the good efficiency of the photo-Fenton process with the cocktail of 21 micropollutants. The majority of the micropollutants possessed a large affinity for the surface of the iron-impregnated Faujasite. Except for sulfamethoxazole and PFOA, the concentrations of all the other micro-contaminants became lower than the limit of quantification of the LC-MS/MS after 30 minutes or 6 hours of photo-Fenton treatment depending on their initial concentrations. These results emphasize the important role of the adsorption affinity of micropollutants into the surface of the used catalyst, in facilitating the removal of the present micropollutants. The degradation efficiency was also compared to that of TiO_2 P25 which remains the state of the art photocatalyst. Faster micropollutants removal occurred with the zeolite due to the larger adsorption of the micropollutants, coupled to the greatest production of OH radicals in the presence of hydrogen peroxide.

Our results establish that the Faujasite based heterogeneous photo-Fenton process can efficiently remove a real cocktail of micropollutants from river water at very low concentrations. Although, this behaviour has been expected, it has been barely reported in the scientific literature. This study is also the starting point of research for the development of treatment processes for water reuse.

The photo-Fenton degradation performances of the iron impregnated Faujasite towards the cocktails of micropollutants prove to be promising. Moreover, the removal of micropollutants at such low concentration is representative of the emerging contaminant concentration level (ng L^{-1}) encountered at the outlet of the WWTP. Consequently, and as perspectives, the results can be directly applied at the level of industrial scale in wastewater treatment plants. Future work will extend the present work to address more specifically the degradation mechanisms (byproducts), and also chemical engineering aspects such as reactor design in order to evaluate the potential scale-up of this process to real wastewater treatment plants.

Procédé photo-Fenton hétérogène pour l'élimination des micropolluants à très faible concentration de la rivière Meurthe

Résumé

Ce travail de thèse concerne le développement de catalyseurs Fe/Faujasite afin de dégrader un cocktail de micropolluants provenant d'une eau réelle de rivière dans la Meurthe (France) avec le procédé photo-Fenton hétérogène. Les micropolluants étudiés appartiennent à 4 grandes familles : des principes actifs pharmaceutiques, des produits de soins cosmétiques, des perturbateurs endocriniens, et des composés perfluorés. Pour la première fois, dans cette thèse, la dégradation d'un mélange de 21 micropolluants à l'état de traces (2 – 80 ng/L) provenant d'une réelle eau de rivière non-dopée a été effectuée. Cependant, le fait de travailler avec des concentrations très faibles en polluants reste un challenge notamment en ce qui concerne les aspects de chimie analytiques. Ce travail de thèse est donc divisé en deux grandes parties. Dans un premier temps, il a été nécessaire de trouver la meilleure eau réelle contenant un nombre élevé de micropolluants de différentes natures à des concentrations de l'ordre de quelques ng/L mais inférieures à 100 ng/L. Pour cela différentes campagnes de prélèvement ont été effectuées dans les deux principales rivières de la région Lorraine, la Meurthe et la Moselle, en différents lieux et différentes périodes de l'année. L'eau provenant du site de Moulin Noir a été choisie. Dans une deuxième partie, nous avons développé des catalyseurs fer/Faujasite pour pouvoir tester leur efficacité pour la dégradation des micropolluants provenant du site de Moulin Noir par le procédé photo-Fenton hétérogène. Dans une étape intermédiaire, l'optimisation des paramètres opératoires du procédé photo-Fenton avec nos catalyseurs a été effectuée en utilisant deux macropolluants modèles, phénol et diclofenac.

Mots clés: Eau de rivière, Micropolluants, Photo-Fenton hétérogène, Faujasite, LC-MS/MS.

Heterogeneous photo-fenton process for removal of micropollutants at very low concentration from Meurthe river

Abstract

Twenty one 21 micropollutants including pharmaceuticals, personal cares product, endocrine disruptors and perfluorinated compounds presenting at ng/L in the real water of Meurthe river, were successfully quantified and removed using heterogeneous photo-Fenton process. To achieve this goal, an analytical-catalytic methodology was developed and the work steps were performed linked together in a cycle-like manner. The use of the sensitive and efficient multi-residual SPE-LC-MS/MS analytical method allowed us to analyze and quantify the mixture of micropollutants present in a complex matrix during 3 periods of the year with different weather conditions, from 5 sampling sites. Results showed that the highest concentrations of most of the present micropollutants are observed in October at ng/L, Moulin Noir sampling site found to contain the largest number and type of these pollutants, the WWTP was not efficient in the removal of the micropollutants present in water and the drinking water used from tab was totally safe from micropollutants. The calculation of the fluxes and estimation of the mass balance at the rivers confluence confirmed the good precision and reliability of our measurement methodology, and specify the most suitable site for water to be taken from to be used in the removal tests which was Moulin Noir. Having the appropriate water sample, an efficient iron impregnated Faujasite catalyst was developed and used in a photo-Fenton process for the micropollutant removal tests. After characterization and optimization of the different experimental factors using the 2 model macropollutants, phenol and diclofenac, the real tests were performed on real water samples from Moulin Noir. The results demonstrated the good efficiency of the photo-Fenton process with the cocktail of 21 micropollutants. Except for sulfamethoxazole and PFOA, the concentrations of all the other micro-contaminants became lower than the limit of quantification of the LC-MS/MS after 30 minutes or 6 hours of photo-Fenton treatment depending on their initial concentrations under the effect of both adsorption and Fenton mechanisms. Comparing the photo-Fenton process to heterogeneous photocatalytic degradation over TiO₂, Faster micropollutants removal occurred with the zeolite.

Key words: River water, Micropollutants, Heterogeneous photo-Fenton, Faujasite, LC-MS/MS.

